APPENDIX 3.9.2
OS187H TRANSFER CASK BODY STRUCTURAL ANALYSIS

TABLE OF CONTENTS

3.9.2 OS187H TRANSFER CASK BODY STRUCTURAL ANALYSIS 3.9.2-1

3.9.2.1 Introduction 3.9.2-1

3.9.2.2 ANSYS Analysis 3.9.2-7

3.9.2.3 ANSYS Analysis Results and Reporting Methodology 3.9.2-28

3.9.2.4 Transfer Cask Trunnion Local Stresses 3.9.2-29

3.9.2.5 References 3.9.2-39

LIST OF TABLES

3.9.2-1 Summary of OS-187H Transfer Cask Stress Analysis

3.9.2-2 Computation Spreadsheet for the 6*g* Lifting, Top Trunnion, Local Stresses at Trunnion Pad

3.9.2-3 Computation Spreadsheet for the 6*g* Lifting, Top Trunnion, Local Stresses at Pad - Shell Intersection

3.9.2-4 Computation Spreadsheet for the (DW + 1.0*g* Axial) Transfer Load, Bottom Trunnion – Local Shell Stresses

3.9.2-5 Computation Spreadsheet for the (DW + 1.0*g* Vertical) Transfer Load, Bottom Trunnion – Local Shell Stresses

3.9.2-6 Computation Spreadsheet for the (DW + 1.0*g* transverse) Transfer Load, Bottom Trunnion – Local Shell Stresses

3.9.2-7 Computation Spreadsheet for the (DW + 0.5*g* axial + 0.5*g* vertical + 0.5*g* trans.) Transfer Load, Bottom Trunnion – Local Shell Stresses

3.9.2-8 NUHOMS®-OS187H Transfer Cask Local Shell Stresses and Allowables

LIST OF FIGURES

3.9.2-1 NUHOMS®-OS187H Transfer Cask Key Components and Dimensions

3.9.2-2 2-Dimensional Finite Element Model, Element Plot

3.9.2-3 3-Dimensional Finite Element Model, Element Plot

3.9.2-3A Cask Top Cover/Flange/Bolt Model

3.9.2-3B Cask Bottom Ram Access/Cover/Bolt Model

3.9.2-3C Cask Top Cover/Flange Contac52 Element Representation

3.9.2-3D Cask Shell/Lead Contac52 Element Representation

3.9.2.3E Cask Bottom Access/Shell/Flange/Lead Contac52 Element Representation

3.9.2-4 115°F Ambient Temperature Distribution

3.9.2-5 -20°F Ambient Temperature Distribution

3.9.2-6 6g Lifting Boundary Conditions

3.9.2-7 30 psi Internal Pressure Boundary Conditions

3.9.2-8 Transfer Loads Boundary Conditions

3.9.2-9 75*g* Bottom End Drop Boundary Conditions

3.9.2-10 75*g* Top End Drop Boundary Conditions

3.9.2-11 75*g* Side Drop Boundary Conditions

3.9.2-12 Local Trunnion Stress Computation Sheet

3.9.2 OS187H TRANSFER CASK BODY STRUCTURAL ANALYSIS

3.9.2.1 Introduction

This appendix presents the structural analyses of the NUHOMS®-OS187H Transfer Cask body including the top cover, cylindrical shell assembly, bottom assembly, and the local stresses at the trunnion/cask body interface. The specific methods, models, and assumptions used to analyze the cask body for the various individual loading conditions specified in 10CFR72 [1] are described. The maximum stresses in each of the major components of the transfer cask are reported for each load case and load combination in Section 3.9.2.2.4. The results are evaluated against the ASME Code [2] design criteria described in Section 3.9.2.1.3.

The OS187H transfer cask body structural analyses generally use static linear elastic methods. The stresses and deformations due to the applied loads are generally determined using the ANSYS [4] computer program.

Other components associate with the transfer cask are described and analyzed in the following Appendices:

Appendix 3.9.3 – OS187H transfer cask top cover and RAM access cover bolt analyses
Appendix 3.9.4 – OS187H transfer cask lead slump and inner shell buckling analyses
Appendix 3.9.5 – OS187H transfer cask trunnion analysis
Appendix 3.9.6 – OS187H transfer cask shield shell panel structural analyses

The analysis methods described in this appendix and used to evaluate the cask body for the loading conditions are:

ANSYS Analysis
- Axisymmetric and
- Asymmetric Loads

3.9.2.1.1 OS187H Transfer Cask Geometry Description

Key dimensions of the transfer cask are shown in Figure 3.9.2-1. The shell, or cask body cylinder assembly, is an open ended (at the top) cylindrical unit with an integral closed bottom end. This assembly consists of concentric inner shell (SA-240, Type 304) and an outer shell (SA-240, Type 304) welded to a massive closure flange (SA-182, Type F304N) at the top and bottom ends. The annulus between the shells is filled with lead shielding. The lead is poured into the annulus in a molten state using a carefully controlled procedure. The top cover is bolted to the top flange by 24-1 1/2 in. diameter high strength bolts and sealed with O-ring. A cover plate is provided to seal the bottom hydraulic ram access penetration of the cask (by 12-1/2 in. high strength bolt with O-ring) during fuel loading and transferring the canister to the ISFSI.

Two lifting trunnions are provided for handling the transfer cask in the plant's fuel/reactor building using a lifting yoke and an overhead crane. Lower support trunnions are provided on the cask for pivoting the transfer cask from/to the vertical and horizontal positions on the support skid/transport trailer.

The overall dimensions of the OS187H transfer cask are 197.07 inches long and 92.20 inches in diameter. The transfer cask structural shell is 82.70 inches in diameter. The transfer cask cavity is 186.60 inches long and 70.50 inches in diameter. A detailed physical description of the transfer cask is provided in Chapter One. Chapter One also contains reference drawings of the NUHOMS®-OS187H cask which are the source of dimensions and other information used to develop analysis models.

The gross weight of the loaded transfer cask is 114.3 tons (228.68 kips) including a maximum payload of 54.4 tons (108.76 kips). Sections 3.9.2.1.2 and Figure 3.9.2-1 summarize the component weights and key dimensions of the NUHOMS®-OS187H transfer cask.

This appendix evaluates the structural integrity of the OS187H Transfer Cask main structural members during all normal and hypothetical accident condition loadings.

3.9.2.1.2 Transfer Cask Component Weights

The following tables summarize the component weights of the NUHOMS®-OS187H Transfer Cask as well as the dry loaded NUHOMS®-DSC weight, that are used for the transfer cask structural evaluation.

OS-187H Transfer Cask Component Weights

Transfer Cask Component	Weight (lb. x 1000)
Structural Shell	20.85
Inner Shell	5.86
Lead Gamma Shield	62.37
Top Flange	3.18
Bottom Flange	3.37
Top Cover	5.20
Bottom Assembly	3.46
Neutron Shield Panel (including water)	12.75
Upper Trunnions (2)	1.61
Lower Trunnions (2)	1.27
Total Transfer Cask Weight	**119.92**

Dry Loaded 32PTH DSC Weight

Transfer Cask Payload	Weight (lb. x 1000)	Weight Used for Analysis (lb. x 1000)
32PTH Canister	28.19	
32PTH Basket	29.85	
Fuel Assemblies (32)	50.72	
Total 32PTH DSC Weight	**108.76**	**115.00**

3.9.2.1.3 Stress Criteria

The resulting stresses are compared with the allowable stresses set forth by ASME B&PV Code, Section III, Subsection NC [2] for normal conditions and ASME B&PV Code, Section III, Appendix F [3] for accident conditions. The allowable stresses for both normal and accident conditions are summarized in the following table.

Service Level	Stress Category	Stress Criteria
A (Normal Conditions)	Primary Membrane Stress, P_m	S_m
	Primary Membrane + Bending Stress, $P_m + P_b$	$1.5\ S_m$
	Primary + Secondary Stress, $P_m + P_b + Q$	$3\ S_m$
D (Accident Conditions)	Primary Membrane Stress, P_m	Lesser of $2.4\ S_m$ or $0.7\ S_u$
	Primary Local Membrane Stress, P_L	150% of P_m Stress Limit
	Primary Membrane + Bending Stress, $P_m + P_b$	Lesser of $3.6\ S_m$ or S_u

3.9.2.1.4 Material Properties

The NUHOMS®-OS187H Transfer Cask is primarily constructed from SA-240 Type 304 stainless steel. The top cover is constructed to SA-240 Type XM-19. SA-540 Grade B24 Class 1 is used for the top cover and bottom cover bolts. Chemical lead is used for radial gamma shielding, Vyal B [5] resin material is used for the solid axial neutron shielding, and liquid water is used for radial neutron shielding.

Since various temperature distributions are applied to the transfer cask model, temperature dependent Modulus of Elasticity, E, and Coefficient of Thermal Expansion, α, are used to model each material. The following material properties are used in the transfer cask model.

Transfer Cask Body (SA-240, type 304 Stainless Steel)

Temperature	Modulus of Elasticity, E (psi) [6]	Coefficient of Thermal Expansion, α (in./in.°F) [6]	Density, ρ (lb. /in^3.) [7]	Poisson's ratio, ν [7]
70° F	28.3×10^6	8.5×10^{-6}	0.29	0.3
200° F	27.6×10^6	8.9×10^{-6}	0.29	0.3
300° F	27.0×10^6	9.2×10^{-6}	0.29	0.3
400° F	26.5×10^6	9.5×10^{-6}	0.29	0.3
500° F	25.8×10^6	9.7×10^{-6}	0.29	0.3
600° F	25.3×10^6	9.8×10^{-6}	0.29	0.3

Top Cover (SA-240, type XM-19 Stainless Steel)

Temperature	Modulus of Elasticity, E (psi) [6]	Coefficient of Thermal Expansion, α (in./in.°F) [6]	Density, ρ (lb. /in^3.) [7]	Poisson's ratio, ν [7]
70° F	28.3×10^6	8.2×10^{-6}	0.29	0.3
200° F	27.6×10^6	8.5×10^{-6}	0.29	0.3
300° F	27.0×10^6	8.8×10^{-6}	0.29	0.3
400° F	26.5×10^6	8.9×10^{-6}	0.29	0.3
500° F	25.8×10^6	9.1×10^{-6}	0.29	0.3
600° F	25.3×10^6	9.2×10^{-6}	0.29	0.3

Top Cover Bolts and RAM Access Cover Bolts (SA-540 Grade B24 Class 1)

Temperature	Modulus of Elasticity, E (psi) [6]	Coefficient of Thermal Expansion, α (in./in.°F) [6]	Density, ρ (lb. /in^3.) [7]	Poisson's ratio, ν [7]
70° F	27.8×10^6	6.4×10^{-6}	0.29	0.3
200° F	27.1×10^6	6.7×10^{-6}	0.29	0.3
300° F	26.7×10^6	6.9×10^{-6}	0.29	0.3
400° F	26.1×10^6	7.1×10^{-6}	0.29	0.3
500° F	25.7×10^6	7.3×10^{-6}	0.29	0.3
600° F	25.2×10^6	7.4×10^{-6}	0.29	0.3

Gamma Shield (ASTM B-29, Chemical Lead)

Temperature	Modulus of Elasticity, E (psi) [8]	Coefficient of Thermal Expansion, α (in./in.°F) [8]	Density, ρ (lb. /in^3.) [7]	Poisson's ratio, ν [7]
70° F	2.35×10^6	16.21×10^{-6}	0.41	0.45
200° F	2.28×10^6	16.70×10^{-6}	0.41	0.45
300° F	2.06×10^6	17.34×10^{-6}	0.41	0.45
400° F	$1.92\times10^{6*}$	$18.12\times10^{-6*}$	0.41	0.45

*Extrapolated from available Reference 8 Data.

The resin material properties used to model the bottom neutron shield plate for the axisymmetric load cases are taken from available data in References 5 and 12 and are as follows.

Temperature	Modulus of Elasticity, E (psi) [12]	Coefficient of Thermal Expansion, α (in./in.°F)	Density, ρ (lb. /in^3.) [5]	Poisson's ratio, ν [5]
Room Temperature	0.16×10^6	-*	0.065	0.20

* The coefficient of thermal expansion for the resin material is not used in the finite element model. The resin material is not a structural component, and since the resin has a very low Modulus of Elasticity (relative to stainless steel) it's thermal expansion is not expected to affect the stresses in the structural components significantly.

3.9.2.2 ANSYS Analysis

3.9.2.2.1 Geometry Description

The top cover, inner shell, structural shell, and bottom assembly are the primary structural members of the cask. Key components and dimensions of the confinement vessel are shown in Figure 3.9.2-1. Chapter 1 contains reference drawings of the NUHOMS®-OS187H transfer cask which are the source of dimensions and other information used to develop analysis models.

3.9.2.2.2 Allowable Stresses

Allowable stresses are based on the material properties of each component taken at their corresponding maximum temperatures. Based on the 115°F hot ambient thermal analysis performed in Chapter 4, and shown in Figure 3.9.2-4, the maximum temperatures of the various transfer cask components are as shown in the following table.

Transfer Cask Component	Maximum Temperature	Temperature Used to Compute Allowable Stress
Structural Shell*	280	300° F
Top Cover	196	300° F
Inner Shell	340	400° F
Bottom End Plates**	216	300° F
RAM access and Cover	197	200° F

* Includes outer structural shell and top and bottom flanges.
** Includes Bottom End Plate and Bottom Neutron Shield Plate

The NUHOMS®-OS187H transfer cask is broken down into 5 major components for ease of stress evaluation as seen in the table above. The above table also lists the temperatures used to determine the allowable stress for each major component. The temperature chosen for each component is conservatively higher than the maximum temperature experienced during the 115° F hot ambient condition.

The following transfer cask component allowable stresses are computed based on the stress criteria and component temperatures described above, and the material properties provided in Reference 6.

Transfer Cask Component	Service Level	Stress Category	Allowable Stress
Structural Shell*	A	P_m	20.00
		$(P_m \text{ or } P_L) + P_b$	30.00
		$P_L + P_b + Q$	60.00
	D	P_m	46.34
		P_L	66.20
		$(P_m \text{ or } P_L) + P_b$	66.20
Top Cover	A	P_m	31.40
		$(P_m \text{ or } P_L) + P_b$	47.10
		$P_L + P_b + Q$	94.20
	D	P_m	65.94
		P_L	94.20
		$(P_m \text{ or } P_L) + P_b$	94.20
Inner Shell	A	P_m	18.70
		$(P_m \text{ or } P_L) + P_b$	28.05
		$P_L + P_b + Q$	56.10
	D	P_m	44.80
		P_L	64.00
		$(P_m \text{ or } P_L) + P_b$	64.00
Bottom End Plates**	A	P_m	20.00
		$(P_m \text{ or } P_L) + P_b$	30.00
		$P_L + P_b + Q$	60.00
	D	P_m	46.34
		P_L	66.20
		$(P_m \text{ or } P_L) + P_b$	66.20
RAM access and Cover	A	P_m	20.00
		$(P_m \text{ or } P_L) + P_b$	30.00
		$P_L + P_b + Q$	60.00
	D	P_m	48.00
		P_L	71.00
		$(P_m \text{ or } P_L) + P_b$	71.00

* Includes outer structural shell and top and bottom flanges.
** Includes Bottom End Plate and Bottom Neutron Shield Plate

3.9.2.2.3 ANSYS Cask Finite Element Models

Two separate FEMs were constructed. The first is a 2-dimensional, axisymmetric representation of the cask, which is constructed with plane elements. The second model is a 180°, 3-dimensional "brick" element representation.

3.9.2.2.3A 2-Dimensional Finite Element Model Description

A 2-dimensional axisymmetric ANSYS [4] finite element model, constructed primarily from PLANE42 elements, is used to analyze all axisymmetric load cases. The Basic dimensions of the transfer cask are provided in Figure 3.9.2-1. An element plot of the 2-dimensional FEM is shown in Figure 3.9.2-2.

Model Material Properties

The elastic material properties listed above are used to model the transfer cask materials. For all load cases, except for the -20° F Ambient load cases, the temperature distribution for the 115° F Ambient condition is applied to the finite element model. Figure 3.9.2-4 shows the 115° F ambient temperature distribution as applied to the 2-dimensional model. The 115° F Ambient temperature distribution is used to determine the appropriate temperature dependent material property to be used at each node. However, non-zero coefficients of thermal expansion are used only in the load cases where thermal stresses are to be evaluated. For all other load cases, all material coefficients of thermal expansion are set to zero, so that no thermal stresses are induced.

Unmodeled Components

Only the structural steel section of the top cover (3 in. thick.) is modeled. The top neutron shield resin, the ¼ in. thickness top cover outer plate, and hoist ring standoffs are not modeled since they are not intended to provide any structural support. However, their inertial load is accounted for by increasing the density of the structural portion of the top cover. The weight of the unmodeled portion of the top cover assembly is as follows.

Weight of unmodeled top cover components = 678 lb. (resin) + 422 lb. (1/4" top cover outer plate) + 20 lb. (standoffs) = 1,120 lb.

The volume and weight of the structural steel portion of the top cover is 14,051 in.^{3} and 4,075 lb. respectively. Therefore the density of the top cover, ρ_l, is increased as follow.

$$\rho_l = [1{,}120 \text{ lb.} + 4{,}075 \text{ lb.}] / 14{,}051 \text{ in.}^3 = 0.37 \text{ lb./in.}^3$$

For conservatism, the density of the top cover used in this analysis is increased to 0.38 lb./in.^{3}

The radial neutron shield (water) and neutron shield panel are also not modeled, because they are not considered structural components of the transfer cask. Therefore, the density of the structural shell of the transfer cask is increased to account for the unmodeled components. The weight of

the unmodeled radial neutron shield assembly is 12,746 lb.

The volume and weight of the structural shell is 71,895 in.^{3} and 20,850 lb. respectively. Therefore the density of the structural shell, ρ_s, is increased as follow.

$$\rho_l = [12{,}746 \text{ lb.} + 20{,}850 \text{ lb.}] / 71{,}895 \text{ in.}^3 = 0.47 \text{ lb./in.}^3$$

For conservatism, the density of the structural shell used in this analysis is increased to 0.49 lb./in.^{3}

Top Cover and RAM Access Cover Bolts

The top cover and RAM access cover bolts are modeled with axisymmetric BEAM3 elements, and are only used in the model to simulate the overall behavior of the closure joints. The stresses in the top cover and RAM access cover bolts are evaluated separately in Appendix 3.9.3. The element real constants are computed in the following way for the top cover and RAM access cover bolts.

Top Cover Bolts

There are 24, 1½ in - 8UN 2A bolts used to mount the transfer cask top cover to the flange. However, the size used to model the transfer cask top cover bolts is 1½ in. - 10UN 2A bolts, which have a negligible difference in geometry relative to that of the 1½ in - 8UN 2A bolts. The bolt diameter used for stress analysis, D_{tc}, is computed using formulae given in Table 5.1 of Reference 9, as follows.

$$D_{tc} = 1.50 - 0.9743(1/10) = 1.403 \text{ in.}$$

The total tensile stress area for all 24 top cover bolts, A_{tc2d}, is computed as follows.

$$A_{tc2d} = (\pi/4) \times 1.403^2 \times 24 \text{ bolts} = 1.546 \times 24 \text{ bolts} = 37.104 \text{ in.}^2$$

The total moment of inertia of all 24 top cover bolts, I_{tc2d}, is,

$$I_{tc2d} = (\pi/64) \times 1.403^4 \times 24 \text{ bolts} = 4.565 \text{ in.}^4$$

The total height of the top cover bolts, H_{tc2d}, is computed assuming the following equivalent height method.

$$H_{tc2d} = \sqrt{A_{tc2d}} = \sqrt{1.546} = 1.243 \text{ in.}$$

RAM Access Cover Bolts

There are 12, ½ in - 13UNC 2A bolts used to mount the transfer cask RAM access cover to the bottom of the cask. The bolt diameter used for stress analysis, D_{ra}, is computed as follows.

$$D_{ra} = 0.50 - 0.9743(1/13) = 0.425 \text{ in.}$$

The total tensile stress area for all 12 RAM access cover bolts, A_{ra2d}, is computed as follows.

$$A_{ra2d} = (\pi/4) \times 0.425^2 \times 12 \text{ bolts} = 0.142 \times 12 \text{ bolts} = 1.704 \text{ in.}^2$$

The total moment of inertia of all 12 RAM access cover bolts, I_{ra2d}, is,

$$I_{ra2d} = (\pi/64) \times 0.425^4 \times 12 \text{ bolts} = 0.01922 \text{ in.}^4$$

The height of the RAM access cover bolts, H_{ra2d}, used in the model is,

$$H_{ra2d} = \sqrt{0.142} = 0.3768 \text{ in.}$$

For both the top cover bolts and the RAM access cover bolts, a bolt preload stress of 25,000 psi. is used. This bolt preload stress is applied to the model by placing an initial strain in the beam elements that are used to model the bolts.

Contact Elements

CONTAC12 elements are placed between all surfaces of the top flange and top cover, between the RAM access cover and RAM access penetration that contact each other, and between the lead gamma shielding and the inner and structural shells. These contact elements are used to model the reaction forces that occur between these surfaces.

The contact elements introduce nonlinearities in the analysis depending whether they are open or closed. Initially, at all contact surfaces, the gaps are closed. The contact element spring constant, K_n, is calculated in the following way.

$$K_n = f E h \text{ [4]}$$

Where,

f = A factor usually between 0.01 to 100.
E = Modulus of elasticity (27.0×10^6 psi for SA-240, type 304 @ 300°F)
h = contact target length (i.e., the square root of target area).
Typical element length $\approx$ 1/2 in.
Typical element width $\approx$ 1 in.
Typical target length, $h = (0.5 \times 1.0)^{0.5} = 1.22$ in.

Therefore,

$$K_n = 27.0\times10^6 \times 1.22 \times f \approx 3.29\times10^5 \text{ to } 3.29\times10^9 \text{ lb./in}$$

Thus, there is very wide range for K_n value. For the 2-D finite element model, the structure responded well with a spring constant value of 1.0×10^6 lb/in. for the lead shield contact elements and 1.0×10^7 lb/in. for the top cover and RAM access cover contact elements.

Boundary Conditions

Separate sets of boundary conditions are required for the various loading cases analyzed. The boundary condition sets are used to prevent rigid body motion and are assigned based on the specific loading configuration. In each of the boundary condition sets, displacement constraints are fixed such that no displacement is permitted in the prescribed direction.

3.9.2.2.3B 3-Dimensional Finite Element Model Description

A 3-dimensional axisymmetric ANSYS [4] finite element model, constructed primarily from SOLID45 elements, is used to analyze all non-axisymmetric load cases. The 3-dimensional model represents 180° of the full 360° cask, or a half model. An element plot of the 3-dimensional FEM is shown in Figures 3.9.2-3, 3A, 3B, 3C, 3D, and 3E.

Model Material Properties

The elastic material properties listed in the material properties section are used to model the transfer cask materials. As in the 2-dimensional finite element model, the temperature distribution for the 115° F Ambient condition is applied to the finite element model unless otherwise stated. The 115° F Ambient temperature distribution however, is used to determine the appropriate temperature dependent material property to be used at each node. But, material coefficients of thermal expansion are only used for thermal stress load cases.

Modeled Component Weights

Only the structural steel section of the top cover is modeled. The top neutron shield resin, top cover outer plate (1/4" thick.), and hoist ring standoffs are not modeled since they are not intended to provide any structural support. However, their inertial load is accounted for by increasing the density of the structural portion of the top cover. The weight of the unmodeled portion of the top cover assembly is as follows.

Weight of unmodeled top cover components = 678 lb. (resin) + 422 lb. (top cover outer plate) + 20 lb. (standoffs) = 1,120 lb.

The volume and weight of the structural steel portion of the lid are 14,051 in.^{3} and 4,075 lb. respectively. Therefore the density of the top cover, ρ_l, is increased as follow.

$$\rho_l = [1{,}120 \text{ lb.} + 4{,}075 \text{ lb.}] / 14{,}051 \text{ in.}^3 = 0.37 \text{ lb./in.}^3$$

For conservatism, the density of the unmodeled top cover components used in this analysis is increased 0.38 lb./in.^{3}

The radial neutron shield (water) and shield panel are not modeled, because they are not considered structural components of the transfer cask. Therefore, the density of the structural shell of the transfer cask is increased to account for the unmodeled components. The weight of the unmodeled radial neutron shield assembly is 12,746 lb.

The volume and weight of the structural shell are 71,895 in.^{3} and 20,850 lb. respectively. Therefore the density of the structural shell, ρ_s, is increased as follow.

$$\rho_s = [12{,}746 \text{ lb.} + 20{,}850 \text{ lb.}] / 71{,}895 \text{ in.}^3 = 0.47 \text{ lb./in.}^3$$

For conservatism, the density of the structural shell used in this analysis is increased to 0.53 lb./in.^{3}

The bottom neutron shield (resin) is also not modeled, because it is not considered a structural component for the non-axisymmetric load cases. Therefore, the density of the bottom end plate, bottom neutron shield plate, and the bottom flange is increased to account for the unmodeled component. The weight of the unmodeled bottom neutron shield is 551 lb.

The volume and weight of the bottom end plate, bottom neutron shield plate, and the bottom flange are 19,871 in.^{3} and 5,763 lb. respectively. Therefore the density of the cask bottom components, ρ_b, is increased as follow.

$$\rho_b = [5{,}763 \text{ lb.} + 551 \text{ lb.}] / 19{,}871 \text{ in.}^3 = 0.318 \text{ lb./in.}^3$$

For conservatism, the density of the bottom components used in this analysis is increased to 0.32 lb./in.^{3}

Top Cover and RAM Access Cover Bolts

The top cover and RAM access cover bolts are modeled with BEAM4 elements, and are only used in the model to simulate the overall behavior of the closure joints. The stresses in the top cover and RAM access cover bolts are evaluated separately in Appendix 3.9.3. The element real constants are computed in the following way for the top cover and RAM access cover bolts.

Top Cover Bolts

There are 24, 1½ in - 8UN 2A bolts used to mount the transfer cask top cover to the cask flange. However, the size used to model the transfer cask top cover bolts is 1½ in. - 10UN 2A bolts, which have a negligible difference in geometry relative to that of the 1½ in - 8UN 2A bolts. The bolt diameter used for stress analysis, computed above, is D_{tc} = 1.403 in. The tensile stress area for a single top cover bolt, A_{tc3d}, is computed as follows.

$$A_{tc3d} = (\pi/4) \times 1.403^2 = 1.546 \text{ in.}^2$$

The moment of inertia for a single top cover bolt, I_{tc3d}, is,

$$I_{tc3d} = (\pi/64) \times 1.403^4 = 0.190 \text{ in.}^4$$

The height for a single top cover bolt, H_{tc3d}, is computed assuming the following equivalent height method.

$$H_{tc3d} = \sqrt{A_{tc3d}} = \sqrt{1.546} = 1.243 \text{ in.}$$

RAM Access Cover Bolts

There are 12, ½ in - 13UNC 2A bolts used to mount the transfer cask RAM access cover to the bottom of the cask. The bolt diameter used for stress analysis, computed above is $D_{ra} = 0.425$ in.

The tensile stress area for a single RAM access cover bolt, A_{ra3d}, is computed as follows.

$$A_{ra3d} = (\pi/4) \times 0.425^2 = 0.142 \text{ in.}^2$$

The moment of inertia for a single RAM access cover bolt, I_{ra3d}, is,

$$I_{ra3d} = (\pi/64) \times 0.425^4 = 0.00160 \text{ in.}^4$$

The height for a single RAM access cover bolt, H_{ra3d}, is,

$$H_{ra3d} = \sqrt{0.142} = 0.3768 \text{ in.}$$

The top cover bolt and RAM access cover bolt preload strain, ε_b, used in the finite element model, is the same as that used in the 2-dimensional model. Again, the preload strain is applied to the model bolt elements to simulate a preload stress of 25,000 psi, due to the applied preload torque.

Contact Elements

CONTAC52 elements are placed between all surfaces of the top flange and top cover, between the RAM access cover and RAM access penetration that contact each other, and between the lead gamma shielding and the inner and structural shells. These contact elements are used to model the reaction forces that occur between closure surfaces. LINK8 elements with a very low Modulus of Elasticity and density are placed in all locations where CONTAC52 elements exist in order to maintain overall stability of the model. This is only required in the 3-dimensional model.

The contact elements introduce nonlinearities in the analysis depending whether they are open or closed. Initially, at all contact surfaces, the gaps are closed. The contact element spring constant, K_n, is calculated in the following way.

$$K_n = f E h \text{ [4]}$$

Where,

f = A factor usually between 0.01 to 100.
E = Modulus of elasticity (27.0×10^6 psi for SA-240, type 304 @ 300°F)
h = contact target length (i.e., the square root of target area).
Typical element length $\approx$ 1/2 in.
Typical element width $\approx$ 1 in.
Typical target length, $h = (0.5 \times 1.0)^{0.5} = 1.22$ in.

Therefore,

$$K_n = 25.8\times10^6 \times 1.22 \times f \approx 3.39\times10^5 \text{ to } 3.39\times10^9 \text{ lb./in}$$

Thus, there is very wide range for K_n value. For the 3-D finite element model, the structure responded well with a spring constant value of 1.0×10^7 lb/in. for the lead shield contact elements and 1.0×10^8 lb/in. for the top cover and RAM access cover contact elements.

3.9.2.2.4 Load Cases

The following two tables describe the normal (Level A) and accident (Level D) condition load cases analyzed in this calculation. The load cases considered consist of 115° F hot ambient and -20° F cold ambient environments, 30 psig internal, vacuum drying conditions, transfer loads, and 75g accident condition end and side drops. The normal and accident load conditions are summarized in the following table.

Summary of Normal and Accident Load Conditions

Load Case Number	Loading Condition	Service Level	Applied Load
1	6*g* Vertical Lifting	A	Cask vertical, supported at top trunnions, 6*g* vertical accel. + 30 psi. internal pressure.
1A	6*g* Vertical Lifting + Thermal Loads	A	Cask vertical, supported at top trunnions, 6*g* vertical accel. + 30 psi. internal pressure + 115° F ambient.
2	Vacuum Drying	A	Cask vertical, supported at cask bottom, 15 psi. external pressure + vacuum drying thermal loads
3	30 psi. Internal Pressure	A	30 psi. internal pressure
4	115°F Ambient Hot Thermal Environment	A	115° F ambient environment
5	-20°F Ambient Cold Thermal Environment	A	-20° F ambient environment
6	Transfer Inertial Loads (2*g* Vertical + 2*g* Transverse + 2*g* Axial)	A	Cask horizontal, supported at top and bottom trunnions, 2*g* acceleration in all directions
6A	Transfer Loads + Internal Pressure	A	Cask horizontal, supported at top and bottom trunnions, 2*g* acceleration in all directions + 30 psi. internal pressure
6B	Transfer Loads + 115° F Ambient + Internal Pressure	A	Cask horizontal, supported at top and bottom trunnions, 2*g* acceleration in all directions +30 psi. internal pressure + 115° F ambient
6C	Transfer Loads + -20° F Ambient + Internal Pressure	A	Cask horizontal, supported at top and bottom trunnions, 2*g* acceleration in all directions + 30 psi internal pressure + -20° F ambient
7	75*g* Bottom End Drop + Internal Pressure	D	Cask vertical, supported at bottom, 75*g* vertical up acceleration + 30 psi. internal pressure
8	75*g* Top End Drop + Internal Pressure	D	Cask vertical, supported at top, 75*g* vertical down acceleration + 30 psi. internal pressure
9	75*g* Side Drop + Internal Pressure	D	Cask horizontal, supported on side, 75*g* transverse acceleration + 30 psi. internal pressure
10	Transfer Thermal Accident (Fire)	D	30 psi. internal pressure + thermal accident loads

Method of Applying Load to the Cask Body

Pressures applied in the axial direction are calculated based on load divided by pressure area calculation. For example, to calculate the pressure applied due to internal loading on the inner surface of the bottom transfer cask due to an end drop on the bottom end, divide the total applied load by the cross-sectional area of the inner surface of the bottom transfer cask.

Pressures applied in the radial direction in the 3-dimensional finite element model are based on cosine distributed pressure functions. These pressure distributions simulate the internal cask contents applying pressure to the inner cask wall. The pressure distribution is assumed to be in the longitudinal direction over a specified length and vary with a cosine distribution around the circumference of the cask.

The following sections describe the boundary conditions used for each individual load case and load combination.

Load Case 1: 6g Lifting (3-D FEM)

The 6*g* Lifting Load case consists of the loaded transfer cask in the vertical position, supported by the top two trunnions. A 6*g* vertical acceleration is conservatively used to bound the normal lifting load. An internal pressure of 30 psi. is also conservatively applied to the model to bound any possible pressure build up inside the cask.

The weight of the transfer cask internals (canister, basket, and fuel assemblies) is accounted for by applying equivalent pressures. The weight of the cask internals used in this analysis is 115,000 lb. The transfer cask inner radius is 35.25 in., and the inner radius of the ram access penetration is 10.00 in. The inertial load of the transfer cask internals reacts against the annular surface bounded by these two radii during a lifting. Therefore the area of the reaction surface, A_{6gi}, is as follows.

$$A_{6gl} = \pi(35.25^2 - 10.00^2) = 3{,}589.47 \text{ in}^2.$$

The pressure equivalent to the inertial load of the internals during a 6*g* lift, P_{6gi}, is,

$$P_{6gl} = [115{,}000 / 3{,}589.47] \times 6\ gs = 192.229 \text{ psi}.$$

Symmetry displacement boundary conditions are applied along the y-axis of the 3-dimensionsal axisymmetric model.

A depiction of the 6*g* Lifting load case boundary conditions is provided in Figure 3.9.2-6.

Load Case 2: Vacuum Drying

The stresses generated during the vacuum drying process are computed by hand in the following way.

The applied loads used to calculate the maximum stress in the transfer cask during vacuum drying include a 15 psi external pressure, a maximum radial temperature gradient, and a 1*g* axial (gravity) load. The stresses generated in the transfer cask shell by these three loads are computed using hand calculations. Since the primary load during vacuum drying is caused by the radial temperature gradient, the maximum transfer cask stress is computed for the outer radial structural shell.

A uniform 15 psi pressure is applied to the external radial surface of the cask, generating a hoop stress in the cask structural shell. The hoop stress, σ_p, in the shell is computed in the following way.

σ_p = external pressure × the mean structural shell radius / the minimum structural shell thickness
= 15 psi × (78.70 + 1.50)/2 in. / 1.50 in. = 401 psi.

The stress generated in the structural shell by the 1g axial load is conservatively computed assuming that the weight of the entire transfer cask is taken by the cross sectional area of the structural shell. The weight of the transfer cask is conservatively taken to be 250,000 lb., which is higher than the actual weight (119,920 lb.). The 1*g* axial stress in the structural shell, σ_g, is computed as follows.

σ_g = 1g × maximum transfer cask weight / minimum cross sectional area of the structural shell
= 1g × 250,000 / [$(\pi/4)\times(81.70^2 - 78.70^2)$] = 661 psi.

The maximum hoop stress generated by the radial thermal gradient during the vacuum drying process will occur in the outer structural shell due to the thermal expansion of the lead gamma shield. From Chapter 4, the maximum temperature difference between the lead gamma shield and the structural shell occurs during the drying process C at 42 hours, when the lead and structural shell are at 271° F and 217° F, respectively.

The change in the outer radius of the lead gamma shield, ΔR_l, is computed as follows.

$\Delta R_l = R_l \times \alpha_l \times \Delta T_l$ = 39.35 in. × 17.34 ×10^{-6} in./in.°F (@300 °F) × (271 – 70)°F
= 0.1372 in.

The change in the inner radius of the structural shell, ΔR_s, is computed as follows.

$\Delta R_s = R_s \times \alpha_s \times \Delta T_s$ = 39.35 in. × 9.2 ×10^{-6} in./in.°F (@300 °F) × (217 – 70)°F
= 0.0532 in.

Therefore the differential radial expansion between the lead and structural shell, ΔR, is as follows.

$$\Delta R = 0.1372 \text{ in.} - 0.0532 \text{ in.} = 0.084 \text{ in.}$$

Therefore, the lead cylinder, if it were free, would grow 0.084 in. more than the inner surface of the structural shell. If all of the differential expansion is accommodated in the lead, the lead strain, ε_l, would be the following.

$$\varepsilon_l = \Delta R / R_l = 0.084 \text{ in.} / 39.35 \text{ in.} = 0.00213 \text{ in./in.}$$

If the lead remained linear elastic, the maximum hoop stress in the lead would be,

$$\sigma_l = E_l \times \varepsilon_l = 2.06 \times 10^6 \text{ psi. (@300°F)} \times 0.00213 \text{ in./in.} = 4{,}388 \text{ psi.}$$

Conservatively assuming that the lead remains linear elastic, the interference pressure on the outer structural shell required to exert an average hoop stress of 4,388 psi. in the lead can be determined in the following way.

$$P_{interface} = \sigma_l \times \text{lead thickness} / R_{interface} = 4{,}388 \text{ psi.} \times 3.60 \text{ in.} / 39.35 \text{ in.} = 401 \text{ psi.}$$

This interference pressure would generate the following hoop stress in the structural shell.

$$\sigma_s = P_{interface} \times R_{interface} / t_s = 401 \text{ psi.} \times 39.35 / 1.50 = 10{,}520 \text{ psi.}$$

The total combine maximum stress intensity, σ, in the transfer cask during vacuum drying operations is then,

$$\sigma = 401 \text{ psi.} + 661 \text{ psi.} + 10{,}520 \text{ psi.} = 11{,}582 \text{ psi.}$$

Load Case 3: 30 psi Internal Pressure (2-D FEM)

A uniform 30 psi pressure is applied to all internal surfaces of the transfer cask up to the top cover and RAM access cover seal locations. Symmetry displacement boundary conditions are applied along the *y*-axis of the 2-dimensionsal axisymmetric model, and transfer cask is held in the *y*-direction at one location to prevent rigid body motion. A depiction of the Internal Pressure load case boundary conditions is provided in Figure 3.9.2-7.

Load Case 4: 115 °F Ambient Hot Thermal Environment (2-D FEM)

The temperature distribution resulting from a 115°F Ambient Environment, shown in Figure 3.9.2-4, is computed in Chapter 4, and is applied to all nodes of the transfer cask model. An ANSYS macro is used to assign each node of the transfer cask model to a node in the ANSYS thermal model (described in Chapter 4) that is closest to that node. The macro then applies these nodal temperatures to the transfer cask model. The temperature dependant coefficients of thermal expansion are applied to each of the corresponding material types, in order to induce thermal stresses in the model.

Symmetry displacement boundary conditions are applied along the *y*-axis of the 2-dimensionsal axisymmetric model, and transfer cask is held in the *y*-direction at one location to prevent rigid body motion.

Load Case 5: -20 °F Ambient Cold Thermal Environment (2-D FEM)

The temperature distribution resulting from a -20° F Ambient Environment, shown in Figure 3.9.2-5, is computed in Chapter 4, and is applied to all nodes of the transfer cask model. Again, an ANSYS macro is used to assign each node of the transfer cask model to a node in the ANSYS thermal model (described in Chapter 4) that is closest to that node. The macro then applies these nodal temperatures to the transfer cask model. The temperature dependent coefficients of thermal expansion are applied to each corresponding material types, in order to induce thermal stresses in the model.

Symmetry displacement boundary conditions are applied along the *y*-axis of the 2-dimensionsal axisymmetric model, and transfer cask is held in the *y*-direction at one location to prevent rigid body motion.

Load Case 6: Transfer Loads (3-D FEM)

The Transfer load case consists of the loaded transfer cask in the horizontal position, supported at both top and bottom trunnions. An acceleration of 2*g* in all directions is applied to the transfer cask model in order to bound all possible transfer accelerations, and an internal pressure of 30 psi. is conservatively applied to the model to bound any possible pressure build up inside the cask.

The vertical and transverse accelerations are combined, so that a single horizontal acceleration is applied to the finite element model in the following way.

Horizontal Acceleration = [$2g^2$ transverse $+2g^2$ vertical]$^{1/2}$ = 2.828g

The horizontal inertial load of the transfer cask internals is accounted for by applying a cosine varying pressure on the inside surface of the cask inner shell. Assuming that the transfer cask internals react upon 90° arc of the inside surface, then the inertial load of the internals, $P_{(\theta)}$, which varies with angle, θ, ($\theta = 0$ is at the impact point), is governed by the following expression.

$$P_{(\theta)} = P_{max} \cos(2\theta)$$

Where P_{max} is the maximum load at the impact point ($\theta = 0$). Assuming the axial length of the applied load is L, the inside radius of the cask inner shell is R, and the load distribution, $P_{(\theta)}$ above, then the total inertial load generated by the internals, F, is the following.

$$F = \int_{\frac{-\pi}{4}}^{\frac{\pi}{4}} P_{\max} \cos(2\theta)\cos(\theta) LR d\theta$$

or,

$$F = \frac{P_{\max} LR}{2} \int_{\frac{-\pi}{4}}^{\frac{\pi}{4}} \cos((2+1)\theta) + \cos((2-1)\theta) d\theta$$

By integrating we get the following.

$$F = \left[\frac{P_{\max} LR}{2}\right]\left[\frac{\sin(3\theta)}{3} + \sin(\theta)\right]\Bigg|_{\frac{-\pi}{4}}^{\frac{\pi}{4}}$$

Therefore,

$$F = \left[\frac{P_{\max} LR}{2}\right]\left[\frac{\sin\left(\frac{3\pi}{4}\right)}{3} + \sin\left(\frac{\pi}{4}\right) - \frac{\sin\left(\frac{-3\pi}{4}\right)}{3} - \sin\left(\frac{-\pi}{4}\right)\right]$$

$$F = P_{\max} LR\left[\frac{\sin\left(\frac{3\pi}{4}\right)}{3} + \sin\left(\frac{\pi}{4}\right)\right]$$

The transfer cask inner shell inner diameter, $R = 35.25$ in., and the axial length of the applied load, $L = 183.6$ in. The total applied force, F, is equal to the inertial load of the cask internals, which is the following.

$$F = 115{,}000 \text{ lb.} \times \sqrt{8}\, g = 325{,}269 \text{ lb.}$$

Therefore, P_{max} is the following.

$$P_{max} = \frac{325{,}269}{(183.60)(35.25)} \left[\frac{\sin\left(\frac{3\pi}{4}\right)}{3} + \sin\left(\frac{\pi}{4}\right) \right]^{-1} = 53.307 \text{ psi.}$$

The axial inertial load of the transfer cask internals is accounted for by applying a pressure on the inside surface of the cask top cover. For a 2g inertial load, the applied axial pressure, P_a, is as follows.

$$P_a = 115{,}000 \text{ lb.} \times 2g / [\, \pi \times 35.70^2 \,] = 57.444 \text{ psi}$$

Symmetry displacement boundary conditions are applied along the y-axis of the 3-dimensionsal axisymmetric model.

A depiction of the Transfer Loads load case boundary conditions is provided in Figure 3.9.2-8.

<u>Load Case 7:</u> 75g Bottom End Drop (2-D FEM)

The weight of the transfer cask internals (canister, basket, and fuel assemblies) is accounted for by applying equivalent pressures. The actual weights of the canister, basket, and fuel assemblies are 28.19 kips, 29.85 kips, and 50.72 kips, respectively. Therefore, the total actual weight of the cask internals is 108.76 kips. For conservatism, the weight of the cask internals used in this analysis is increased to 115 kips. The transfer cask inner radius is 35.25 in., and the inner radius of the ram access penetration is 10.00 in. The inertial load of the transfer cask internals reacts against the annular surface bounded by these two radii during a bottom end drop. The area of this reaction surface, A_{bi}, is as follows.

$$A_{bi} = \pi(35.25^2 - 10.00^2) = 3{,}589.47 \text{ in}^2.$$

The pressure equivalent to the inertial load of the internals under accident conditions, P_{bi}, is,

$$P_{in} = [115{,}000 / 3{,}589.47] \times 75\, gs = 2{,}403.86 \text{ psi.}$$

Symmetry displacement boundary conditions are applied along the y-axis of the 2-dimensionsal axisymmetric model. The bottom end of the transfer cask is held in the axial direction in order to simulate the rigid reaction force generated by the impact target. A 75 g inertial load in the positive y-direction is also applied to the model for the accident condition load case.

A depiction of the Bottom End Drop load case boundary conditions is provided in Figure 3.9.2-9.

Load Case 8: 75g Top End Drop (2-D FEM)

The weight of the transfer cask internals (canister, basket, and fuel assemblies) is accounted for by applying equivalent pressures. The weight of the canister internals used in this analysis is 115,000 lb. The inertial load of the transfer cask internals reacts against the inside surface of the top cover assembly during a top end drop. The outer radius of the inside surface of the transfer cask top cover assembly is 35.70 in. Therefore the area of the reaction surface, A_{bi}, is as follows.

$$A_{bi} = \pi(35.70^2) = 4{,}003.93 \text{ in}^2.$$

The pressure equivalent to the inertial load of the internals under accident conditions, P_{bi}, is,

$$P_{in} = [115{,}000 / 4{,}003.93] \times 75 \text{ gs} = 2{,}154.13 \text{ psi}.$$

Symmetry displacement boundary conditions are applied along the y-axis of the 2-dimensionsal axisymmetric model. The outer surface of the top cover is held in the axial direction in order to simulate the rigid reaction force generated by the impact target. A 75 *g* inertial load in the negative y-direction is also applied to the model for the accident condition load case.

A depiction of the Top End Drop load case boundary conditions is provided in Figure 3.9.2-10.

Load Case 9: 75g Side Drop (3-D FEM)

During the 75*g* Side Drop load case, the loaded transfer cask is dropped onto a concrete target generating a transverse acceleration of 75g.

The impact side of the transfer cask is supported in the cask radial direction along the entire length of the cask. The radial support spans 15° of the model. The radial support is intended to model the reaction of the concrete target during impact.

The inertial load of the transfer cask internals is accounted for by applying a cosine varying pressure on the inside surface of the cask inner shell using the same method that was used for the Transfer Loads case. The total applied force, *F*, is equal to the inertial load of the cask internals, which is the following.

$$F = 115{,}000 \text{ lb.} \times 75g = 8{,}625{,}000 \text{ lb.}$$

Therefore, using the formula derived for the Transfer Loads case, P_{max} is the following.

$$P_{max} = \frac{8{,}625{,}000}{(183.60)(35.25)}\left[\frac{\sin\left(\frac{3\pi}{4}\right)}{3} + \sin\left(\frac{\pi}{4}\right)\right]^{-1} = 1{,}413.53 \text{ psi.}$$

Symmetry displacement boundary conditions are applied along the y-axis of the 3-dimensionsal axisymmetric model. An internal pressure of 30 psi. is conservatively to the model to bound any possible pressure build up inside the cask.

A depiction of the 75*g* Side Drop load case boundary conditions is provided in Figure 3.9.2-11.

Load Case 10: Transfer Thermal Accident (Fire)

The stresses generated during the thermal accident are computed by hand, and use the thermal stresses generated from the Transfer Loads load case, computed with ANSYS.

The applied loads used to calculate the maximum stress in the transfer during fire accident event, include a maximum radial temperature gradient, and normal conditions transfer loads. The stresses generated in the transfer cask shell by the temperature gradient are computed using hand calculations. The resulting stresses caused by the thermal temperature gradient are added to the stresses computed for the transfer load case. Since the primary load for the fire accident is caused by the radial temperature gradient, the maximum transfer cask stress is computed for the outer radial structural shell.

The maximum stress generated by the radial thermal gradient fire accident will occur in the outer structural shell due to the thermal expansion of the lead gamma shield. From Chapter 4, the maximum temperature difference between the lead gamma shield and the structural shell occurs when the lead and structural shell are at 618° F and 553° F, respectively.

The change in the outer radius of the lead gamma shield, ΔR_l, is computed as follows.

$$\Delta R_l = R_l \times \alpha_l \times \Delta T_l = 39.35 \text{ in.} \times 19.68\times10^{-6} \text{ in./in.°F (@600°F)} \times (618 - 70)° \text{ F}$$
$$= 0.4243 \text{ in.}$$

The change in the inner radius of the structural shell, ΔR_s, is computed as follows.

$$\Delta R_s = R_s \times \alpha_s \times \Delta T_s = 39.35 \text{ in.} \times 9.8\times10^{-6} \text{ in./in.°F (@600°F)} \times (553 - 70)° \text{ F}$$
$$= 0.1863\text{in.}$$

Therefore the differential radial expansion between the lead and structural shell, ΔR, is as follows.

$$\Delta R = 0.4243 \text{ in.} - 0.1863 \text{ in.} = 0.238 \text{ in.}$$

Therefore, the lead cylinder, if it were free, would grow 0.238 in. more than the inner surface of the structural shell. If all of the differential expansion is accommodated in the lead, the lead strain, ε_l, would be the following.

$$\varepsilon_l = \Delta R/R_l = 0.238 \text{ in.} / 39.35 \text{ in.} = 0.006 \text{ in./in.}$$

If the lead remained linear elastic, the residual hoop stress in the lead would be,

$$\sigma_l = E_l \times \varepsilon_l = 1.64\times10^6 \text{ psi. (@600°F)} \times 0.006 \text{ in./in.} = 9{,}840 \text{ psi.}$$

Conservatively assuming that the lead remains linear elastic, the interference pressure on the outer structural shell required to exert an average hoop stress of 9,840 psi. in the lead can be determined in the following way.

$$P_{interface} = \sigma_l \times \text{lead thickness} / R_{interface} = 9{,}840 \text{ psi.} \times 3.60 \text{ in.} / 39.35 \text{ in.} = 900 \text{ psi.}$$

This interference pressure would generate the following hoop stress in the structural shell.

$$\sigma_s = P_{interface} \times R_{interface} / t_s = 900 \text{ psi.} \times 39.35 / 1.50 = 23{,}610 \text{ psi.} \approx 23.61 \text{ ksi}$$

The total combine maximum stress, σ, in the transfer cask during the fire accident is then,

$$\begin{aligned}\sigma &= 5.02 \text{ ksi (stress due to 30 psi internal pressure from load case 3)} + 23.61 \text{ ksi} \\ &= 28.63 \text{ ksi}\end{aligned}$$

3.9.2.3 ANSYS Analysis Results and Reporting Methodology

The maximum nodal stress intensities in various components of the NUHOMS®-OS187H Transfer Cask are extracted from the ANSYS results files for all load cases. These stresses are compared to the normal and accident condition allowable stresses set forth by ASME B&PV Code Subsection NC [2]. Allowable Stresses are derived from material properties taken from Reference 6 at the various component temperatures listed in the Material Properties section. A summary of the maximum transfer cask component stresses and corresponding allowable stresses are presented in Table 3.9.2-1.

The maximum nodal stress intensities ($P_m + P_b$) are conservatively compared to the allowable membrane stress intensities, unless otherwise stated. In load cases where the nodal stress intensity exceeds the membrane allowable stress, individual membrane and membrane plus bending stresses are computed by linearizing the maximum component stresses through the thickness of the component. The resulting linearized stresses are then compared to their corresponding P_m and $P_m + P_b$ allowable stresses.

For the load combinations involving mechanical loads and thermal loads (i.e. 6*g* Lifting plus 115° F ambient), the maximum stresses from the mechanical load case and the maximum stress from the thermal load case are simply summed for each of the major cask components. This method of computing the maximum load combination stresses is very conservative, because, in general, the maximum stress caused by a mechanical load and the maximum stress caused by a thermal load will not occur at the same location in the transfer cask.

Typically, fictitious stresses at nodes where point contact exists with a beam element used to model a transfer cask bolt is ignored. These unrealistic stresses usually occur in the top cover at locations where the top cover bolts are fixed to the cover by node coupling (in all degrees of freedom) at a single node.

3.9.2.4 Transfer Cask Trunnion Local Stresses

The purpose of this section is to evaluate the local stress intensities in the NUHOMS®-OS187H Transfer Cask radial shells near the top and bottom trunnions, due to all applied loads during fuel loading and transfer operations.

3.9.2.4.1 Approach

The NUHOMS®-OS187H Transfer Cask has two top trunnions made of SA-182 Gr. FXM19 (22Cr-13Ni-5Mn Forging) and two bottom trunnions made of SA-182 Gr. F304. The transfer cask radial shells are made of SA-240, Gr. 304 (18Cr-8Ni).

The two top trunnions are used to first lift the cask, containing an empty DSC into a fuel pool for loading of the spent fuel. After the spent fuel has been loaded into the DSC, the cask is lifted to a decontamination area. After draining and drying of the pool water, welding of the canister cover, and bolting of the cask top cover, the cask is placed on a trailer for transfer to onsite HSM-H.

The transfer cask is vertically lifted into the trailer and rests its bottom trunnions on a support frame mounted to the top of the trailer. Then the cask is allowed to rotate, using the bottom trunnion supports as the pivot points, into a horizontal position until the top trunnions rest on their supports on the trailer. Throughout the operation the maximum total load is applied to the cask top trunnions. After the cask has been placed in the trailer, it is supported by all four trunnions and is subject to a set of specified handling loads.

The following two load cases are analyzed for the four cask trunnions and adjoining shell:

(a) Lifting Loads (Cask lifted from the pool to the decontamination area and then to the trailer)
The two top trunnions are analyzed for vertical 6 g and 10g loads as required by ANSI N14.6 [11]. The two bottom trunnions are not used during lifting of the cask.

(b) Handling Loads (Cask in a horizontal position inside trailer)
All four trunnions rest on the supports in the trailer. These four trunnions are designed to resist the following transfer loads:

DW (dead weight) + 1*g* Axial
DW + 1*g* Transverse
DW + 1*g* Vertical
DW + 1/2*g* Axial + 1/2*g* Transverse +1/2*g* Vertical

(Directions are relative to a horizontal cask)

All four trunnions carry the axial and vertical loads while only one top trunnion and one bottom trunnion on the same side of the cask will carry the transverse load. The bottom trunnion has the same cross section geometry as the top trunnion. However, the structural shell near the bottom trunnion is thinner (1.5 inches) than the shell near the top trunnion (2 inches). Also, there is a 1 inch thick reinforcing pad at top trunnion location. Thus, the bottom trunnion is critical with respect to stress generated by the handling load. The transfer loads are therefore analyzed only for the weaker bottom trunnions.

The outer neutron shield cylinder and structural cylinder are welded to the trunnion. Therefore, both cylinders resist the trunnion loads. However, for conservatism, support of outer shell is neglected in the analysis.

The trunnions and cask shells are assumed to be at a 300° F uniform temperature during transfer, which is conservative compared to the maximum temperature computed in Chapter 4 for the 115° F ambient environment condition (see Figure 3.9.2-4).

The following calculations are based on the method described in Reference 10. A spreadsheet, based on Figure 3.9.2-12 taken from Reference 10, was created to aid in the computation. Tables 3.9.2-2 through 3.9.2-7 are hardcopies of this spreadsheet for the various load cases analyzed. Typical parameters used in the spread sheet are hand calculated for load case 2D (DW + 0.5*g* Axial + 0.5*g* Vertical + 0.5*g* Transverse in Table 3.9.2-7) to illustrate the calculation process.

3.9.2.4.2 Load Cases

The weights of NUHOMS®-OS187H Transfer Cask components are the same as the component weights listed in Section 3.9.2.1.2. The weight for the NUHOMS®-OS187H Transfer Cask is 240,530 lb., including the loaded DSC and water in the canister and annulus (11,850 lb). However, for conservatism, a weight of 250,000 lb. is used in this analysis.

The following moment arms are used for the two load cases:

Load Case	*g* Load	Moment Arm Length	Reaction Support
Lifting	6*g* axial	9.750 in.*	Top two trunnions only
Transfer Loads	DW +1*g* Axial DW+1*g* vertical DW+1*g* transverse DW + 0.5*g* Axial + 0.5*g* Vertical + 0.5*g* Transverse	7.135 in.**	All four top and bottom trunnions

* [105.96 (trunnion outside) – 2×0.38 in. (trunnion lip) – 3.00 in. (average outer shoulder width) – 82.70 in. (shell outer diameter)] / 2 = 9.75 in.

** [49.61 – 81.7/2 – 3.25/2] = 7.135 in.

3.9.2.4.3 Material Properties

The following pertinent material properties are taken from Reference 6 at 300° F.

Property	SA-240, Type 304 stainless steel (cask shells and pad)
S_m	20 ksi
S_y	22.4 ksi
S_u	66.2

3.9.2.4.4 Stress Criteria

All load cases analyzed are normal condition (Level A) load cases. According to ASME Code, Section III, Subsection NC [2], the maximum allowable local membrane (P_l) and local membrane plus bending ($P_l + P_b$) stress intensities for normal conditions are $1.5S_m$ and $3.0S_m$ respectively.

The transfer cask radial shells are constructed from SA-240, Type 304 stainless steel. The shell material properties are conservatively taken at 300° F, which bounds the maximum inner shell and structural shell temperatures generated during the 115° F ambient transfer condition.

Therefore, the maximum allowable membrane and membrane plus bending stress intensities are as follows.

Stress Category	S_m for SA-240 Type 304 at 300° F [6]	Stress Criteria	Maximum Allowable Stress
P_m	20.0 ksi.	$1.5S_m$	30.0 ksi.
$P_m + P_b$	20.0 ksi.	$3.0S_m$	60.0 ksi.

3.9.2.4.5 Stress Computation

Note that all calculation results performed here are rounded to significant figures, even though the results computed in the attached spreadsheets (Tables 3.9.2-2 through 3.9.2-7) are not rounded.

Load Case 1. 6g Lifting

The 6*g* lifting loads are as follows.

Direction	*g*-load
Longitudinal	6.0*g*
Vertical	0.0*g*
Lateral	0.0*g*

At the top trunnions the *g*-load per trunnion is:

6.0*g* (Axial) / 2 = 3.0 *g* Axial per trunnion.

The following analytical method is taken from Reference 10. See Figure 3.9.2-12 for derivation of the following terms and equations.

Trunnion loads:

$P = 0.0$ lb.
$M_L = 3.0 \times 1.1 \times 250{,}000 \times 9.75 = 8{,}043{,}750$ in. lb.
$M_C = 0.0$ in. lb.
$M_T = 0.0$ in. lb.
$V_L = 3.0 \times 1.1 \times 250{,}000 = 825{,}000$ lb.
$V_C = 0.0$ lb.

The following parameters based on the nominal geometry and Reference 10 formulae are calculated as follows.

At Trunnion – Pad intersection:

Trunnion radius, $r_0 = 8.575$ in.
Mean radius, $R_m = 39.35 + 3.0/2 = 40.85$ in.
Shell and Pad thickness, $T = 2.0 + 1.0 = 3.0$ in

At Pad – Shell intersection:

Trunnion Pad radius, $r_0 = 13.575$ in.
Mean radius, $R_m = 39.35 + 2.0/2 = 40.35$ in.
Shell thickness, $T = 2.0$ in

Shell stresses are calculated at Trunnion-Pad intersection (in Table 3.9.2-2) and at Pad – Shell intersection (in Table 3.9.2-3).

Load Case 2. Transfer Loads

Load Case 2A. *DW + 1g Axial*

The transfer loads are as follows:

Direction	g-load
Axial	1.0g
Vertical (DW)	1.0g
Lateral	0g

At the top and bottom trunnions the g-load per trunnion is:

1.0g (axial) / 2 sides / 2 set trunnions = 0.25g axial per trunnion.
1.0g (vertical) / 2 sides / 2 set trunnions = 0.25g vertical per trunnion

Due to the above loads, stresses in the bottom trunnion locations will be critical since shell thickness at the bottom trunnion intersection is thinner relative to that of the top trunnions.

Trunnion loads:

$P = 0$ lb.
$M_L = 0.25 \times 250{,}000 \times 7.135 = 445{,}938$ in. lb.
$M_C = 0.25 \times 250{,}000 \times 7.135 = 445{,}938$ in. lb.
$M_T = 0.0$ in. lb.
$V_L = 0.25 \times 250{,}000 = 62{,}500$ lb.
$V_C = 0.25 \times 250{,}000 = 62{,}500$ lb.

At bottom trunnion locations:

Trunnion radius, $r_0 = 8.575$ in.
Mean radius, $R_m = 39.35 + 1.5/2 = 40.1$ in.
Shell thickness, $T = 1.5$ in

See Table 3.9.2-4 for shell stresses calculations and results.

Load Case 2B. *DW + 1g Vertical*

The transfer loads are as follows:

Direction	*g*-load
Axial	0*g*
Vertical (DW)	1.0*g* +1.0*g* = 2.0*g*
Transverse	0*g*

At the top and bottom trunnions the *g*-load per trunnion is:

2.0*g* (vertical) / 2 sides / 2 set trunnions = 0.5*g* vertical per trunnion

Trunnion loads:

$P = 0$ lb.
$M_L = 0$ in. lb.
$M_C = 0.5 \times 250{,}000 \times 7.135 = 891{,}875$ in. lb.
$M_T = 0.0$ in. lb.
$V_L = 0$ lb.
$V_C = 0.5 \times 250{,}000 = 125{,}000$ lb.

At bottom trunnion locations:

Trunnion radius, $r_0 = 8.575$ in.
Mean radius, $R_m = 39.35 + 1.5/2 = 40.1$ in.
Shell thickness, $T = 1.5$ in

See Table 3.9.2-5 for shell stresses calculations and results.

Load Case 2C. *DW + 1g Transverse*

The transfer loads are as follows:

Direction	g-load
Axial	0g
Vertical (DW)	1.0g
Transverse	1.0g

At the top and bottom trunnions the g-load per trunnion is:

1.0g (vertical) / 2 sides / 2 set trunnions = 0.25g vertical per trunnion
1.0g (transverse) / 2 sides / 1 set trunnions = 0.5g transverse per trunnion

Trunnion loads:

P = 0.5 x 250,000 = 125,000 lb.
M_L = 0 in. lb.
M_C = 0.25×250,000×7.135 = 445,938 in. lb.
M_T = 0.0 in. lb.
V_L = 0 lb.
V_C = 0.25×250,000 = 62, 5 00 lb.

At bottom trunnion locations:

Trunnion radius, r_0 = 8.575 in.
Mean radius, R_m = 39.35 + 1.5/2 = 40.1 in.
Shell thickness, T = 1.5 in

See Table 3.9.2-6 for shell stresses calculations and results.

Load Case 2D. *DW + 0.5g Axial + 0.5g Vertical + 0.5g Transverse*

The transfer loads are as follows:

Direction	g-load
Axial	0.5g
Vertical (DW)	1.0g + 0.5 = 1.5g
Transverse	0.5g

At the top and bottom trunnions the g-load per trunnion is:

0.5g (axial) / 2 sides / 2 set trunnions = 0.125g axial per trunnion
1.5g (vertical) / 2 sides / 2 set trunnions = 0.375g vertical per trunnion
0.5g (transverse) / 2 sides / 1 set trunnions = 0.25g axial per trunnion

Trunnion loads:

$P = 0.25 \times 250{,}000 = 62{,}500$ lb.
$M_L = 0.125 \times 250{,}000 \times 7.135 = 222{,}969$ in. lb.
$M_C = 0.375 \times 250{,}000 \times 7.135 = 668{,}906$ in. lb.
$M_T = 0.0$ in. lb.
$V_L = 0.125 \times 250{,}000 = 31{,}250$ lb.
$V_C = 0.375 \times 250{,}000 = 93{,}750$ lb.

At bottom trunnion locations:

Trunnion radius, $r_0 = 8.575$ in.
Mean radius, $R_m = 39.35 + 1.5/2 = 40.1$ in.
Shell thickness, $T = 1.5$ in

See Table 3.9.2-7 for shell stresses calculations and results.

These transfer load case parameter values are determined from tables in Reference 10. The following calculated parameters for load case 2D are given here to illustrate the typical procedure used in spreadsheet Tables 3.9.2-2 through 3.9.2-7.

$\gamma = R_m/T = 26.7333$

$\beta = 0.875 \times r_0/R_m = 0.1871$

$$\frac{P}{R_M T} = \frac{62{,}500}{40.1(1.5)} = 1{,}039$$

$$\frac{6P}{T^2} = \frac{6(62{,}500)}{1{,}5^2} = 166{,}667$$

$$\frac{M_C}{R_M^2 \beta T} = \frac{668{,}906}{40.1^2(0.1871)(1.5)} = 1{,}482$$

$$\frac{6M_C}{R_M \beta T^2} = \frac{6(668{,}906)}{40.1(0.1871)(1.5^2)} = 237{,}747$$

$$\frac{M_L}{R_M^2 \beta T} = \frac{222{,}969}{40.1^2(0.1871)(1.5)} = 494$$

$$\frac{6M_L}{R_M \beta T^2} = \frac{6(222{,}969)}{40.1(0.1871)(1.5^2)} = 79{,}249$$

$$\tau_{X\phi} \text{ for } V_C = \frac{V_C}{\pi r_0 T} = \frac{93{,}750}{\pi(8.575)(1.5)} = 2{,}320$$

$$\tau_{X\phi} \text{ for } V_L = \frac{V_L}{\pi r_0 T} = \frac{31{,}250}{\pi(8.575)(1.5)} = 773$$

It may be noted that some numbers in hand calculation do not exactly match the spreadsheet (Table 3.9.2-7) numbers. The reason is that hand calculation results are rounded as compared to the results in the spreadsheets.

3.9.2.4.6 Stress Intensity Calculation

Membrane plus bending Stress intensities are calculated in the following way.

$$S.I. = Max.\ of \begin{cases} \frac{1}{2}\left[(\sigma_x + \sigma_\phi) \pm \sqrt{(\sigma_x - \sigma_\phi)^2 + 4\tau^2}\right] \\ \sqrt{(\sigma_x - \sigma_\phi)^2 + 4\tau^2} \end{cases}$$

In order to calculate the membrane or bending stress intensity, only those components associated with membrane or bending stress, respectively, are summed to calculate σ_ϕ, σ_x and τ.

3.9.2.4.7 Local Shell Stress Results

The Table 3.9.2-8 summarizes the maximum stress intensities for both loading conditions.

3.9.2.4.8 Local Shell Stress Conclusions

All calculated local membrane stresses are less than the allowable local membrane stress of 30,000 psi., and all local membrane plus bending stress intensities are less than the allowable local membrane plus bending stress of 60,000 psi. Therefore, the NUHOMS®-OS187H Transfer Cask shells adjoining the trunnions are structurally adequate with respect to local stresses generated during lifting and transfer operations.

3.9.2.5 References

1. 10CFR Part 72, Licensing Requirement for Storage of Spent Fuel in an Independent Spent Fuel Storage Installation.

2. ASME Code Section III, Subsection NC and Appendices, 1998, including 2000 Addendum.

3. American Society of Mechanical Engineers, ASME Boiler and Pressure Vessel Code, Section III, Appendix F, 1998, including 2000 addenda.

4. ANSYS Users Manual, Rev. 5.6, 1998.

5. Pascale, Abadie, Qualification Du Material Vyal B, Rapport D'Essais N° 99 023-1, Cogema Logistics, March 13, 2003.

6. American Society of Mechanical Engineers, ASME Boiler and Pressure Vessel Code, Section II, Part D, 1998, including 2000 addenda.

7. Baumeister & Marks, Standard Handbook for Mechanical Engineers, 7th Edition.

8. An Assessment of Stress-Strain Data Suitable for Finite Element Elastic-Plastic Analysis of Shipping Containers, NUREG/CR-0481.

9. Stress Analysis of Closure Bolts for Shipping Casks, NUREG/CR-6007, April 1992.

10. Welding Research Council (WRC), Local Stresses in Spherical and Cylindrical Shells Due To External Loadings, Bulletin 107.

11. Special Lifting Devices for Shipping Containers Weighing 10,000 Pounds or More, ANSI N14.6, 1993.

12. NUHOMS 32P-ISFSI Transfer Cask Structural Analysis, TN Calculation No. 1095-35, Rev. 0.

Table 3.9.2-1
Summary of OS-187H Transfer Cask Stress Analysis

Load Case Number	Loading Condition	Service Level	Component		Maximum Stress Intensity (ksi)	Allowable Membrane Stress Intensity (ksi)
1	6g Vertical Lifting	A	Structural Shell	P_m	12.13	20.00
				$P_m + P_b$	27.75	30.00
			Top Cover		7.49	31.40
			Inner Shell		15.39	18.70
			Bottom End plates	P_m	14.68	20.00
				$P_m + P_b$	28.51	30.00
			RAM Acc. and Cover	P_m	13.08	20.00
				$P_m + P_b$	20.48	30.00
1A	6g Vertical Lifting + Thermal Loads	A	Structural Shell		46.69	60.00(1)
			Top Cover		16.05	94.20(1)
			Inner Shell		36.60	56.10(1)
			Bottom End plates		38.79	60.00(1)
			RAM Access and Cover		33.42	60.00(1)
2	Vacuum Drying	A	Structural Shell		11.58	60.00(1)
3	30 psi. Internal Pressure	A	Structural Shell		5.02	20.00
			Top Cover		5.54	31.40
			Inner Shell		4.41	18.70
			Bottom End plates		5.16	20.00
			RAM Access and Cover		4.71	20.00
4	115°F Ambient Hot Thermal Environment	A	Structural Shell		19.04	60.00(1)
			Top Cover		8.56	94.20(1)
			Inner Shell		21.21	56.10(1)
			Bottom End plates		10.28	60.00(1)
			RAM Access and Cover		12.94	60.00(1)

Table 3.9.2-1 (continued)
Summary of OS-187H Transfer Cask Stress Analysis

Load Case Number	Loading Condition	Service Level	Component	Maximum Stress Intensity (ksi)	Allowable Membrane Stress Intensity (ksi)
5	-20°F Ambient Cold Thermal Environment	A	Structural Shell	18.32	60.00(1)
			Top Cover	7.30	94.20(1)
			Inner Shell	24.84	56.10(1)
			Bottom End plates	10.53	60.00(1)
			RAM Access and Cover	11.73	60.00(1)
6	Transfer Inertial Loads (2*g* Vertical + 2*g* Transverse + 2*g* Axial)	A	Structural Shell	11.18	20.00
			Top Cover	17.60	31.40
			Inner Shell	6.06	18.70
			Bottom End plates	1.76	20.00
			RAM Access and Cover	2.89	20.00
6A	Transfer Loads + Internal Pressure	A	Structural Shell	9.49	20.00
			Top Cover	17.69	31.40
			Inner Shell	5.40	18.70
			Bottom End plates	4.75	20.00
			RAM Access and Cover	4.15	20.00
6B	Transfer Loads + 115° F Ambient + Internal Pressure	A	Structural Shell	28.53	60.00(1)
			Top Cover	26.25	94.20(1)
			Inner Shell	26.61	56.10(1)
			Bottom End plates	15.03	60.00(1)
			RAM Access and Cover	17.09	60.00(1)
6C	Transfer Loads + -20° F Ambient + Internal Pressure	A	Structural Shell	27.81	60.00(1)
			Top Cover	24.99	94.20(1)
			Inner Shell	30.24	56.10(1)
			Bottom End plates	15.28	60.00(1)
			RAM Access and Cover	15.88	60.00(1)
7	75*g* Bottom End Drop + Internal Pressure	D	Structural Shell	35.16	46.34
			Top Cover	10.07	65.94
			Inner Shell	13.02	44.80
			Bottom End plates	28.23	46.34
			RAM Access and Cover	38.46	48.00

Table 3.9.2-1 (continued)
OS-187H Transfer Cask Maximum Stresses

Load Case Number	Loading Condition	Service Level	Component		Maximum Stress Intensity (ksi)	Allowable Membrane Stress Intensity (ksi)
8	75g Top End Drop + Internal Pressure	D	Structural Shell		19.11	46.34
			Top Cover		27.89	65.94
			Inner Shell		10.07	44.80
			Bottom End plates		6.56	46.34
			RAM Access and Cover		4.83	48.00
9	75g Side Drop + Internal Pressure	D	Structural Shell	P_m	42.95	46.34
				$(P_m$ or $P_L) + P_b$	58.17	66.20(3)
			Top Cover	P_m	60.38	65.94
				P_L	77.81(4)	94.20(4)
				$(P_m$ or $P_L) + P_b$	91.90	94.20(3)
			Inner Shell	P_m	33.43	44.80
				$(P_m$ or $P_L) + P_b$	49.86	64.00(3)
			Bottom End plates	P_m	43.88	46.34
				P_L	51.26(4)	66.2(4)
				$(P_m$ or $P_L) + P_b$	48.28	66.20(3)
			RAM Access and Cover	P_m	37.14	48.00
				$(P_m$ or $P_L) + P_b$	47.74	71.00(3)
10	Transfer Thermal Accident (Fire)	D	Structural Shell		28.63	58.32(2)

(1) $P_L + P_b + Q$ allowable stress.
(2) Sm = 16.2 ksi. For SA-240 type 304 at a temperature of 650° F. (the maximum transfer cask temperature is 618° F during the thermal accident [Chapter 4]). The allowable is taken as $3.6S_m$.
(3) Membrane plus bending [$(P_m$ or $P_L) + P_b$] allowable stress.
(4) Stresses at the edge of the impact target support at the 15° location is considered local and are compared to P_L allowable stresses.

Table 3.9.2-2
Computation Spreadsheet for the 6g Lifting, Top Trunnion, Local Stresses at Trunnion Pad

Allplied Loads			Geometry			Geometric Parameters							
W	250000		T	3		gamma	13.6167						
P	0		r0	8.575		beta	0.1837						
ML	8043750		Rm	40.85									
MC	0												
MT	0												
VL	825000												
VC	0												
					column # =	1	2	3	4	5	6	7	8
from fig	read curves	for	multiplier	abs. stress	values	Au	Al	Bu	Bl	Cu	Cl	Du	Dl
3C AND 4C	0	0	0	0	0	0	0	0	0	0	0	0	0
1C AND 2C-1	0	0	0	0	0	0	0	0	0	0	0	0	0
3A	0		0	0						0	0	0	0
1A	- 0		0	0						0	0	0	0
3B	1.4		8748	12247		-12247	-12247	12247	12247				
1B OR 1B-1	0.046		714702	32876		-32876	32876	32876	-32876				
			Summation of phi stresses => sigma phi =			-45123	20629	45123	-20629	0	0	0	0
3C AND 4C	0	0	0	0	0	0	0	0	0	0	0	0	0
1C-1 AND 2C	0	0	0	0	0	0	0	0	0	0	0	0	0
4A	0		0	0						0	0	0	0
2A	0		0	0						0	0	0	0
4B	0.48		8748	4199		-4199	-4199	4199	4199				
2B OR 2B-1	0.072		714702	51459		-51459	51459	51459	-51459				
			Summation of X stresses => sigma X =			-55658	47260	55658	-47260	0	0	0	0
			Shear stress due to torsion MT		0	0	0	0	0	0	0	0	0
			Shear stress due to load VC		0	0	0	0	0				
			Shear stress due to load VL		10208					-10208	-10208	10208	10208
			Summation of shear stresses tau =			0	0	0	0	-10208	-10208	10208	10208
			stress intensities =>			55658	47260	55658	47260	20416	20416	20416	20416
			membrane components of sigma phi =>			-12247	-12247	12247	12247	0	0	0	0
			membrane components of sigma X =>			-4199	-4199	4199	4199	0	0	0	0
			tau =>			0	0	0	0	-10208	-10208	10208	10208
			membrane stress intensities =>			12247	12247	12247	12247	20416	20416	20416	20416

Table 3.9.2-3
Computation Spreadsheet for the 6g Lifting, Top Trunnion, Local Stresses at Pad - Shell Intersection

Allplied Loads			Geometry			Geometric Parameters							
W	250000		T	2		gamma	20.1750						
P	0		r0	13.575		beta	0.2944						
ML	8043750		Rm	40.35									
MC	0												
MT	0												
VL	825000												
VC	0												
					column # =	1	2	3	4	5	6	7	8
from fig	read curves	for	multiplier	abs. stress	values	Au	Al	Bu	Bl	Cu	Cl	Du	Dl
3C AND 4C	0	0	0	0	0	0	0	0	0	0	0	0	0
1C AND 2C-1	0	0	0	0	0	0	0	0	0	0	0	0	0
3A	0		0	0						0	0	0	0
1A	0		0	0						0	0	0	0
3B	2		8391	16783		-16783	-16783	16783	16783				
1B OR 1B-1	0.024		1015785	24379		-24379	24379	24379	-24379				
				Summation of phi stresses => sigma phi =		-41162	7596	41162	-7596	0	0	0	0
3C AND 4C	0	0	0	0	0	0	0	0	0	0	0	0	0
1C-1 AND 2C	0	0	0	0	0	0	0	0	0	0	0	0	0
4A	0		0	0						0	0	0	0
2A	0		0	0						0	0	0	0
4B	0.84		8391	7049		-7049	-7049	7049	7049				
2B OR 2B-1	0.043		1015785	43679		-43679	43679	43679	-43679				
				Summation of X stresses => sigma X =		-50728	36630	50728	-36630	0	0	0	0
				Shear stress due to torsion MT	0	0	0	0	0	0	0	0	0
				Shear stress due to load VC	0	0	0	0	0				
				Shear stress due to load VL	9672					-9672	-9672	9672	9672
				Summation of shear stresses tau =		0	0	0	0	-9672	-9672	9672	9672
				stress intensities =>		50728	36630	50728	36630	19345	19345	19345	19345
				membrane components of sigma phi =>		-16783	-16783	16783	16783	0	0	0	0
				membrane components of sigma X =>		-7049	-7049	7049	7049	0	0	0	0
				tau =>		0	0	0	0	-9672	-9672	9672	9672
				membrane stress intensities =>		16783	16783	16783	16783	19345	19345	19345	19345

Table 3.9.2-4
Computation Spreadsheet for the (DW + 1.0g Axial) Transfer Load, Bottom Trunnion – Local Shell Stresses

Alplied Loads			Geometry			Geometric Parameters							
W	250000		T	1.5		gamma	26.7333						
P	0		r0	8.575		beta	0.1871						
ML	445938		Rm	40.1									
MC	445938												
MT	0												
VL	62500												
VC	62500												
					column # =	1	2	3	4	5	6	7	8
from fig	read curves	for	multiplier	abs. stress	values	Au	Al	Bu	Bl	Cu	Cl	Du	Dl
3C AND 4C	3.5	4.5	0	0	0	0	0	0	0	0	0	0	0
1C AND 2C-1	0.088	0.054	0	0	0	0	0	0	0	0	0	0	0
3A	- 1.1		988	1087						-1087	-1087	1087	1087
1A	0.09		158490	14264						-14264	14264	14264	-14264
3B	3		988	2964		-2964	-2964	2964	2964				
1B OR 1B-1	0.034		158490	5389		-5389	5389	5389	-5389				
		Summation of phi stresses => sigma phi =				-8353	2424	8353	-2424	-15351	13177	15351	-13177
3C AND 4C	3.5	4.5	0	0	0	0	0	0	0	0	0	0	0
1C-1 AND 2C	0.084	0.052	0	0	0	0	0	0	0	0	0	0	0
4A	1.7		988	1680						-1680	-1680	1680	1680
2A	0.044		158490	6974						-6974	6974	6974	-6974
4B	1		988	988		-988	-988	988	988				
2B OR 2B-1	0.05		158490	7924		-7924	7924	7924	-7924				
		Summation of X stresses => sigma X =				-8913	6936	8913	-6936	-8653	5294	8653	-5294
		Shear stress due to torsion MT			0	0	0	0	0	0	0	0	0
		Shear stress due to load VC			1547	1547	1547	-1547	-1547				
		Shear stress due to load VL			1547					-1547	-1547	1547	1547
		Summation of shear stresses tau =				1547	1547	-1547	-1547	-1547	-1547	1547	1547
					stress intensities =>	10205	7416	10205	7416	15691	13470	15691	13470
					membrane components of sigma phi =>	-2964	-2964	2964	2964	-1087	-1087	1087	1087
					membrane components of sigma X =>	-988	-988	988	988	-1680	-1680	1680	1680
					tau =>	1547	1547	-1547	-1547	-1547	-1547	1547	1547
					membrane stress intensities =>	3812	3812	3812	3812	3150	3150	3150	3150

Table 3.9.2-5
Computation Spreadsheet for the (DW + 1.0*g* Vertical) Transfer Load, Bottom Trunnion – Local Shell Stresses

Allplied Loads			Geometry			Geometric Parameters							
W	250000		T	1.5		gamma	26.7333						
P	0		r0	8.575		beta	0.1871						
ML	0		Rm	40.1									
MC	891875												
MT	0												
VL	0												
VC	125000												
					column # =	1	2	3	4	5	6	7	8
from fig	read curves	for	multiplier	abs. stress	values	Au	Al	Bu	Bl	Cu	Cl	Du	Dl
3C AND 4C	3.5	4.5	0	0	0	0	0	0	0	0	0	0	0
1C AND 2C-1	.0.088	0.054	0	0	0	0	0	0	0	0	0	0	0
3A	1.1		1976	2174						-2174	-2174	2174	2174
1A	0.09		316979	28528						-28528	28528	28528	-28528
3B	3		0	0		0	0	0	0				
1B OR 1B-1	0.034		0	0		0	0	0	0				
					Summation of phi stresses => sigma phi =	0	0	0	0	-30702	26354	30702	-26354
3C AND 4C	3.5	4.5	0	0	0	0	0	0	0	0	0	0	0
1C-1 AND 2C	0.084	0.052	0	0	0	0	0	0	0	0	0	0	0
4A	1.7		1976	3360						-3360	-3360	3360	3360
2A	0.044		316979	13947						-13947	13947	13947	-13947
4B	1		0	0		0	0	0	0				
2B OR 2B-1	0.05		0	0		0	0	0	0				
					Summation of X stresses => sigma X =	0	0	0	0	-17307	10588	17307	-10588
					Shear stress due to torsion MT	0	0	0	0	0	0	0	0
					Shear stress due to load VC	3093	3093	3093	-3093	-3093			
					Shear stress due to load VL	0					0	0	0	0
					Summation of shear stresses tau =		3093	3093	-3093	-3093	0	0	0	0
					stress intensities =>		6187	6187	6187	6187	30702	26354	30702	26354
					membrane components of sigma phi =>		0	0	0	0	-2174	-2174	2174	2174
					membrane components of sigma X =>		0	0	0	0	-3360	-3360	3360	3360
					tau =>		3093	3093	-3093	-3093	0	0	0	0
					membrane stress intensities =>		6187	6187	6187	6187	3360	3360	3360	3360

Table 3.9.2-6
Computation Spreadsheet for the (DW + 1.0*g* transverse) Transfer Load, Bottom Trunnion – Local Shell Stresses

Allplied Loads			Geometry			Geometric Parameters							
W	250000		T	1.5		gamma	26.7333						
P	125000		r0	8.575		beta	0.1871						
ML	0		Rm	40.1									
MC	445938												
MT	0												
VL	0												
VC	62500												
					column # =	1	2	3	4	5	6	7	8
from fig	read curves	for	multiplier	abs. stress	values	Au	Al	Bu	Bl	Cu	Cl	Du	Dl
3C AND 4C	3.5	4.5	2078	7273	9352	-9352	-9352	-9352	-9352	-7273	-7273	-7273	-7273
1C AND 2C-1	0.088	0.054	333333	29333	18000	-18000	18000	-18000	18000	-29333	29333	-29333	29333
3A	1.1		988	1087						-1087	-1087	1087	1087
1A	0.09		158490	14264						-14264	14264	14264	-14264
3B	3		0	0		0	0	0	0				
1B OR 1B-1	0.034		0	0		0	0	0	0				
					Summation of phi stresses => sigma phi =	-27352	8648	-27352	8648	-51958	35237	-21256	8883
3C AND 4C	3.5	4.5	2078	7273	9352	-7273	-7273	-7273	-7273	-9352	-9352	-9352	-9352
1C-1 AND 2C	0.084	0.052	333333	28000	17333	-28000	28000	-28000	28000	-17333	17333	-17333	17333
4A	1.7		988	1680						-1680	-1680	1680	1680
2A	0.044		158490	6974						-6974	6974	6974	-6974
4B	1		0	0		0	0	0	0				
2B OR 2B-1	0.05		0	0		0	0	0	0				
					Summation of X stresses => sigma X =	-35273	20727	-35273	20727	-35338	13275	-18032	2688
					Shear stress due to torsion MT	0	0	0	0	0	0	0	0
					Shear stress due to load VC	1547	1547	1547	-1547	-1547			
					Shear stress due to load VL	0					0	0	0	0
					Summation of shear stresses tau =	1547	1547	-1547	-1547	0	0	0	0
					stress intensities =>	35565	20921	35565	20921	51958	35237	21256	8883
					membrane components of sigma phi =>	-9352	-9352	-9352	-9352	-8360	-8360	-6187	-6187
					membrane components of sigma X =>	-7273	-7273	-7273	-7273	-11031	-11031	-7672	-7672
					tau =>	1547	1547	-1547	-1547	0	0	0	0
					membrane stress intensities =>	10176	10176	10176	10176	11031	11031	7672	7672

Table 3.9.2-7
Computation Spreadsheet for the (DW + 0.5*g* axial + 0.5*g* vertical + 0.5*g* trans.) Transfer Load, Bottom Trunnion – Local Shell Stresses

Alplied Loads			Geometry			Geometric Parameters							
W	250000		T	1.5		gamma	26.7333						
P	62500		r0	8.575		beta	0.1871						
ML	222969		Rm	40.1									
MC	668906												
MT	0												
VL	31250												
VC	93750												
					column # =	1	2	3	4	5	6	7	8
from fig	read curves	for	multiplier	abs. stress	values	Au	Al	Bu	Bl	Cu	Cl	Du	Dl
3C AND 4C	3.5	4.5	1039	3637	4676	-4676	-4676	-4676	-4676	-3637	-3637	-3637	-3637
1C AND 2C-1	0.088	0.054	166667	14667	9000	-9000	9000	-9000	9000	-14667	14667	-14667	14667
3A	1.1		1482	1630						-1630	-1630	1630	1630
1A	0.09		237734	21396						-21396	21396	21396	-21396
3B	3		494	1482		-1482	-1482	1482	1482				
1B OR 1B-1	0.034		79245	2694		-2694	2694	2694	-2694				
					Summation of phi stresses => sigma phi =	-17852	5536	-9499	3112	-41330	30796	4723	-8736
3C AND 4C	3.5	4.5	1039	3637	4676	-3637	-3637	-3637	-3637	-4676	-4676	-4676	-4676
1C-1 AND 2C	0.084	0.052	166667	14000	8667	-14000	14000	-14000	14000	-8667	8667	-8667	8667
4A	1.7		1482	2520						-2520	-2520	2520	2520
2A	0.044		237734	10460						-10460	10460	10460	-10460
4B	1		494	494		-494	-494	494	494				
2B OR 2B-1	0.05		79245	3962		-3962	3962	3962	-3962				
					Summation of X stresses => sigma X =	-22093	13831	-13180	6895	-26322	11932	-363	-3950
					Shear stress due to torsion MT	0	0	0	0	0	0	0	0
					Shear stress due to load VC	2320	2320	2320	-2320	-2320			
					Shear stress due to load VL	773.3					-773	-773	773	773
					Summation of shear stresses tau =	2320	2320	-2320	-2320	-773	-773	773	773
					stress intensities =>	23116	14436	14301	7997	41370	30827	5316	8858
					membrane components of sigma phi =>	-6158	-6158	-3194	-3194	-5267	-5267	-2006	-2006
					membrane components of sigma X =>	-4131	-4131	-3143	-3143	-7195	-7195	-2156	-2156
					tau =>	2320	2320	-2320	-2320	-773	-773	773	773
					membrane stress intensities =>	7676	7676	5488	5488	7467	7467	2858	2858

Table 3.9.2-8
NUHOMS®-OS187H Transfer Cask Local Shell Stresses and Allowables

Load Case Number	Load	Maximum Local Stress		Allowable (ksi)	Reference Table
		Type	Magnitude (ksi)		
1	6*g* Lifting (Pad)	P_l	20.42	30.0	Table 3.9.2-2
		$P_l + P_b$	55.66	60.0	Table 3.9.2-2
	6*g* Lifting (Shell)	P_l	19.35	30.0	Table 3.9.2-3
		$P_l + P_b$	50.73	60.0	Table 3.9.2-3
2A.	Transfer, DW + 1*g* Axial	P_l	3.81	30.0	Table 3.9.2-4
		$P_l + P_b$	15.69	60.0	Table 3.9.2-4
2B.	Transfer, DW + 1*g* Vertical	P_l	6.19	30.0	Table 3.9.2-5
		$P_l + P_b$	30.70	60.0	Table 3.9.2-5
2C.	Transfer, DW + 1*g* Transverse	P_l	11.03	30.0	Table 3.9.2-6
		$P_l + P_b$	51.96	60.0	Table 3.9.2-6
2D.	Transfer, DW + 0.5*g* Axial + 0.5*g* Vertical + 0.5*g* Transverse	P_l	7.68	30.0	Table 3.9.2-7
		$P_l + P_b$	41.37	60.0	Table 3.9.2-7

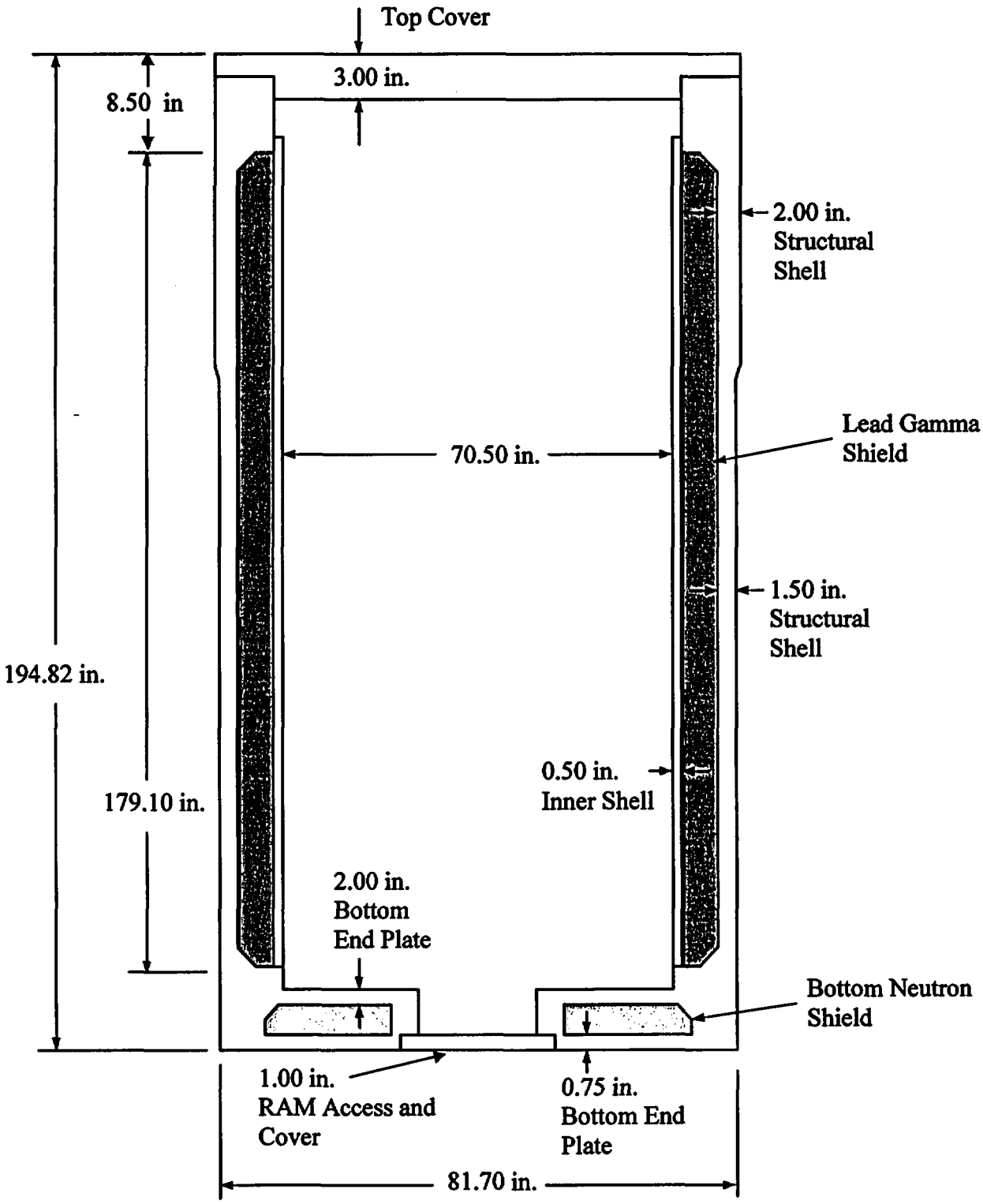

Figure 3.9.2-1
NUHOMS®-OS187H Transfer Cask Key Components and Dimensions (Drawing Not to Scale)

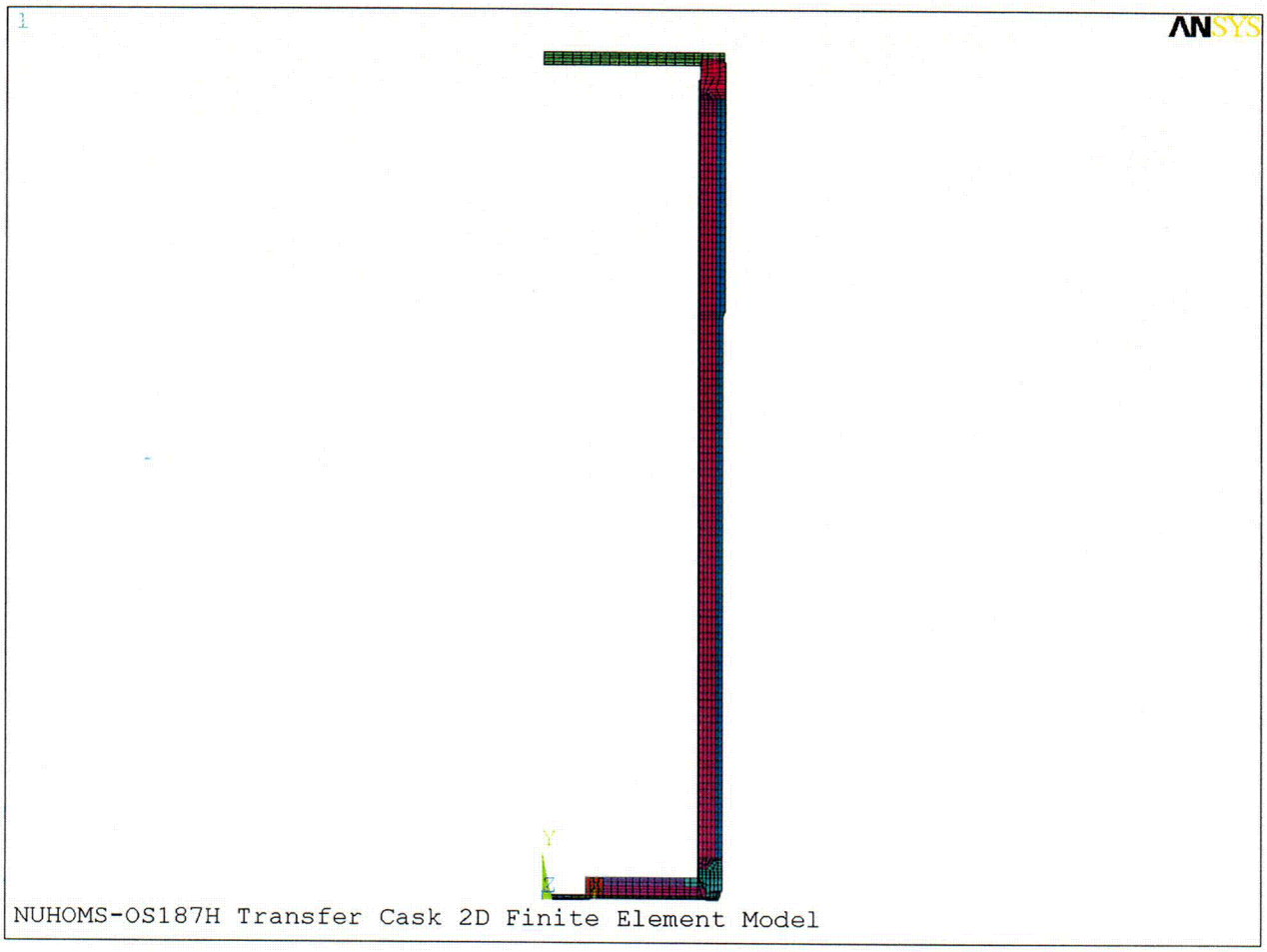

Figure 3.9.2-2
2-Dimensional Finite Element Model, Element Plot

C01

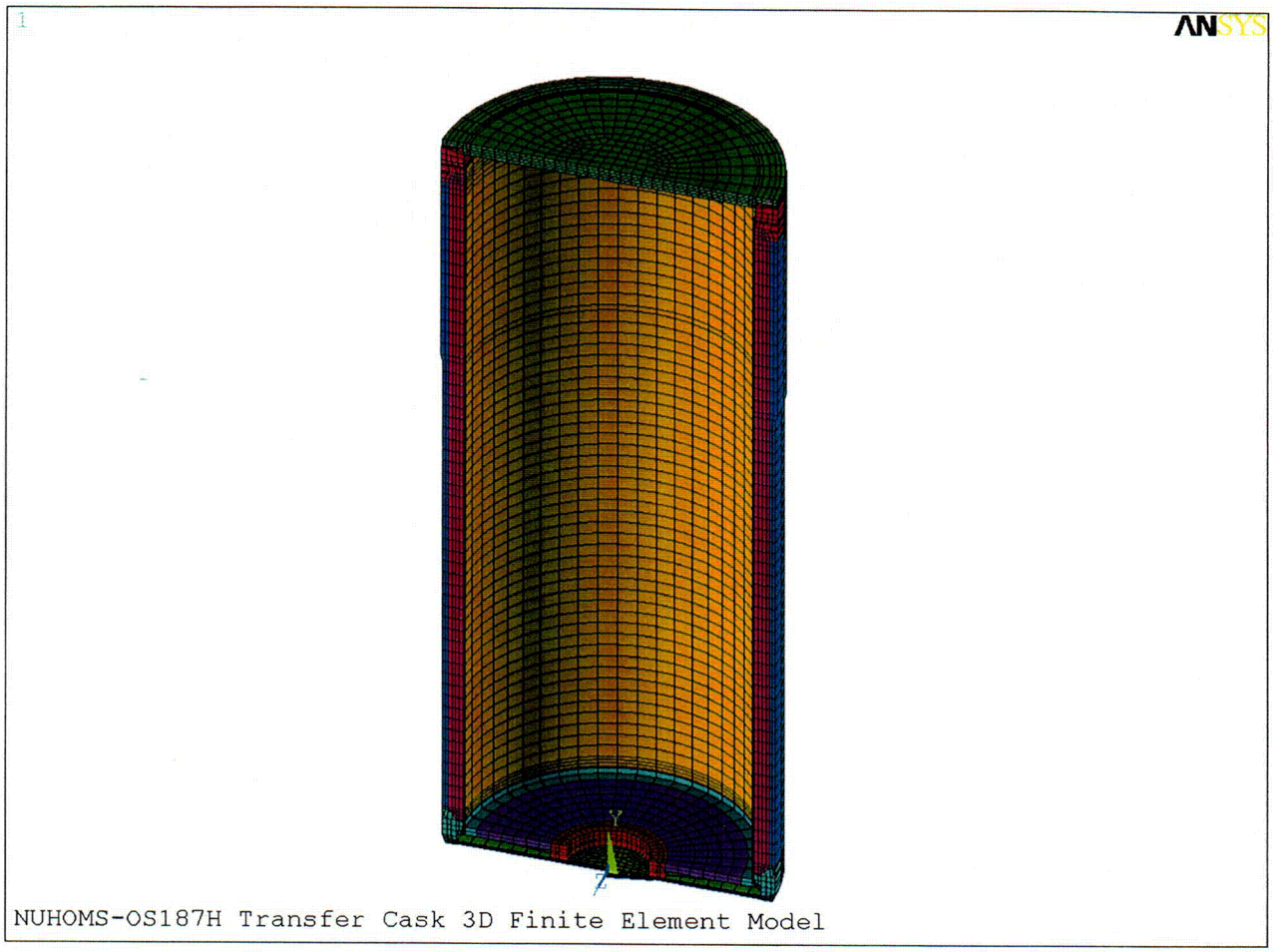

Figure 3.9.2-3
3-Dimensional Finite Element Model, Element Plot

C02

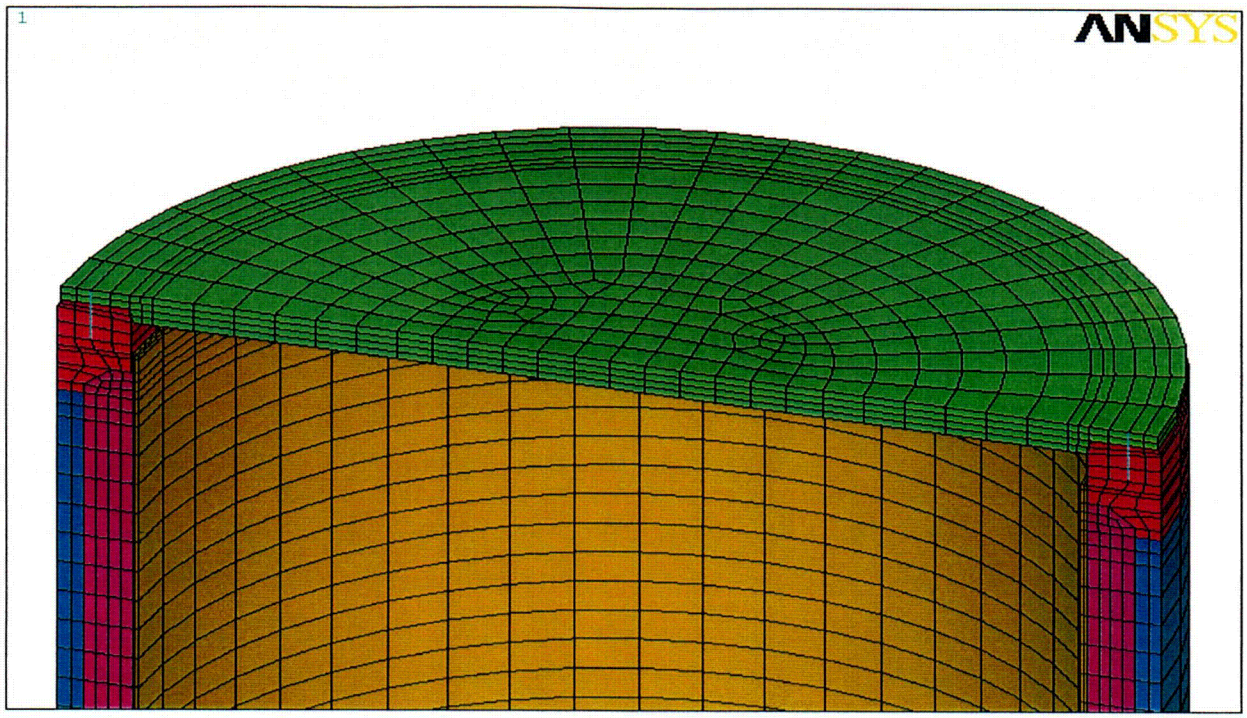

Figure 3.9.2-3A
Cask Top Cover / Flange / Bolt Model

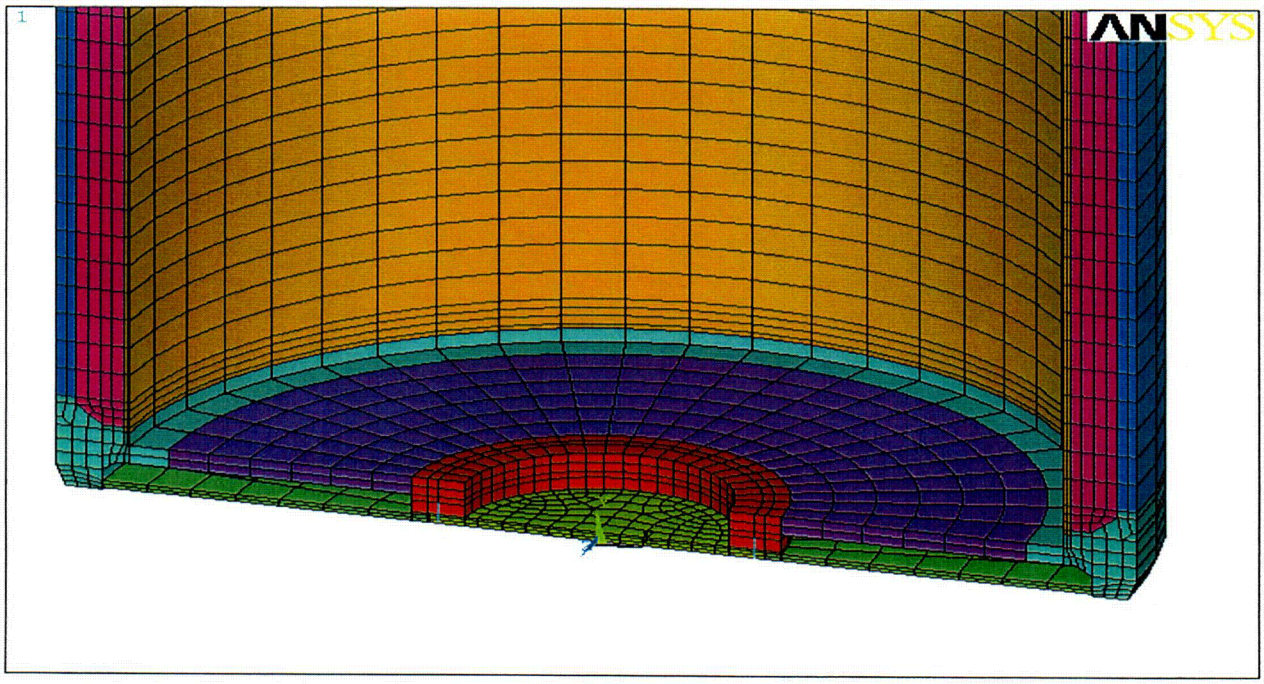

Figure 3.9.2-3B
Cask Bottom Ram Access/Cover/Bolt Model

C03

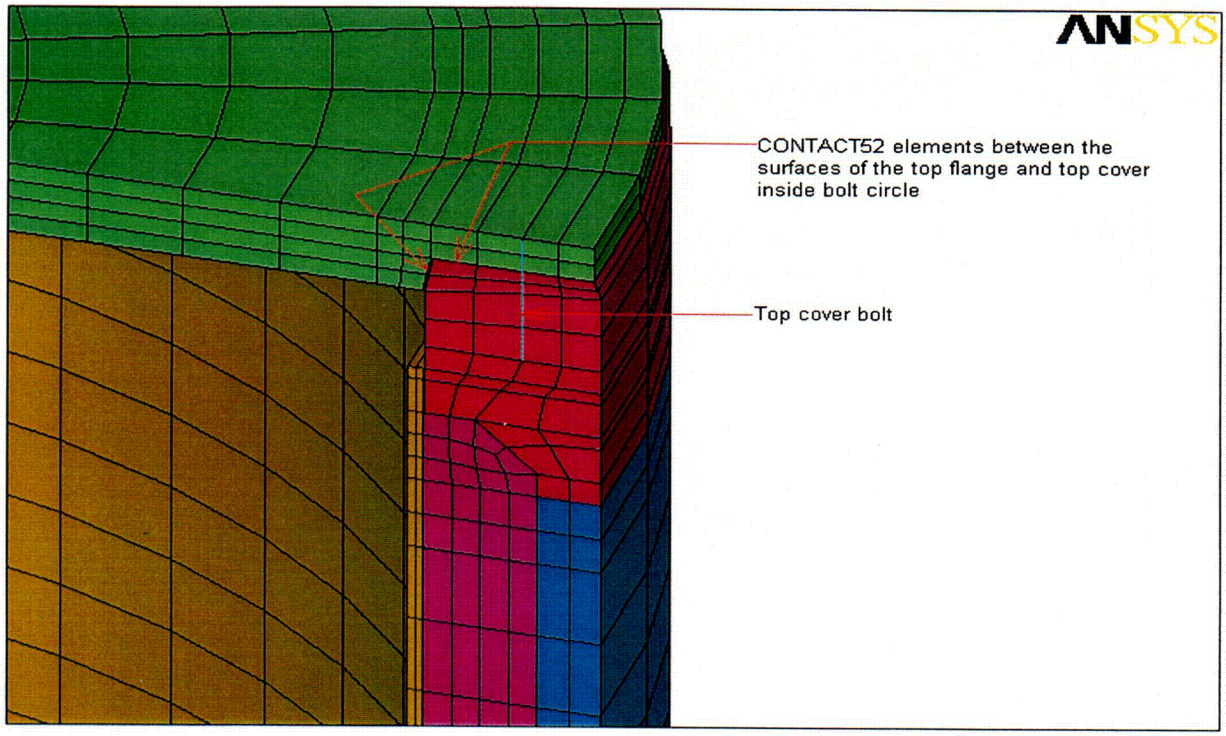

Figure 3.9.2-3C
Cask Top Cover / Flange CONTAC52 Element Representation

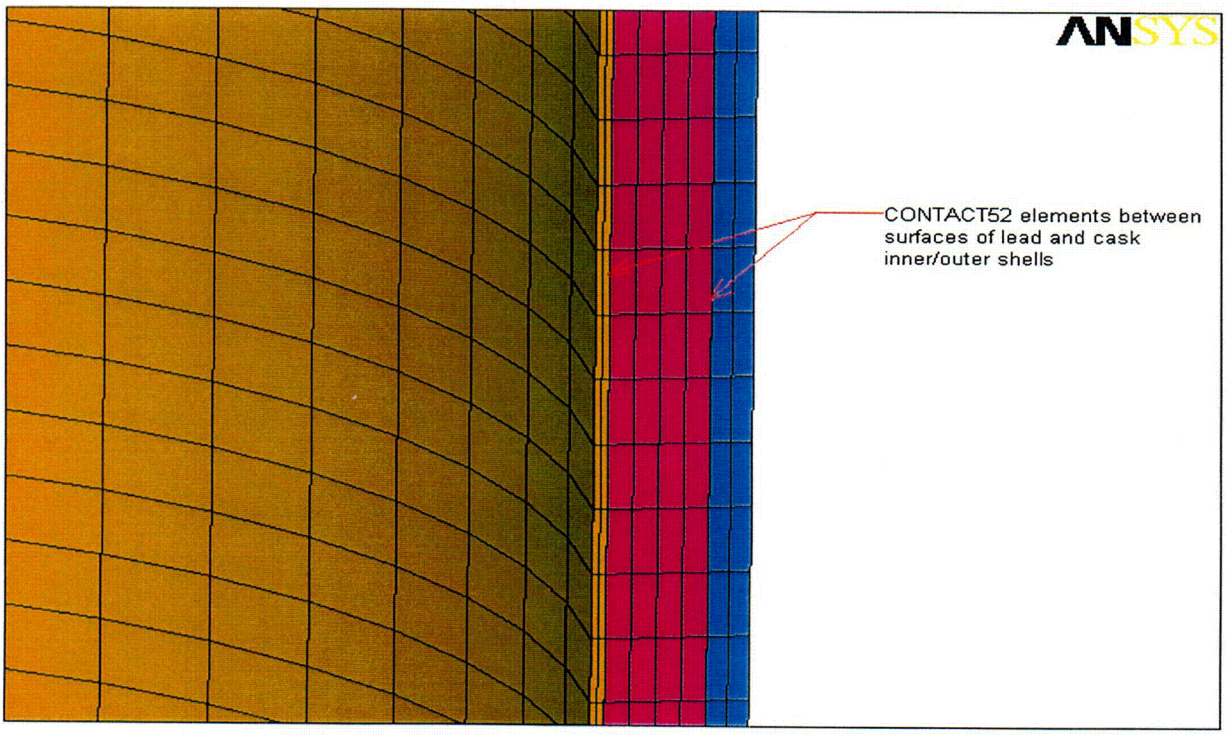

Figure 3.9.2-3D
Cask Shell / Lead CONTAC52 Element Representation

C04

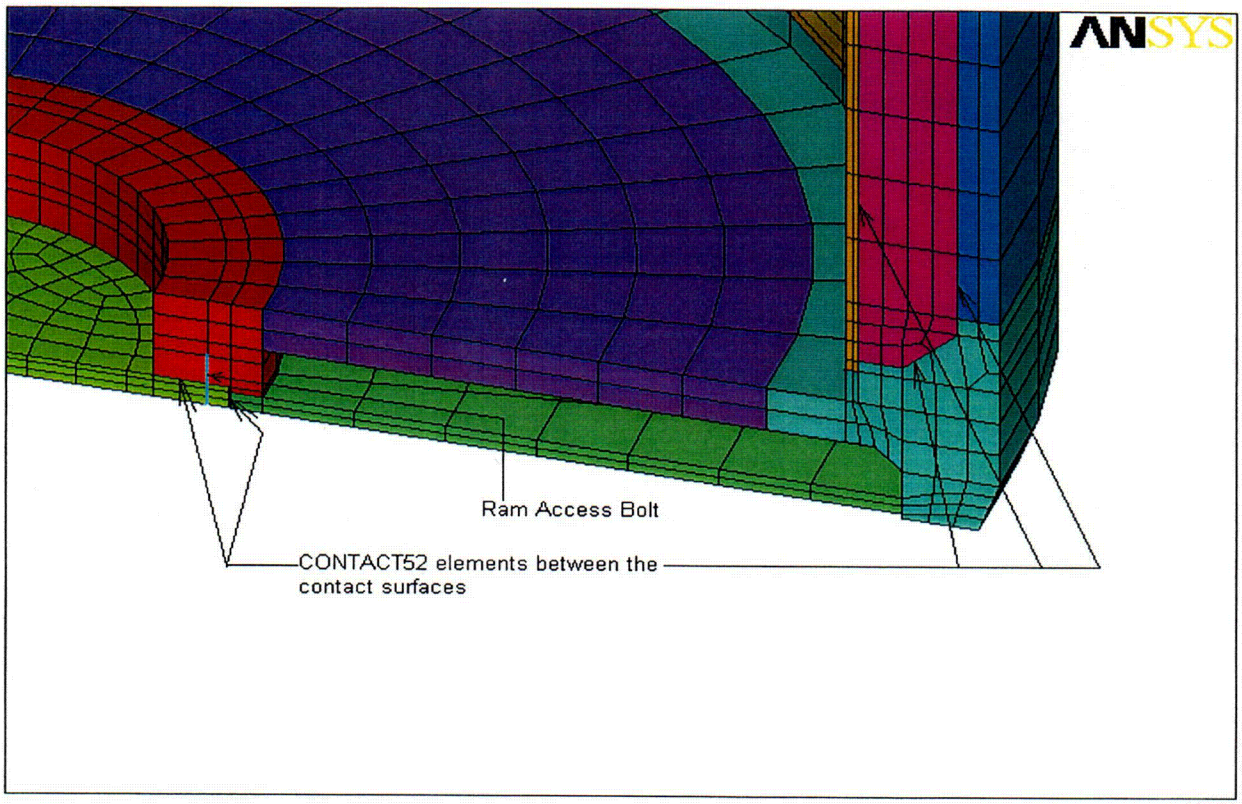

FIGURE 3.9.2-3E
Cask Bottom Access / Shell / Flange / Lead CONTAC52 Element Representation

C05

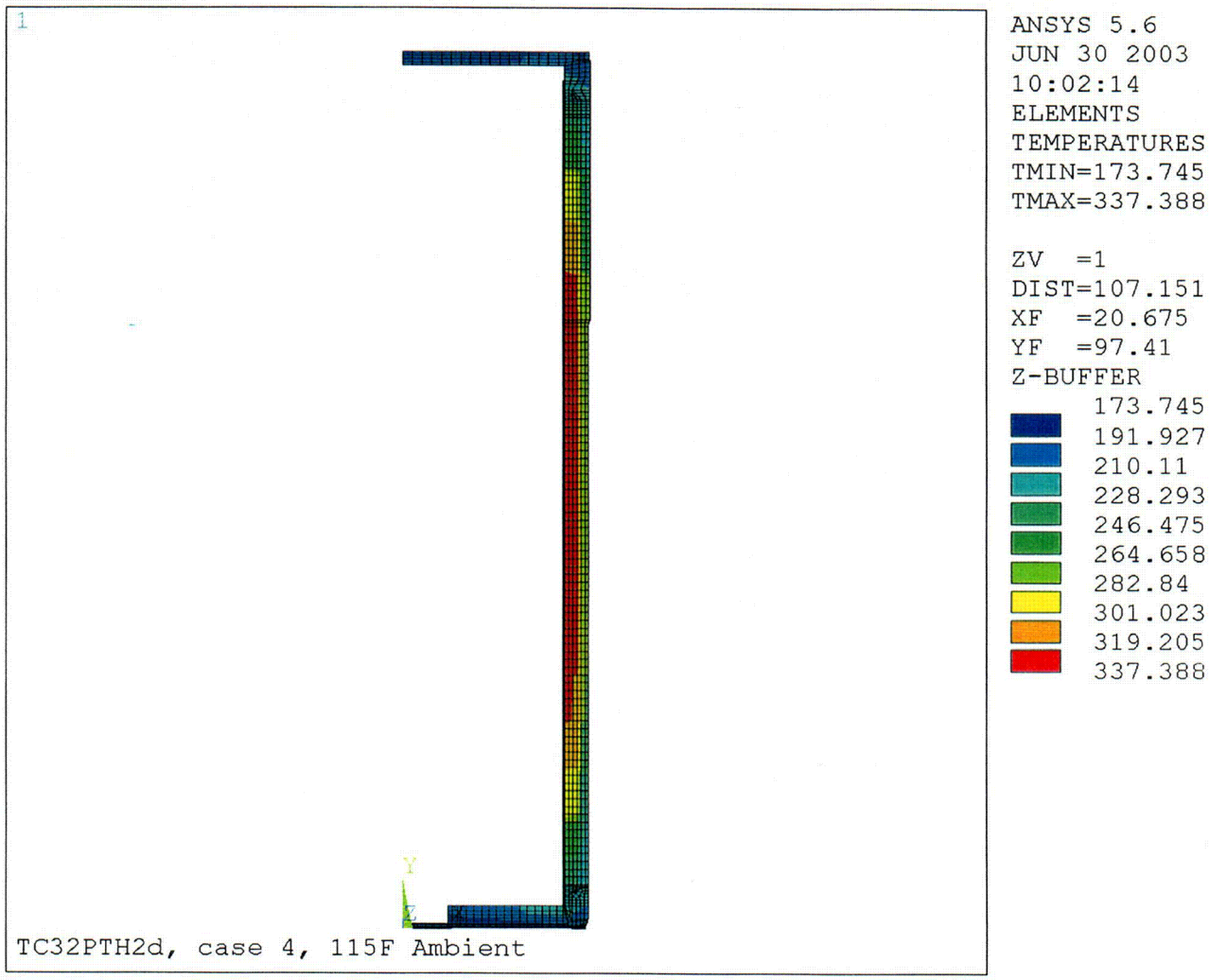

Figure 3.9.2-4
115°F Ambient Temperature Distribution

C06

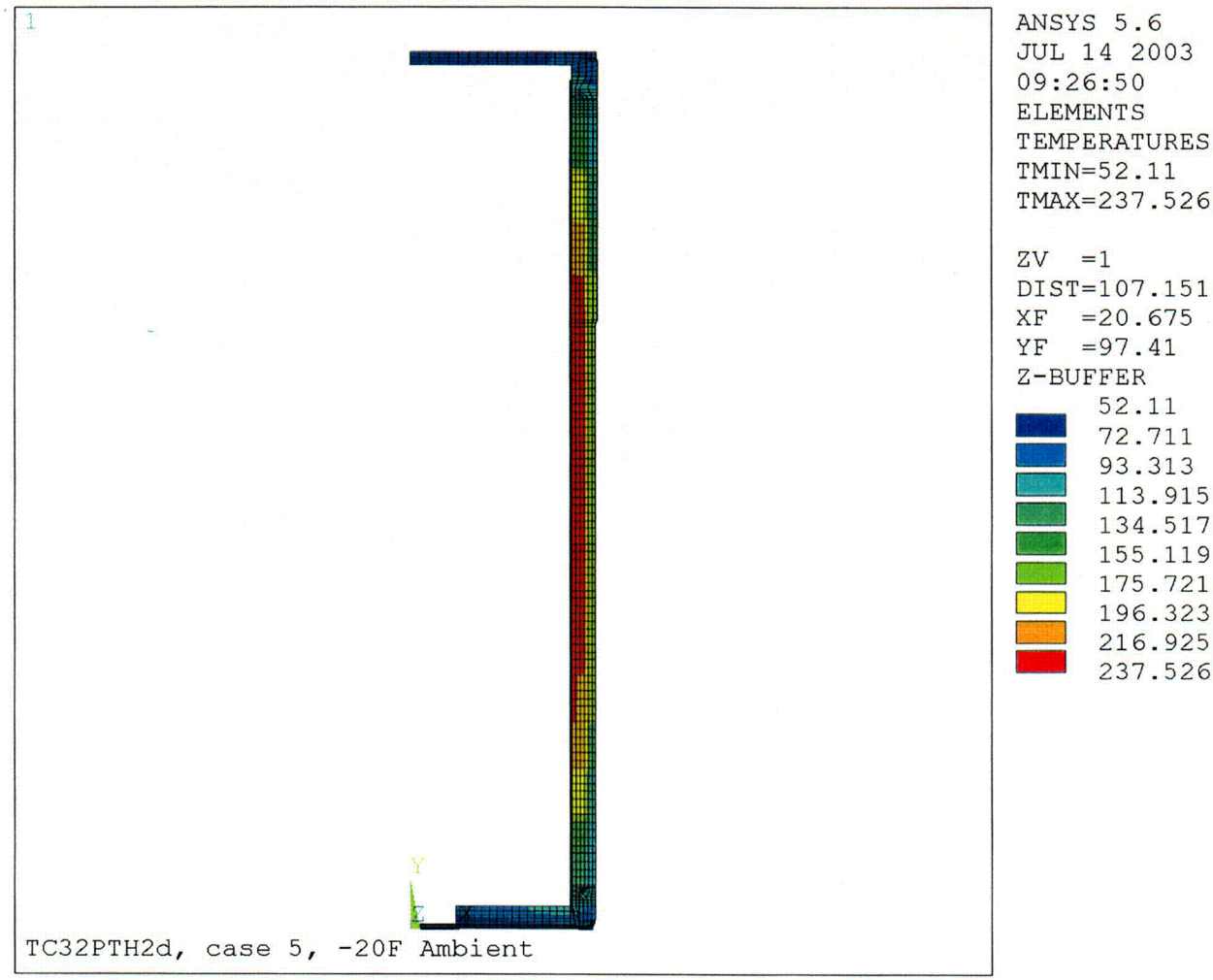

Figure 3.9.2-5
-20°F Ambient Temperature Distribution

C07

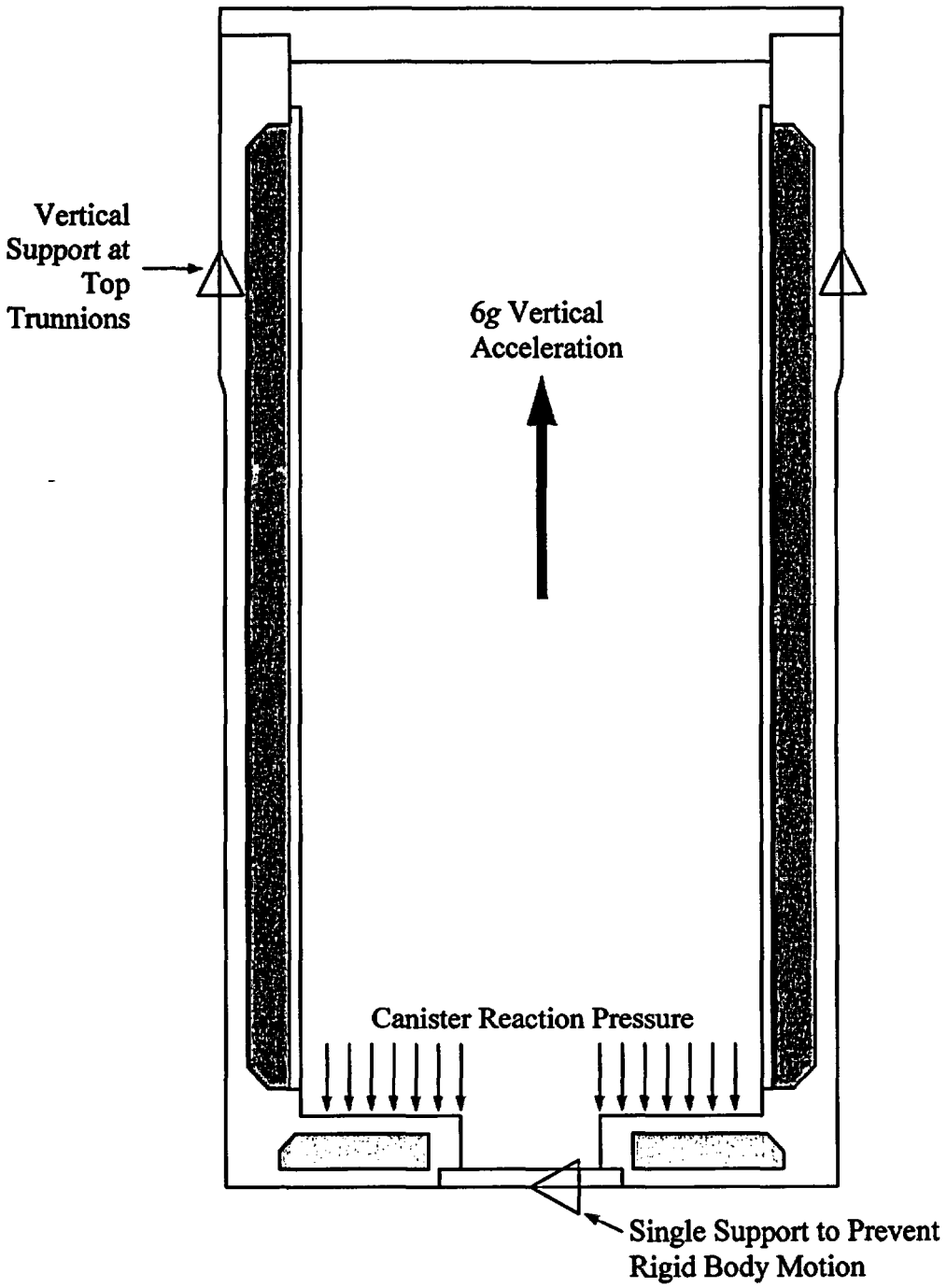

Figure 3.9.2-6
6g Lifting Boundary Conditions
(3D Model)

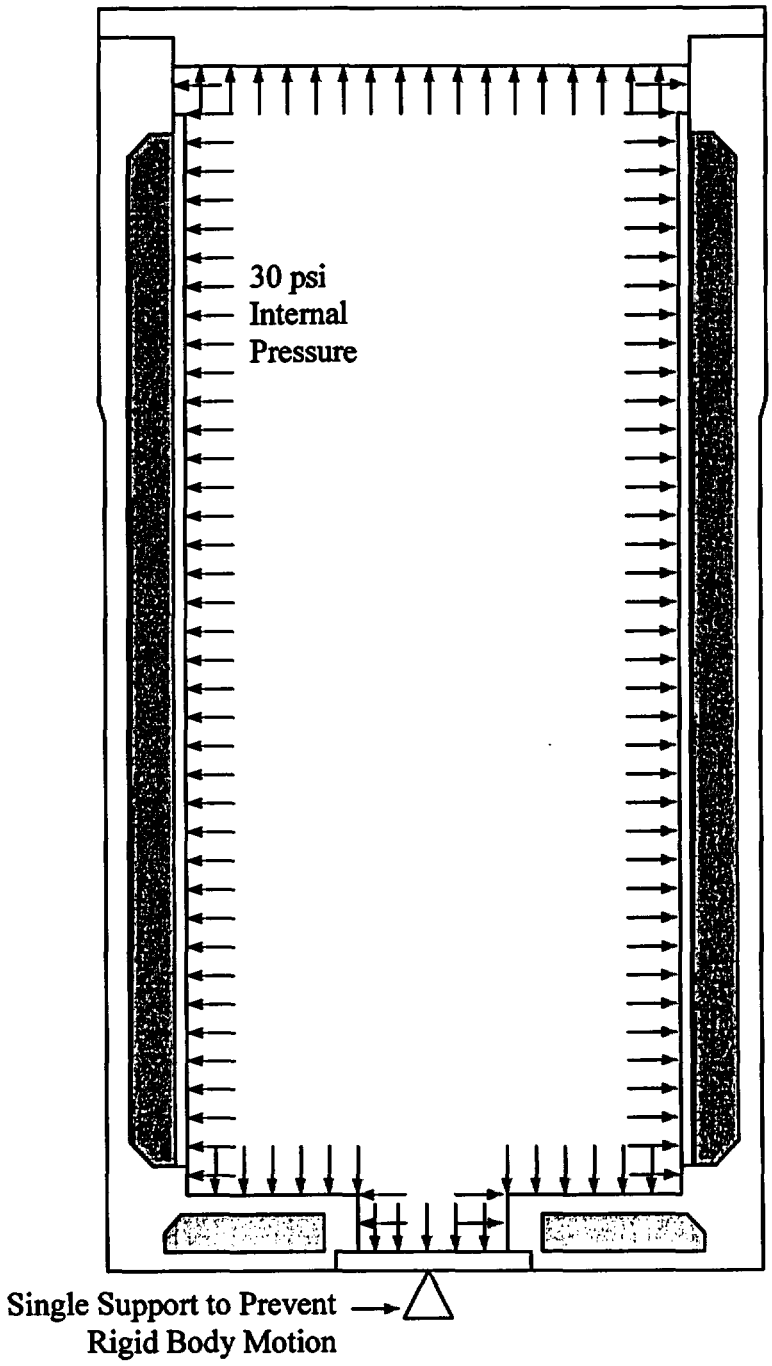

Figure 3.9.2-7
30 psi Internal Pressure Boundary Conditions
(2D Model)

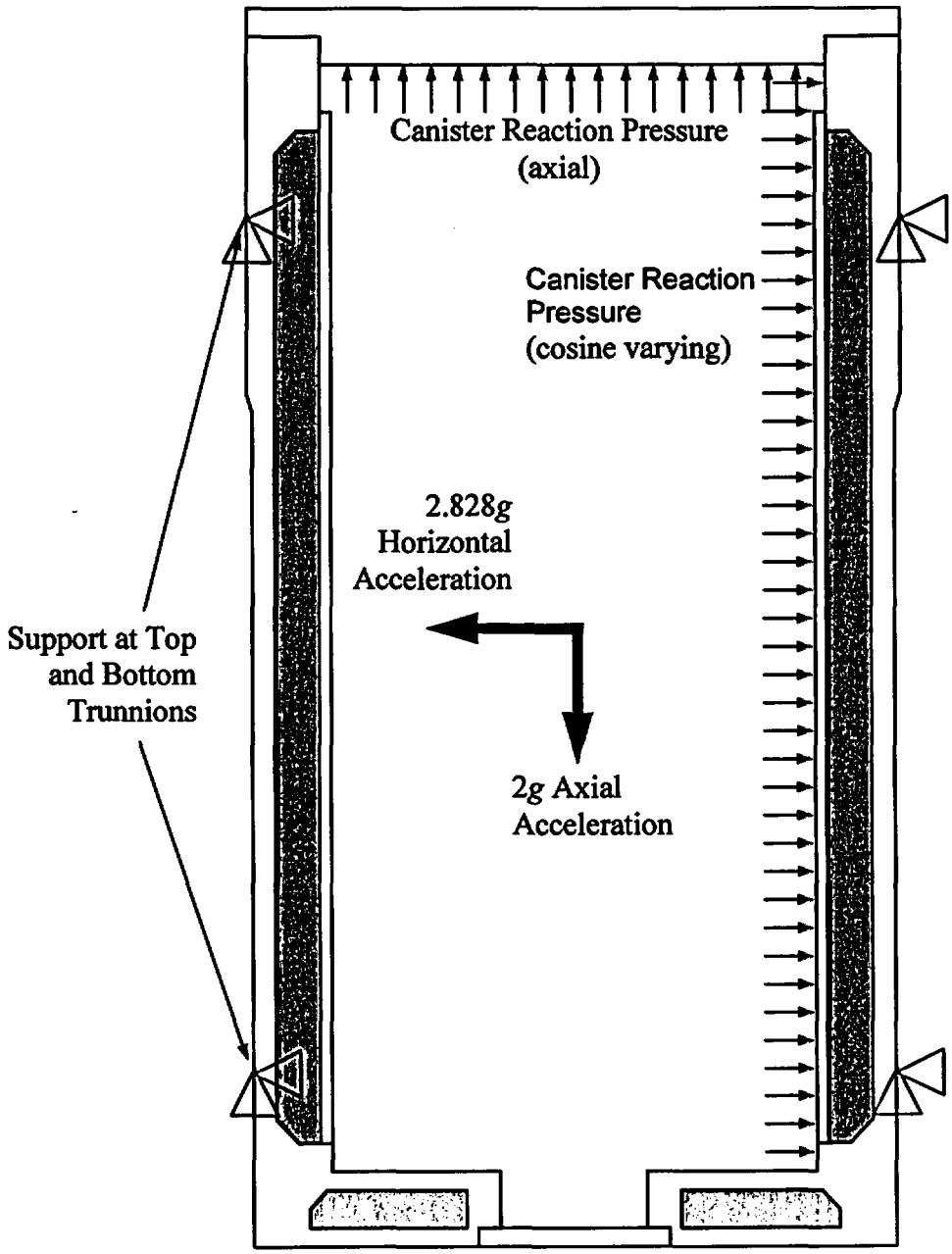

Figure 3.9.2-8
Transfer Loads Boundary Conditions
(3D Model)

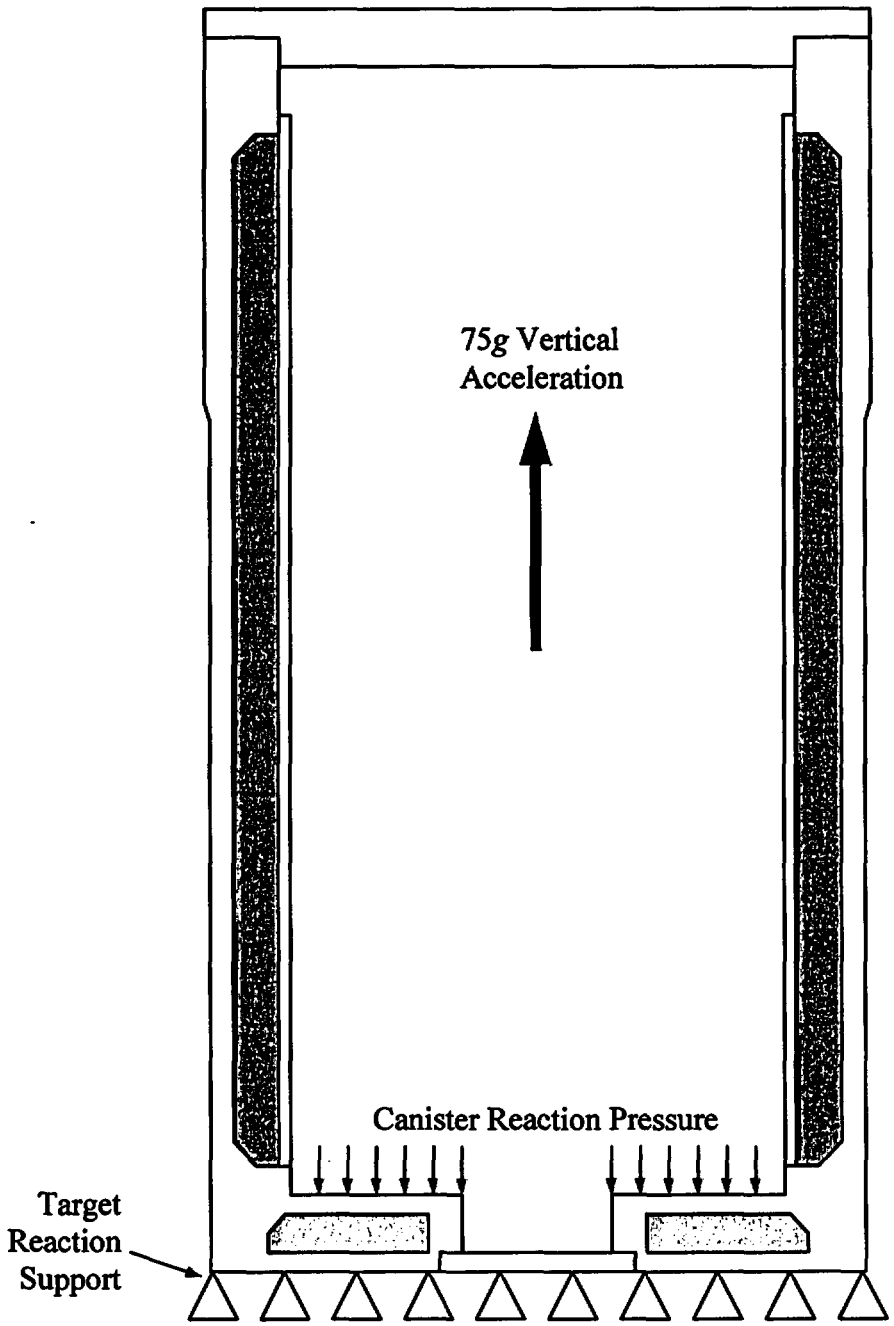

Figure 3.9.2-9
75g Bottom End Drop Boundary Conditions
(2D Model)

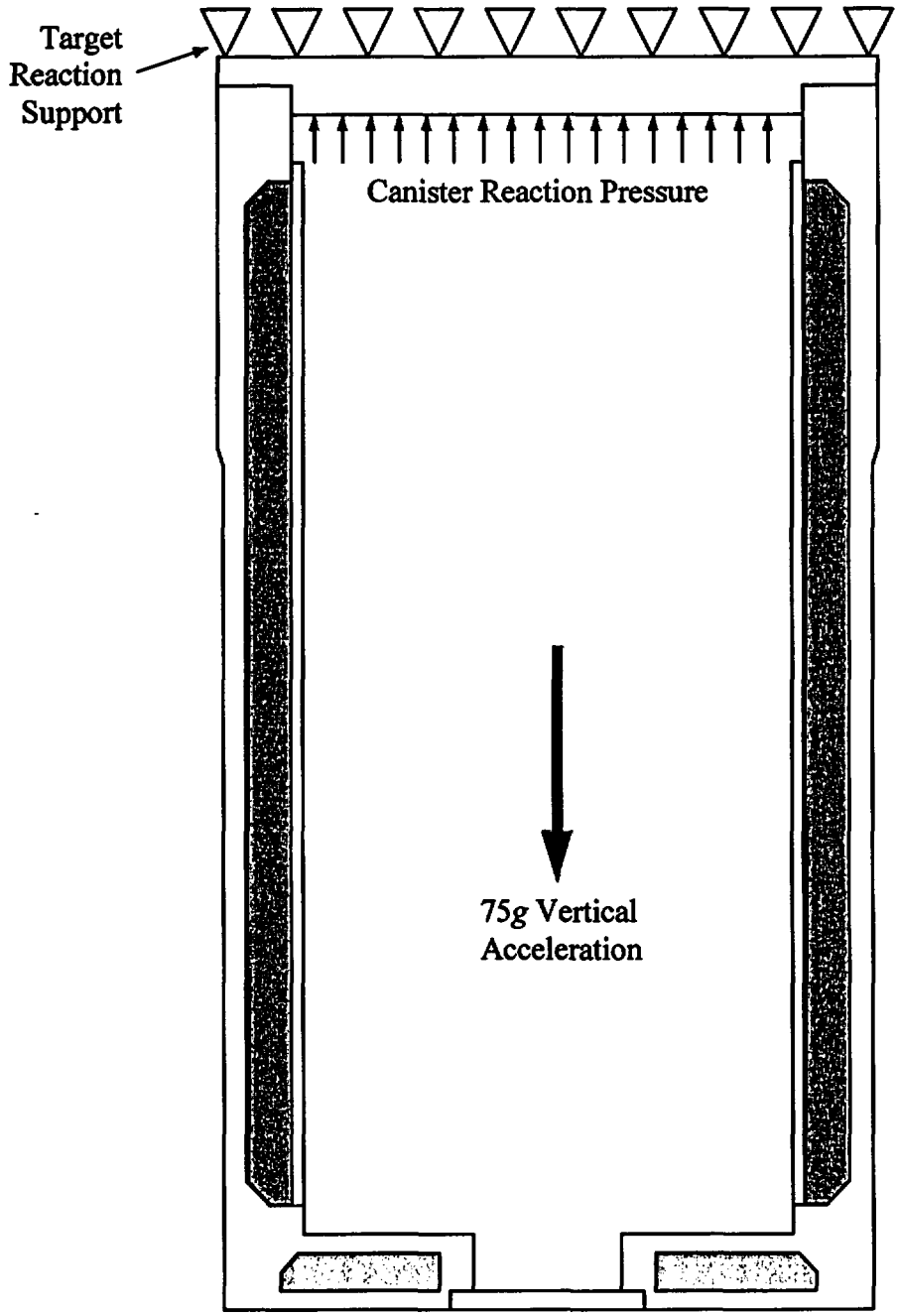

Figure 3.9.2-10
75g Top End Drop Boundary Conditions
(2D Model)

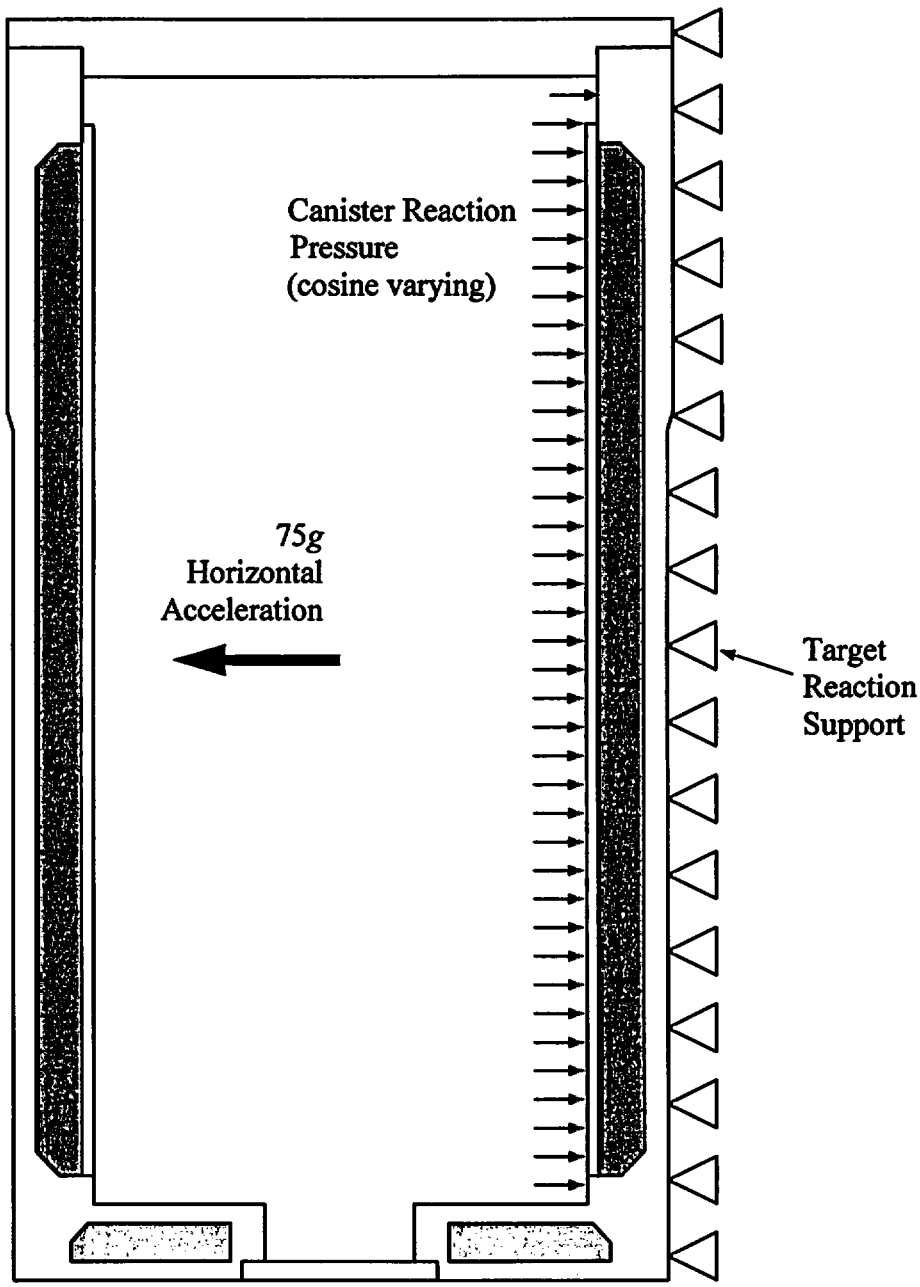

Figure 3.9.2-11
75g Side Drop Boundary Conditions
(3D Model)

1. APPLIED LOADS

RADIAL LOAD	P = _____	LB.
CIRC. MOMENT	M_c = _____	IN-LB.
LONG. MOMENT	M_L = _____	IN-LB.
TORSION MOMENT	M_T = _____	IN-LB.
SHEAR LOAD	V_c = _____	LB.
SHEAR LOAD	V_L = _____	LB.

* NOTE: ENTER ALL FORCE VALUES IN ACCORDANCE WITH SIGN CONVENTION

2. GEOMETRY

VESSEL THICKNESS	T = _____	IN.
ATTACHMENT RADIUS	r_o = _____	IN.
VESSEL RADIUS	R_m = _____	IN.

3. GEOMETRIC PARAMETERS

$\gamma = \frac{R_m}{T} =$ _____

$\beta = (0.875)\frac{r_o}{R_m} =$ _____

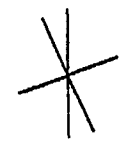

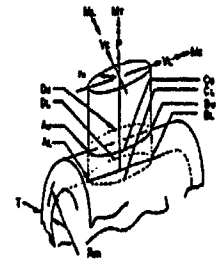

FROM FIG.	READ CURVES FOR	COMPUTE ABSOLUTE VALUES OF STRESS AND ENTER RESULT	STRESSES – IF LOAD IS OPPOSITE THAT SHOWN, REVERSE SIGNS SHOWN A_c	A_L	B_c	B_L	C_c	C_L	D_c	D_L
3C AND 4C	$\frac{M_c}{W/R_m}$ =	$\left(\frac{M_c}{W/R_m}\right)\cdot\frac{P}{R_m T}$ =	+	+	+	+	+	+	+	+
1C AND 2C-1	$\frac{M_c}{V}$ =	$\left(\frac{M_c}{V}\right)\cdot\frac{6P}{T^2}$ =	+	−	+	−	+	−	+	−
3A	$\frac{M_c}{M_c/R_m\beta}$ =	$\left(\frac{M_c}{M_c/R_m\beta}\right)\cdot\frac{M_c}{R_m\beta T}$ =					−	−	+	+
1A	$\frac{M_c}{M_c/R_m\beta}$ =	$\left(\frac{M_c}{M_c/R_m\beta}\right)\cdot\frac{6M_c}{R_m\beta T^2}$ =					−	+	+	−
3B	$\frac{M_L}{M_L/R_m\beta}$ =	$\left(\frac{M_L}{M_L/R_m\beta}\right)\cdot\frac{M_L}{R_m\beta T}$ =	−	−	+	+				
1B OR 1B-1	$\frac{M_L}{M_L/R_m\beta}$ =	$\left(\frac{M_L}{M_L/R_m\beta}\right)\cdot\frac{6M_L}{R_m\beta T^2}$ =	−	+	+	−				
ADD ALGEBRAICALLY FOR SUMMATION OF σ_θ STRESSES σ_θ =										
3C AND 4C	$\frac{M_c}{W/R_m}$ =	$\left(\frac{M_c}{W/R_m}\right)\cdot\frac{P}{R_m T}$ =	+	+	+	+	+	+	+	+
1C-1 AND 2C	$\frac{M_c}{V}$ =	$\left(\frac{M_c}{V}\right)\cdot\frac{6P}{T^2}$ =	+	−	+	−	+	−	+	−
4A	$\frac{M_c}{M_c/R_m\beta}$ =	$\left(\frac{M_c}{M_c/R_m\beta}\right)\cdot\frac{M_c}{R_m\beta T}$ =					−	−	+	+
2A	$\frac{M_c}{M_c/R_m\beta}$ =	$\left(\frac{M_c}{M_c/R_m\beta}\right)\cdot\frac{6M_c}{R_m\beta T^2}$ =					−	+	+	−
4B	$\frac{M_L}{M_L/R_m\beta}$ =	$\left(\frac{M_L}{M_L/R_m\beta}\right)\cdot\frac{M_L}{R_m\beta T}$ =	−	−	+	+				
2B OR 2B-1	$\frac{M_L}{M_L/R_m\beta}$ =	$\left(\frac{M_L}{M_L/R_m\beta}\right)\cdot\frac{6M_L}{R_m\beta T^2}$ =	−	+	+	−				
ADD ALGEBRAICALLY FOR SUMMATION OF σ_L STRESSES σ_L =										
SHEAR STRESS DUE TO TORSION M_T		$\tau_{\theta L} = \tau_{L\theta} = \frac{M_T}{2R_m T^2}$	+	+	+	+	+	+	+	+
SHEAR STRESS DUE TO LOAD V_c		$\tau_{L\theta} = \frac{V_c}{R_m T}$	+	+	−	−				
SHEAR STRESS DUE TO LOAD V_L		$\tau_{\theta L} = \frac{V_L}{R_m T}$					+	+	−	−
ADD ALGEBRAICALLY FOR SUMMATION OF SHEAR STRESSES τ =										

	LONGITUDINAL σ_L	CIRCUMFERENTIAL σ_θ
PRESSURE STRESS	$\frac{PR-0.4PT}{2T}$ = _____	$\frac{PR-0.4PT}{T}$ = _____
LONGITUDINAL BENDING STRESS	= _____	
TOTAL MEMBRANE STRESS	= _____ ≤ _____	= _____ ≤ _____
TOTAL SURFACE STRESS	= _____ ≤ _____	= _____ ≤ _____

NOZZLE NO. _____

PIPING LOAD CODE _____

ANALYSIS POINT _____

COMPUTATION SHEET FOR LOCAL STRESSES IN CYLINDRICAL SHELLS

Figure 3.9.2-12
Local Trunnion Stress Computation Sheet

APPENDIX 3.9.3
OS187H TRANSFER CASK TOP COVER AND RAM COVER BOLT ANALYSES

TABLE OF CONTENTS

3.9.3 OS187H TRANSFER CASK TOP COVER AND RAM COVER BOLT ANALYSES 3.9.3-1

3.9.3.1 Introduction 3.9.3-1

3.9.3.2 Top Cover Bolt Calculations 3.9.3-3

3.9.3.3 Top Cover Bolt Load Combinations 3.9.3-8

3.9.3.4 Top Cover Bolt Stress Calculations 3.9.3-10

3.9.3.5 Top Cover Bolt Analysis Results 3.9.3-13

3.9.3.6 Minimum Engagement Length for Top Cover Bolt and Flange 3.9.3-14

3.9.3.7 RAM Access Cover Bolt Calculations 3.9.3-16

3.9.3.8 RAM Access Cover Bolt Load Combinations 3.9.3-21

3.9.3.9 RAM Access Cover Bolt Stress Calculations 3.9.3-23

3.9.3.10 RAM Access Cover Bolt Analysis Results 3.9.3-26

3.9.3.11 Minimum Engagement Length for RAM Access Cover Bolt 3.9.3-27

3.9.3.12 Conclusions 3.9.3-29

3.9.3.13 References 3.9.3-30

LIST OF TABLES

3.9.3-1 Design Parameters for Top Cover Bolt Analysis

3.9.3-2 Design Parameters for Ram Access Cover Bolt Analysis

3.9.3-3 Bolt Data

3.9.3-4 Allowable Stresses in Closure Bolts for Normal Conditions

3.9.3-5 Allowable Stresses in Closure Bolts for Hypothetical Accident Conditions

3.9.3 OS187H TRANSFER CASK TOP COVER AND RAM ACCESS COVER BOLT ANALYSES

3.9.3.1 Introduction

This calculation evaluates the top cover bolts and RAM access cover bolts of the NUHOMS®-OS187H Transfer Cask under normal and accident conditions. Also evaluated in this calculation is the bolt thread engagement length. The stress analysis is performed in accordance with NUREG/CR-6007 [1].

The NUHOMS®-OS187H transfer cask top cover closure arrangement is shown in drawings 10494-72-16 and 17. The 3.0 inch thick cover is bolted directly to the end of the vessel top flange by 24 high strength steel 1.50 inch diameter bolts. Close fitting alignment pins ensure that the top cover is centered in the vessel. The top cover bolt material is SA-540 Gr. B24 class 1 which has a minimum yield strength of 150 ksi at room temperature [2].

The OS-187H Transfer Cask RAM access cover arrangement is shown in drawings 10494-72-16 and 18. The 1.0 inch thick cover is bolted directly to the end of the RAM access penetration ring by 12 high strength 0.50 inch diameter bolts. The RAM access cover bolt material is SA-540 Gr B24 Class 1, which has a minimum yield strength of 150 ksi at room temperature [2].

The following ways to minimize bolt forces and bolt failures for shipping casks are taken directly from NUREG/CR-6007, page xiii [1]. All of the following design methods are employed in the NUHOMS®-OS187H transfer cask closure system.

- Use materials with similar thermal properties for the closure bolts, the top cover, and the cask wall to minimize the bolt forces generated by fire accident
- Apply sufficiently large bolt preload to minimize fatigue and loosening of the bolts by vibration.
- Lubricate bolt threads to reduce required preload torque and to increase the predictability of the achieved preload.
- Use closure top cover design which minimizes the prying actions of applied loads.
- When choosing a bolt preload, pay special attention to the interactions between the preload and thermal load and between the preload and the prying action.

The following evaluations are presented in this section:

- Top over and RAM cover bolt torque
- Bolt preload
- Gasket seating load
- Pressure load
- Temperature load
- Impact load
- Thread engagement length evaluation
- Bearing stress
- Load combinations for normal and accident conditions
- Bolt stresses and allowable stresses

3.9.3.2 Top Cover Bolt Load Calculations

The design parameters of the top cover are summarized in Table 3.9.3-1. The top cover bolt data and material allowables are presented in Tables 3.9.3-3 through 3.9.3-5. A temperature of 300° F is used in the top cover bolt region during normal and accident conditions. The following load cases are considered in the analysis.

- Preload + Temperature Load (normal condition)
- Pressure Load (normal condition)
- Pressure + 80 inch Corner Drop (accident condition)

Symbols and terminology used in this analysis are taken from NUREG/CR-6007 [1] and are reproduced in Table 3.9.3-1.

3.9.3.2.1 Top Cover Bolt Preload and Bolt Torque

A bolt torque range of 450 to 580 ft. lb. has been selected.

Using the minimum torque,

$$F_a = Q/KD_b = 450\times12/(0.132\times1.50) = 27{,}270 \text{ lb., and}$$

Preload stress = F_a / Stress Area (Table 3.9.3-3) = 27,270/1.406 = 19,400 psi.

Using the maximum torque,

$$F_a = Q/KD_b = 580\times12/(0.132\times1.50) = 35{,}150\text{lb., and}$$

Preload stress = F_a / Stress Area (Table 3.9.3-3) = 35,150/1.406 = 25,000 psi.

Residual torsional moment for minimum torque of 450 ft. lb. is,

$$M_{tr} = 0.5Q = .5(450\times12) = 2{,}700 \text{ in. lb.}$$

Residual torsional moment for maximum torque of 580 ft. lb. is,

$$M_{tr} = 0.5Q = .5(580\times12) = 3{,}480 \text{ in. lb.}$$

Residual tensile bolt force for maximum torque,

$$F_{ar} = F_a = 35{,}150 \text{ lb.}$$

3.9.3.2.2 Top Cover Gasket Seating Load

Since a self energizing o-ring is used, the gasket seating load is negligible.

3.9.3.2.3 Pressure Loads ([1], Table 4.3)

Axial force per bolt due to internal pressure is

$$F_a = \frac{\pi D_{lg}^2 (P_{li} - P_{lo})}{4N_b}.$$

D_{lg} (median lid seal diameter) = 74.19 in. Then,

$$F_a = \frac{\pi(74.19^2)(30-0)}{4(24)} = 5{,}404 \text{ lb./bolt.}$$

The fixed edge closure lid force is,

$$F_f = \frac{D_{lb}(P_{li} - P_{lo})}{4} = \frac{77.70(30)}{4} = 582.8 \text{ lb. in.}^{-1}.$$

The fixed edge closure lid moment is,

$$M_f = \frac{(P_{li} - P_{lo})D_{lb}^2}{32} = \frac{30(77.70^2)}{32} = 5{,}660 \text{ in. lb. in.}^{-1}.$$

The shear bolt force per bolt is,

$$F_s = \frac{\pi E_l t_l (P_{li} - P_{lo}) D_{lb}^{\ 2}}{2N_b E_c t_c (1 - N_{ul})} = \frac{\pi(27.0\times10^6)(3.0)(30)(77.70)^2}{2(24)(27.0\times10^6)(5.575)(1-0.3)} = 9{,}113 \text{ lb./bolt.}$$

The top cover shoulder takes this shear force, so that $F_s = 0$.

3.9.3.2.4 Temperature Loads

From reference 2, the top cover bolt material is SA-540, Grade B24, which is 2 Ni 3/4Cr 1/3Mo. The top cover is constructed from of SA-240 Type XM-19, which is 23Cr 13Ni 5Mn, and the flange is constructed from of SA-240 Type 304, which is 18Cr 8Ni. Therefore the bolts have a coefficient of thermal expansion of 6.9×10^{-6} in./in.°F^{-1} at 300° F, the lid has a coefficient of thermal expansion of 8.8×10^{-6} in./in.°F^{-1} at 300° F, and the flange has a coefficient of thermal expansion of 9.2×10^{-6} in./in.°F^{-1} at 300 °F.

Therefore, the tensile load in the bolt due to different thermal expansion is,

$$F_a = 0.25\ \pi D_b^2\ E_b\ (a_l\ T_l - a_b\ T_b)$$

$$F_a = 0.25(\pi)(1.50^2)(26.7\times10^6)[(8.8\times10^{-6})(230) - (6.9\times10^{-6})(230)] = 20{,}620 \text{ lb.}$$

Even though the top cover and flange are constructed from different materials, the shear force per bolt, F_s, due to a temperature change of 230° F is, 0 psi, since the clearance holes in the lid are oversized (1.688 in. diameter) allowing the lid to grow in the radial direction.

$$F_s = 0.$$

The temperature difference between the inside and outside of the top cover will always be less than one degree (see Chapter 4). Consequently, the resulting bending moment is negligible.

$$M_f = 0.$$

3.9.3.2.5 Impact Loads ([1], Table 4.5)

The non-prying tensile bolt force per bolt, F_a, is,

$$F_a = \frac{1.34\sin(xi)(DLF)(ai)(W_l + W_c)}{N_b} = \frac{1.34\sin(xi)(1.1)(ai)(115{,}500)}{24} = 7{,}094(ai)\sin(xi) \text{ lb./bolt.}$$

Note: $W_l + W_c$ is conservatively assumed to be 115,500 lbs. [see table 3.9.3-1]

The shear bolt force is,

$$F_s = \frac{\cos(xi)(ai)(W_l)}{N_b} = \frac{5{,}500(ai)\cos(xi)}{24} = 229.2(ai)\cos(xi) \text{ lb./bolt.}$$

The lid shoulder during normal and accident condition drops takes shear force. Therefore,

$$F_s = 0.$$

The fixed-edge closure lid force, F_f, is,

$$F_f = \frac{1.34\sin(xi)(DLF)(ai)(W_l + W_c)}{\pi D_{lb}} = \frac{1.34\sin(xi)(1.1)(ai)(115{,}500)}{\pi(77.70)} = 697.4\sin(xi)(ai) \text{ lb. in.}^{-1}$$

The fixed-edge closure lid moment, M_f, is,

$$M_f = \frac{1.34\sin(xi)(DLF)(ai)(W_l + W_c)}{8\pi} = \frac{1.34\sin(xi)(1.1)(ai)(115{,}500)}{8\pi} = 6{,}774\sin(xi)(ai) \text{ in.lb.in}^{-1}$$

The accident condition impact load is taken to be the axial acceleration due to corner drop. The following accident condition corner drop acceleration and impact angle bound the 15.9*g* C.G. over corner drop acceleration computed in Appendix 3.9.7.

$$ai = 25\ gs, \text{ and } xi = 60°$$

Therefore,

$F_a = 7{,}094 \times 25 \times \sin(60°) = 153{,}600$ lb./bolt

$F_s = 0$ lb./bolt

$F_f = 697.4 \times 25 \times \sin(60°) = 15{,}100$ lb./bolt, and

$M_f = 6{,}774 \times 25 \times \sin(60°) = 146{,}700$ lb./bolt.

The top cover individual load is summarized in the following table.

Top Cover Bolt Individual Load Summary

Load Case	Applied Load		Non-Prying Tensile Force, F_a (lb.)	Torsional Moment, M_t (in. lb.)	Prying Force, F_f (lb.in.$^{-1}$)	Prying Moment, M_f (in. lb. in.$^{-1}$)
Preload	Residual	Minimum Torque	27,270	2,700	0	0
		Maximum Torque	35,150	3,480	0	0
Gasket	Seating Load		0	0	0	0
Pressure	50 psig Internal		5,404	0	582.8	5,660
Thermal	300°F		20,620	0	0	0
Impact	Accident Condition Drop		153,600	0	15,100	146,700

3.9.3.3 Top Cover Bolt Load Combinations ([1], Table 4.9)

A summary of normal and accident condition load combinations is presented in the following table.

Top Cover Bolt Normal and Accident Load Combinations

Load Case	Combination Description		Non-Prying Tensile Force, F_a (lb.)	Torsional Moment, M_t (in. lb.)	Prying Force, F_f (lb.in.$^{-1}$)	Prying Moment, M_f (in. lb. in.$^{-1}$)
1.	Preload + Temperature (Normal Condition)	Minimum Torque	47,890	2,700	0	0
		Maximum Torque	55,770	3,480	0	0
2.	Pressure (Normal Condition)		5,404	0	582.8	5,660
3.	Pressure + Accident Impact (Accident Condition)		159,000	0	15,680	152,400

Additional Prying Bolt Force

It is shown in the above table, Top Cover Bolt Normal and Accident Load Combinations, that all loading conditions cause outward acting loads only. Outward acting loads generate no additional prying bolts forces, because the gap between the lid and flange at the outer edge prevents the creation of a prying moment.

Bolt Bending Moment ([1], Table 2.2)

The maximum bending bolt moment, M_{bb}, generated by the applied load is evaluated as follows:

$$M_{bb} = \left(\frac{\pi D_{lb}}{N_b}\right)\left[\frac{K_b}{K_b + K_l}\right]M_f$$

The K_b and K_l are based on geometry and material properties and are defined in Reference 1, Table 2.2. By substituting the values given above,

$$K_b = \left(\frac{N_b}{L_b}\right)\left(\frac{E_b}{D_{lb}}\right)\left(\frac{D_b^4}{64}\right) = \left(\frac{24}{1.5}\right)\left(\frac{26.7\times10^6}{77.70}\right)\left(\frac{1.50^4}{64}\right) = 4.349 \times 10^5, \text{ and}$$

$$K_l \frac{E_l t_l^3}{3\left[\left(1-N_{ul}^2\right)+\left(1-N_{ul}\right)^2\left(\frac{D_{lb}}{D_{lo}}\right)^2\right]D_{lb}} = \frac{27.0\times10^6(3.0^3)}{3\left[\left(1-0.3^2\right)+\left(1-0.3\right)^2\left(\frac{77.70}{82.20}\right)^2\right]77.70}$$

$$= 2.320 \times 10^6$$

Therefore,

$$M_{bb} = \left(\frac{\pi 77.70}{24}\right)\left[\frac{4.349\times10^5}{4.349\times10^5 + 2.320\times10^6}\right]M_f = 1.606\, M_f.$$

For load case 2, M_f = 5,660 in. lb. Substituting this value into the equation above gives,

M_{bb} = 9,090 in. lb. / bolt.

3.9.3.4 Top Cover Bolt Stress Calculations ([1], Table 5.1)

3.9.3.4.1 Average Tensile Stress

A summary of the applied loads for the transfer cask lid bolts is provided in the Top Cover Bolt Normal and Accident Load Combinations Table on page 3.9.3-8.

For the normal condition load cases, the applied bolt preload maintains closure of the transfer cask top cover. The closure force per bolt generated by the minimum lid bolt torque, with or without the additional closure force generated by thermal loads, is greater than the normal condition forces trying to open the top cover.

For accident conditions, the impact loads may instantaneously relax pressure on the top cover seals. However the accident condition loads will not cause lid bolt failure, as shown below and immediately following the accident impact, the top closure seal will be reseated by the bolt preload.

Normal Condition

$$S_{ba} = 1.2732\frac{F_a}{D_{ba}^2} = 1.2732\frac{55{,}770}{1.378^2} = 37{,}390\,\text{psi.} = 37.4\ \text{ksi.}$$

Accident Condition

$$S_{ba} = 1.2732\frac{F_a}{D_{ba}^2} = 1.2732\frac{159{,}000}{1.378^2} = 106{,}600\,\text{psi.} = 106.6\ \text{ksi.}$$

3.9.3.4.2 Bending Stress

Normal Condition

$$S_{bb} = 10.186\frac{M_{bb}}{D_{ba}^3} = 10.186\frac{9{,}090}{1.378^3} = 35{,}390\,\text{psi.} = 35.4\ \text{ksi.}$$

3.9.3.4.3 Shear Stress

For both normal and accident conditions, the average shear stress caused by shear bolt force F_s is,

$$S_{bs} = 0.$$

For normal and accident conditions the maximum shear stress caused by the torsional moment M_t is,

$$S_{bt} = 5.093\frac{M_t}{D_{ba}^3} = 5.093\frac{3{,}480}{1.378^3} = 6{,}773\,\text{psi.} = 6.8\text{ ksi.}$$

3.9.3.4.4 Maximum Combined Stress Intensity

The maximum combined stress intensity is calculated in the following way (Ref. 1, Table 5.1).

$$S_{bi} = [(S_{ba} + S_{bb})^2 + 4(S_{bs} + S_{bt})^2]^{0.5}$$

For normal conditions combine tension, shear, bending, and residual torsion.

$$S_{bi} = [(37{,}390 + 35{,}390)^2 + 4\,(0 + 6{,}773)^2]^{0.5} = 74{,}030\text{ psi.} = 74.0\text{ ksi.}$$

3.9.3.4.5 Stress Ratios

In order to meet the stress ratio requirement, the following relationship must hold for both normal and accident conditions.

$$R_t^2 + R_s^2 < 1$$

Where R_t is the ratio of average tensile stress to allowable average tensile stress, and R_s is the ratio of average shear stress to allowable average shear stress.

For normal conditions

$$R_t = 37{,}390/92{,}400 = 0.405,$$

$$R_s = 6{,}773/55{,}400 = 0.122,$$

$$R_t^2 + R_s^2 = (0.405)^2 + (0.122)^2 = 0.179 < 1.$$

For accident conditions

$$R_t = 106{,}600/115{,}500 = 0.923,$$

$$R_s = 6{,}773/69{,}300 = 0.098,$$

$$R_t^2 + R_s^2 = (0.923)^2 + (0.098)^2 = 0.862 < 1.$$

3.9.3.4.6 Bearing Stress (Under Bolt Head)

A standard 1.50 in. washer placed under the head of each top cover bolt. The inside and outside diameter of a standard 1.50 in. washer is 1.50 in. and 3.00 in. respectively. The diameter of the bolt clearance hole in the top cover is 1.688 in. Therefore, the total bearing area under the top cover bolts, A_b, is the following.

$$A_b = (\pi/4)\ [\ 3.00^2 - 1.688^2\ ] = 4.831 \text{ in.}^2$$

According to Reference 1, bearing stresses are only required to be evaluated for normal condition loads. For normal conditions, the maximum bearing stress under the washer, σ_b, is the following.

$$\sigma_b = 55{,}770 \text{ lb.} / 4.831 \text{ in.}^2 = 11{,}540 \text{ psi.}$$

The normal condition allowable bearing stress on the cover is taken to be the yield stress of the cover material at 300° F. The cover is manufactured out of SA-240 Type XM-19, which has a yield stress of 43.3 ksi. at 300° F.

3.9.3.5 Top Cover Bolt Analysis Results

A summary of the stresses calculated above is listed in the following table:

Summary of Top Cover Bolt Stresses and Allowables

Stress Type	Normal Condition		Accident Condition	
	Stress	Allowable	Stress	Allowable
Average Tensile (ksi.)	37.4	92.4	106.6	115.5
Shear (ksi)	6.8	55.4	6.8	69.3
Combined (ksi)	74.0	124.7	Not Required [1]	
Interaction Equation $R_t^2 + R_s^2 < 1$	0.179	1	0.862	1
Bearing (ksi) Allowable (ksi) (S_y of lid material)	11.5	43.3	Not Required [1]	

3.9.3.6 Minimum Engagement Length for Top Cover Bolt and Flange

For a 1 1/2"– 8UN – 2A bolt, the material is SA-540 GR. B24 CL.1, with

S_u = 165 ksi., and
S_y = 150 ksi (at room temperature)

The helicoil insert is neglected in the thread engagement length computation. It is conservative to neglect the helicoil insert, because it has a much higher tensile strength (200 ksi. [3] than the flange material. The flange material is constructed from type 304 stainless steel and has the following material properties.

S_u = 75 ksi., and

S_y = 30 ksi (at room temperature)

The minimum engagement length, L_e, for the bolt and flange is [4],

$$L_e = \frac{2A_t}{3.1416K_{n\max}\left[\frac{1}{2}+.57735n\left(E_{s\min}-K_{n\max}\right)\right]}.$$

Where,

A_t = tensile stress area = 1.491 in.^{2},
n = number of threads per inch = 8,
$K_{n\,max}$ = maximum minor diameter of internal threads = 1.390 in. [4]
$E_{s\,min}$ = minimum pitch diameter of external threads = 1.4093 in. [4]

Substituting the values given above,

$$L_e = \frac{2(1.491)}{(3.1416)1.390\left[\frac{1}{2}+.57735(8)(1.4093-1.390)\right]} = 1.159 \text{ in.}$$

$$J = \frac{A_s \times S_{ue}}{A_n \times S_{ui}}. \text{ [5]}$$

Where, S_{ue} is the tensile strength of external thread material, and S_{ui} is the tensile strength of internal thread material.

A_s = shear area of external threads = $3.1416\, nL_e\, K_{n\,max}\, [1/(2n) + .57735\, (E_{s\,min} - K_{n\,max})]$

A_n = shear area of internal threads = $3.1416\, nL_e\, D_{s\,min}\, [1/(2n) + .57735(D_{s\,min} - E_{n\,max})]$

For the bolt / Helicoil insert connection:

$E_{n\,max}$ = maximum pitch diameter of internal threads = 1.4283 in. [4]
$D_{s\,min}$ = minimum major diameter of external threads = 1.4828 in. [4]

Therefore,

$$A_s = 3.1416(8)(1.159)(1.390)[1/(2\times8) + .57735\,(1.4093 - 1.390)] = 2.982 \text{ in.}^2$$

$$A_n = 3.1416(8)(1.159)(1.4828)[1/(2\times8) + .57735\,(1.4828 - 1.4283)] = 4.059 \text{ in.}^2$$

So,

$$J = \frac{2.982(165.0)}{4.059(75.0)} = 1.616$$

$$Q = L_e J = (1.159)(1.616) = 1.873 \text{ in.}$$

The actual minimum engagement length:

4.50 in. bolt length – 1.50 in. cover thickness – 0.180 in. washer thickness = 2.82 in. > 1.873 in.

3.9.3.7 RAM Access Cover Bolt Calculations

The design parameters of the RAM access cover bolts are summarized in Table 3.9.3-2. The RAM access cover bolt data and material allowables are presented in Tables 3.9.3-3 through 3.9.3-5. A temperature of 300° F is used in the RAM access cover bolt region during normal and accident conditions. The following load cases are considered in the analysis.

- Preload + Temperature Load (normal condition)
- Pressure Load (normal condition)
- Pressure + 80 inch Corner Drop (accident condition)

Symbols and terminology used in this analysis are taken from NUREG/CR-6007 [1] and are reproduced in Table 3.9.3-2.

3.9.3.7.1 RAM Access Cover Bolt Preload and Bolt Torque

A bolt torque range of 15 to 20 ft. lb. has been selected.

Using the minimum torque,

$$F_a = Q/KD_b = 15\times12/(0.132\times0.50) = 2{,}727 \text{ lb., and}$$

Preload stress = F_a / Stress Area (Table 3.9.3-3) = 2,727 /0.142 = 19,204 psi.

Using the maximum torque,

$$F_a = Q/KD_b = 20\times12/(0.132\times0.50) = 3{,}636 \text{ lb., and}$$

Preload stress = F_a / Stress Area (Table 3.9.3-3) = 3,636/0.142 = 25,610 psi.

Residual torsional moment for minimum torque of 15 ft. lb. is,

$$M_{tr} = 0.5Q = .5(15\times12) = 90 \text{ in. lb.}$$

Residual torsional moment for maximum torque of 20 ft. lb. is,

$$M_{tr} = 0.5Q = .5(20\times12) = 120 \text{ in. lb.}$$

Residual tensile bolt force for maximum torque,

$$F_{ar} = F_a = 3{,}636 \text{ lb.}$$

3.9.3.7.2 RAM Access Cover Gasket Seating Load

Since a self energizing o-ring is used, the gasket seating load is negligible.

3.9.3.7.3 Pressure Loads ([1], Table 4.3)

Axial force per bolt due to internal pressure is

$$F_a = \frac{\pi D_{lg}^2 (P_{li} - P_{lo})}{4N_b}.$$

D_{lg} (median cover seal diameter) = 21.16 in. Then,

$$F_a = \frac{\pi(21.16^2)(30-0)}{4(12)} = 879.1 \text{ lb./bolt.}$$

The fixed edge cover force is,

$$F_f = \frac{D_{lb}(P_{li} - P_{lo})}{4} = \frac{23.50(30)}{4} = 176.3 \text{ lb. in.}^{-1}.$$

The fixed edge cover moment is,

$$M_f = \frac{(P_{li} - P_{lo})D_{lb}^2}{32} = \frac{30(23.50^2)}{32} = 517.7 \text{ in. lb. in.}^{-1}.$$

The shear bolt force per bolt is,

$$F_s = \frac{\pi E_l t_l (P_{li} - P_{lo}) D_{lb}{}^2}{2N_b E_c t_c (1 - N_{ul})} = \frac{\pi(27.0\times10^6)(1.0)(30)(23.50)^2}{2(12)(27.0\times10^6)(4.0)(1-0.3)} = 774.5 \text{ lb./bolt.}$$

The radial growth of the access ring due to an internal pressure of 30 psi is, δ_r, is given by the following equation.

$$\delta_r = \frac{Pr^2}{Et}$$

Where, P is the applied pressure (30 psi.), r is the mean radius of the RAM access penetration (12.00 in.), E is the material modulus of elasticity (27.0×10^6 psi. @ 300° F [2]), and t is the radial thickness of the penetration (4.00 in.). Therefore,

$$\delta_r = \frac{(30)(12.00)^2}{(27\times10^6)(4.00)} = 4.00\times10^{-5} \text{ in.}$$

Since the radial growth due to internal pressure is less than the RAM access bolt clearance (0.563 in. – ½ in. bolt = 0.063 in.), no shear force is generated in the RAM access cover bolts. Therefore,

$$F_s = 0.$$

3.9.3.7.4 Temperature Loads

The cover bolt material is SA-540 Grade B24 Class 1, which is 2Ni ¾ Cr 1/3 Mo. The RAM access penetration and cover are both constructed from of SA-240 Type 304, which is 18Cr 8Ni. Therefore the bolts have a coefficient of thermal expansion of 6.9×10^{-6} in./in. °F^{-1} at 300° F, the RAM access penetration and cover has a coefficient of thermal expansion of 9.2×10^{-6} in./in. °F^{-1} at 300° F. The tensile load in the bolt due to different thermal expansion is,

$$F_a = 0.25\ \pi D_b^2\ E_b\ (a_l\ T_l - a_b\ T_b)$$

$$F_a = 0.25(\pi)(0.50^2)(26.7\times10^6)[(9.2\times10^{-6})(230) - (6.9\times10^{-6})(230)] = 2{,}773 \text{ lb./bolt}$$

The shear force per bolt, F_s, due to a temperature change of 230° F is 0 lb, since there is negligible differential thermal expansion between the RAM access penetration and cover, which are both constructed from the same material, and since the clearance holes in the cover are oversized (0.563 in. diameter). Therefore,

$$F_s = 0.$$

The temperature difference between the inside and outside of the cover will always be less than one degree (see Chapter 4). Consequently, the resulting bending moment is negligible.

$$M_f = 0.$$

3.9.3.7.5 Impact Loads ([1], Table 4.5)

The DSC inside the NUHOMS®-OS187H Transfer Cask is supported in the axial direction at the bottom of the cask by the bottom end plate. During a free drop event, the inertial load of the transfer cask internals is transferred through the bottom end plate, bottom neutron shield, and neutron shield plate to the impact target. Consequently, only the inertial load of the RAM access cover itself generates loads in the bolts.

The non-prying tensile bolt force per bolt, F_a, is,

$$F_a = \frac{1.34\sin(xi)(DLF)(ai)(W_l + W_c)}{N_b} = \frac{1.34\sin(xi)(1.1)(ai)(200)}{12} = 24.57(ai)\sin(xi)\text{ lb./bolt.}$$

Note: $W_l + W_c$ is assumed to be only the weight of the RAM access cover, $W_c = 200$ lbs. [see table 3.9.3-2]

The shear bolt force is,

$$F_s = \frac{\cos(xi)(ai)(W_l)}{N_b} = \frac{200(ai)\cos(xi)}{12} = 16.67(ai)\cos(xi)\text{ lb./bolt.}$$

The fixed-edge cover force, F_f, is,

$$F_f = \frac{1.34\sin(xi)(DLF)(ai)(W_l + W_c)}{\pi D_{lb}} = \frac{1.34\sin(xi)(1.1)(ai)(200)}{\pi(23.50)} = 3.993\sin(xi)(ai)\text{ lb. in.}^{-1}$$

The fixed-edge cover moment, M_f, is,

$$M_f = \frac{1.34\sin(xi)(DLF)(ai)(W_l + W_c)}{8\pi} = \frac{1.34\sin(xi)(1.1)(ai)(200)}{8\pi} = 11.73\sin(xi)(ai)\text{ in.lb.in}^{-1}$$

The accident condition impact load is taken to be the axial acceleration due to corner drop. The following accident condition corner drop acceleration and impact angle bound the 15.9g C.G. over corner drop acceleration computed in Appendix 3.9.7.

$$ai = 25\ gs, \text{ and } xi = 60°$$

Therefore,

$F_a = 24.57 \times 25 \times \sin(60°) = 531.9$ lb./bolt
$F_s = 16.67 \times 25 \times \cos(60°) = 208.4$ lb./bolt,
$F_f = 3.993 \times 25 \times \sin(60°) = 86.45$ lb./in., and
$M_f = 11.73 \times 25 \times \sin(60°) = 254.0$ in.lb./in.

The ram cover bolt individual load is summarized in the following table.

Ram Access Cover Bolt Individual Load Summary

Load Case	Applied Load		Non-Prying Tensile Force, F_a (lb.)	Torsional Moment, M_t (in. lb.)	Shear Force, F_s (lb.)	Prying Force, F_f (lb.in.$^{-1}$)	Prying Moment, M_f (in. lb. in.$^{-1}$)
Preload	Residual	Minimum Torque	2,727	90	0	0	0
		Maximum Torque	3,636	120	0	0	0
Gasket	Seating Load		0	0	0	0	0
Pressure	30 psig Internal		879.1	0	0	176.3	517.7
Thermal	300°F		2,773	0	0	0	0
Impact	Accident Condition Drop		531.9	0	208.4	86.45	254.0

3.9.3.8 RAM Access Cover Bolt Load Combinations ([1], Table 4.9)

A summary of normal and accident condition load combinations is presented in the following table.

Ram Access Cover Bolt Normal And Accident Load Combinations

Load Case	Combination Description		Non-Prying Tensile Force, F_a (lb.)	Torsional Moment, M_t (in. lb.)	Shear Force, F_s (lb.)	Prying Force, F_f (lb.in.$^{-1}$)	Prying Moment, M_f (in. lb. in.$^{-1}$)
1.	Preload + Temperature (Normal Condition)	Minimum Torque	5,500	90	0	0	0
		Maximum Torque	6,409	120	0	0	0
2.	Pressure (Normal Condition)		879.1	0	0	176.3	517.7
3.	Pressure + Accident Impact (Accident Condition)		1,411	0	208.4	262.8	771.7

Additional Prying Bolt Force

It is shown in the above table, Ram Access Cover Bolt Normal and Accident Load Combinations, that all loading conditions cause outward acting loads only. Outward acting loads generate no additional prying bolts forces, because the gap between the cover and the ram access penetration ring at the outer edge prevents the creation of a prying moment.

Bolt Bending Moment ([1], Table 2.2)

The maximum bending bolt moment, M_{bb}, evaluated for normal conditions only, is evaluated as follows:

$$M_{bb} = \left(\frac{\pi D_{lb}}{N_b}\right)\left[\frac{K_b}{K_b + K_l}\right]M_f$$

The K_b and K_l are based on geometry and material properties and are defined in Reference 1, Table 2.2. By substituting the values given above,

$$K_b = \left(\frac{N_b}{L_b}\right)\left(\frac{E_b}{D_{lb}}\right)\left(\frac{D_b^4}{64}\right) = \left(\frac{12}{0.34}\right)\left(\frac{26.7\times10^6}{23.50}\right)\left(\frac{0.50^4}{64}\right) = 3.916\times10^4, \text{ and}$$

$$K_l = \frac{E_l t_l^3}{3\left[\left(1-N_{ul}^2\right)+\left(1-N_{ul}\right)^2\left(\frac{D_{lb}}{D_{lo}}\right)^2\right]D_{lb}} = \frac{27.0\times10^6(1.00^3)}{3\left[\left(1-0.3^2\right)+\left(1-0.3\right)^2\left(\frac{23.50}{25.45}\right)^2\right]23.50}$$

$$= 2.884\times10^5$$

Therefore,

$$M_{bb} = \left(\frac{\pi 23.50}{12}\right)\left[\frac{3.619\times10^4}{3.619\times10^4 + 2.884\times10^5}\right]M_f = 0.7355\,M_f.$$

For load case 2, M_f = 517.7 in.lb./in. Substituting this value into the equation above gives,

M_{bb} = 380.8 in. lb. / bolt.

3.9.3.9 RAM Access Cover Bolt Stress Calculations ([1], Table 5.1)

3.9.3.9.1 Average Tensile Stress

A summary of the applied loads for the transfer cask RAM access cover bolts is provided in the Ram Access Cover Bolt Normal and Accident Load Combinations Table on page 3.9.3-21.

For both normal and accident condition load cases, the applied bolt preload maintains closure of the transfer cask RAM access cover. The closure force per bolt generated by the minimum RAM access cover bolt torque, with or without the additional closure force generated by thermal loads, is greater than all loads trying to open the RAM access cover.

Normal Condition

$$S_{ba} = 1.2732\frac{F_a}{D_{ba}^2} = 1.2732\frac{6{,}409}{0.425^2} = 45{,}180\,\text{psi.} = 45.2\text{ ksi.}$$

Accident Condition

$$S_{ba} = 1.2732\frac{F_a}{D_{ba}^2} = 1.2732\frac{6{,}409}{0.425^2} = 45{,}180\,\text{psi.} = 45.2\text{ ksi.}$$

3.9.3.9.2 Bending Stress

Normal Condition

$$S_{bb} = 10.186\frac{M_{bb}}{D_{ba}^3} = 10.186\frac{380.8}{0.425^3} = 50{,}530\,\text{psi.} = 50.5\text{ ksi.}$$

3.9.3.9.3 Shear Stress

For normal conditions, the average shear stress caused by shear bolt force F_s is,

$$S_{bs} = 0.$$

For accident conditions, the average shear stress caused by shear bolt force F_s is,

$$S_{bs} = 1.2732\frac{F_s}{D_{ba}^{\ 2}} = 1.2732\frac{208.4}{0.425^2} = 1{,}469\text{ psi.} = 1.5\text{ ksi.}$$

For normal and accident conditions the maximum shear stress caused by the torsional moment M_t is,

$$S_{bt} = 5.093\frac{M_t}{D_{ba}^3} = 5.093\frac{120}{0.425^3} = 7{,}961\text{ psi.} = 8.0\text{ ksi.}$$

3.9.3.9.4 Maximum Combined Stress Intensity

The maximum combined stress intensity is calculated in the following way (Ref. 1, Table 5.1).

$$S_{bi} = [(S_{ba} + S_{bb})^2 + 4(S_{bs} + S_{bt})^2]^{0.5}$$

For normal conditions combine tension, shear, bending, and residual torsion.

$$S_{bi} = [(45{,}180 + 50{,}530)^2 + 4\,(0 + 7{,}961)^2]^{0.5} = 97{,}030\text{psi.} = 97.0\text{ ksi.}$$

3.9.3.9.5 Stress Ratios

In order to meet the stress ratio requirement, the following relationship must hold for both normal and accident conditions.

$$R_t^2 + R_s^2 < 1$$

Where R_t is the ratio of average tensile stress to allowable average tensile stress, and R_s is the ratio of average shear stress to allowable average shear stress.

For normal conditions

$$R_t = 45{,}180/92{,}400 = 0.740,$$

$$R_s = 0/55{,}400 = 0,$$

$$R_t^2 + R_s^2 = (0.740)^2 + (0)^2 = 0.548 < 1.$$

For accident conditions

$$R_t = 45{,}180/115{,}500 = 0.531,$$

$$R_s = 1{,}469/69{,}300 = 0.021,$$

$$R_t^2 + R_s^2 = (0.531)^2 + (0.021)^2 = 0.282 < 1.$$

3.9.3.9.6 Bearing Stress (Under Bolt Head)

A ½ in. standard washer is placed under the head of each RAM access cover bolt. The inside and outside diameter the washer is 0.531 in. and 1.062 in. respectively. The diameter of the bolt clearance hole in the cover is 0.563 in. Therefore, the total bearing area under the top cover bolts, A_b, is the following.

$$A_b = (\pi/4)\ [\ 1.062^2 - 0.563^2\ ] = 0.637 \text{ in.}^2$$

According to Reference 1, bearing stresses are only required to be evaluated for normal condition loads. For normal conditions, the maximum bearing stress under the washer, σ_b, is the following.

$$\sigma_b = 6{,}409 \text{ lb.} / 0.637 \text{ in.}^2 = 10{,}060 \text{ psi.}$$

The normal condition allowable bearing stress on the cover is taken to be the yield stress of the cover material at 300° F. The cover is manufactured out of SA-240 Type 304, which has a yield stress of 22.4 ksi. at 300° F.

3.9.3.10 RAM Access Cover Bolt Analysis Results

A summary of the stresses calculated above is listed in the following table:

Summary Of Stresses And Allowables

Stress Type	Normal Condition		Accident Condition	
	Stress	Allowable	Stress	Allowable
Average Tensile (ksi.)	45.2	92.4	45.2	115.5
Shear (ksi)	8.0	55.4	9.5	69.3
Combined (ksi)	90.7	124.7	Not Required [1]	
Interaction E.Q. $R_t^2 + R_s^2 < 1$	0.548	1	0.282	1
Bearing (ksi) Allowable (ksi) (S_y of lid material)	10.1	22.4	Not Required [1]	

3.9.3.11 Minimum Engagement Length for RAM Access Cover Bolt

For a 1/2"– 13UNC – 2A bolt, the material is SA-540 GR. B24 CL.1, with

S_u = 165 ksi., and
S_y = 150 ksi (at room temperature)

The RAM access penetration and threaded insert material are both constructed from type 304 stainless steel and have the following material properties.

S_u = 75 ksi., and
S_y = 30 ksi (at room temperature)

The minimum engagement length, L_e, for the bolt and flange is [4],

$$L_e = \frac{2A_t}{3.1416K_{n\max}\left[\frac{1}{2}+.57735n(E_{s\min}-K_{n\max})\right]}.$$

Where,

A_t = tensile stress area = 0.142 in.^{2},
n = number of threads per inch = 13
$K_{n\,max}$ = maximum minor diameter of internal threads = 0.434 in. [4]
$E_{s\,min}$ = minimum pitch diameter of external threads = 0.4435 in. [4]

Substituting the values given above,

$$L_e = \frac{2(0.142)}{(3.1416)0.434\left[\frac{1}{2}+.57735(13)(0.4435-0.434)\right]} = 0.365 \text{ in.}$$

$$J = \frac{A_s \times S_{ue}}{A_n \times S_{ui}} \quad [4]$$

Where, S_{ue} is the tensile strength of external thread material, and S_{ui} is the tensile strength of internal thread material.

A_s = shear area of external threads = 3.1416 $nL_e K_{n\,max}$ [1/(2n) + .57735 ($E_{s\,min} - K_{n\,max}$)]

A_n = shear area of internal threads = 3.1416 $nL_e D_{s\,min}$ [1/(2n) + .57735($D_{s\,min} - E_{n\,max}$)]

For the bolt / Helicoil insert connection:

$E_{n\,max}$ = maximum pitch diameter of internal threads = 0.4565 in. [4]
$D_{s\,min}$ = minimum major diameter of external threads = 0.4876 in. [4]

Therefore,

$$A_s = 3.1416(13)(0.365)(0.434)[1/(2\times13) + .57735\,(0.4435 - 0.434)] = 0.2843 \text{ in.}^2$$

$$A_n = 3.1416(13)(0.365)(0.4876)[1/(2\times13) + .57735\,(0.4876 - 0.4565)] = 0.4101 \text{ in.}^2$$

So,

$$J = \frac{0.2843(165.0)}{0.4101(75.0)} = 1.525$$

$$Q = L_e J = (0.365)(1.525) = 0.557 \text{ in.}$$

The actual minimum engagement length is,

1.25 in. bolt length – 1.00 in. cover thickness + 0.66 in. cover counter bore– 0.125 in. washer thickness = 0.785 in. > 0.557 in.

3.9.3.12 Conclusions

1. Top cover and RAM access cover bolt stresses meet the acceptance criteria of NUREG/CR-6007 "Stress Analysis of Closure Bolts for Shipping Casks".

2. The top cover and RAM cover bolt, insert, and flange thread engagement length is acceptable.

3.9.3.13 References

1. Stress Analysis of Closure Bolts for Shipping Cask, NUREG/CR-6007, 1992.

2. American Society of Mechanical Engineers, ASME Boiler and Pressure Vessel Code, Section II, Part D, 1998 with 2000 addenda.

3. Helicoil Catalog, Heli-Coil 8-Pitch Inserts, Bulletin 913B.

4. Machinery Handbook, 21st Ed, Industrial Press, 1979.

5. Baumeister, T., Marks, L. S., *Standard Handbook for Mechanical Engineers*, 7th Edition, McGraw-Hill, 1967.

Table 3.9.3-1
Design Parameters for Top cover Bolt Analysis

- D_b Nominal diameter of closure bolt; 1.500 in.
- K Nut factor for empirical relation between the applied torque and achieved preload is 0.132
- Q Applied torque for the preload (in.-lb.)
- D_{lb} Closure lid diameter at bolt circle, 77.70 in.
- D_{lg} Closure lid diameter at the seal = 74.19 in.
- E_c Young's modulus of cask wall material, 27.0×10^6 psi. @ 300° F.
- E_l Young's modulus of lid material, 27.0×10^6 psi. @ 300° F.
- N_b Total number of closure bolts, 24
- N_{ul} Poisson's ratio of closure lid, 0.3, [5].
- P_{ei} Inside pressure of cask, 30 psig.
- D_{lo} Closure lid diameter at outer edge, 82.20 in.
- P_{li} Pressure inside the closure lid, 30 psig.
- t_c Thickness of flange, 5.575 in.
- t_l Thickness of lid, 3.0in./1.5 in.
- a_b Thermal coefficient of expansion, bolt material, 6.9×10^{-6} in. in.$^{-1}$ °F^{-1} at 300°F
- a_c Thermal coefficient of expansion, cask, 9.2×10^{-6} in. in.$^{-1}$ °F^{-1} at 300°F
- a_l Thermal coefficient of expansion, lid, 8.8×10^{-6} in. in.$^{-1}$ °F^{-1} at 300°F
- E_b Young's modulus of bolt material, 26.7×10^6 psi. at 300°F
- ai Maximum rigid-body impact acceleration (g) of the cask
- DLF Dynamic load factor to account for any difference between the rigid body acceleration and the acceleration of the contents and closure lid = 1.1
- W_c weight of contents = 50,720 lb. (fuel) + 29,854 lb. (basket) + 28,191 lb. (canister) = 108,765 lbs., conservatively use 110,000 lbs.
- W_l weight of closure lid = 5,195 lb., conservatively use 5,500 lb.
- W_c+W_l 110,000 + 5,500 = 115,500 lbs.
- xi Impact angle between the cask axis and target surface
- S_{yl} Yield strength of closure lid material, 43.3 ksi. @ 300° F.
- S_{ul} Ultimate strength of closure lid, 94.2 ksi @ 300° F.
- S_{yb} Yield strength of bolt material (see Table 3.9.3-3).
- S_{ub} Ultimate strength of bolt material (see Table 3.9.3-4).
- P_{lo} Pressure outside the lid.
- P_{co} Pressure outside the cask, 0 psig. (worst case scenario)
- L_b Bolt length between the top and bottom surfaces of closure, 1.50 in.

Table 3.9.3-2
Design Parameters for Ram Access Cover Bolt Analysis

- D_b Nominal diameter of closure bolt; 0.50 in.
- K Nut factor for empirical relation between the applied torque and achieved preload is 0.132
- Q Applied torque for the preload (in.-lb.)
- D_{lb} RAM access cover diameter at bolt circle, 23.50 in.
- D_{lg} RAM access cover diameter at the seal = 21.16 in.
- E_c Young's modulus of RAM access penetration wall material, 27.0×10^6 psi. @ 300° F.
- E_l Young's modulus of cover material, 27.0×10^6 psi. @ 300° F.
- N_b Total number of closure bolts, 12
- N_{ul} Poisson's ratio of closure RAM access cover, 0.3, [5].
- P_{ci} Inside pressure of RAM access penetration, 30 psig.
- D_{lo} Cover diameter at outer edge, 25.45 in.
- D_{li} Cover diameter at inner edge, 20.00 in.
- P_{li} Pressure inside the cover, 30 psig.
- t_c Thickness of RAM access penetration, 4.00 in.
- t_l Thickness of cover, 1.0 in.
- a_b Thermal coefficient of expansion, bolt material, 6.9×10^{-6} in. in.$^{-1}$ °F^{-1} at 300°F
- a_c Thermal coefficient of expansion, RAM access penetration, 9.2×10^{-6} in. in.$^{-1}$ °F^{-1} at 300°F
- a_l Thermal coefficient of expansion, cover, 9.2×10^{-6} in. in.$^{-1}$ °F^{-1} at 300°F
- E_b Young's modulus of bolt material, 26.7×10^6 psi. at 300°F
- ai Maximum rigid-body impact acceleration (g) of the cask
- DLF Dynamic load factor to account for any difference between the rigid body acceleration and the acceleration of the contents and cover = 1.1.
- W_c the inertial load of the transfer cask contents does not affect the cover bolts.
- W_l weight of RAM access cover = 148 lb., conservatively use 200 lb.
- W_c+W_l 0 + 200 = 200 lbs.
- xi Impact angle between the cask axis and target surface.
- S_{yl} Yield strength of closure cover material, 22.4 ksi. @ 300° F.
- S_{ul} Ultimate strength of closure lid, 66.2 ksi @ 300° F.
- S_{yb} Yield strength of bolt material (see Table 3.9.3-4).
- S_{ub} Ultimate strength of bolt material (see Table 3.9.3-5).
- P_{lo} Pressure outside the cover, 0 psig. (worst case scenario)
- P_{co} Pressure outside the RAM access penetration, 0 psig. (worst case scenario)
- L_b Bolt length between the top and bottom surfaces of closure, 0.34 in.

Table 3.9.3-3
Bolt Data ([1], Table 5.1)

Top cover Bolts

Bolt: 1 1/2"– 8UN – 2A

N: no of threads per inch = 8

p: Pitch = 1/8" = .125 in.

D_b: Nominal Diameter = 1.50 in.

D_{ba}: Bolt diameter for stress calculations = D_b - .9743p = 1.50 - .9743 (0.125) = 1.378 in.

Stress Area = $\pi/4\ (1.378)^2 = 1.491\ in^2$

Ram Closure Bolts:

Bolt: 1/2"– 13UNC – 2A

N: no of threads per inch = 13

p: Pitch = 1/13" = .0769 in.

D_b: Nominal Diameter = 0.50 in.

D_{ba}: Bolt diameter for stress calculations = D_b - .9743p = 0.50 - .9743 (0.0769) = 0.425 in.

Stress Area = $\pi/4\ (0.425)^2 = 0.142\ in^2$

Table 3.9.3-4
Allowable Stresses in Closure Bolts for Normal Conditions
(MATERIAL: SA-540 Gr. B24 CL.1)

Temperature (°F)	Yield Stress[1] (ksi)	Normal Condition Allowables		
		F_{tb}[2,4] (ksi)	F_{vb}[3,4] (ksi)	$S.I.$[5] (ksi)
100	150	100.0	60.0	135.0
200	143.4	95.6	57.4	129.1
300	138.6	92.4	55.4	124.7
400	134.4	89.6	53.8	121.0
500	130.2	86.8	52.1	117.2
600	124.2	82.8	49.7	111.8

Notes:

1. Yield stress values are from ASME Code, Section II, Table 4 (Ratio: $S_y = 3S_m$) [2]
2. Allowable Tensile stress, $F_{tb} = 2/3\ S_y$ (Ref. 1, Table 6.1)
3. Allowable shear stress, $F_{vb} = 0.4\ S_y$ (Ref. 1, Table 6.1)
4. Tension and shear stresses must be combined using the following interaction equation:

$$\frac{\sigma_{tb}^2}{F_{tb}^2} + \frac{\tau_{vb}^2}{F_{vb}^2} \leq 1.0 \text{ [1]}$$

Stress intensity from combined tensile, shear and residual torsion loads, $S.I. \leq 0.9\ S_y$ (Ref. 1, Table 6.1)

Table 3.9.3-5
Allowable Stresses in Closure Bolts for Hypothetical Accident Conditions
(MATERIAL: SA-540 Gr. B24 Cl.1)

Temperature (°F)	Yield Stress(1) (ksi)	Accident Condition Allowables		
		$0.6\ S_y$(3) (ksi)	F_{tb}(2,4) (ksi)	F_{vb}(3,4) (ksi)
100	150.0	90.0	115.5	69.3
200	143.4	86.0	115.5	69.3
300	138.6	83.2	115.5	69.3
400	134.4	80.6	115.5	69.3
500	130.2	78.1	115.5	69.3
600	124.2	74.5	115.5	69.3

Notes:

1. Yield and tensile stress values are from ASME Code, [2] Table 4, Note that S_u is 165.0 ksi at all temperatures of interest.

2. Allowable Tensile stress, F_{tb} = MINIMUM(0.7 S_u, S_y), where 0.7 S_u = 0.7 (165.0) = 115.5 ksi. (Ref. 1, Table 6.3)

3. Allowable shear stress, F_{vb} = MINIMUM(0.42 S_u, 0.6 S_y), where 0.42 S_u = 0.42 (165.0) = 69.3 ksi. (Ref. 1, Table 6.3)

4. Tension and shear stresses must be combined using the following interaction equation:

$$\frac{\sigma_{tb}^2}{F_{tb}^2} + \frac{\tau_{vb}^2}{F_{vb}^2} \leq 1.0 \quad [1]$$

APPENDIX 3.9.4
OS187H TRANSFER CASK LEAD SLUMP AND INNER SHELL BUCKLING ANALYSIS

TABLE OF CONTENTS

3.9.4 OS187H TRANSFER CASK LEAD SLUMP AND INNER SHELL BUCKLING ANALYSIS 3.9.4-1

3.9.4.1 Introduction 3.9.4-1

3.9.4.2 Material Properties 3.9.4-2

3.9.4.3 Finite Element Model 3.9.4-6

3.9.4.4 FEA Results 3.9.4-11

3.9.4.5 Conclusions 3.9.4-12

3.9.4.6 References 3.9.4-13

LIST OF FIGURES

3.9.4-1 Loads and Boundary Conditions for Transfer Cask Bottom End Drop Model (Top End, 115° F Ambient Case)

3.9.4-2 Loads and Boundary Conditions for Transfer Cask Bottom End Drop Model (Bottom End, 115° F Ambient Case)

3.9.4-3 Loads and Boundary Conditions for Transfer Cask Bottom End Drop Model (Top End, -20° F Ambient Case)

3.9.4-4 Loads and Boundary Conditions for Transfer Cask Bottom End Drop Model (Bottom End, -20° F Ambient Case)

3.9.4-5 Loads and Boundary Conditions for Transfer Cask Top End Drop Model (Top End, 115° F Ambient Case)

3.9.4-6 Loads and Boundary Conditions for Transfer Cask Top End Drop Model (Bottom End, 115° F Ambient Case)

3.9.4-7 Loads and Boundary Conditions for Transfer Cask Top End Drop Model (Top End, -20° F Ambient Case)

3.9.4-8 Loads and Boundary Conditions for Transfer Cask Top End Drop Model (Bottom End, -20° F Ambient Case)

3.9.4-9 Deformed Shape of Transfer Cask for 75g Bottom End Drop (Top End, 115° F Ambient Case)

3.9.4-10 Deformed Shape of Transfer Cask for 75g Bottom End Drop (Top End, -20° F Ambient Case)

3.9.4-11 Deformed Shape of Transfer Cask for 75g Top End Drop (Bottom End, 115° F Ambient Case)

3.9.4-12 Deformed Shape of Transfer Cask for 75g Top End Drop (Bottom End, -20° F Ambient Case)

3.9.4-13 Construction of Collapse Load for Transfer Cask Bottom End Drop

3.9.4 OS187H TRANSFER CASK LEAD SLUMP AND INNER SHELL BUCKLING ANALYSIS

3.9.4.1 Introduction

The purpose of this Appendix is to evaluate the structural adequacy of the OS187H Transfer Cask inner shell with respect to bucking, and to determine the extent of lead slump. The load considered includes an internal pressure of 30 psig and a 75*g* top and bottom end drop load in both hot (115° F) and cold (-20° F) ambient environments. The calculations for the component stresses and their evaluations under these loads were conducted and reported in Appendix 3.9.2 and Appendix 3.9.3 for the top cover and ram cover bolts.

During a hypothetical accident condition end drop, permanent deformation of the lead gamma shield may occur. The lead gamma shield is supported by friction between the lead and transfer cask shells, in addition to bearing at the end of the lead column.

A nonlinear finite element analysis is performed in order to quantify the amount of lead slump generated during an end drop event. A 2-dimensional axisymmetric ANSYS [1] finite element model is constructed for this purpose. The results of the finite element analysis provide both stresses and displacements generated during the end drop event. The displacement results are used in this section to determine the maximum size of the axial gap that develops between the lead gamma shield column and the structural shell of the transfer cask. The effect of this cavity size on the shielding ability of the transfer package is evaluated in Chapter 5. Both stress and displacement distributions computed by the finite element analysis are also used to perform a buckling evaluation of inner containment shell of the OS187H transfer cask.

An ANSYS elastic-plastic buckling analysis is performed for the transfer cask end drop cases. A 100*g* drop load, which is greater than the design load of 75*g*, is applied to the ANSYS model. This100*g* drop load was ramped in small increments by many load sub-steps. The ANSYS solution was set to stop and exit at any load sub-step that fails to result in a converged solution. The failure of convergence represents the onset of buckling of the structure. The acceptance criteria (allowable buckling loads) are taken from the ASME Code, Section III, Appendix F [2], paragraph F-1341.3, Collapse Load. The allowable buckling load is determined by plastic analysis collapse load according to the criteria given in Section III, Subsection NB, Paragraph NB-3213.25 [2].

3.9.4.2 Material Properties

The maximum normal condition temperature in each transfer cask component from Chapter 4 was used to obtain the tangent modulus of the material. The following table summarizes the maximum transfer cask component temperatures taken from Chapter 4.

Cask Component	Material	Temperature Used in Analysis
Lid	SA-240 Type XM-19	300 °F
Inner Shell	SA-240 Type 304	350 °F
Top and Bottom Flanges, Ram Access Penetration Ring	SA-182 Gr. F304N	300 °F
Outer Structural Shell, Bottom Neutron Shield plate, Bottom End and Cover plates	SA-240 Type 304	300 °F
Top Lid and Bottom RAM access Cover Bolts	SA-540-Gr. B24 Cl.1	300 °F
Gamma Shield	B-29, Chemical Lead	350 °F

The following is a summary of the transfer cask material properties evaluated at the temperatures listed above.

A. Lid Material (SA-240 Type XM-19)

Temperature	Modulus of Elasticity, E (psi) [2]	Density, ρ (lb./in.3) [3]	Poisson's ratio, ν [3]
70° F	28.3×10^6	0.29	0.3
200° F	27.6×10^6	0.29	0.3
300° F	27.0×10^6	0.29	0.3
400° F	26.5×10^6	0.29	0.3

@ 300° F,

$E = 27.0\times10^6$ psi. [2]

$S_y = 43.3$ ksi. [2]

$S_u = 94.2$ ksi. [2]

Tangent Modulus, $E_T = 5\%$ of $E = 0.05 \times 27.0\times10^6$ psi $= 1.35 \times10^6$ psi

B. Inner Shell (SA-240 Type 304)

Temperature	Modulus of Elasticity, E (psi) [2]	Density, ρ (lb./in.3) [3]	Poisson's ratio, ν [3]
70° F	28.3×10^6	0.29	0.3
200° F	27.6×10^6	0.29	0.3
300° F	27.0×10^6	0.29	0.3
400° F	26.5×10^6	0.29	0.3

@ 350° F,

$E = 26.75 \times10^6$ psi. [2]
$S_y = 21.55$ ksi. [2]
$S_u = 65.1$ ksi. [2]
Tangent Modulus, E_T = 5% of $E = 0.05 \times 26.75\times10^6$ psi = 1.34×10^6 psi

C. Top and Bottom Flanges, and Ram Access Penetration Ring (SA-182 Gr. F304N)

Temperature	Modulus of Elasticity, E (psi) [2]	Density, ρ (lb./in.3) [3]	Poisson's ratio, ν [3]
70° F	28.3×10^6	0.29	0.3
200° F	27.6×10^6	0.29	0.3
300° F	27.0×10^6	0.29	0.3
400° F	26.5×10^6	0.29	0.3

@ 300° F,

$E = 27.0\times10^6$ psi. [2]
$S_y = 25$ ksi. [2]
$S_u = 76.1$ ksi. [2]
Tangent Modulus, E_T = 5% of $E = 0.05 \times 27.0\times10^6$ psi = 1.35×10^6 psi

D. Outer Structural Shell, Bottom Neutron Shield plate, Bottom End plate, and Bottom cover plate (SA-240 Type 304)

Temperature	Modulus of Elasticity, E (psi) [2]	Density, ρ (lb./in.3) [3]	Poisson's ratio, ν [3]
70° F	28.3×10^6	0.29	0.3
200° F	27.6×10^6	0.29	0.3
300° F	27.0×10^6	0.29	0.3
400° F	26.5×10^6	0.29	0.3

@ 300° F,

$E = 27.0\times10^6$ psi. [2]
$S_y = 22.4$ ksi. [2]
$S_u = 66.2$ ksi. [2]
Tangent Modulus, E_T = 5% of $E = 0.05 \times 27.0\times10^6$ psi $= 1.35 \times10^6$ psi

E. Bolts for Top Lid and Bottom RAM Access Cover (SA-54 Gr. 24 CL 1)

Temperature	Modulus of Elasticity, E (psi) [2]	Density, ρ (lb./in.3) [3]	Poisson's ratio, ν [3]
70° F	27.8×10^6	0.29	0.3
200° F	27.1×10^6	0.29	0.3
300° F	26.7×10^6	0.29	0.3
400° F	26.1×10^6	0.29	0.3

@ 300 °F,

$E = 26.7\times10^6$ psi. [2]
$S_y = 138.6$ ksi. [2]
$S_u = 165$ ksi. [2]
Tangent Modulus, E_T = 5% of $E = 0.05 \times 26.7\times10^6$ psi $= 1.335 \times10^6$ psi

F. Chemical Lead (B-29)

Temperature	Modulus of Elasticity, E (psi) [2]	Density, ρ (lb./in.3) [3]	Poisson's ratio, ν [3]
70° F	2.49×10^6	0.41	0.45
200° F	2.28×10^6	0.41	0.45
300° F	2.06×10^6	0.41	0.45
400° F	$1.78\times10^{6*}$	0.41	0.45

*Extrapolated from available Reference 4 Data.

@ 350° F,
Multi-linear Stress/Strain Curve: [4] [5]

Strain (in/in)	Stress (psi)
	350° F
0.000485	1,208*
0.030	1,500
0.100	2,100
0.300	2,400
0.500	2,700

*Values adjusted for consistence with modulus of elasticity listed in above table.

3.9.4.3 Finite Element Model

3.9.4.3.1 Approach

A 2-dimensional axisymmetric ANSYS [1] finite element model, constructed primarily from PLANE42 elements, is used in this analysis. Beam3 elements are used to model the lid and RAM port cover bolts. Contact elements are used to model the interaction between the lead gamma shield and the cask inner and outer shells. The coefficient of sliding friction for lead on mild steel varies from 0.3 for lubricated surfaces to 0.95 for dry surfaces [3]. A lower bound coefficient of static friction of 0.25 is conservatively used for this buckling analysis.

In order to determine the buckling load of the inner shell and the amount of lead slump settling, an elastic-plastic analysis is required. The material properties of the lid, bottom, inner shell and outer shell of the transfer cask are modeled with bilinear stress-strain curves, while the lead material is modeled with a multilinear stress-strain curve. Above tables list these material properties.

3.9.4.3.2 Unmodeled Components

Only the structural steel section of the top cover is modeled. The top neutron shield resin, top cover plate, and hoist ring standoffs are not modeled since they are not intended to provide any structural support. However, their inertial load is accounted for by increasing the density of the structural portion of the top cover. The weight of the unmodeled portion of the top cover assembly is as follows.

Weight of unmodeled lid components = 678 lb. (resin) + 422 lb. (cover plate) + 20 lb. (standoffs)
= 1,120 lb.

The volume and weight of the structural steel portion of the lid is 14,051 in.^{3} and 4,075 lb. respectively. Therefore the weight of the structural steel portion of the lid, ρ_l, is the following.

$$\rho_l = [1{,}120 \text{ lb.} + 4{,}075 \text{ lb.}] / 14{,}051 \text{ in.}^3 = 0.37 \text{ lb./in.}^3$$

For conservatism, the density of the top cover used in this analysis is increased 0.38 lb./in.^{3}

The radial neutron shield and shell are also not modeled, because they are not considered structural components of the transfer cask. Therefore, the density of the outer structural steel shell of the transfer cask is increased to account for the un-modeled components. The weight of the un-modeled radial neutron shield assembly is 12,746 lb.

The volume and weight of the outer structural shell is 71,895 in.^{3} and 20,850 lb. respectively. Therefore the weight of the structural steel portion of the lid, ρ_s, is the following.

$$\rho_l = [12{,}746 \text{ lb.} + 20{,}850 \text{ lb.}] / 71{,}895 \text{ in.}^3 = 0.47 \text{ lb./in.}^3$$

For conservatism, the density of the outer structural steel shell used in this analysis is increased 0.49 lb./in.^{3}

3.9.4.3.3 Attachment Bolt Modeling

The top cover and RAM access cover bolts are modeled with axisymmetric BEAM3 elements. The top cover and RAM access bolts are constructed from SA-540 grade B24 class 1 material. The element real constants are computed in the following way for the top cover and RAM access bolts.

There are 24, 1½ in - 8UN 2A bolts used to mount the transfer cask top cover. The bolt diameter used for stress analysis, D_{tc}, is computed using formulae given in Table 5.1 of Reference 6, as follows.

$$D_{tc} = 1.50 - 0.9743(1/8) = 1.378 \text{ in.}$$

The total tensile stress area for all 24 top cover bolts, A_{tc2d}, is computed as follows.

$$A_{tc2d} = (\pi/4) \times 1.378^2 \times 24 \text{ bolts} = 1.491 \times 24 \text{ bolts} = 35.793 \text{ in.}^2$$

The total moment of inertia of all 24 top cover bolts, I_{tc2d}, is,

$$I_{tc2d} = (\pi/64) \times 1.378^4 \times 24 \text{ bolts} = 4.248 \text{ in.}^4$$

The total height of the top cover bolts, H_{tc2d}, is computed assuming the following equivalent height method.

$$H_{tc2d} = \sqrt{A_{tc2d}} = \sqrt{1.491} = 1.221 \text{ in.}$$

There are 12, ½ in - 13UNC 2A bolts used to mount the transfer cask RAM access cover. The bolt diameter used for stress analysis, D_{ra}, is computed as follows.

$$D_{ra} = 0.50 - 0.9743(1/13) = 0.425 \text{ in.}$$

The total tensile stress area for all 12 RAM access cover bolts, A_{ra2d}, is computed as follows.

$$A_{ra2d} = (\pi/4) \times 0.425^2 \times 12 \text{ bolts} = 0.142 \times 12 \text{ bolts} = 1.704 \text{ in.}^2$$

The total moment of inertia of all 12 RAM access cover bolts, I_{ra2d}, is,

$$I_{ra2d} = (\pi/64) \times 0.425^4 \times 12 \text{ bolts} = 0.01922 \text{ in.}^4$$

The height of the RAM access cover bolts, H_{ra2d}, used in the model is,

$$H_{ra2d} = \sqrt{0.142} = 0.3768 \text{ in.}$$

For both the top cover bolts and the RAM access cover bolt, a bolt preload stress of 25,000 psi. is used. Since the top cover bolts and RAM access cover bolts are constructed from the same material, SA-540, type B24. Both sets of bolts are torqued to the same preload stress, and their corresponding preload strains, ε_b, used in the finite element model are computed as follows.

$$\varepsilon_b = \text{preload stress / bolt modulus of elasticity}$$

3.9.4.3.4 Contact Elements

CONTAC12 elements are places between all surfaces of the top flange and lid as well as the RAM access cover and RAM access penetration that contact each other. These contact elements are used to model the reaction forces that occur between closure surfaces.

The contact elements introduce nonlinearities in the analysis depending whether they are open or closed. Initially, at all contact surfaces, the gaps are closed. The contact element spring constant, K_n, is calculated in the following way.

$$K_n = f E h \text{ [7]}$$

Where,

f = A factor usually between 0.01 to 100.
E = Modulus of elasticity (27.0×10^6 psi for SA-240, type 304 @ 300°F [2])
h = contact target length (i.e., the square root of target area).
Typical element length $\approx$ 1/2 in.
Typical element width $\approx$ 1 in.
Typical target length, $h = (0.5 \times 1.0)^{0.5} = 1.22$ in.

$$K_n = 27.0\times10^6 \times 1.22 \times f \approx 3.29\times10^5 \text{ to } 3.29\times10^9 \text{ lb./in}$$

Thus, there is very wide range for K_n value. For the 2-D finite element model, an upper value of 3×10^9 lb/in was used to minimize penetrations in the contact elements.

3.9.4.3.5 Bottom End Drop Boundary Conditions

The weight of the transfer cask internals (canister, basket, and fuel assemblies) is accounted for by applying equivalent pressures. The actual weights of the canister, basket, and fuel assemblies

are 28.19 kips, 29.85 kips, and 50.72 kips. respectively. Therefore, the total actual weight of the cask internals is 108.77 kips. For conservatism, the weight of the cask internals used in this analysis is increased to 115.00 kips. The transfer cask inner radius is 35.25 in., and the inner radius of the ram access penetration is 10.00 in. The inertial load of the transfer cask internals reacts against the annular surface bounded by these two radii during a bottom end drop. The area of this reaction surface, A_{bi}, is as follows.

$$A_{bi} = \pi(35.25^2 - 10.00^2) = 3{,}589.47 \text{ in}^2.$$

The pressure equivalent to the inertial load of the internals under accident conditions, P_{bi}, is,

$$P_{in} = [115{,}000 / 3{,}589.47] \times 100 \text{ gs} = 3205.15 \text{ psi}.$$

Symmetry displacement boundary conditions are applied along the y-axis of the 2-dimensionsal axisymmetric model. The bottom end of the transfer cask is held in the axial direction in order to simulate the rigid reaction force generated by the impact target. A 100 g inertial load in the positive y-direction is also applied to the model for the accident condition load case.

A depiction of the bottom end drop load case boundary conditions is provided in Figures 3.9.4-1 and 3.9.4-2 for the 115° F ambient condition, and Figures 3.9.4-3 and 3.9.4-4 for the -20° F ambient condition.

3.9.4.3.6 Top End Drop Boundary Conditions

The weight of the transfer cask internals (canister, basket, and fuel assemblies) is accounted for by applying equivalent pressures. The weight of the canister internals used in this analysis is 115.00 kips. The inertial load of the transfer cask internals reacts against the inside surface of the top cover assembly during a top end drop. The outer radius of the inside surface of the transfer cask top cover assembly is 35.70 in. Therefore the area of the reaction surface, A_{bi}, is as follows.

$$A_{bi} = \pi(35.70^2) = 4{,}003.93 \text{ in}^2.$$

The pressure equivalent to the inertial load of the internals under accident conditions, P_{bi}, is,

$$P_{in} = [115{,}000 / 4{,}003.93] \times 100 \text{ gs} = 2{,}872.17 \text{ psi}.$$

Symmetry displacement boundary conditions are applied along the *y*-axis of the 2-dimensionsal axisymmetric model. The outer surface of the top cover is held in the axial direction in order to simulate the rigid reaction force generated by the impact target. A 100*g* inertial load in the negative *y*-direction is also applied to the model for the accident condition load case.

A depiction of the top end drop load case boundary conditions is provided in Figures 3.9.4-5 and 3.9.4-6 for the 115° F ambient condition, and Figures 3.9.4-7 and 3.9.4-8 for the -20° F ambient condition.

3.9.4.3.7 Thermal Loads

Two thermal load cases are applied to each drop orientation load case, yielding a total of four load combinations. The two temperature distributions applied correspond to the 115° F. and -20° F ambient temperature environments. Both temperature distributions applied to the finite element model are taken from Chapter 4.

3.9.4.4 FEA Results

- Lead Slump

The ANSYS solutions have converged at all load sub-steps in each case of the 100*g* drop loads. Figures 3.9.4-9 and 3.9.4-10 show the deformed shape of the transfer cask for 75*g* bottom end drop, and Figures 3.4.9-11 and 3.9.4-12 show the deformed shape of the transfer cask for the 75*g* top end drop. The calculated maximum lead slumps in each case are listed in the following table.

Load Combination	Lead Slump Cavity Length
75*g* Bottom End Drop, Hot Environment	0.787 in.
75*g* Bottom End Drop, Cold Environment	0.755 in.
75*g* Top End Drop, Hot Environment	0.770 in.
75*g* Top End Drop, Cold Environment	0.719 in.

- Shell Buckling

Using the methodology described earlier for the cask model, the allowable collapse load has been determined for the 75g bottom end drop load case (this load case has resulting maximum deformation) in Figure 3.9.4-13. The allowable collapse load for the shell is 100g which is higher than the 75g side drop impact load.

3.9.4.5 Conclusions

The analysis indicates that the transfer cask will not buckle during 75*g* end drops in both 115° F and -20° F ambient environments. The table above shows that the maximum longitudinal gap, caused by lead slump, is 0.787 inches, and occurs during accident condition bottom end drop, in the hot environment. The effect of the gap on the shielding ability of the NUHOMS®-OS187H transfer cask is analyzed in Chapter 7.

3.9.4.6 References

1. ANSYS User's Manual, Rev 6.0

2. American Society of Mechanical Engineers, ASME Boiler and Pressure Vessel Code, Section II, Part D and Section III, Subsection NB and Appendix F, 1998, including 2000 addenda.

3. Baumeister & Marks, Standard Handbook for Mechanical Engineers, 7th Edition.

4. An Assessment of Stress-Strain Data Suitable for Finite-Element Elastic-Plastic Analysis of Shipping Containers, NUREG/CR-0481.

5. A Survey of Strain Rate Effects for some Common Structural Materials Used in Radioactive Material Packaging and Transportation Systems, U.S. Energy Research and Development Administration, Battelle Columbus Laboratories, August 1976.

6. "Stress Analysis of Closure Bolts for Shipping Casks", NUREG/CR-6007, April 1992

7. ANSYS User's Manual, Rev 5.6

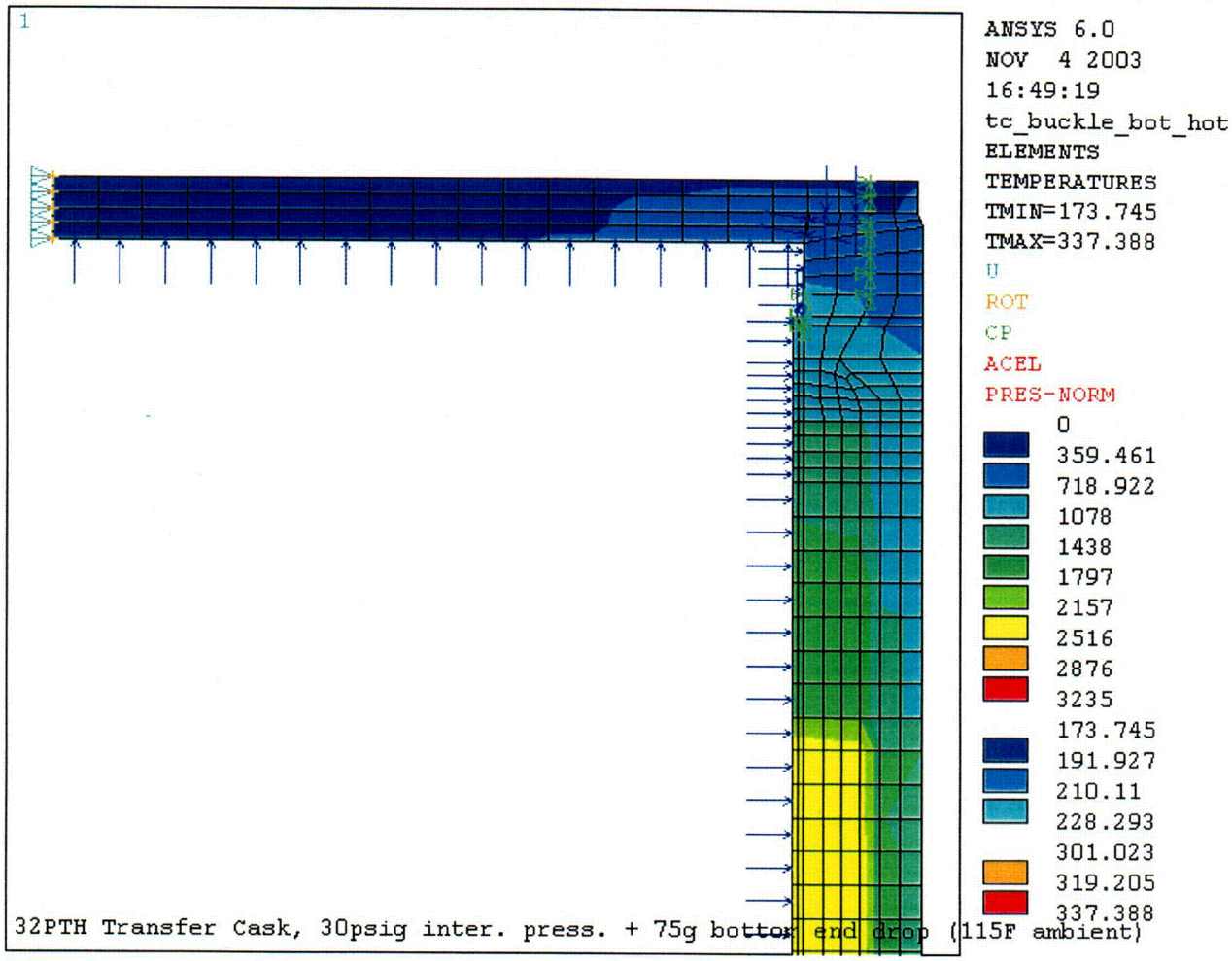

Figure 3.9.4-1
Loads and Boundary Conditions for Transfer Cask Bottom End Drop Model (Top End, 115° F Ambient Case)

C08

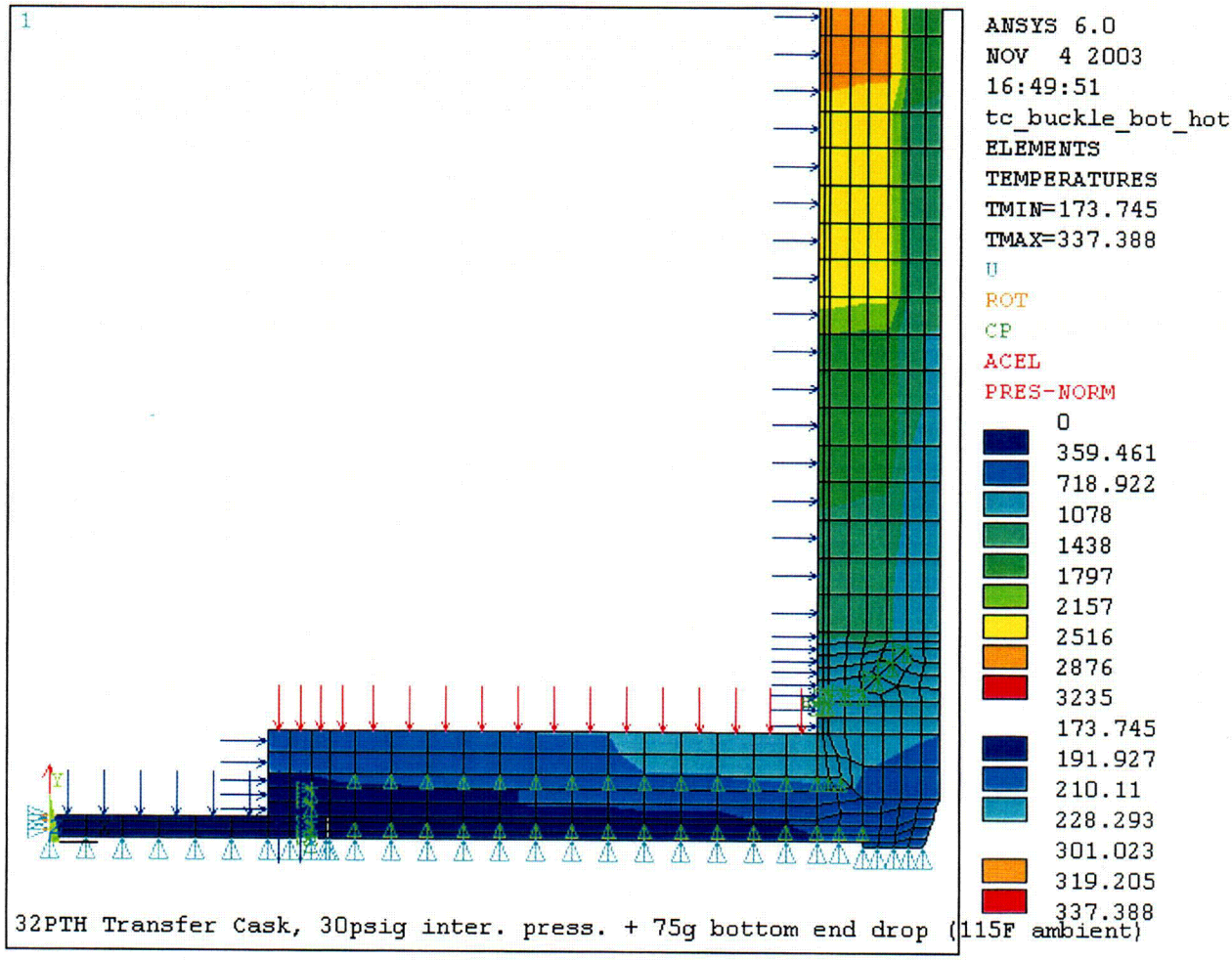

Figure 3.9.4-2
Loads and Boundary Conditions for Transfer Cask Bottom End Drop Model (Bottom End, 115° F Ambient Case)

C09

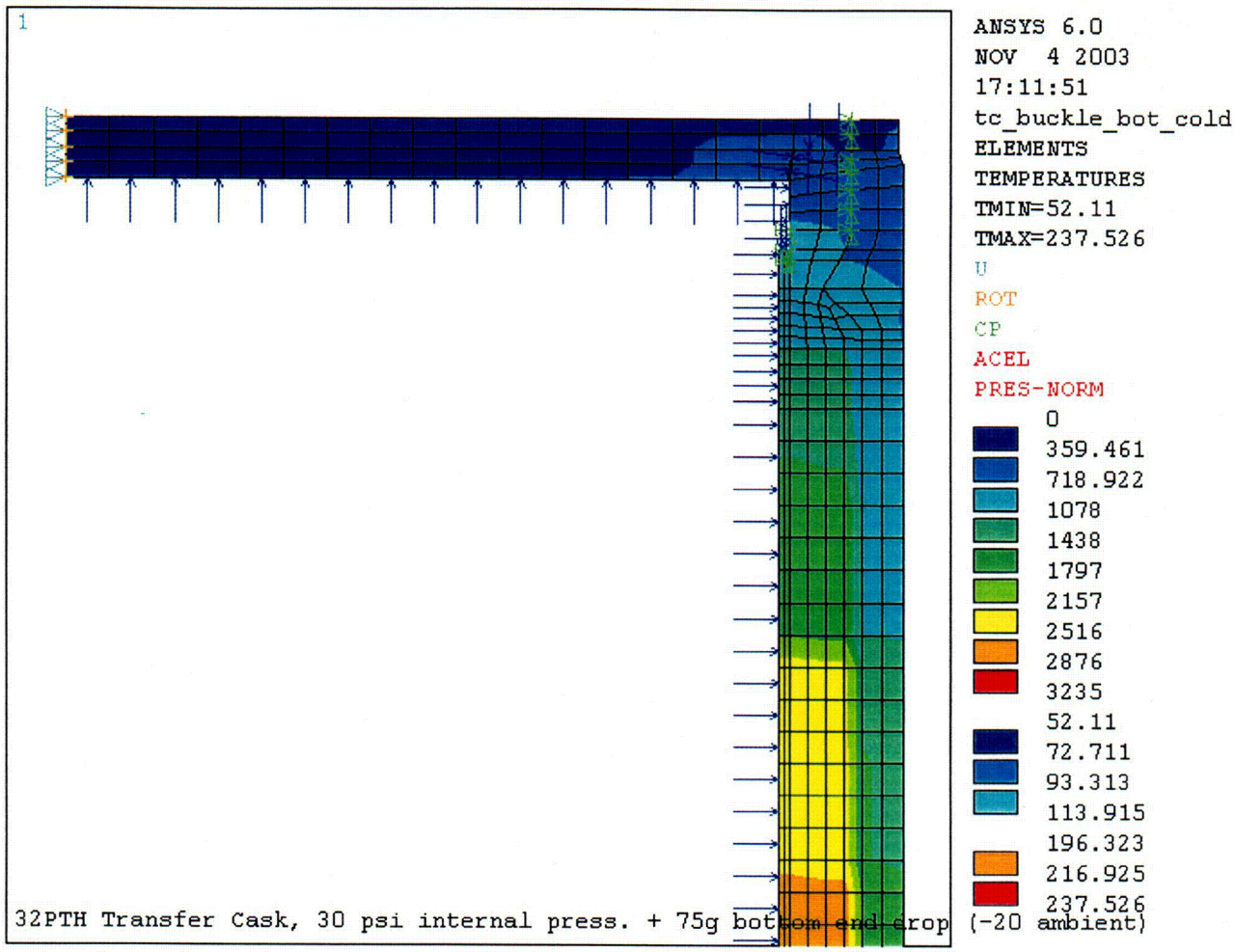

Figure 3.9.4-3
Loads and Boundary Conditions for Transfer Cask Bottom End Drop Model (Top End, -20° F Ambient Case)

C10

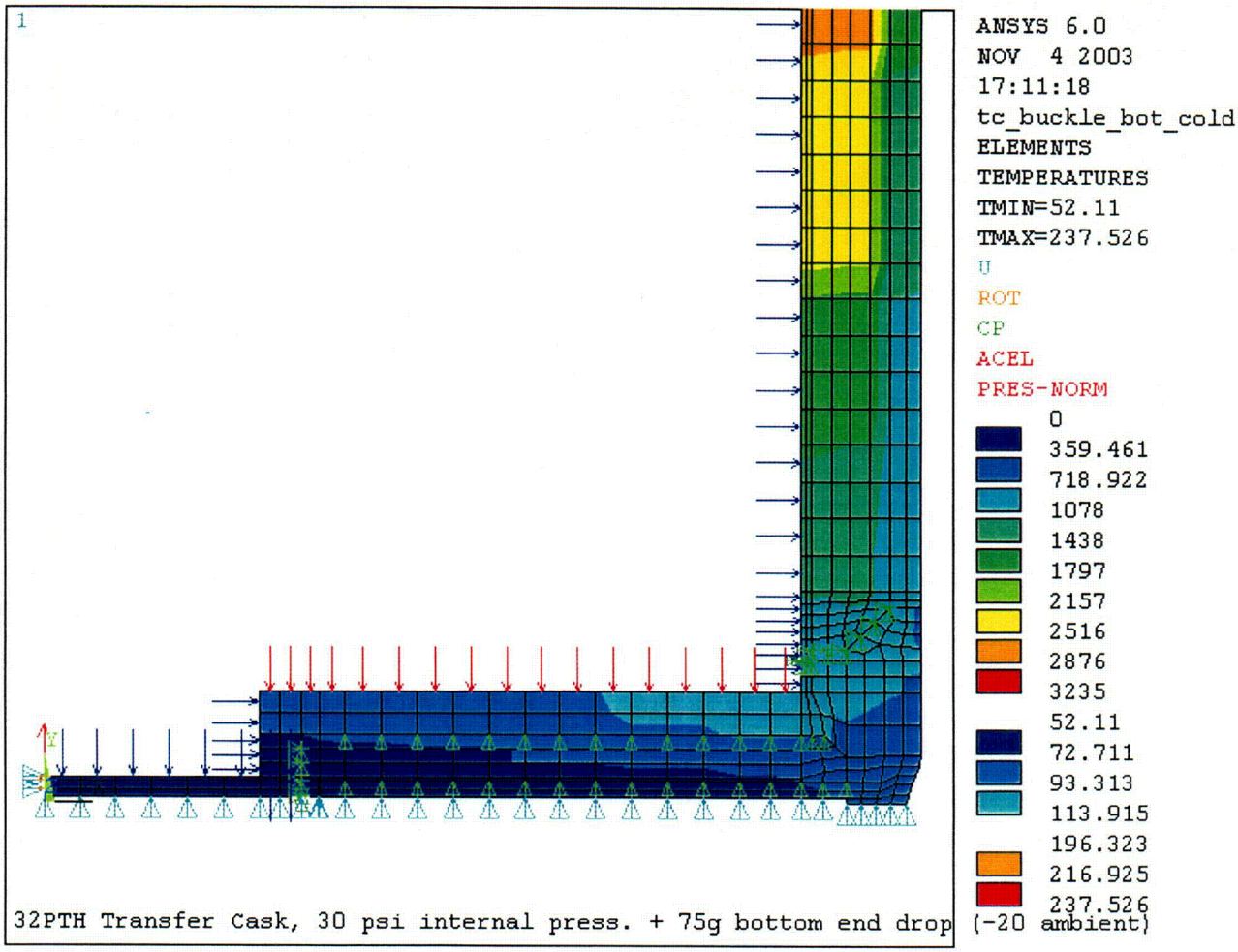

Figure 3.9.4-4
Loads and Boundary Conditions for Transfer Cask Bottom End Drop Model (Bottom End, -20° F Ambient Case)

C11

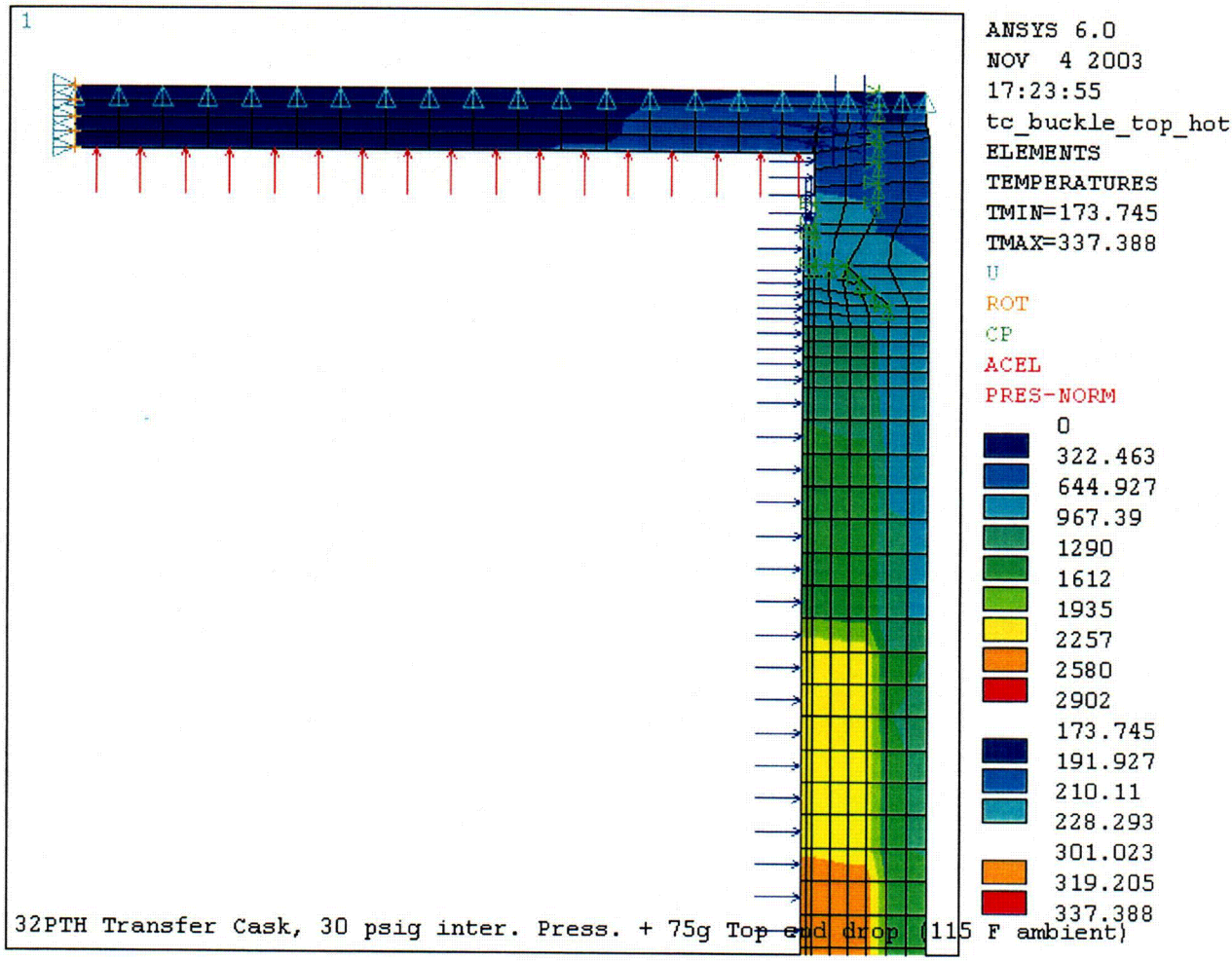

Figure 3.9.4-5
Loads and Boundary Conditions for Transfer Cask Top End Drop Model (Top End, 115° F Ambient Case)

C12

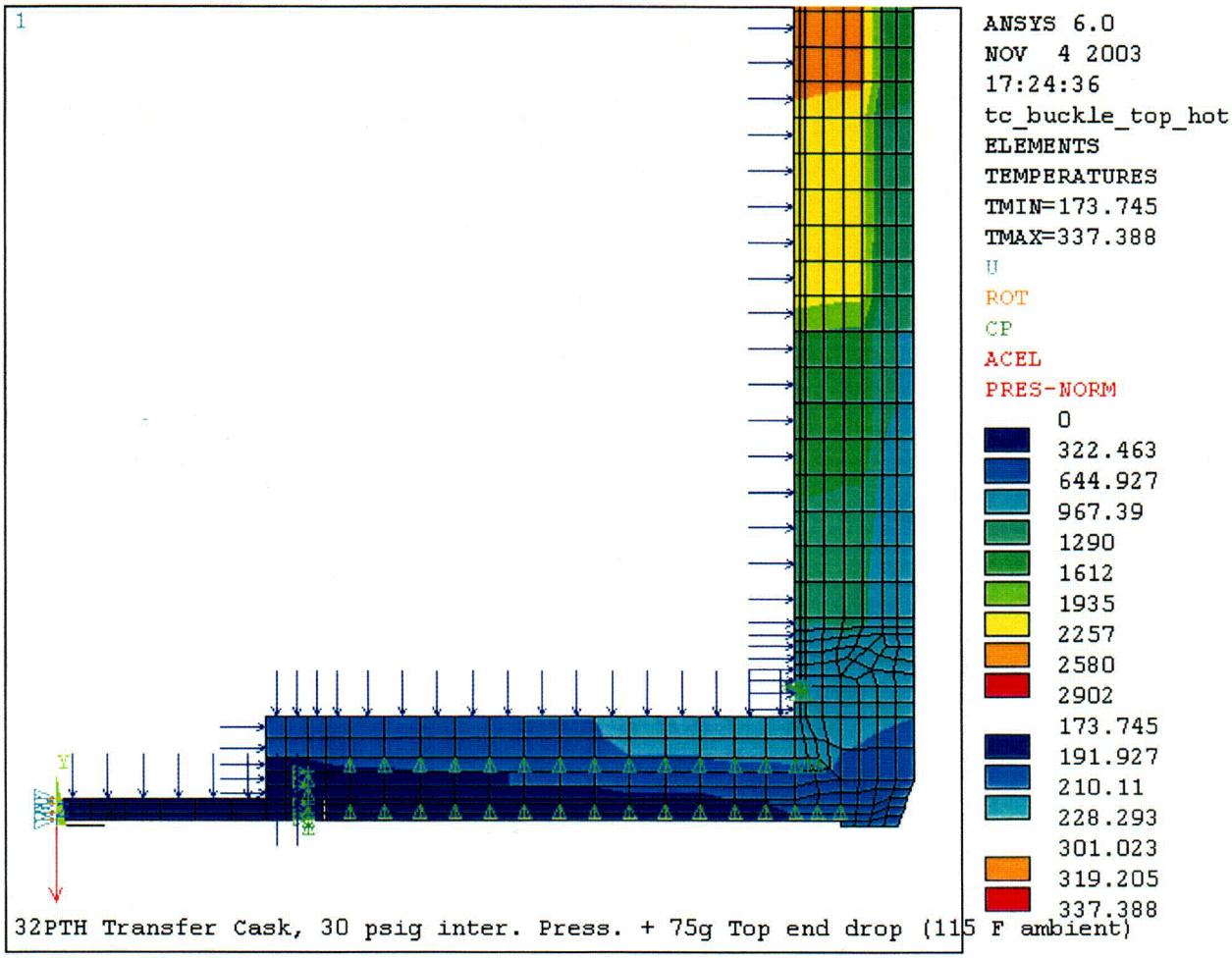

Figure 3.9.4-6
Loads and Boundary Conditions for Transfer Cask Top End Drop Model (Bottom End, 115° F Ambient Case)

C13

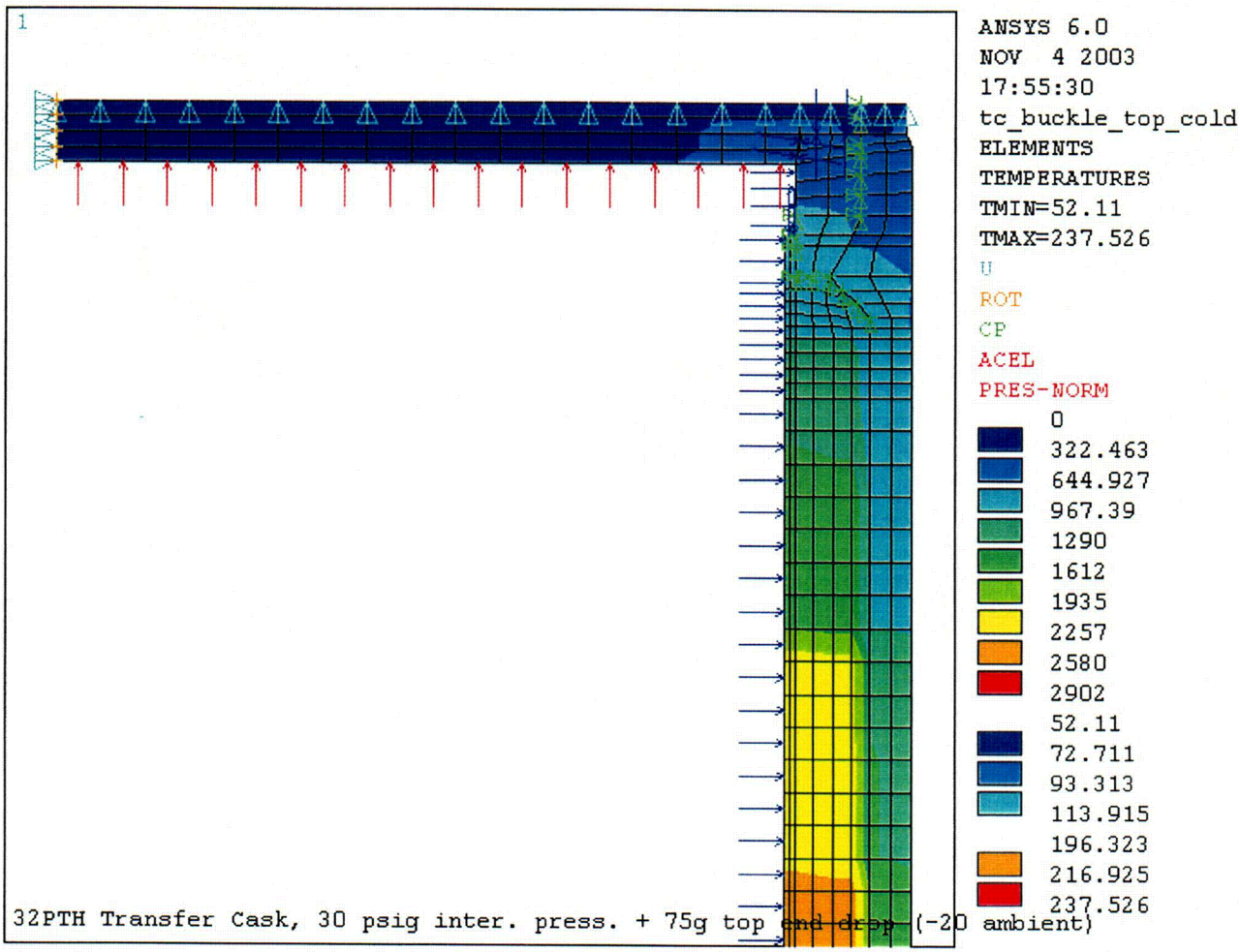

Figure 3.9.4-7
Loads and Boundary Conditions for Transfer Cask Top End Drop Model (Top End, -20° F Ambient Case)

C14

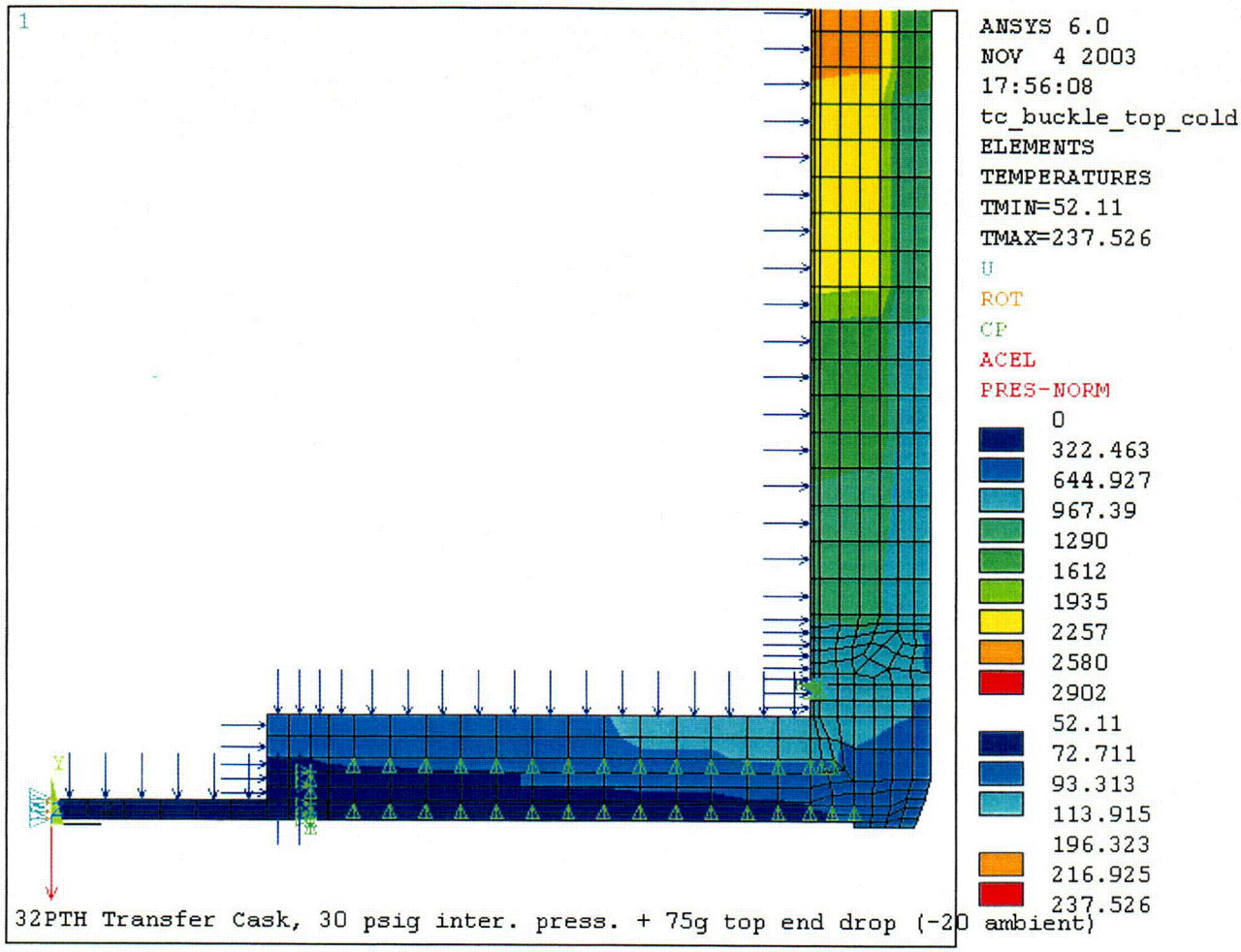

Figure 3.9.4-8
Loads and Boundary Conditions for Transfer Cask Top End Drop Model (Bottom End, -20° F Ambient Case)

C15

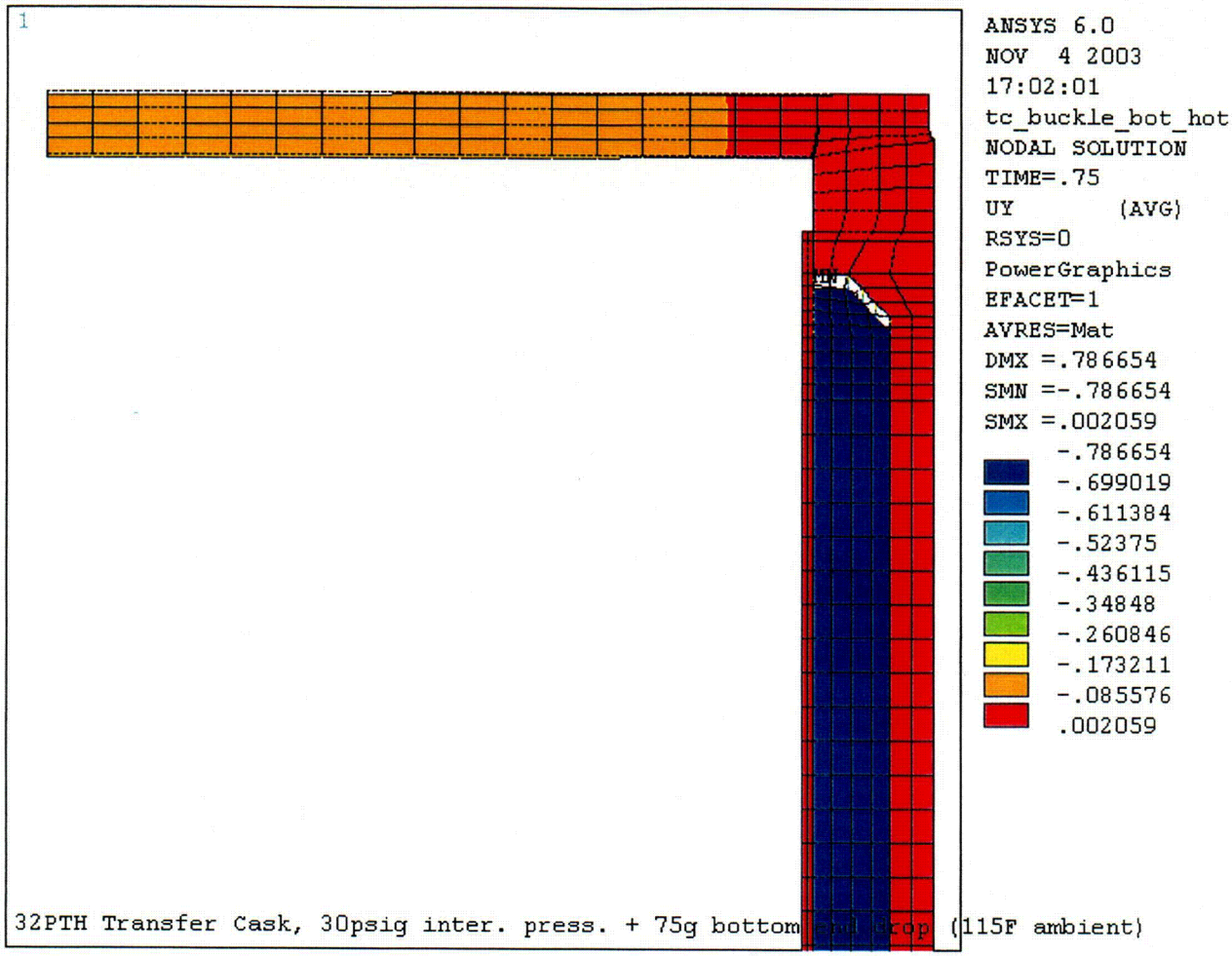

Figure 3.9.4-9
Deformed Shape of Transfer Cask for 75g Bottom End Drop
(Top End, 115° F Ambient Case)

C16

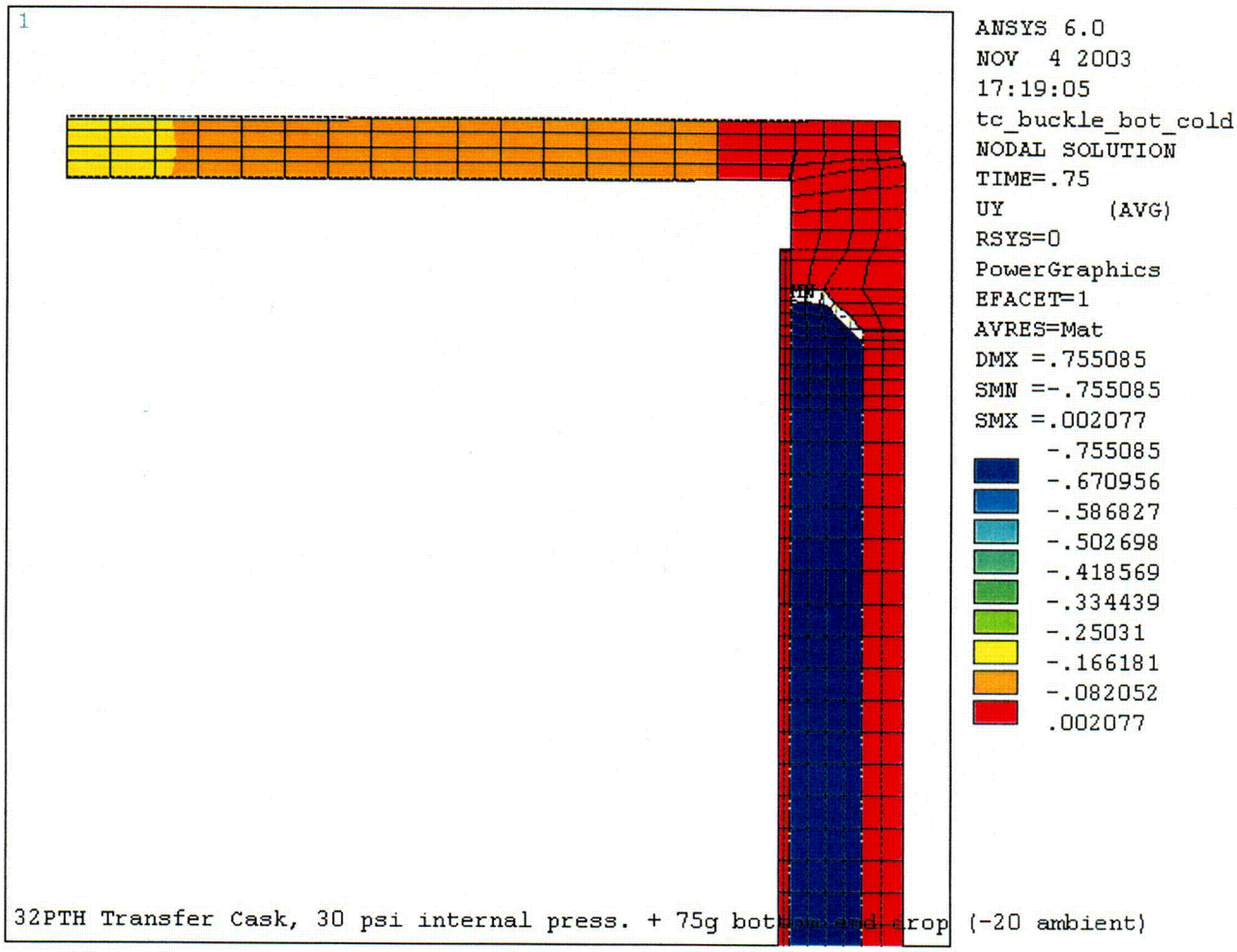

Figure 3.9.4-10
Deformed Shape of Transfer Cask for 75g Bottom End Drop
(Top End, -20° F Ambient Case)

C17

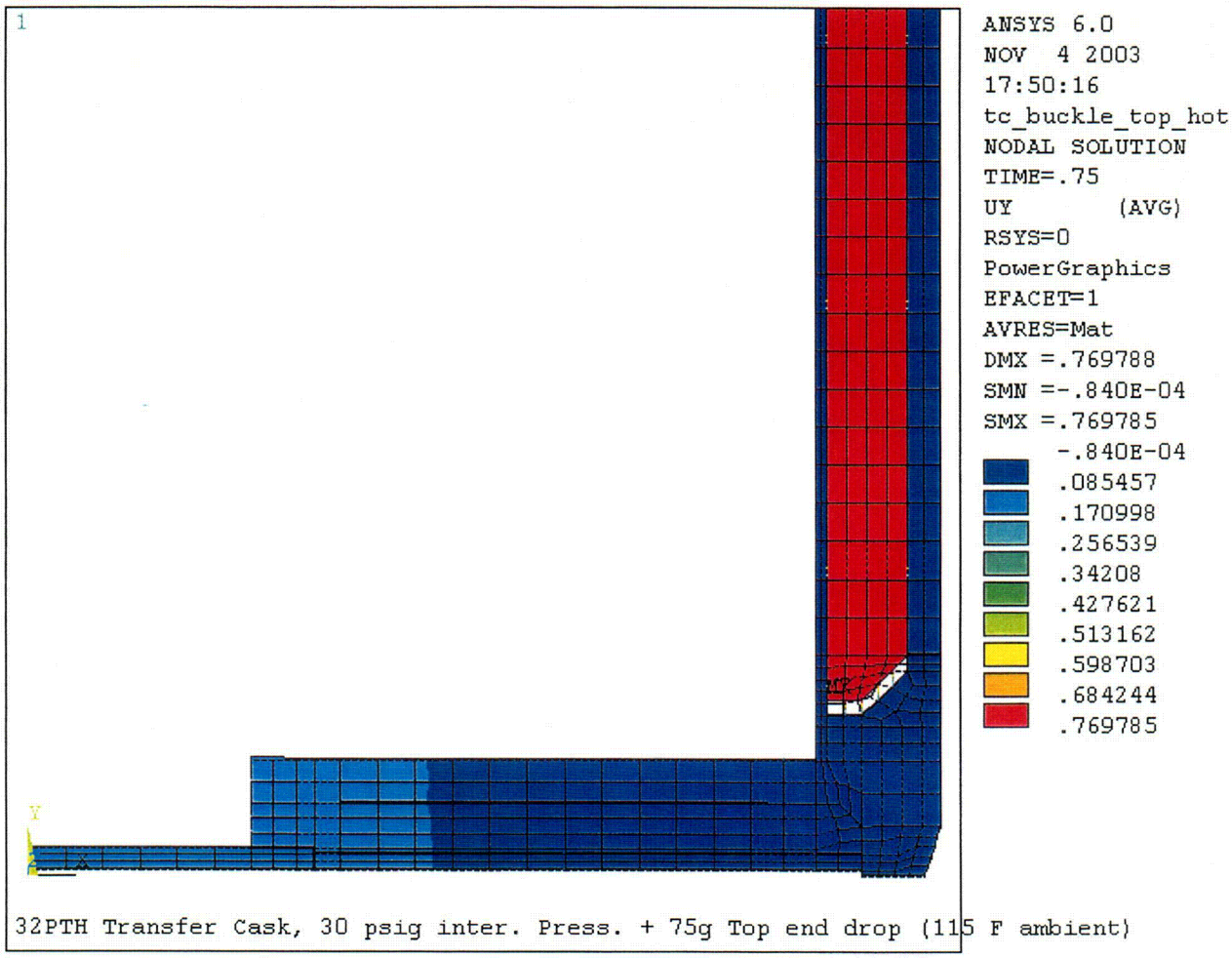

Figure 3.9.4-11
Deformed Shape of Transfer Cask for 75g Top End Drop (Bottom End, 115° F Ambient Case)

C18

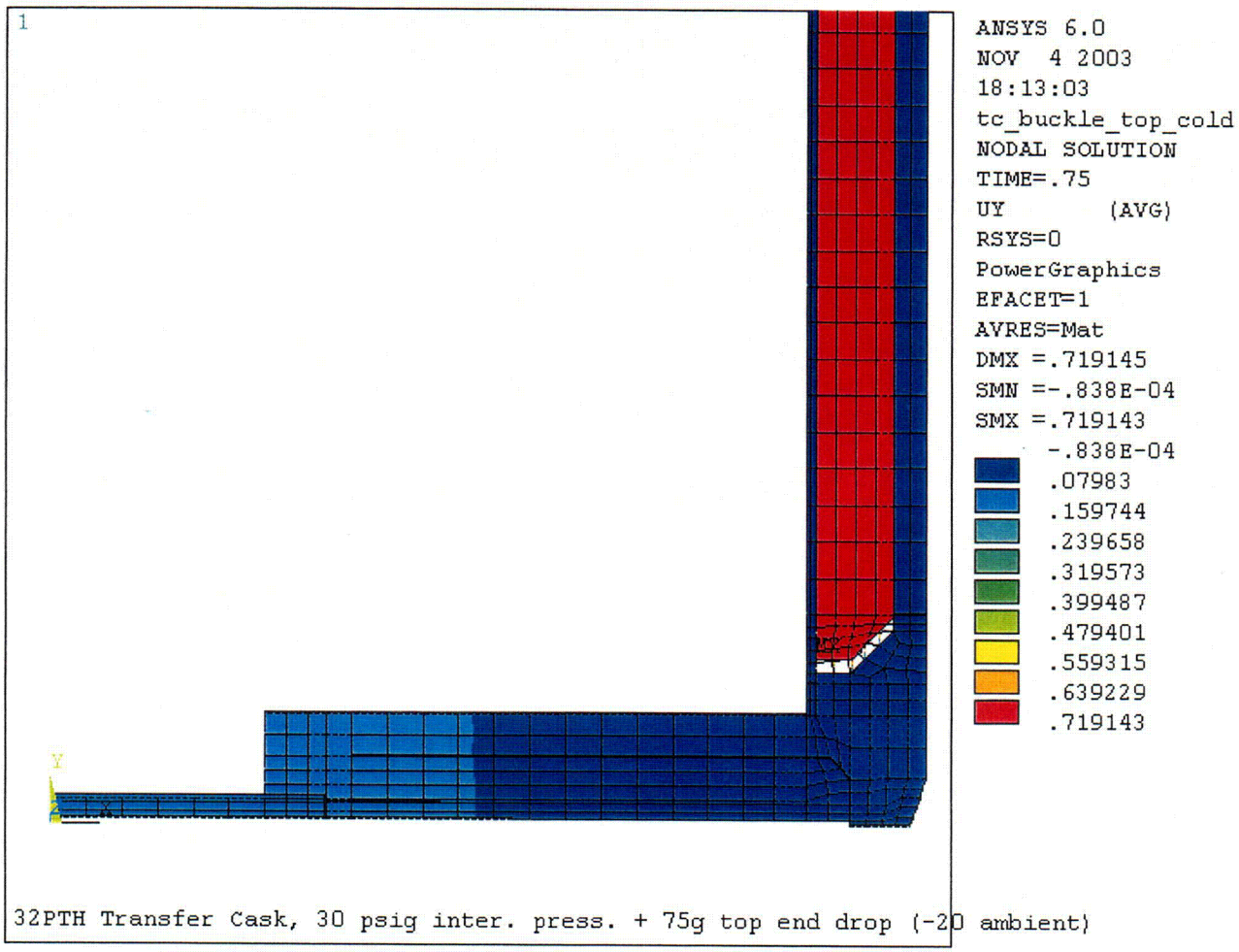

Figure 3.9.4-12
Deformed Shape of Transfer Cask for 75g Top End Drop (Bottom End, -20° F Ambient Case)

C19

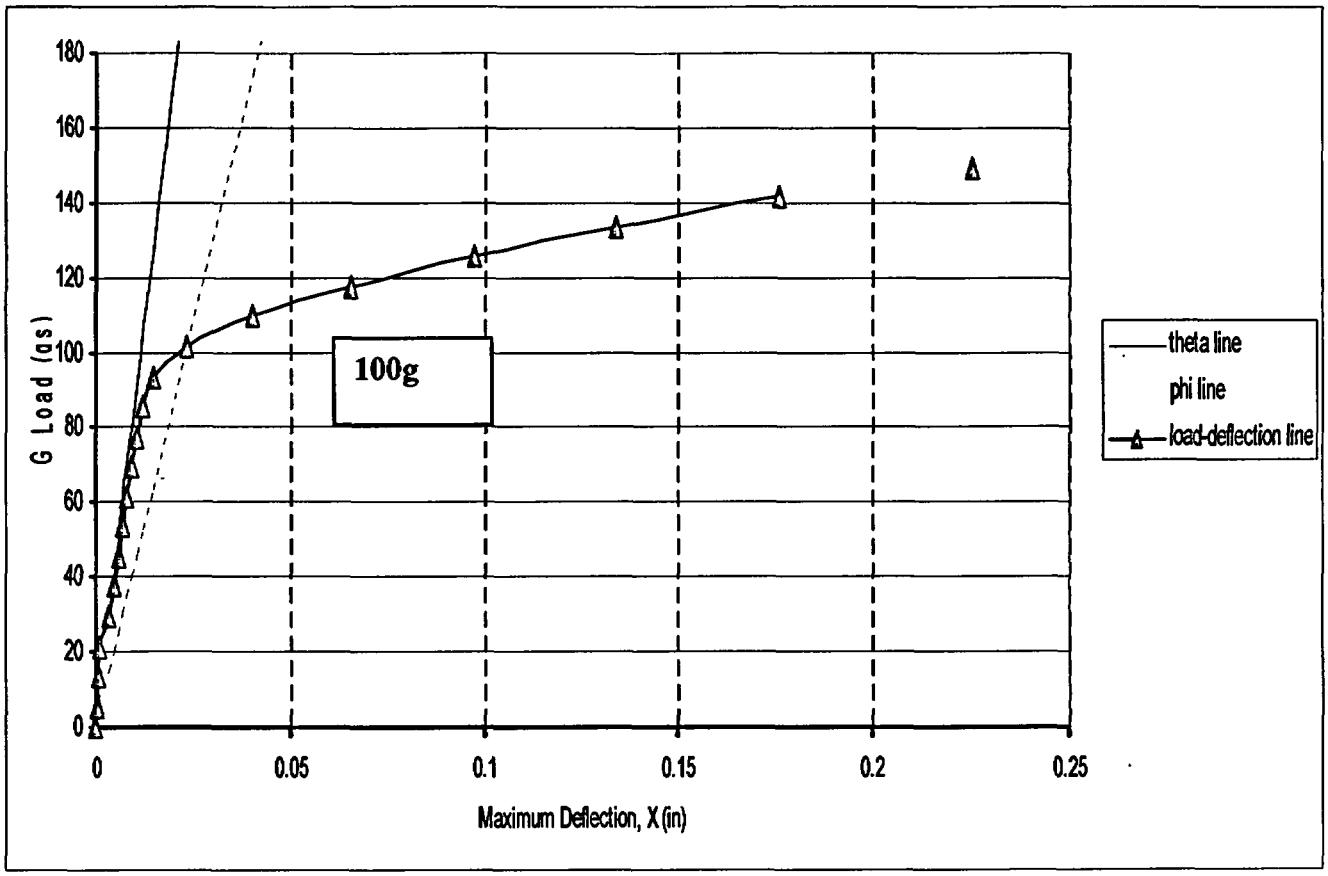

Figure 3.9.4-13
Construction of Collapse Load for Transfer Cask Bottom End Drop

APPENDIX 3.9.5
OS187H TRANSFER CASK TRUNNION ANALYSIS

TABLE OF CONTENTS

3.9.5 OS187H TRANSFER CASK TRUNNION ANALYSIS 3.9.5-1

3.9.5.1 Introduction 3.9.5-1

3.9.5.2 Component Weights 3.9.5-2

3.9.5.3 Load Cases 3.9.5-2

3.9.5.4 Material Properties 3.9.5-3

3.9.5.5 Stress Criteria 3.9.5-3

3.9.5.6 Stress Computation 3.9.5-3

3.9.5.7 Summary of Computed Stresses 3.9.5-13

3.9.5.8 Conclusions 3.9.5-13

3.9.5.9 References 3.9.5-14

LIST OF TABLES

3.9.5-1 Summary of Computed and Allowable Trunnion Stresses

LIST OF FIGURES

3.9.5-1 OS187H Transfer Cask Bottom Trunnion (Top View)

3.9.5-2 OS187H Transfer Cask Top Trunnion (Top View)

3.9.5-3 Opening in the Lifting Yoke Arm Geometry

3.9.5 OS187H TRANSFER CASK TRUNNION ANALYSIS

3.9.5.1 Introduction

This appendix presents the evaluation of the NUHOMS®-OS187H Transfer Cask Trunnion stresses due to all applied loads during fuel loading and transfer operations.

NUHOMS® OS187H transfer cask has two top trunnions constructed from SA-182 Gr. FXM19 (22Cr-13Ni-5Mn Forging) and two bottom trunnions constructed from SA-182 Gr. F304. The cask shells are made of SA-240, Gr. 304 (18Cr-8Ni) stainless steel. The two top trunnions are used to first lift the cask, containing a canister and an empty basket, into a fuel pool for loading of the spent fuel. After the spent fuel has been loaded into the basket, the cask is lifted to a decontamination area. After draining and drying of the pool water, welding of the canister cover, and bolting of the cask lid, the cask is placed in a trailer for transfer to onsite HSM. The cask is vertically lifted onto the trailer and is initially supported by the bottom trunnions which are mated to transfer trailer. Then the cask is allowed to pivot about the bottom trunnions, into a horizontal position until the top trunnions rest on their supports in the trailer. Throughout the operation the maximum total load is applied to the cask top trunnions. After the cask has been placed on the trailer, it is supported by all four trunnions and is subject to a set of specified design handling loads.

The following two load cases are analyzed for the four transfer cask trunnions:

A. Lifting Loads (Cask lifted from the pool to the decontamination area and then to the trailer). The two top trunnions are analyzed for 6*g* and 10*g* vertical loads as required by ANSI N14.6 [1]. The two bottom trunnions are not used during lifting of the cask.

B. Handling Loads (Cask in a horizontal position on transfer trailer). All four trunnions rest on the supports on the trailer. The four trunnions are designed to resist the following transfer loads:

   DW (Dead Weight) + 1g Axial
   DW + 1g Transverse
   DW + 1g Vertical
   DW + ½*g* Axial + ½*g* Transverse + ½*g* Vertical

   (Directions are relative to a horizontal cask)

The transfer cask shell and trunnions are assumed to be at 300° F during transfer. This assumption is conservative based on the thermal evaluation performed in Chapter 4.

3.9.5.2 Component Weights

The weight of the NUHOMS®-OS187H Transfer Cask is 228.72 kips, including the loaded DSC (Section 3.2). However, for conservatism, a weight of 250.00 kips. is used in this analysis.

3.9.5.3 Load Cases

The following moment arms are used for the two load cases:

Load Case	*g* Load	Moment Arm Length	Reaction Support
Lifting	6g and 10g longitudinal	9.750 in.*	Top two trunnions only
Transfer Loads	DW +1*g* Axial DW+1*g* vertical DW+1*g* transverse DW + 0.5g Axial + 0.5g Vertical + 0.5g Trans.	7.135 in.**	All four top and bottom trunnions

* See Figure 3.9.5-2 (11.63"- 0.38"- 1.5" = 9.75")
** See Figure 3.9.5-1 (8.76"-1.625" = 7.135")

3.9.5.4 Material Properties

The following material properties, used for the trunnion stress analysis, are taken from Reference 2 at 300°F.

Property	SA-182, Gr. FXM-19 (Top Trunnions)	SA-182, Gr. F304 (Bottom Trunnions, t >5")
S_m	31.4 ksi	20 ksi
S_y	43.3 ksi	22.4 ksi
S_u	94.2 ksi	66.2 ksi

3.9.5.5 Stress Criteria

ANSI N14.6 requires the maximum tensile and shear stresses in the lifting trunnion due to 6*g* and 10*g* load be checked against the material yield and ultimate stresses respectively. The handling loads are normal condition (Level A) loads and are compared with the allowable stresses in ASME Code, Section III, Subsection NC [3].

3.9.5.6 Stress Computation

3.9.5.6.1 Lifting Load Stresses in Top Trunnions

The top trunnion material (SA-182 Gr. FXM19) ultimate and yield stresses at 300° F are 94,200 psi and 43,300 psi respectively. Since the ratio of two design lifting loads for each top trunnion is 1.667 (10*g* / 6*g*), is less than the ratio of the allowable stresses, 2.175 (94,200psi / 43,300 psi), it is not necessary to check stresses in the trunnions for the higher 10*g* design load.

The 6*g* Vertical load on one top trunnion, F_1, is,

$$F_1 = 250{,}000 \text{ lb} \times 6g \times 1.1 \times 1/2 = 825{,}000 \text{ lb}$$

A dynamic load factor, DLF, of 1.1 is used in this calculation.

The 2.5 inch thick lifting yoke plate is to be positioned in the middle of the 3 inch wide top trunnion groove. Therefore, the lift weight acts at the center of the 3 inch trunnion groove. (See Figure 3.9.5-2 for the load location)

A. Stresses at trunnion Section A-A (See Figure 3.9.5-2)

The cross-section area, $A_{A\text{-}A}$, and area moment of inertia, $I_{A\text{-}A}$ are the following.

$$A_{A\text{-}A} = \pi/4\ (8.75^2 - 4^2) = 47.57\ \text{in}^2$$
$$I_{A\text{-}A} = \pi/64\ (8.75^4 - 4^4) = 275.17\ \text{in}^4$$

$$M_{A\text{-}A} = F_1 \times L_{A\text{-}A} = 825{,}000\ \text{lb} \times (3 / 2) = 1{,}237{,}500\ \text{in-lb.}$$

The average shear stress, τ_{avg}, is,

$$\tau_{avg} = F_1 / A_{A\text{-}A} = 825{,}000\ \text{lb} / 47.57\ \text{in}^2 = 17{,}343\ \text{psi}$$

The maximum bending stress, σ_b, is,

$$\begin{aligned}\sigma_b &= (M_{A\text{-}A} / I_{A\text{-}A}) \times (H_{A\text{-}A} /2)\\ &= (1{,}237{,}500\ \text{in-lb} / 275.17\ \text{in}^4)\ (8.75 / 2) = 19{,}675\ \text{psi}\end{aligned}$$

The combined shear stress, τ_{max},

$$\begin{aligned}\tau_{max} &= 0.5 \times [(\sigma_b^2 + 4(\tau_{avg})^2]^{0.5}\\ &= 0.5 \times [19{,}675^2 + 4(17{,}343)^2]^{0.5}\\ &= 19{,}940\ \text{psi} < S_y\end{aligned}$$

The maximum tensile stress, σ_{max}, is the following.

$$\begin{aligned}\sigma_{max} &= \sigma_b / 2 + \tau_{max}\\ &= 19{,}675 /2 + 19{,}940 = 29{,}778\ \text{psi} < S_y\end{aligned}$$

B. Stresses at trunnion Section B-B (See Figure 3.9.5-2)

Cross-section Area, $A_{B\text{-}B}$, Area Moment of Inertia, $I_{B\text{-}B}$, are the following.

$$A_{B\text{-}B} = \pi/4\ (12^2 - 4^2) = 100.53\ \text{in}^2$$
$$I_{B\text{-}B} = \pi/64\ (12^4 - 4^4) = 1{,}005\ \text{in}^4$$

$$M_{B\text{-}B} = 825{,}000\ \text{lb} \times (3'' / 2 + 3.25'') = 3{,}918{,}750\ \text{in-lb.}$$

The average shear stress, τ_{avg}, is,

$$\tau_{avg} = F_1 / A_{B\text{-}B} = 825{,}000\ \text{lb} / 100.53\ \text{in}^2 = 8{,}207\ \text{psi}$$

The maximum bending stress, σ_b, is,

$$\sigma_b = (M_{B\text{-}B} / I_{B\text{-}B}) \times (H_{B\text{-}B} /2)$$
$$= (3{,}918{,}750 \text{ in-lb} / 1{,}005 \text{ in}^4)\ (12 / 2) = 23{,}396 \text{ psi}$$

The combined shear stress, τ_{max},

$$\tau_{max} = 0.5 \times [(\sigma_b^2 + 4(\tau_{avg})^2]^{0.5}$$
$$= 0.5 \times [23{,}396^2 + 4(8{,}207)^2]^{0.5}$$
$$= 14{,}289 \text{ psi} < S_y$$

The maximum tensile stress, σ_{max}, is the following.

$$\sigma_{max} = \sigma_b / 2 + \tau_{max}$$
$$= 22{,}396 / 2 + 14{,}289 = 25{,}987 \text{ psi} < S_y$$

C. Stresses at Section C-C (See Figure 3.9.5-2)

Cross-section Area, $A_{B\text{-}B}$, Area Moment of Inertia, $I_{B\text{-}B}$, are the following.

$$A_{C\text{-}C} = \pi/4\ (17.15^2 - 4^2) = 218.44 \text{ in}^2$$
$$I_{C\text{-}C} = \pi/64\ (17.15^4 - 4^4) = 4{,}234 \text{ in}^4$$

$$M_{C\text{-}C} = F_1 \times L_{C\text{-}C} = 825{,}000 \text{ lb} \times (11.63" - 0.38" - 3" / 2) = 8{,}043{,}750 \text{ in-lb.}$$

The average shear stress, τ_{avg}, is,

$$\tau_{avg} = F_1 / A_{C\text{-}C} = 825{,}000 \text{ lb} / 218.44 \text{ in}^2 = 3{,}777 \text{ psi}$$

The maximum bending stress, σ_b, is,

$$\sigma_b = (M_{C\text{-}C} / I_{C\text{-}C}) \times (H_{C\text{-}C} /2)$$
$$= (8{,}043{,}750 \text{ in-lb} / 4{,}234 \text{ in}^4)\ (17.15 / 2) = 16{,}291 \text{ psi}$$

The combined shear stress, τ_{max},

$$\tau_{max} = 0.5 \times [(\sigma_b^2 + 4(\tau_{avg})^2]^{0.5}$$
$$= 0.5 \times [16{,}291^2 + 4(3{,}777)^2]^{0.5}$$
$$= 8{,}979 \text{ psi} < S_y$$

The maximum tensile stress, σ_{max}, is the following.

$$\sigma_{max} = \sigma_b / 2 + \tau_{max}$$
$$= 16{,}291 /2 + 8{,}979 = 17{,}125 \text{ psi} < S_y$$

D. Bearing Stresses at Trunnion

The following dimensions refer to the Figure 3.9.5-3.

Length AO = 6.5 in., BC = 4.75 in., OC = 5 in., FC = 4.375 in.

Therefore,

$$DO = AO - AD = AO - BC = 6.5 \text{ in.} - 4.75 \text{ in.} = 1.75 \text{ in.}$$

$$\angle DCO = \sin^{-1}(DO/CO) = 20.4873°$$
$$\angle BCE = 90° - \angle DCO = 90° - 20.4873° = 69.5127°$$

During lifting, the 2.5 inch thick lifting arm plate will generate bearing stress in the outer end of the trunnion. The contact between the lifting arm plate and the trunnion is to encompass 69.51°. The projected bearing stress area, A_{br}, is,

$$A_{br} = 2 \times 4.375 \text{ in.} \times \sin 69.51° \times 2.5 \text{ in.} = 20.491 \text{ in.}^2$$

The bearing stress, σ_{br}, is then,

$$\sigma_{br} = 825{,}000 \text{ lb} / 20.491 \text{ in}^2 = 40{,}262 \text{ psi} < S_y$$

3.9.5.6.2 Handling Load Stresses

All four trunnions carry the axial and vertical loads while only one top trunnion and one bottom trunnion on the same side of the cask will carry the transverse load.

A. DW (1*g* vertical) + 1*g* Axial

At the top and bottom trunnions the *g*-loads per trunnion are:

1.0*g* (axial) / 2 sides / 2 set trunnions = 0.25*g* axial per trunnion.
1.0*g* (vertical) / 2 sides / 2 set trunnions = 0.25*g* vertical per trunnion

The bottom trunnions have a larger inner diameter (8 inch diameter of material is removed to reduce the weight, see Figure 3.9.5-1) than the top trunnions (4 inch diameter, see Figure 3.9.5-2). Also, the bottom trunnions material has lower yield and ultimate strengths relative to the top trunnions, and therefore has lower allowable stresses. Thus, the bottom trunnions are critical with respect to stress generated by the handling load. The transfer loads are therefore analyzed only for the weaker bottom trunnions, which are shown in Figure 3.9.5-1.

The vector sum of 0.25g vertical and 0.25*g* axial = $[0.25^2 + 0.25^2]^{1/2}g = 0.354g$

Therefore, the lateral load at each bottom trunnion, F_1, is,

$$F_1 = 250{,}000\text{lb} \times 0.354g = 88{,}500 \text{ lb.}$$

Stresses at Trunnion Section B-B (See Figure 3.9.5-1)

The cross-section Area, $A_{B\text{-}B}$, is,

$$A_{B\text{-}B} = \pi/4\ (12^2 - 8^2) = 62.83 \text{ in}^2$$

Area Moment of Inertia, $I_{B\text{-}B}$, is,

$$I_{B\text{-}B} = \pi/64\ (12^4 - 8^4) = 816.81 \text{ in}^4$$

Therefore, the bending moment, $M_{B\text{-}B}$, is,

$$M_{B\text{-}B} = 88{,}500 \text{ lb} \times (3.25 \text{ in.} / 2) = 143{,}813 \text{ in-lb.}$$

The maximum shear stress due to bending for a hollow circular section, τ_{max}, is the following.

$$\tau_{max} = 2F_1 / A_{B\text{-}B} = 2 \times 88{,}500 \text{ lb} / 62.83 \text{ in}^2 = 2{,}817 \text{ psi}$$

The maximum bending stress due to lateral load, σ_x, is,

$$\sigma_x = (M_{B\text{-}B} / I_{B\text{-}B}) \times (H_{B\text{-}B} /2)$$
$$= (143{,}813 \text{ in-lb} / 816.61 \text{ in}^4)\ (12 \text{ in.} / 2) = 1{,}057 \text{ psi.}$$

The stress intensity, *S.I.*, is then,

$$S.I. = [(\sigma_x^2 + 4(\tau_{max})^2]^{0.5} = [1{,}057^2 + 4(2{,}817)^2]^{0.5}$$
$$= 5{,}732 \text{ psi} < S_m$$

The stress intensity, S.I., calculated here is conservatively considered to be primary membrane stress, P_m, and is evaluated against its allowable stress, S_m, as per ASME B&PV Section III-NC [3].

$$S_m = 20{,}000 \text{ psi (for SA-182 Gr.F304 at 300° F)}$$

Stresses at Section C-C (See Figure 3.9.5-1)

Cross-section Area, $A_{C\text{-}C}$, is,

$$A_{C\text{-}C} = \pi/4\ (17.15^2 - 8^2) = 180.74 \text{ in}^2.$$

Area Moment of Inertia, $I_{C\text{-}C}$, is,

$$I_{C\text{-}C} = \pi/64\ (17.15^4 - 8^4) = 4{,}045 \text{ in}^4.$$

The bending moment, $M_{C\text{-}C}$, is then,

$$M_{C\text{-}C} = F \times L_{C\text{-}C}$$
$$= 88{,}500 \text{ lb} \times (8.75 \text{ in.} - 3.25 \text{ in.} / 2) = 630{,}563 \text{ in-lb.}$$

The maximum shear stress due to bending for a hollow circular section, τ_{max}, is the following.

$$\tau_{max} = 2\ F / A_{C\text{-}C} = 2 \times 88{,}500 \text{ lb} / 180.74 \text{ in}^2 = 979 \text{ psi.}$$

The maximum bending stress due to lateral load, σ_x, is,

$$\sigma_x = (M_{C\text{-}C} / I_{C\text{-}C}) \times (H_{C\text{-}C} /2) + F_a / A_{C\text{-}C}$$
$$= (630{,}563 \text{ in-lb} / 4{,}045 \text{ in.}^4)\ (17.15\text{in.} / 2) = 1{,}337 \text{ psi}$$

The stress intensity, *S.I.*, is,

$$S.I. = [(\sigma_x^2 + 4(\tau_{max})^2]^{0.5}$$
$$= [1{,}337^2 + 4(979)^2]^{0.5} = 2{,}371 \text{ psi} < S_m$$

B. DW (1g vertical) + 1g Vertical

At the top and bottom trunnions the g-load per trunnion is:

2.0g (vertical) / 2 sides / 2 set trunnions = 0.5g vertical per trunnion

The lateral load at each bottom trunnion, F_1 is the following.

$$F_1 = 250{,}000\text{lb} \times 0.5g = 125{,}000 \text{ lb.}$$

Stresses are calculated from Case A by multiplying with a factor 125,000/88,500 = 1.4124

Stresses at trunnion Section B-B (See Figure 3.9.5-1)

Maximum Stress Intensity, *S.I.*, is,

$$S.I. = 1.4124 \times 5{,}732 = 8{,}096 \text{ psi.} < S_m$$

Stresses at trunnion Section C-C (See Figure 3.9.5-1)

Maximum Stress Intensity, *S.I.*, is,

$$S.I. = 1.4124 \times 2{,}371 = 3{,}349 \text{ psi.} < S_m$$

C. DW (1g vertical) + 1g Transverse

At the top and bottom trunnions the g-loads per trunnion are:

1.0g (transverse) / 1 side / 2 set trunnions = 0.5g transverse per trunnion.
1.0g (vertical) / 2 sides / 2 set trunnions = 0.25g vertical per trunnion

Lateral load at each bottom trunnion, F_1, is,

$$F_1 = 250{,}000\text{lb} \times 0.25 = 62{,}500 \text{ lb}$$

Axial Load at bottom trunnion, F_2, is,

$$F_2 = 250{,}000\text{lb} \times 0.5 = 125{,}000 \text{ lb}$$

Stresses at trunnion Section B-B (See Figure 3.9.5-1)

Therefore, the bending moment, $M_{B\text{-}B}$, is,

$$M_{B\text{-}B} = 62{,}500 \text{ lb} \times (3.25 \text{ in.} / 2) = 101{,}563 \text{ in-lb.}$$

The maximum shear stress due to bending for a hollow circular section, τ_{max}, is the following.

$$\tau_{max} = 2F_1 / A_{B\text{-}B} = 2 \times 62{,}500 \text{ lb} / 62.83 \text{ in}^2 = 1{,}989 \text{ psi.}$$

The maximum normal stress, σ_x, is,

$$\begin{aligned}\sigma_x &= \text{max. bending stress due to lateral load + normal stress due to axial load}\\ &= (M_{B\text{-}B} / I_{B\text{-}B}) \times (H_{B\text{-}B} / 2) + F_2 / A_{B\text{-}B}\\ &= (101{,}563 \text{ in-lb} / 816.61 \text{ in}^4)\ (12 \text{ in.} / 2) + 125{,}000 \text{ lb} / 62.83 \text{ in}^2\\ &= 746 + 1989 = 2{,}735 \text{ psi.}\end{aligned}$$

The stress intensity, *S.I.*, is,

$$\begin{aligned}S.I. &= [(\sigma_x^2 + 4(\tau_{max})^2]^{0.5} = [2{,}735^2 + 4(1{,}989)^2]^{0.5}\\ &= 4{,}828 \text{ psi} < S_m\end{aligned}$$

Stresses at Section C-C (See Figure 3.9.5-1)

The bending moment, $M_{C\text{-}C}$, is,

$$\begin{aligned}M_{C\text{-}C} &= F_1 \times L_{C\text{-}C}\\ &= 62{,}500 \text{ lb} \times (8.75 \text{ in.} - 3.25 \text{ in.} / 2) = 445{,}313 \text{ in-lb.}\end{aligned}$$

The maximum shear stress due to bending for a hollow circular section, τ_{max}, is the following.

$$\tau_{max} = 2F / A_{C\text{-}C} = 2 \times 62{,}500 \text{ lb} / 180.74 \text{ in}^2 = 692 \text{ psi.}$$

The maximum normal stress, σ_x, is,

$$\begin{aligned}\sigma_x &= \text{max. bending stress due to lateral load + normal stress due to axial load}\\ &= (M_{C\text{-}C} / I_{C\text{-}C}) \times (H_{C\text{-}C} / 2) + F_a / A_{C\text{-}C}\\ &= (445{,}313 \text{ in-lb} / 4{,}045 \text{ in}^4)\ (17.15 \text{ in.} / 2) + 125{,}000 \text{ lb} / 180.74 \text{ in}^2\\ &= 944 + 692 = 1{,}636 \text{ psi.}\end{aligned}$$

The stress intensity, *S.I.*, is,

$$\begin{aligned}S.I. &= [(\sigma_x^2 + 4(\tau_{max})^2]^{0.5}\\ &= [1{,}636^2 + 4(692)^2]^{0.5} = 2{,}143 \text{ psi} < S_m\end{aligned}$$

D. DW + 0.5*g* Axial + 0.5*g* Vertical + 0.5*g* Transverse

At the top and bottom trunnions the *g*-loads per trunnion are:

0.5*g* (axial) / 2 sides / 2 set trunnions = 0.125*g* axial per trunnion
0.5*g* (transverse) / 1 side / 2 set trunnions = 0.25*g* transverse per trunnion
1.5*g* (vertical) / 2 sides / 2 set trunnions = 0.375*g* vertical per trunnion

The vector sum of 0.375*g* vertical and 0.125*g* axial = $[0.375^2 + 0.125^2]^{1/2}\, g = 0.395g$

Lateral Load at each bottom trunnion, F_1, is,

$$F_1 = 250{,}000\text{lb} \times 0.395g = 98{,}750 \text{ lb}$$

Transverse Load at bottom trunnion, F_2, is,

$$F_2 = 250{,}000\text{lb} \times 0.25g = 62{,}500 \text{ lb}$$

Where, the load, F_2, acts as an axial load on the bottom trunnion.

Stresses at trunnion Section B-B (See Figure 3.9.5-1)

The bending moment, $M_{B\text{-}B}$, is,

$$M_{B\text{-}B} = 98{,}750 \text{ lb} \times (3.25 \text{ in.} / 2) = 160{,}469 \text{ in-lb.}$$

The maximum shear stress due to bending for a hollow circular section, τ_{max}, is the following.

$$\tau_{max} = 2F_1 / A_{B\text{-}B} = 2 \times 98{,}750 \text{ lb} / 62.83 \text{ in}^2 = 3{,}143 \text{ psi.}$$

The maximum normal stress, σ_x, is,

σ_x = max. bending stress due to lateral (F_1) load + normal stress due to F_2 load
$= (M_{B\text{-}B} / I_{B\text{-}B}) \times (H_{B\text{-}B} /2) + F_2 / A_{B\text{-}B}$
$= (160{,}469 \text{ in-lb} / 816.61 \text{ in.}^4)\,(12 \text{ in.} / 2) + 62{,}500 \text{ lb} / 62.83 \text{ in}^2.$
$= 1{,}179 + 995 = 2{,}174$ psi.

The stress intensity, *S.I.*, is,

$$S.I. = [(\sigma_x^2 + 4(\tau_{max})^2]^{0.5} = [2{,}174^2 + 4(3{,}143)^2]^{0.5}$$
$$= 6{,}651 \text{ psi.} < S_m$$

Stresses at Section C-C (See Figure 3.9.5-1)

The bending moment, $M_{C\text{-}C}$, is,

$$M_{C\text{-}C} = F_1 \times L_{C\text{-}C}$$
$$= 98{,}750 \text{ lb} \times (8.75 \text{ in.} - 3.25 \text{ in.} / 2) = 703{,}594 \text{ in-lb.}$$

The maximum shear stress due to bending for a hollow circular section, τ_{max}, is the following.

$$\tau_{max} = 2F_1 / A_{C\text{-}C} = 2 \times 98{,}750 \text{ lb} / \ 180.74 \text{ in}^2 \ = 1{,}093 \text{ psi.}$$

The maximum normal stress, σ_x, is,

$$\sigma_x = \text{max. bending stress due to lateral load + normal stress due to axial load}$$
$$= (M_{C\text{-}C} / I_{C\text{-}C}) \times (H_{C\text{-}C} /2) + F_2 / A_{C\text{-}C}$$
$$= (703{,}594 \text{ in-lb} / 4{,}045 \text{ in.}^4) (17.15 \text{ in.} / 2) + 62{,}500 \text{ lb} / 180.74 \text{ in.}^2$$
$$= 1{,}492 + 346 = 1{,}838 \text{ psi.}$$

The stress intensity, *S.I.*, is,

$$S.I. = [(\sigma_x^2 + 4(\tau_{max})^2]^{0.5}$$
$$= [1{,}838^2 + 4(1{,}093)^2]^{0.5} = 2{,}856 \text{ psi.} < S_m$$

3.9.5.7 Summary of Computed Stresses

The calculated maximum trunnion stresses are summarized in Table 3.9.5-1 and compared with their corresponding allowable stresses.

3.9.5.8 Conclusions

Table 3.9.5-1 shows that all calculated trunnion stresses are less than their corresponding allowable stresses. Therefore, the NUHOMS®-OS187H Transfer Cask top and bottom trunnions are structurally adequate to withstand loads during lifting and transfer operations.

3.9.5.9 References

1. "Special Lifting Devices for Shipping Containers Weighing 10,000 Pounds or More", ANSI N14.6, 1993.

2. American Society of Mechanical Engineers, ASME Boiler and Pressure Vessel Code, Section II, Part D, 1998, including 2000 addenda.

3. American Society of Mechanical Engineers, ASME Boiler and Pressure Vessel Code, Section III, Division 1, Subsection NC, 1998, including 2000 addenda.

Table 3.9.5-1
Summary of Computed and Allowable Trunnion Stresses

Case Number	Load	Maximum Stress		Allowable (ksi)
		Type	Magnitude (ksi)	
1	Lifting 6g	Shear	19.9	43.3 (2)
		Tensile	29.8	43.3 (2)
2	Lifting (1) 10g	Shear	33.2	94.2 (4)
		Tensile	49.6	94.2 (4)
3	Handling DW + 1.0g Axial	P_m	5.7	20.0 (3)
		$P_m + P_b$	5.7	20.0 (3)
4	Handling DW + 1.0g Vertical	P_m	8.1	20.0 (3)
		$P_m + P_b$	8.1	20.0 (3)
5	Handling DW + 1.0g Transverse	P_m	4.8	20.0 (3)
		$P_m + P_b$	4.8	20.0 (3)
6	Handling DW + 0.5g Axial + 0.5g Vertical + 0.5g Transverse	P_m	6.7	20.0 (3)
		$P_m + P_b$	6.7	20.0 (3)

Notes:
(1) Stresses in the trunnions are obtained by direct ratio from 6g load.
(2) Yield stress, S_y, for top trunnion material SA-182-FXM19 at 300° F per ANSI N14.6 [1] criterion.
(3) Design Stress Intensity, S_m, for bottom trunnion material SA-182-F304 at 300° F per ASME Section III-NC [3] criterion. Conservatively, $P_m + P_b$ is compared with S_m.
(4) Ultimate stress, S_u, for trunnion material SA-182-FXM19 at 300° F per ANSI N14.6 [1] criterion.

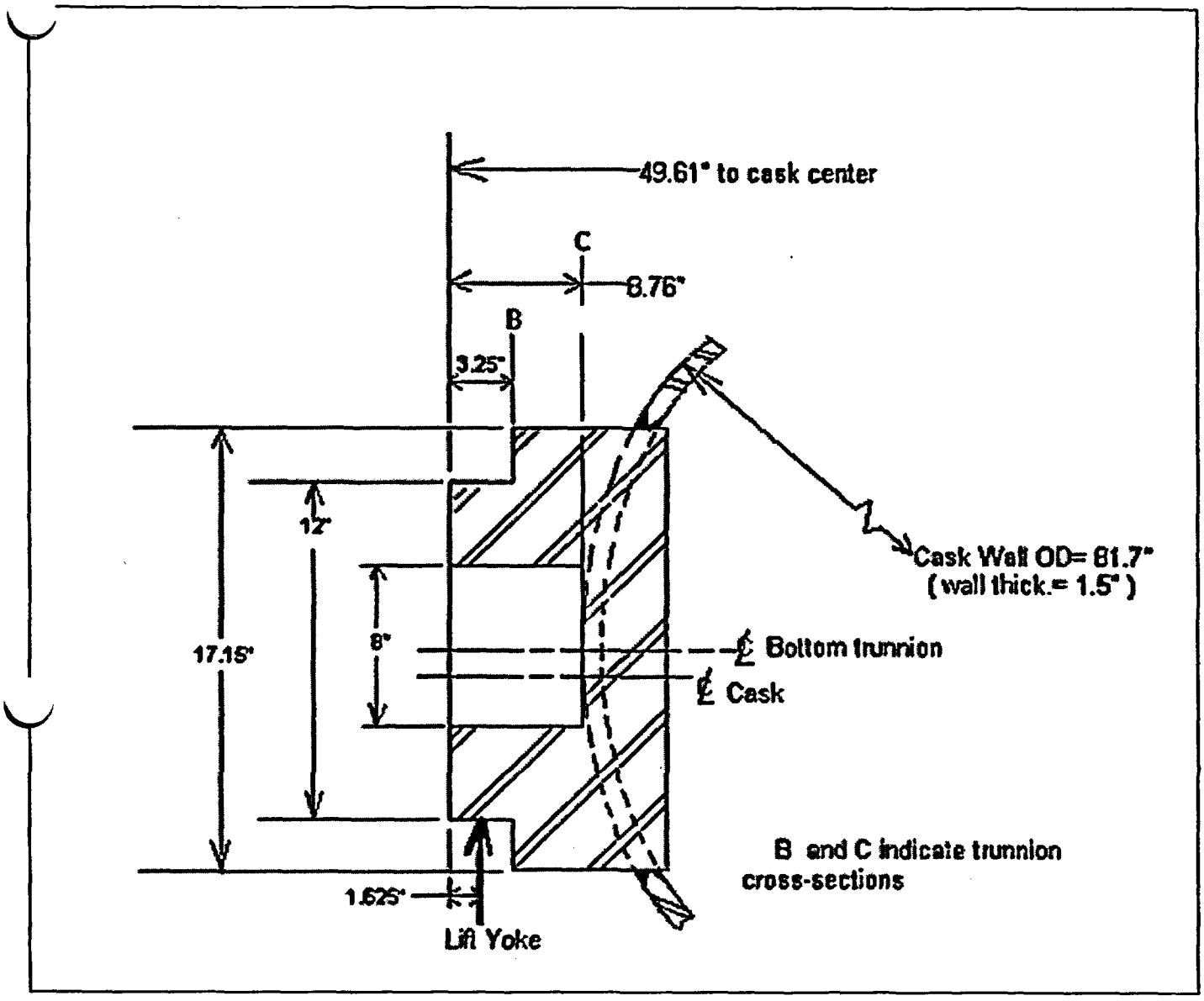

Figure 3.9.5-1
OS187H Transfer Cask Bottom Trunnion (Top View)

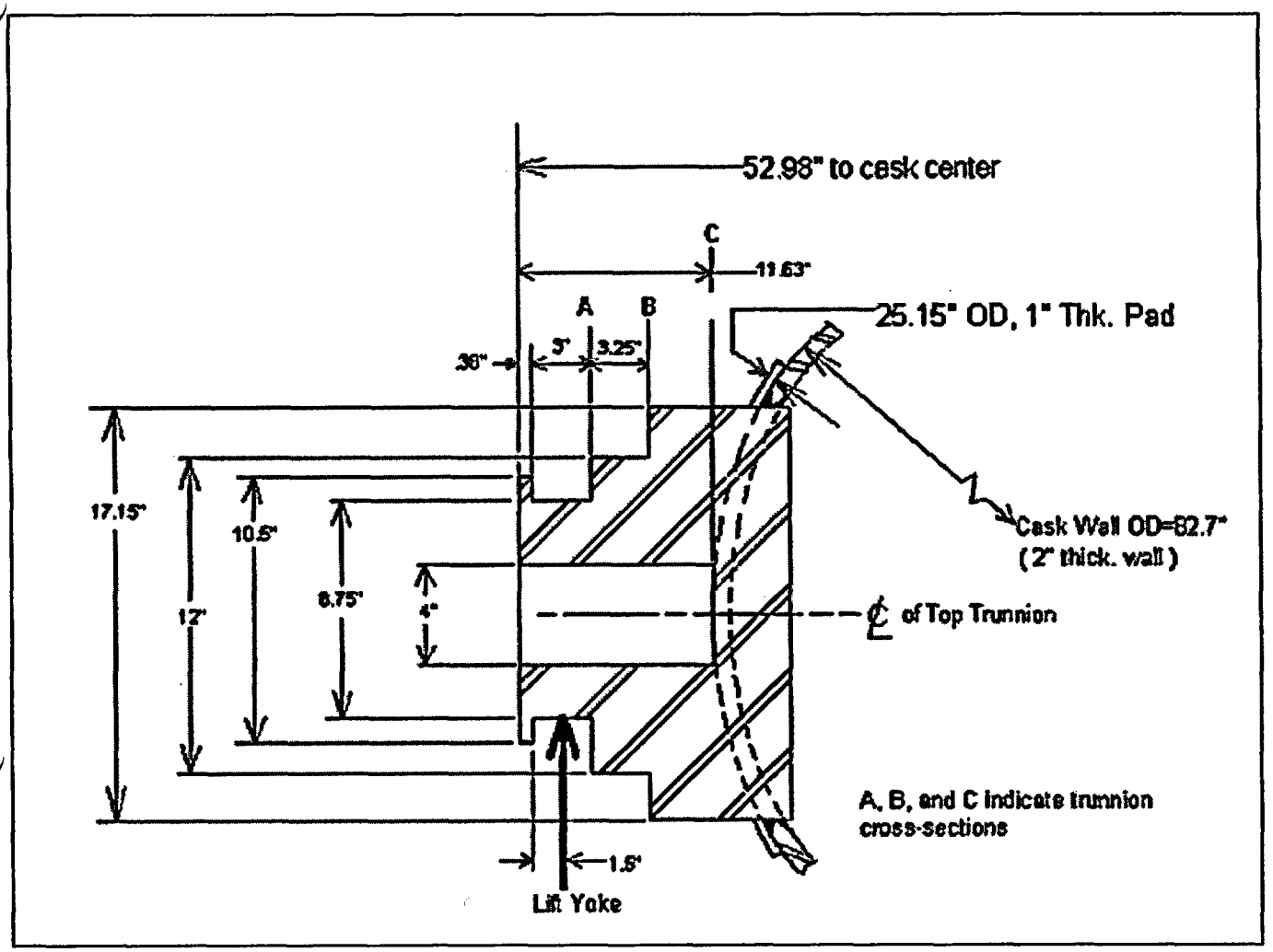

Figure 3.9.5-2
OS187H Transfer Cask Top Trunnion (Top View)

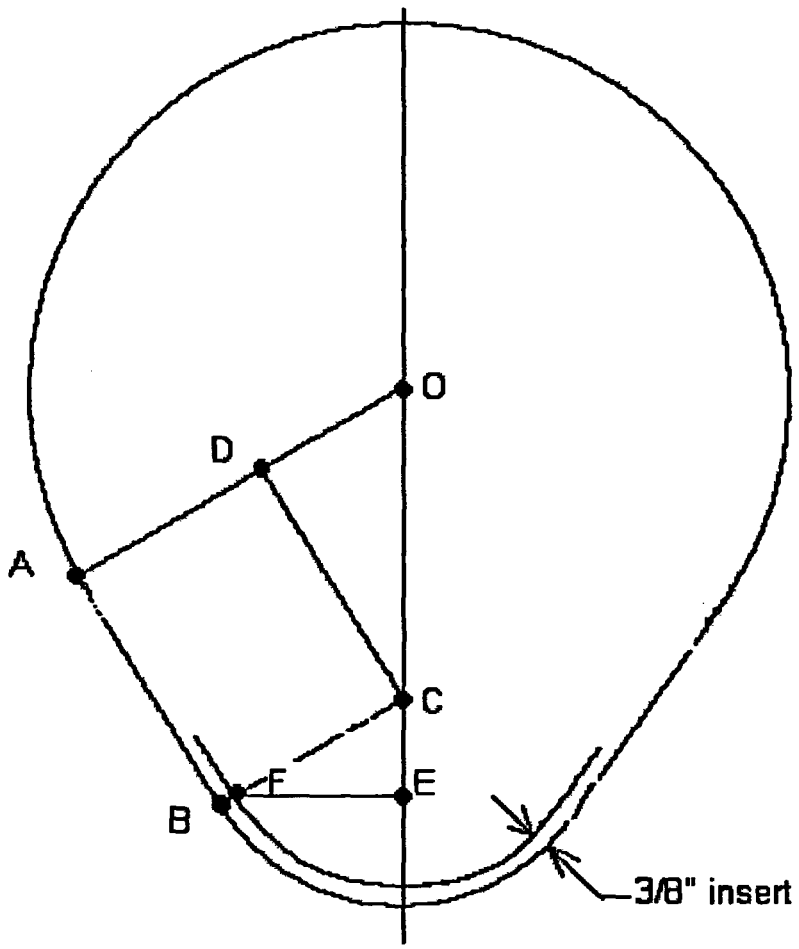

Figure 3.9.5-3
Opening in the Lifting Yoke Arm Geometry

APPENDIX 3.9.6
OS187H TRANSFER CASK SHIELD PANEL STURCTURAL ANALYSIS

TABLE OF CONTENTS

3.9.6 OS187H TRANSFER CASK SHIELD PANEL STURCTURAL ANALYSIS.. 3.9.6-1

3.9.6.1 Introduction 3.9.6-1

3.9.6.2 Material Properties 3.9.6-1

3.9.6.3 Component Weights 3.9.6-2

3.9.6.4 Stress Criteria 3.9.6-2

3.9.6.5 Load Cases 3.9.6-3

3.9.6.6 Stress Calculations 3.9.6-3

3.9.6.7 Conclusions 3.9.6-7

3.9.6.8 References 3.9.6-8

LIST OF TABLES

3.9.6-1 Summary of Computed and Allowable Neutron Shield Shell Stresses

LIST OF FIGURES

3.9.6-1 Neutron Shield Shell Finite Element Model

3.9.6-2 Neutron Shield Shell Finite Element Model, Top Plate Region

3.9.6-3 Neutron Shield Shell Finite Element Model, Bottom Plate Region

3.9.6-4 Neutron Shield Shell Finite Element Model, 3*g* Lifting Boundary Conditions

3.9.6-5 3*g* Lifting Stress Intensity Distribution

3.9.6-6 Neutron Shield Shell Finite Element Model, Transfer Loads Boundary Conditions

3.9.6-7 Transfer Loads Stress Intensity Distribution

3.9.6-8 Cold Ambient Environment Temperature Distribution

3.9.6-9 Hot Ambient Environment Temperature Distribution

4.9.6-10 Transfer Loads plus Cold Ambient Condition Stress Intensity Distribution

4.9.6-11 Transfer Loads plus Hot Ambient Condition Stress Intensity Distribution

3.9.6 OS187H TRANSFER CASK SHIELD PANEL STRUCTURAL ANALYSIS

3.9.6.1 Introduction

The purpose of this appendix is to present the evaluation of the stresses in the NUHOMS®-OS187H Transfer Cask neutron shield shell due to all applied loads during fuel loading and transfer operations.

A finite element model was built for the structural analysis of the outer neutron shield shell, end closure, central plates and structural shell. These components were modeled with the ANSYS Solid PLANE42 elements with axisymmetric option. The top and bottom closure plate welds were also modeled with PLANE42 elements. Double nodes were created at the central plate and shell intersections. These nodes were coupled to simulate the weld effect. Figures 3.9.6-1, 3.9.6-2 and 3.9.6-3 show the overall finite element model and its details. The same finite element model is used for all loading conditions.

3.9.6.2 Material Properties

The transfer cask shell is assumed to be at 300° F uniform temperature during transfer operations. This assumption is conservative based on the thermal evaluations performed in Chapter 4.

All shell components are constructed from stainless steel SA-240, Grade 304. The following mechanical and thermal material properties taken from Reference 1 are used in the analysis:

Material	Temp. °F	S_u (ksi)	S_y (ksi)	S_m (ksi)	E (10^6 psi)	α (10^{-6}) (in/in/°F)	Conductivity (Btu/hr-in-°F)	Density (lb/in^3)
SA-240 Stainless Steel 304	70	75.0	30.0	20.0	28.3	8.5	0.7217	0.29
	200	71.0	25.0	20.0	27.6	8.9	0.775	0.29
	300	66.2	22.4	20.0	27.0	9.2	0.8167	0.29
	400	64.0	20.7	18.7	26.5	9.5	0.8667	0.29

3.9.6.3 Component Weights

The weight of the NUHOMS®-OS187H Transfer Cask neutron shield shell, including the cylindrical shell, the top and bottom support rings, and the 15 central support rings is 4,288 lb. The weight of the neutron shield shell water is 8,458 lb (the transfer component weights are tabulated in Section 3.2). However, for conservatism, a weight of 8,500 lb. is used for the weights of water in this analysis.

For the transfer cask in the vertical orientation, the inertial force due to water weight is applied as pressure in the following way.

The weight of the neutron shield water, W is 8,500 lb. The maximum hydrostatic pressure at the bottom of the neutron shield shell, W_h, is,

$$W_h = 62.4 \text{ lb/ft}^3 \times 177.24 \text{ in} / 12^3 = 6.4 \text{ psi. ... say } 6.5 \text{ psi}$$

This hydrostatic pressure is linear with the axial height of the shield shell and is 0 psi at the top.

In addition to the water weight pressure, an additional internal uniform pressure of 40 psig is used in all load cases.

3.9.6.4 Stress Criteria

All load cases are analyzed and results evaluated to the requirements of ASME Code, Subsection NC [2] as normal condition (Level A) load cases. According to Reference 2, the maximum allowable membrane (P_m) and membrane plus bending ($P_m + P_b$) stress intensities for normal conditions are S_m and 1.5 S_m respectively. Also, average pure shear is limited to 0.6 S_m. The maximum primary plus secondary stress is limited to 3.0 S_m.

The transfer cask inner shell and structural shell are constructed from SA-240, Type 304 stainless steel. Therefore, the maximum allowable membrane and membrane plus bending stress intensities (at 300° F) are as follows:

Stress Category	Stress Criteria	Maximum Allowable Stress
P_m	S_m	20.0ksi.
$P_m + P_b$	$1.5S_m$	30.0 ksi.
$P_m + P_b + Q$	$3.0\ S_m$	60.0 ksi.
Pure Shear	$0.6S_m$	12.0 ksi.

3.9.6.5 Load Cases

The following load cases are considered. When transfer the loaded cask to ISFSI, the transfer loads are 1g axial, 1g transverse, and 1g vertical. For conservatism, a bounding 2g axial + 2g transverse + 2g vertical is used for stress calculations.

Load Case	Applied Load
3*g* Lifting (Cask Vertical)	40 psi. pressure + hydrostatic pressure + 3*g* longitudinal
Transfer Loads (Cask Horizontal)	40 psi. pressure + water pressure + 2*g* longitudinal + 2*g* vertical + 2*g* transverse 40 psi. pressure + water pressure + 2*g* longitudinal + 2*g* vertical + 2*g* transverse + Cold Thermal 40 psi. pressure + water pressure + 2*g* longitudinal + 2*g* vertical + 2*g* transverse + Hot Thermal

3.9.6.6 Stress Calculations

3.9.6.6.1 3*g* Lifting Load Case

The pressure at the bottom plate due to the 3*g* lifting load for water = 3 × 6.5 = 19.5 psi

The ANSYS elastic stress run is made by applying a 40 psi internal pressure and a 19.5 psi hydrostatic pressure. The loading and boundary conditions are shown in Figure 3.9.6-4. A 3g vertical acceleration is applied to account for the inertia loads. As shown in Figure 3.9.6-4, an internal pressure of 59.5 psi. (40 psi. + 19.5 psi.) is applied at the bottom of the shield shell. This pressure tapers linearly to 40 psi at the top.

The resulting stress intensity distribution in the various shell components is shown in Figure 3.9.6-5. It is seen that the maximum nodal stress intensity in the shell model is 24,123 psi. This maximum stress occurs in weld between the bottom plate and cylinder. These stresses are linearized through the shell thickness and presented in Table 3.9.6-1.

3.9.6.6.2 Transfer Load Condition

During transfer operations, the cask is in the horizontal position and the neutron shield shell is subjected to 40 psi internal pressure and transfer handling loads (2*g* vertical + 2*g* lateral + 2*g* axial).

The vertical and lateral loads are combined in the following way.

$$g_{transverse} = (2.0^2 + 2.0^2)^{1/2} = 2.83g$$

The stress due to the 2.83*g* inertia load conservatively assumes that the weight of the shell structure (4,288 lb.) and water (8,500 lb.) are uniformly distributed only over the 177.24 inch length and a 60° arch. Therefore, the equivalent pressure applied to the outer shell is,

$$p_{vl} = [(4{,}288 + 8{,}500) \times 2.83] / [2\,\pi\,(45.913)(177.24)] \times (360°/60°) = 4.25 \text{ psi. ... say 5 psi}$$

Again, the 5 psi load on the 60° sector is conservatively assumed to act on the full 360°. This pressure is added to 40 psi. pressure and applied to the cylinder.

For 2*g* axial acceleration, the pressure due to the water inertial load on the top plate is,

$$p_a = 8{,}500 \times 2.0 / [\pi \times (45.913^2 - 41.35^2)] = 13.6 \text{ psi. ... say 14 psi}$$

Therefore, a pressure of 54 psi. (40 + 14) is applied to the top plate. Also, there is a 40 psi. pressure applied to the bottom plate.

An ANSYS elastic stress run is made by applying the above calculated pressures to the finite element model. The boundary conditions are shown in Figure 3.9.6-6. The resulting stress intensity distribution is shown in Figure 3.9.6-7. It is seen that the maximum nodal stress intensity in the shell model is 20,137 psi. This maximum stress occurs in the outer shell near the bottom plate weld. These stresses are linearized through the shell thickness and presented in Table 3.9.6-1.

3.9.6.6.3 Thermal Analyses

The thermal analysis of the neutron shield shell model is conducted for both cold and hot environmental conditions. Steady-state ANSYS thermal analyses of the model are conducted to obtain the nodal temperatures by impressing the temperatures as the boundary conditions for both cold and hot conditions. Two-dimensional thermal elements (PLANE55) are used in the analyses. Temperature dependent thermal material properties are also used in the analysis

The resulting temperature distributions for cold and hot ambient cases are shown in Figures 3.9.6-8 and 3.9.6-9, respectively.

3.9.6.6.4 Thermal Stress Analyses

Elastic stress analyses of the shield shell structure are conducted in order to evaluate the transfer plus thermal loads. The loads and boundary conditions of model are shown in Figure 3.9.6-6. The nodal temperature distribution from the above thermal analyses results is applied to obtain the thermal stresses in the model.

The nodal stress intensity distribution is plotted Figures 3.9.6-10 for cold condition, and in Figure 3.9.6-11 for 115° F hot ambient case. The critical stress intensities are summarized in Table 3.9.6-1.

It is seen from these figures that the maximum thermal stress intensities are generated in the cold ambient case. The maximum nodal stress intensity in the shell model is 26,045 psi. This maximum stress occurs in the outer shell near the bottom plate weld. Cold and hot stresses are linearized through the shell thickness, and the maximum stresses are summarized and evaluated in Table 3.9.6-1.

3.9.6.6.5 Weld Stresses at Center Support Plates

The center support plates are attached to the cask structural shell by 3/16 inch fillet (3-12) stitch-welds, and to the outer neutron shield cylinder by 1 inch × 0.12 inch plug welds (24 plug welds for each plate). It is seen from stress intensity distribution in Figure 3.9.6-10 that the maximum stress intensity (13,417 psi) occurs during the transfer load plus cold ambient load case. The maximum stressed center support plate is located close to the bottom end closure plate. The maximum weld stresses are also expected to occur at this plate. The following fillet and plug weld stresses are calculated from the nodal forces.

Fillet Weld Stresses

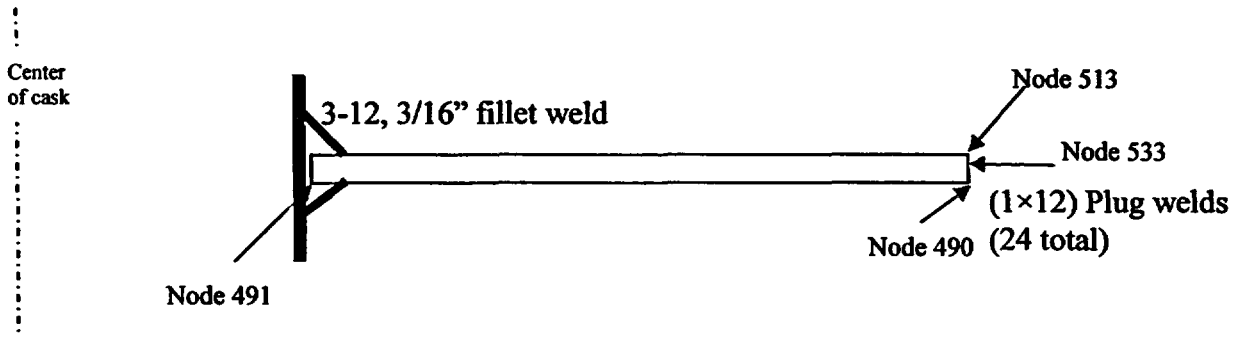

The maximum nodal forces at node 491 (from ANSYS result file) are:

$$F_x = 124{,}800 \text{ lb.} \qquad F_y = -11{,}840 \text{ lb.}$$

The fillet weld tensile/shear area, A_f is,

$$A_f = 3/12\ [\pi(81.7) \times 3/16 \text{ x } 2] = 24.06 \text{ in}^2$$

Therefore, the tensile stress, σ_f is,

$$\sigma_f = 124{,}800 / 24.06 = 5{,}187 \text{ psi}$$

And the shear stress, τ_f, is,

$$\tau_f = 11{,}840 / 24.06 = 492 \text{ psi}$$

The maximum stress intensity, $S.I._f$, is,

$$S.I._f = [(5{,}187)^2 + 4 \times (492^2)]^{0.5} = 5{,}280 \text{ psi,}$$

Which is less than the allowable stress, $S_m = 20.0$ ksi. The maximum shear stress, τ_{fmax}, is,

$$\tau_{fmax} = [(5{,}187/2)^2 + 492^2]^{0.5} = 2{,}640 \text{ psi}$$

Which is less than the allowable shear stress, $0.6S_m = 0.6(20.0) = 12.0$ ksi.

Plug Weld Stress

The maximum forces in the plug weld are the following.

Node	F_x (lb.)	F_y (lb.)
533	0	0
513	-110,100	-130,700
490	59,850	123,800
Total	**-50,250**	**-6,900**

The fillet weld shear area, A_b is,

$$A_b = 24 \text{ plugs} \times (1.0 \times 0.12) = 2.88 \text{ in}^2$$

Therefore, the tensile stress, σ_b is,

$$\sigma_b = 50{,}250/2.88 = 17{,}448 \text{ psi}$$

And the shear stress, τ_b, is,

$$\tau_b = 6{,}900/2.88 = 2{,}396 \text{ psi}$$

The maximum stress intensity, $S.I._b$, is,

$$S.I._b = [(17{,}448)^2 + 4\times(2{,}396^2)]^{0.5} = 18{,}094 \text{ psi}$$

Which is less than the allowable stress, $S_m = 20.0$ ksi. The maximum shear stress, τ_{bmax}, is,

$$\tau_{bmax} = [(17{,}448/2)^2 + 2{,}396^2]^{0.5} = 9{,}047 \text{ psi}$$

Which is less than the allowable shear stress, $0.6S_m = 0.6(20.0) = 12.0$ ksi.

3.9.6.7 Conclusions

Based on the results of the analysis, it is concluded that the outer shell structure is structurally adequate for the specified transfer loads.

3.9.6.8 References

1. American Society of Mechanical Engineers, ASME Boiler and Pressure Vessel Code, Section II, Part D, 1998, including 2000 addenda.

2. American Society of Mechanical Engineers, ASME Boiler and Pressure Vessel Code, Section III, Division 1, Subsection NC, 1998, including 2000 addenda.

Table 3.9.6-1
Summary of Calculated and Allowable Neutron Shield Shell Stresses

Load Case	Stress Category	Maximum Stress (ksi)	Allowable Stress (ksi)
3*g* Lifting	P_m	9.11	20.0
	$P_m + P_b$	21.47	30.0
Transfer Load	P_m	1.52	20.0
	$P_m + P_b$	15.99	30.0
	$P_m + P_b + Q$ (Cold)	21.21	60.0
	$P_m + P_b + Q$ (Hot)	20.6	60.0

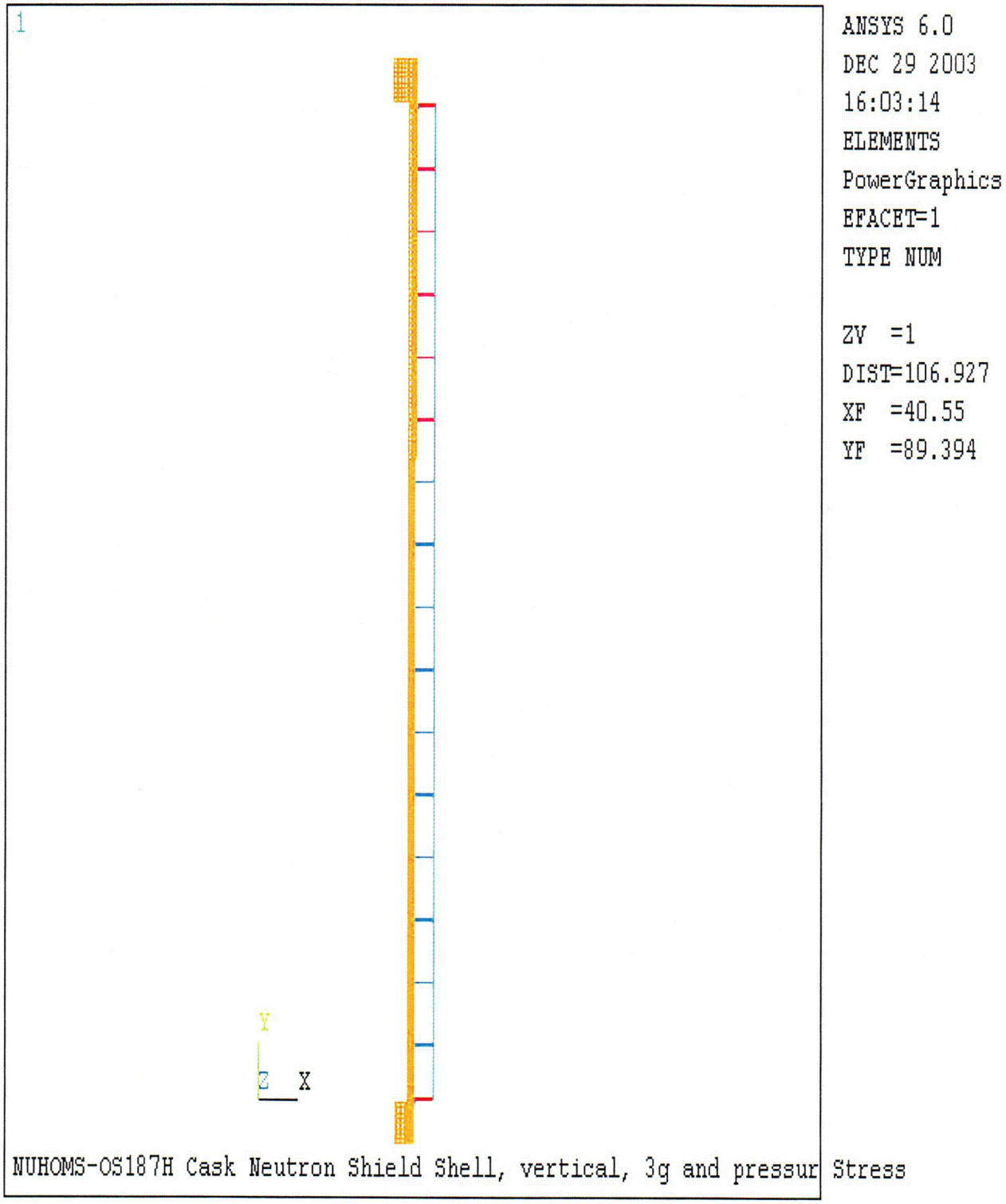

Figure 3.9.6-1
Neutron Shield Shell Finite Element Model

C20

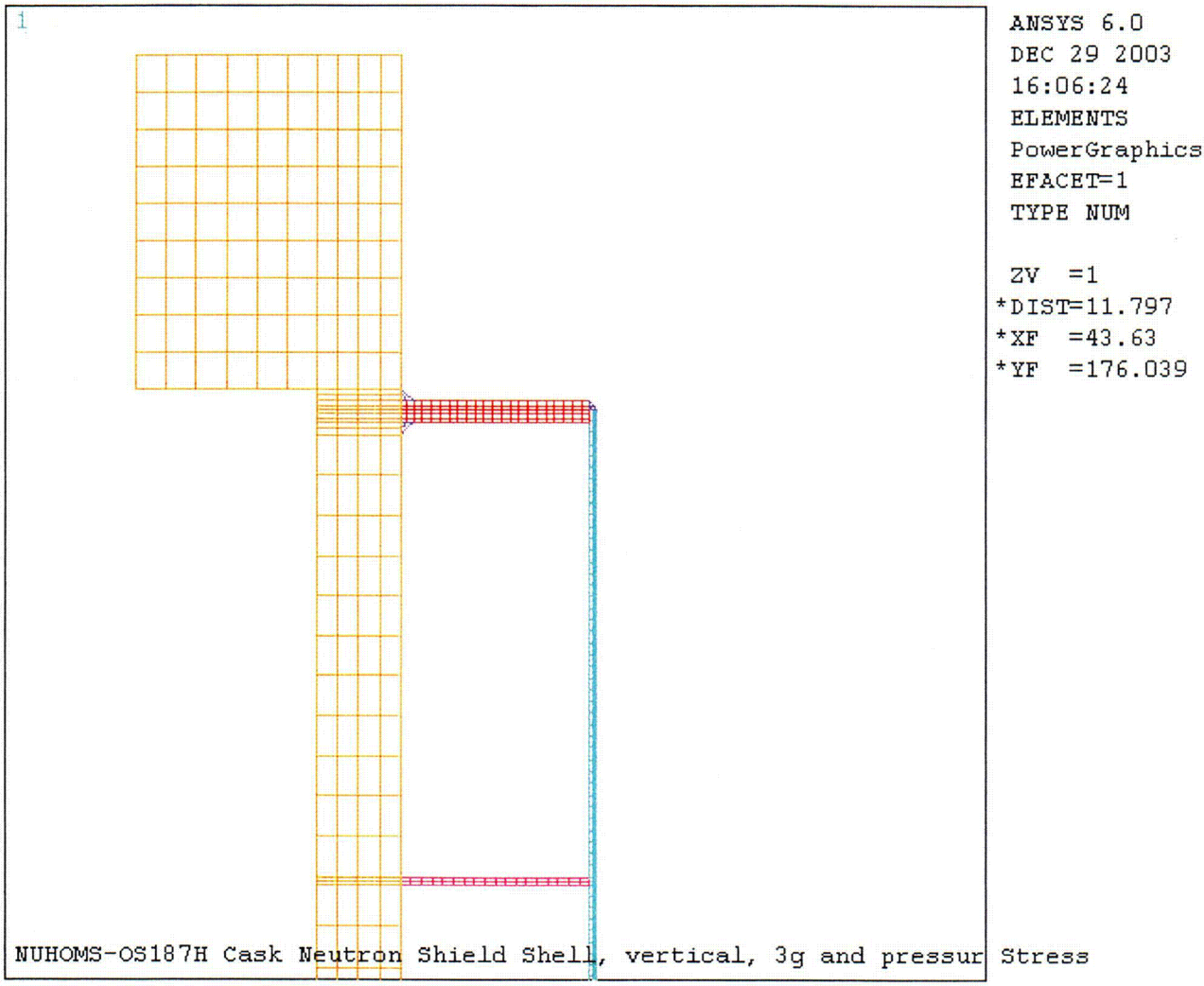

Figure 3.9.6-2
Neutron Shield Shell Finite Element Model, Top Plate Region

C 21

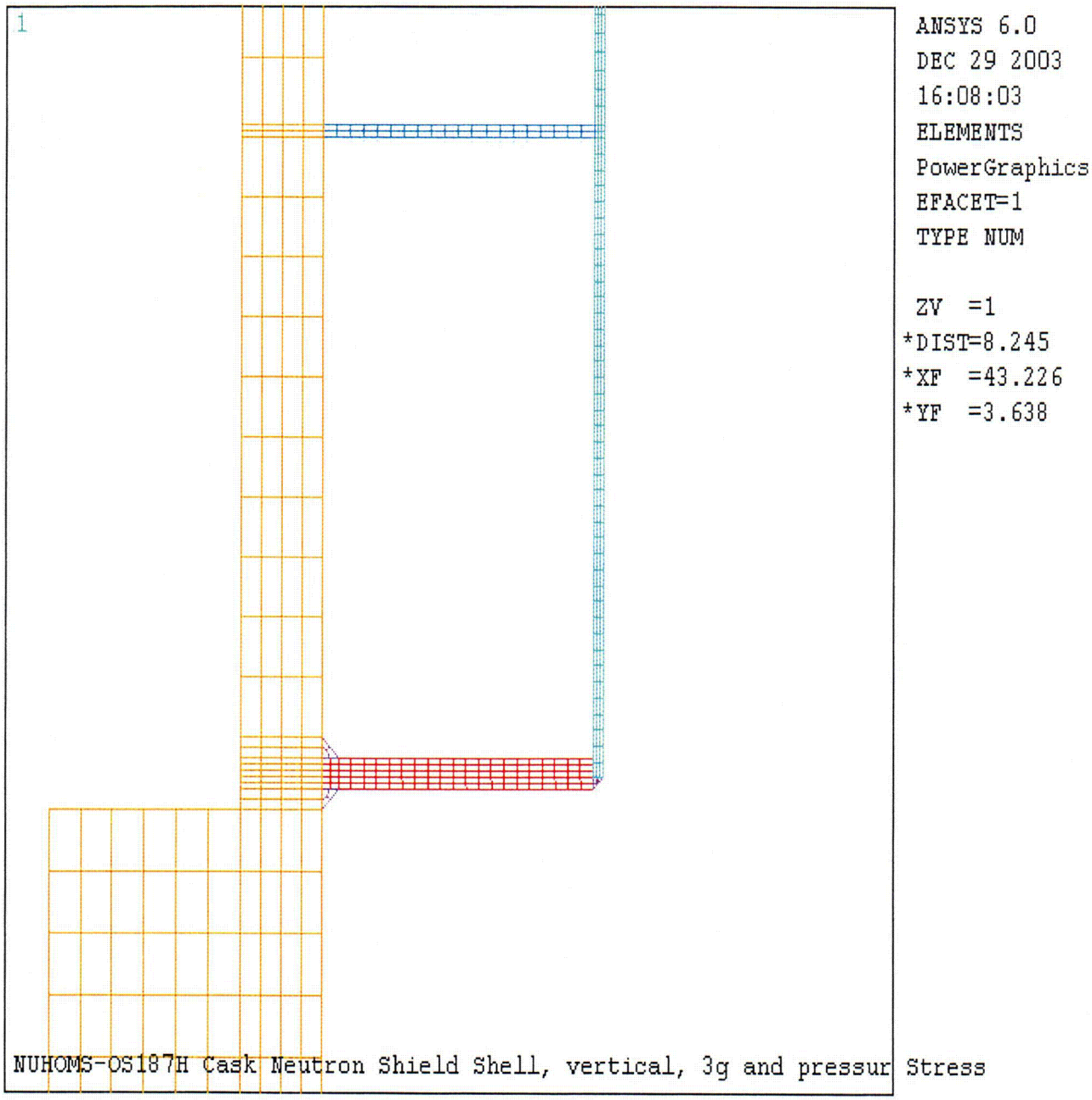

Figure 3.9.6-3
Neutron Shield Shell Finite Element Model, Bottom Plate Region

C 22

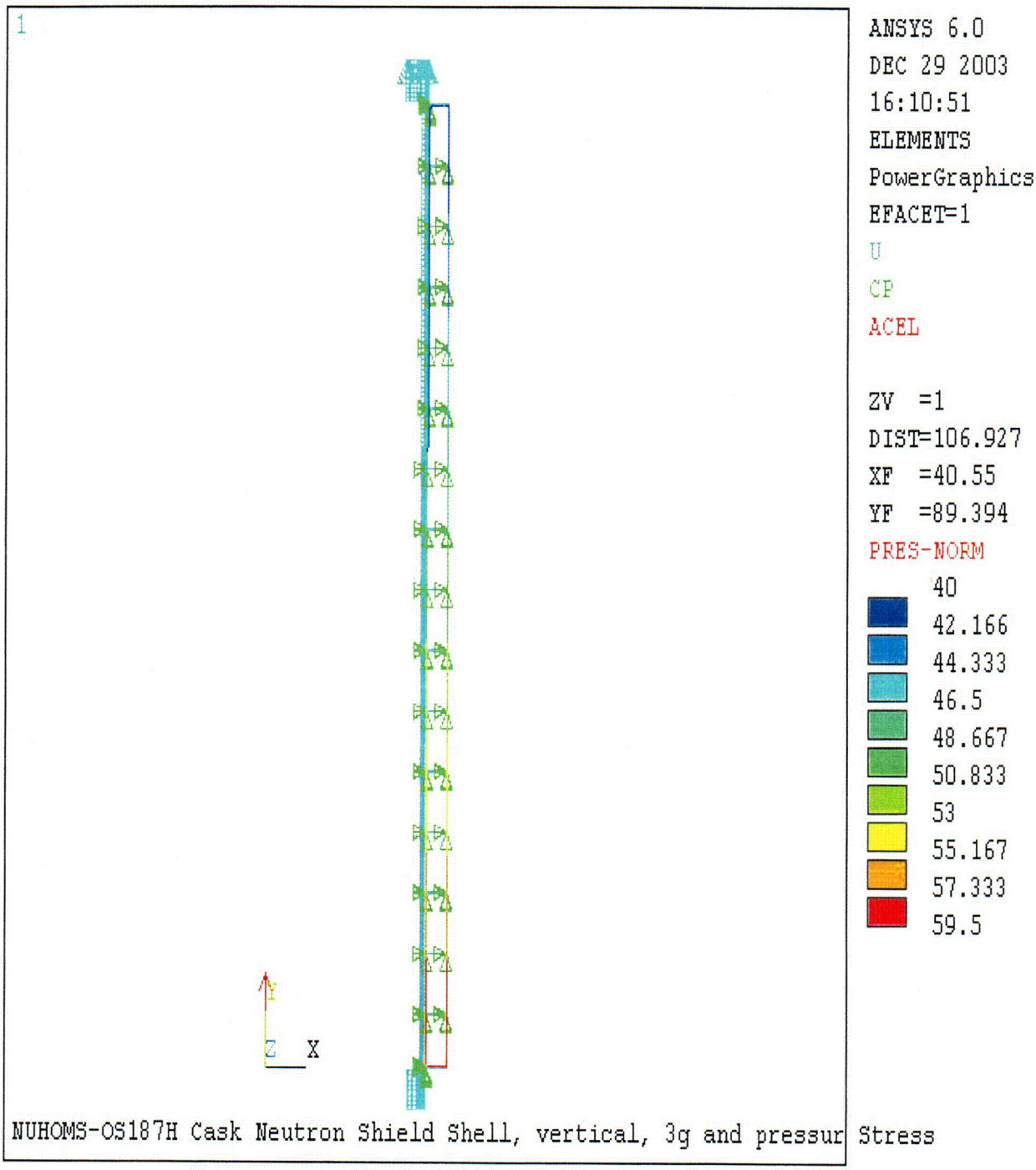

Figure 3.9.6-4
Neutron Shield Shell Finite Element Model, 3*g* Lifting Boundary Conditions

C23

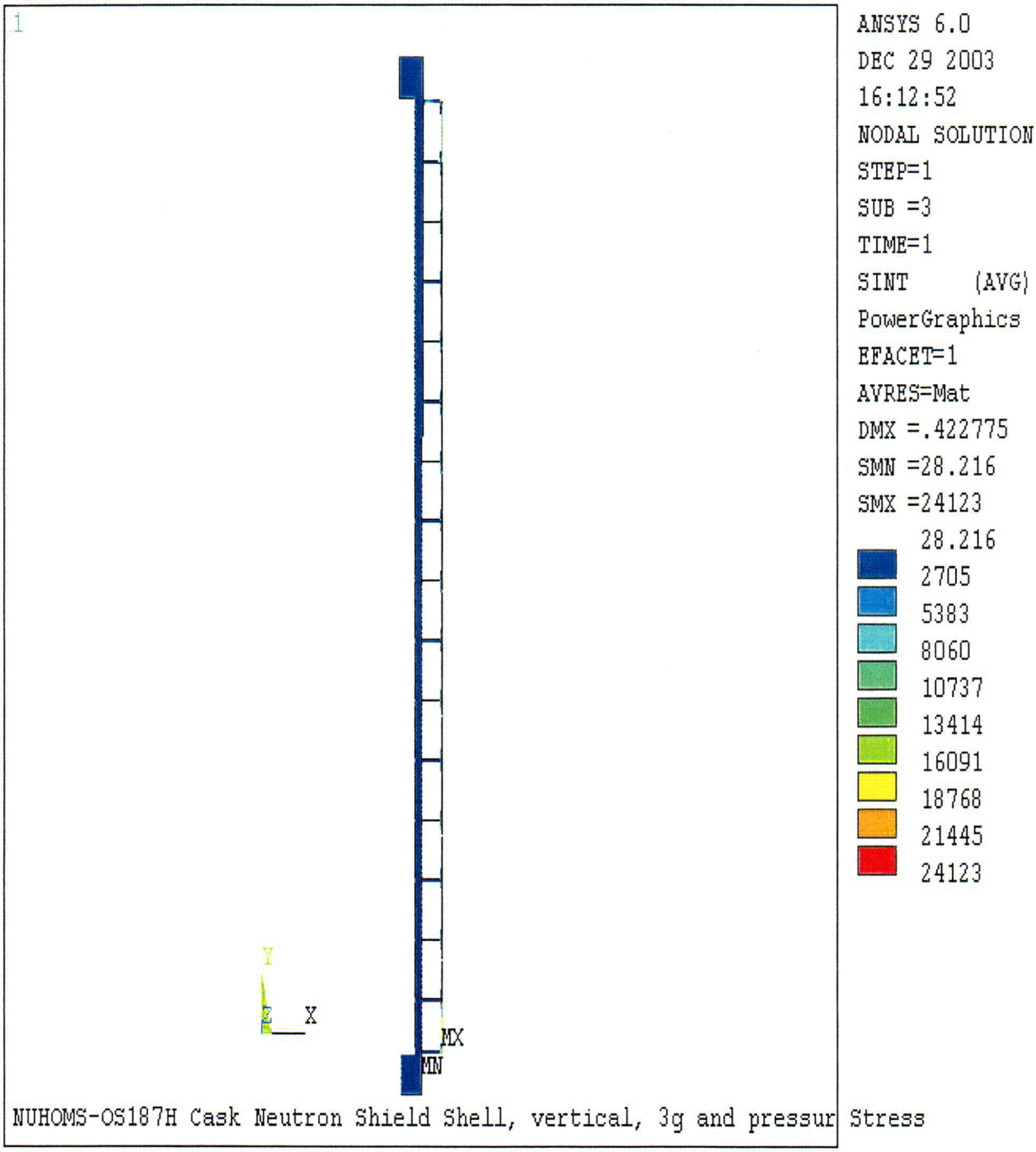

Figure 3.9.6-5
3g Lifting Stress Intensity Distribution

C24

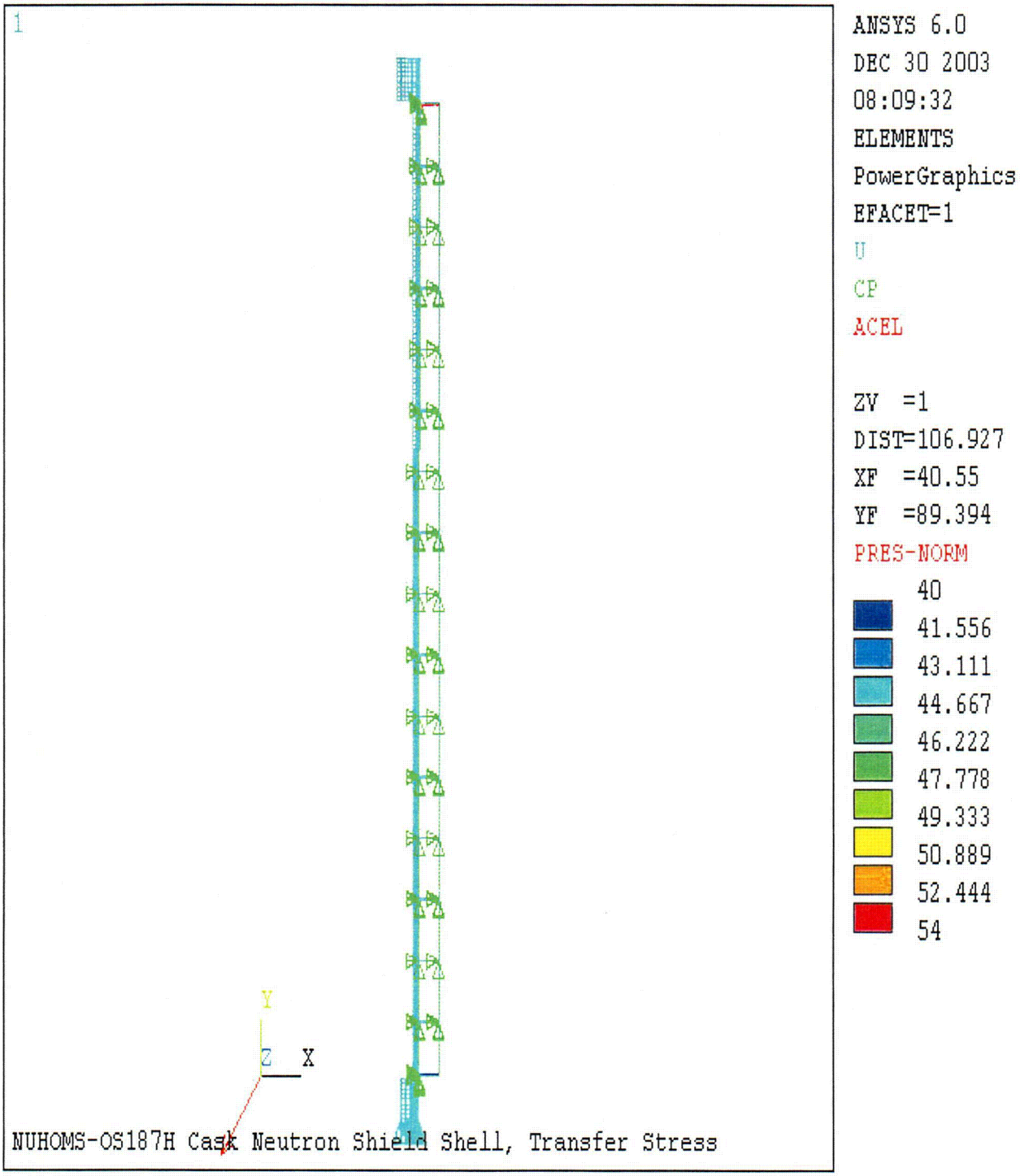

Figure 3.9.6-6
Neutron Shield Shell Finite Element Model, Transfer Loads Boundary Conditions

C25

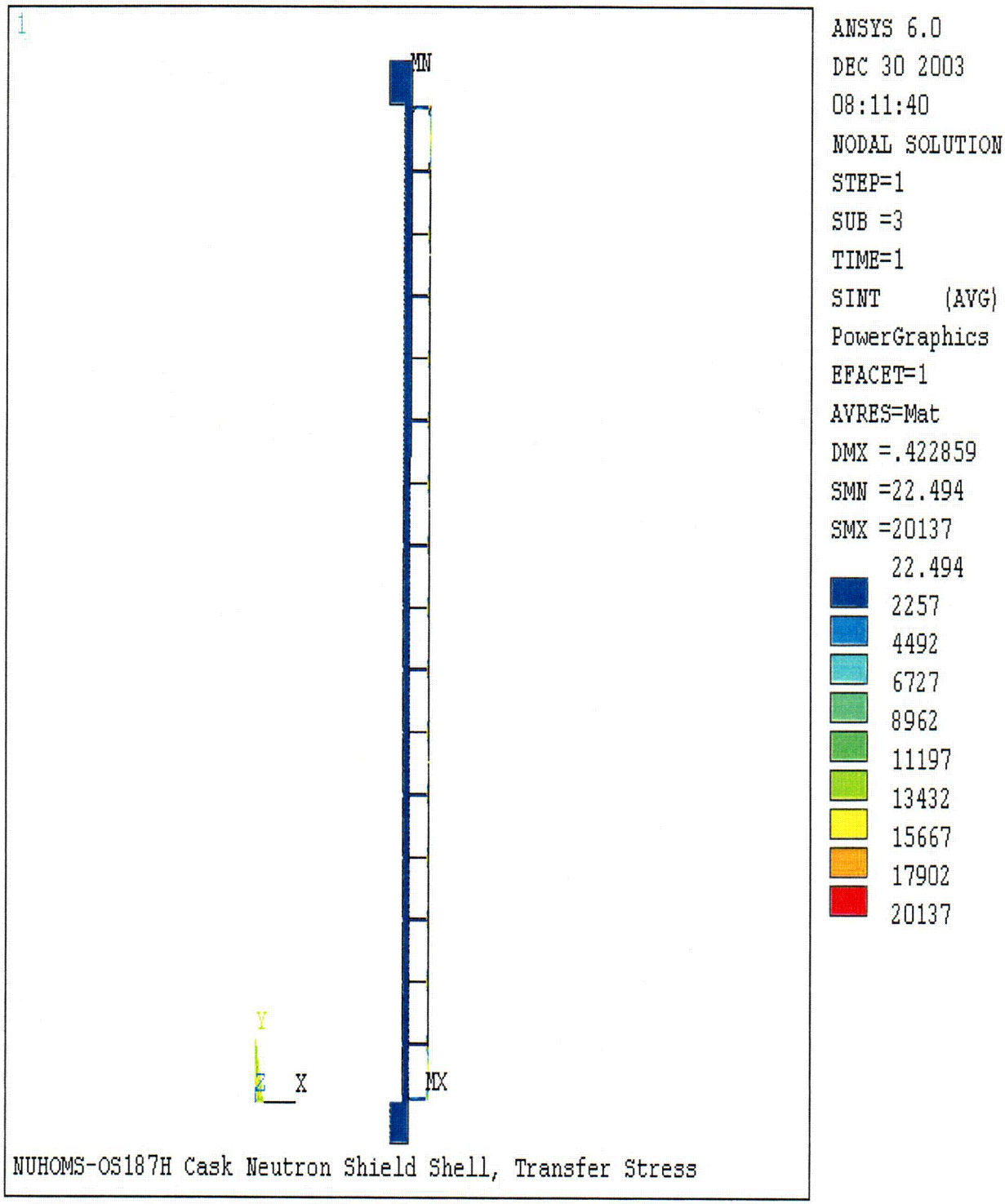

Figure 3.9.6-7
Transfer Loads Stress Intensity Distribution

C 26

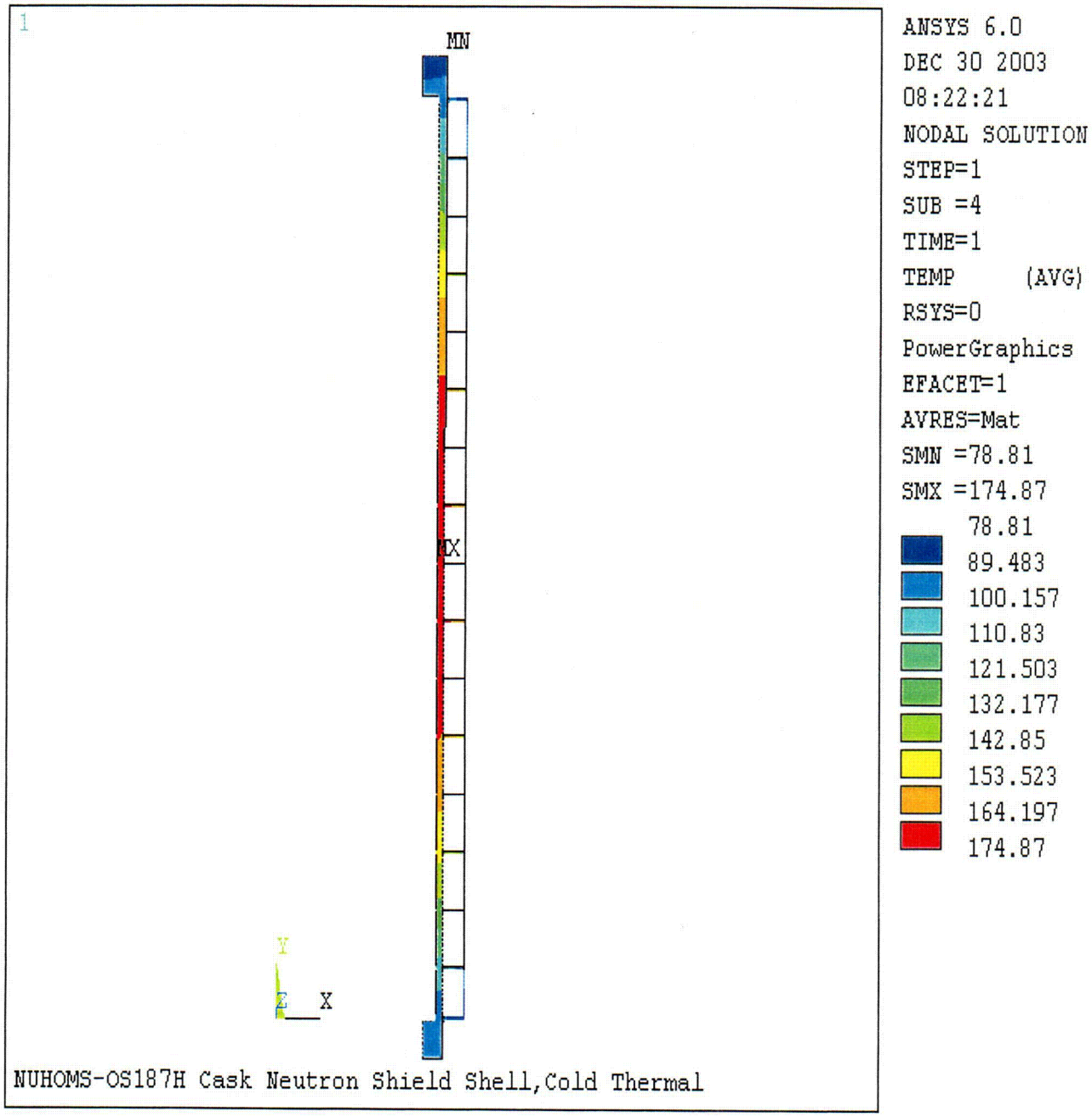

Figure 3.9.6-8
Cold Ambient Environment Temperature Distribution

C 27

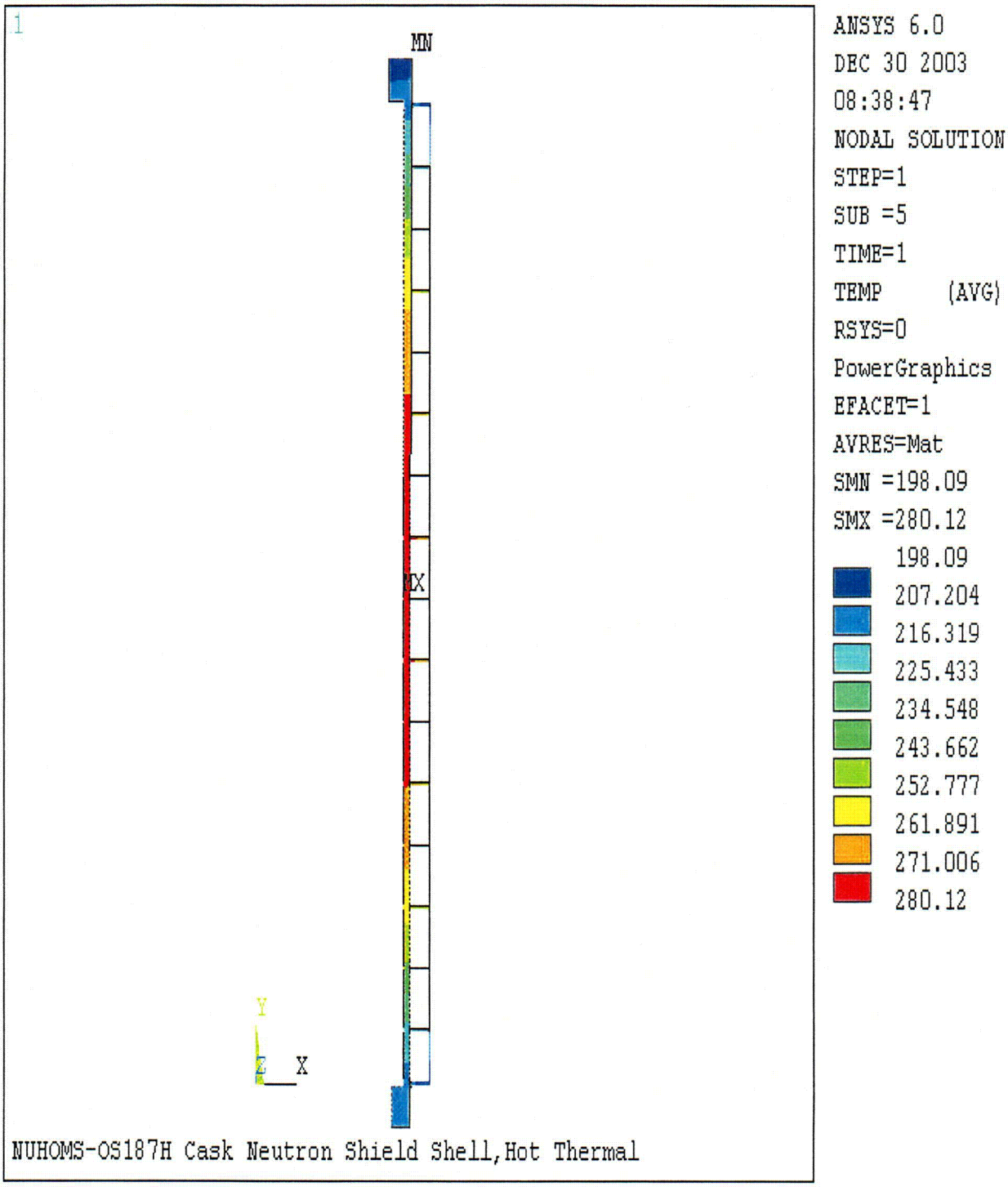

Figure 3.9.6-9
Hot Ambient Environment Temperature Distribution

C 28

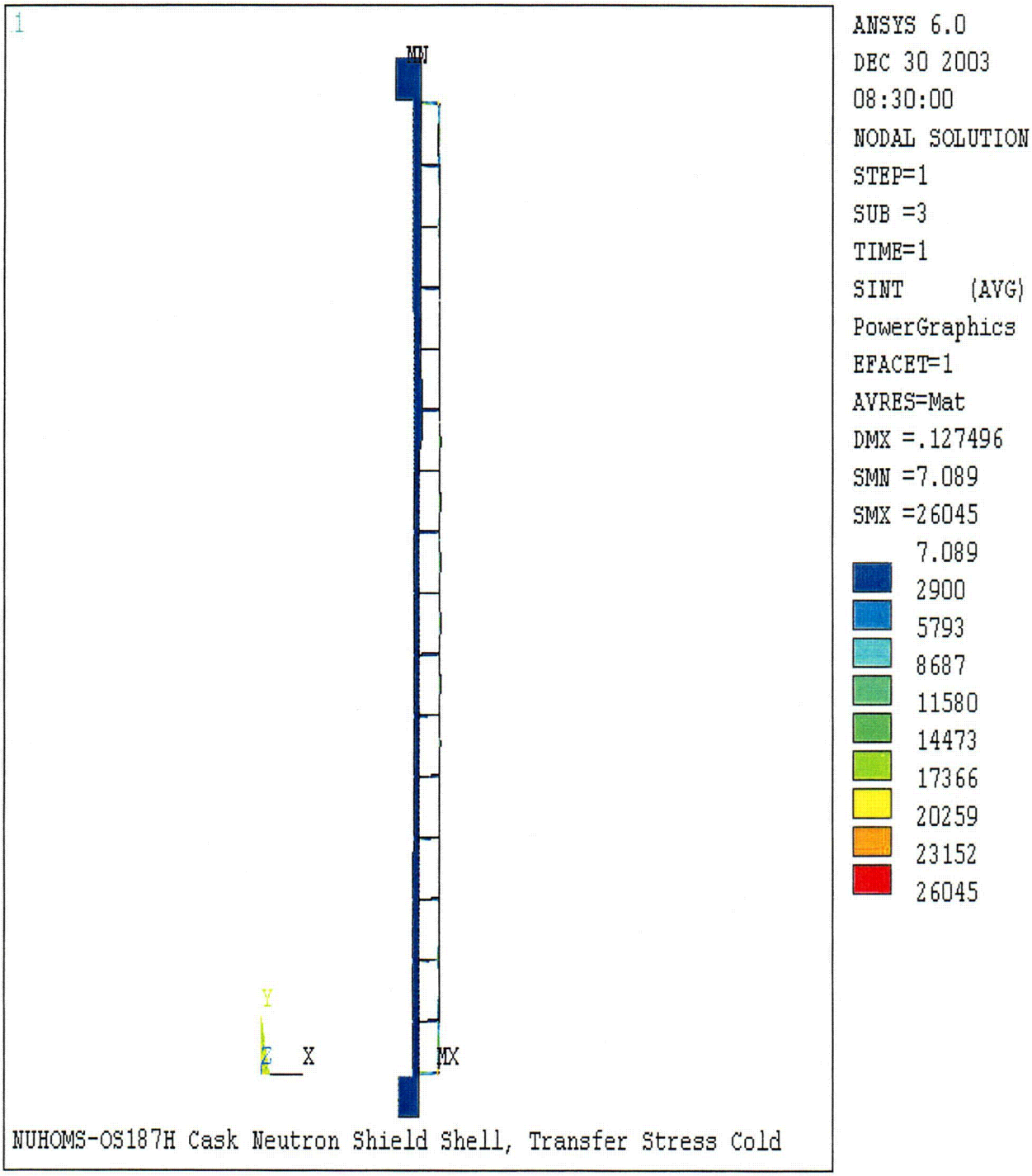

Figure 3.9.6-10
Transfer Loads plus Cold Ambient Condition Stress Intensity Distribution

C 29

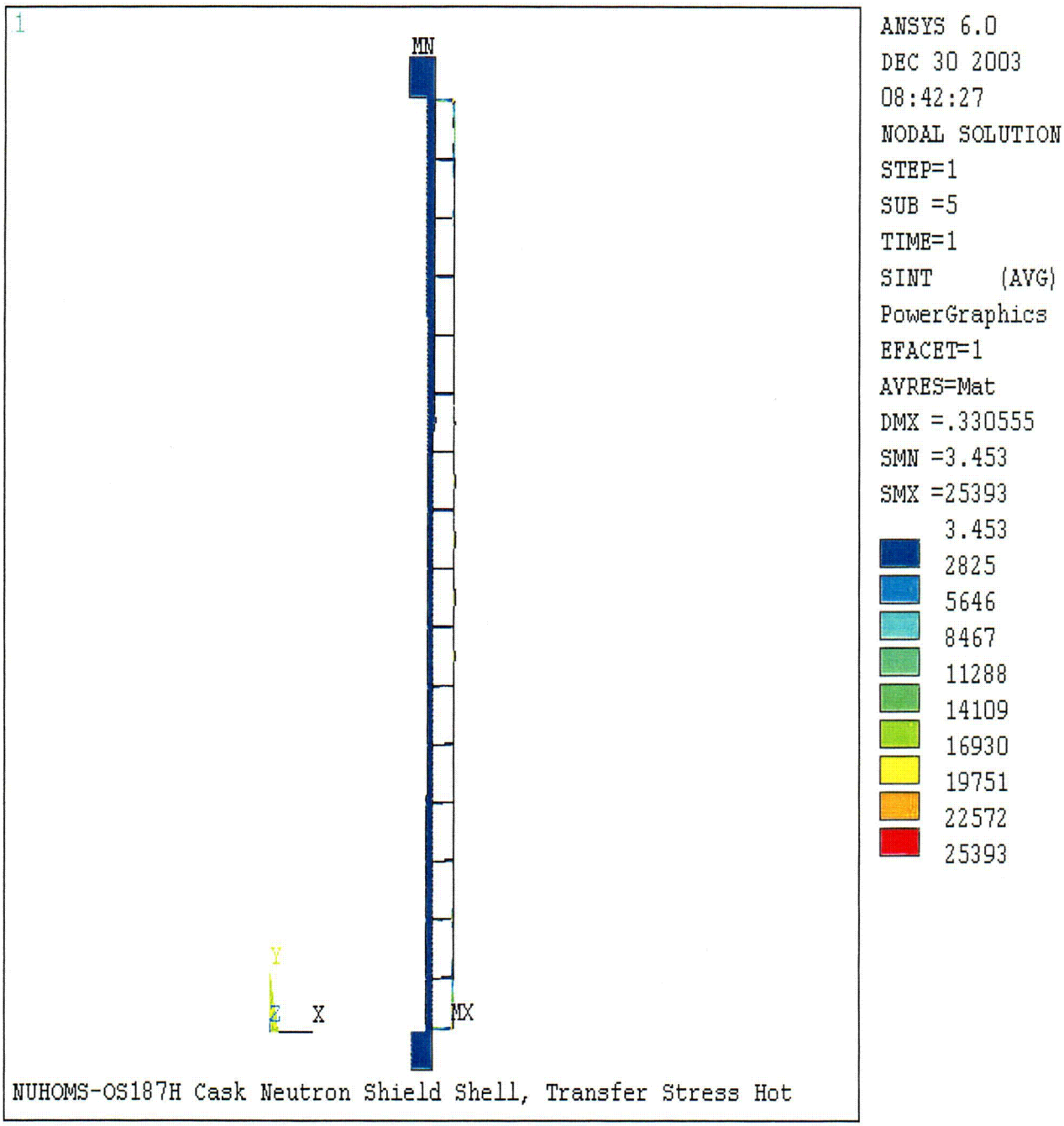

Figure 3.9.6-11
Transfer Loads plus Hot Ambient Condition Stress Intensity Distribution

C 30

APPENDIX 3.9.7
OS187H TRANSFER CASK IMPACT ANALYSIS

TABLE OF CONTENTS

3.9.7 OS187H TRANSFER CASK IMPACT ANALYSIS 3.9.7-1

- **3.9.7.1 Introduction 3.9.7-1**
- **3.9.7.2 Material Properties 3.9.7-1**
- **3.9.7.3 Component Weights 3.9.7-2**
- **3.9.7.4 Geometry and Nomenclature 3.9.7-2**
- **3.9.7.5 Ultimate Capacity of Slab 3.9.7-3**
- **3.9.7.6 End Drop Impact Analysis 3.9.7-4**
- **3.9.7.7 Side Drop Impact Analysis 3.9.7-6**
- **3.9.7.8 Corner Drop Impact Analysis 3.9.7-8**
- **3.9.7.9 Conclusions 3.9.7-9**
- **3.9.7.10 References 3.9.7-10**

LIST OF TABLES

3.9.7-1 Spreadsheet for 80 inch Side Drop Impact Load Calculations (Using Non-Linear *S* vs. *g* relationship)

3.9.7-2 C. G. Over Corner Drop – *L* Calculations

3.9.7-3 C. G. Over Corner Drop – Area Calculations

3.9.7-4 C. G. Over Corner Drop – Energy Calculations

LIST OF FIGURES

3.9.7-1 Force vs. Displacement – End Drop (see Reference 1, Figure 14)

3.9.7-2 *S* vs. *g* Curve for 80 inch Side Drop

3.9.7-3 Geometry of C. G. Over Corner Drop

3.9.7-4 Geometry of C. G. Over Corner Drop (continued)

3.9.7-5 Geometry of the C. G. Over Corner Drop - Area Calculation (continued)

3.9.7-6 C. G. Over Corner Drop – *L* Dimension Calculation

3.9.7 OS187H TRANSFER CASK IMPACT ANALYSIS

3.9.7.1 Introduction

The purpose of this appendix is to present the evaluation of the peak decelerations of NUHOMS® OS187H Transfer Cask during impact, subsequent to the hypothetical accident drop onto the concrete pad/soil system during transfer operations. The hypothetical accident condition drop consists of 80 inch end drop, side drop and center of gravity (C.G.) over corner drop.

For the impact analysis, the transfer cask is assumed rigid as compared to the flexibility of the concrete slab/soil system. The methodology described in Reference 1 is used in this evaluation.

The cask is approximated by a cylinder 197.07 inches long and 81.7 inches in diameter. The effect of the outer shield shell, which is very thin relative to the main structural body of the transfer cask, is neglected. Also, small variations around top cover and cylinder are neglected. The stiffness variation due to the neglected items of the transfer cask is negligible.

The OS187H Transfer Cask is assumed to impact a 36 inch thick concrete pad, with #11 rebar on 12" spacing, at top and bottom of the pad, and 2" coverage.

3.9.7.2 Material Properties

The following material properties, taken from Reference 1, are assumed to model the design basis concrete pad and soil foundation.

E_c = Concrete elastic modulus = 3.6×10^6 psi.
σ_u = Ultimate concrete strength = 4,000 psi.
E_s = Sub-soil modulus = 60,000 psi. (higher value gives higher g load)
S_y = Rebar yield strength = 60,000 psi.
v_c = Poisson's ratio of concrete = 0.17
v_s = Poisson's ratio of soil = 0.49

3.9.7.3 Component Weights

The 32PTH DSC and OS187H Transfer Cask component weights are tabulated in Section 3.2. The following component weights relevant to this analysis are summarized below.

Empty Canister Weight = 28.19 kips
Fuel Basket Weight = 29.85 kips
Fuel Assembly Weight (32) = 50.72 kips
Transfer Cask Weight = 119.95 kips

Total Weight, W = 228.71 kips.

For conservative estimating the g load, a lower weight, 226.9 kips, is used for the impact analysis (lower weight gives higher g load).

3.9.7.4 Geometry and Nomenclature

The technical data used for transfer cask and concrete slab/soil system are:

W = Weight of cask = 226,900 lbs
R = Cask outer radius = 81.7/2 = 40.85 in
A = cask foot print area = π (40.85)^2 = 5,242.4 in^2
L = cask length = 197.07 in.
E_c = Concrete elastic modulus = 3.6×10^6 psi
σ_u = Ultimate concrete strength = 4,000 psi
υ_c = Poisson's ratio of concrete = 0.17
h_c = Concrete pad thickness = 36 inches
S_y = Rebar yield strength = 60,000 psi
E_s = Sub-soil modulus = 60,000 psi (high value of E_s gives higher g load)
υ_s = Poisson's ratio of soil = 0.49
A_s = Rebar (#11) area = π/4 (1.41)^2 = 1.56 in^2

3.9.7.5 Ultimate Capacity of Slab

The ultimate bending capacity of reinforced cement concrete slab, M_u, is computed based on a 1 foot wide pad with a thickness of 36 in., #11 Rebar @ 12 inch spacing and a 2 inch cover. For a 36 inch thick concrete slab, the steel in compression zone is assumed to have no effect and is neglected.

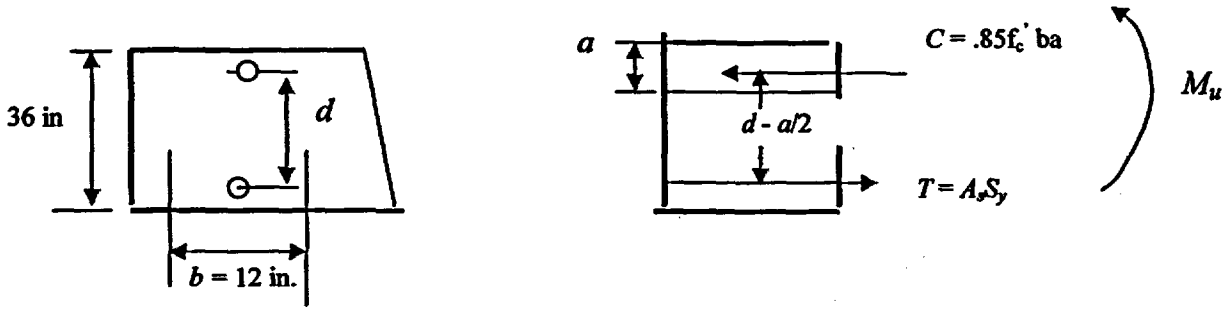

Average depth of steel, d, is the following.

$d = 36 - 4 - 1.41 = 30.59$ in

Therefore,

$C = T = A_sS_y = 0.85f_c' ba$

$a = A_sS_y / 0.85f_c' b = 1.56 \times 60{,}000 / 0.85 \times 4000 \times 12 = 2.294$ in

$M_u = A_sS_y (d - a/2) = 1.56 \times 60{,}000 (30.59 - 2.294/2) = 2.7559 \times 10^6$ in-lb/ft width of slab

3.9.7.6 End Drop Impact Analysis

The results of EPRI NP-7551 report [1] are presented in terms of a target hardness number, S. In general this is given by the following.

$$S = \frac{M_u \sigma_u A}{W^2 \delta_e}$$

Where,

M_u = Ultimate moment capacity of 1 foot section of slab = 2.7559×10^6 in-lb/ft
σ_u = Ultimate concrete strength = 4,000 psi
A = Area of impact surface = 5,242.4 in^2
W = Weight of cask = 226,900 lbs
δ_e = Deflection of cask under weight of cask (1g), in

The deflection, δ_e, is given as:

$$\delta_e = \frac{W}{2Rk}\left(1 - e^{-\beta R}\cos(\beta R)\right)$$

Where,

$$k = \frac{\pi E_s}{1-\upsilon_s^2} = \frac{\pi(60{,}000)}{1-0.49^2} = 248{,}053 \text{ psi/in}$$

$$\beta = \left(\frac{E_s}{4D_c}\right)^{1/4} = \left(\frac{60{,}000}{4 \times 14{,}413 \times 10^6}\right)^{1/4} = 0.03194$$

$$D_c = \frac{E_c h^3}{12(1-\upsilon_c^2)} = \frac{3.6(10)^6(36)^3}{12(1-0.17^2)} = 14{,}413 \times 10^6 \text{ in-lbs}$$

Therefore,

$$\delta_e = \frac{226{,}900}{2 \times 40.85 \times 248{,}053}\left(1 - e^{-0.03194 \times 40.85}\cos 0.03194 \times 40.85\right) = 0.0104 \text{ in}$$

Then,

$$S = \frac{M_u \sigma_u A}{W^2 \delta_e} = \frac{2.7559 \times 10^6 \times 4{,}000 \times 5{,}242.4}{226{,}900^2 \times 0.0104} \approx 10.793 \times 10^4$$

Conservatively using upper bound of Figure 28 from Reference 1 for an 80 inch drop height, the peak force is 49*g* (× weight). To calculate the maximum deformation of the concrete, the force-deformation curve (Figure 3.9.7-1) is obtained by interpolating the data shown on Figure 14 of the EPRI report [1]. From Figure 3.9.7-1, the displacement at the end of elastic phase is about 0.4 inch and elastic-plastic displacement is about 1.0 inch.

We now use energy method to compute final deformation. Using the force – displacement plot on Figure 3.9.7-1 (interpolating $S = 107{,}930$). It is assumed that displacements beyond 1 inch are fully plastic.

Let x be the final plastic deformation. Then, the energy absorbed by target, E_{ab}, is equal to the Area under the Curve (see Figure 3.9.7-1). Therefore,

$$E_{ab} = W[(27.5\times0.4/2) + (27.5 + 39.0)/2\,(0.66 - 0.44) + (39.0 + 48.3)/2\,(1.0 - 0.66) + 49(x - 1.0)]$$

The potential energy of the drop, E_{drop}, is,

$$E_{drop} = W[H + x + 1] = W[81 + x]$$

Equating $E_{ab} = E_{drop}$, gives the following.

$$5.5 + 8.65 + 14.84 + 49x - 49 = 81 + x$$

$$\Rightarrow x = 2.10 \text{ in}$$

Therefore, the total displacement is,

Displacement = 1.0 + 2.10 = 3.10 in

3.9.7.7 Side Drop Impact Analysis

The side drop analysis is conducted in the same manner as for the end drop, except that the expression for δ_e varies, and the target area changes as the depth of penetration increases. Using Reference 1 to evaluate δ_e, we get,

$$I_c = \frac{Lh^3}{12} = 197.07 \times \frac{36^3}{12} = 766{,}208 \text{ in}^4$$

$$\beta = \left(\frac{E_s}{4E_cI_c}\right)^{1/4} = \left(\frac{60{,}000}{4 \times 3.6 \times 10^6 \times 766{,}208}\right)^{1/4} = 0.00859 \text{ in}^{-1}$$

$$k = E_s = 60{,}000 \text{ lb/in}^2$$

$$\delta_e = \frac{W\beta}{2k} = \frac{226{,}900 \times 0.00859}{2 \times 60{,}000} = 0.01624 \text{ in}$$

$$S = \frac{M_u\sigma_u A}{W^2\delta_e} = \frac{2.7559 \times 10^6 \times 4{,}000 \times A}{226{,}900^2 \times 0.01624} = 13.18464A$$

The following sketch shows the geometry of the transfer cask side drop

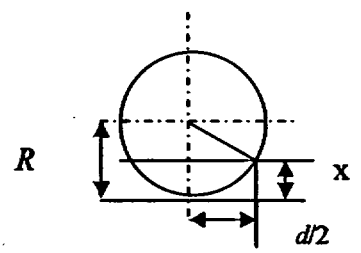

Where,

$$d/2 = [R^2 - (R-x)^2]^{0.5} = [2Rx - x^2]^{0.5}$$

The impact surface area, A, as a function of the penetration depth is,

$$A = 2 \times 197.07\,[81.7\,x - x^2]^{0.5} = 394.14 \times [81.7\,x - x^2]^{0.5}$$

$$S = 13.18464\,A$$

The following data is obtained from Figure 28 of Reference 1.

Target Hardness, S	Acceleration, g
0	6
10,000	17.5
20,000	25.0
30,000	29.8
40,000	33.5
50,000	37.0
60,000	40.0
70,000	43.3
80,000	46.0
90,000	47.8
100,000	49.0

This S vs. g curve is plotted in Figure 3.9.7-2. A spread sheet solution is carried out by incrementing x (penetration depth) to obtain the absorbed energy equal to drop energy. The following steps are carried out on the spreadsheet:

1. Select x
2. Compute Area, $A = 394.14 \times [81.7\,x - x^2]^{0.5}$
3. Compute $S = 13.18464\,A$
4. Obtain g from Figure 3.9.7-2 for computed S
5. Compute Force, $F = W \times g$
6. Compute Energy Increment, $\Delta E = [1/2(F_i + F_{i-1})]\,(x_i - x_{i-1})$
7. Add ΔE to the previous to obtain current total absorbed energy
8. Compute total drop energy $= W(80 + x)$
9. Keep incrementing x until total absorbed energy is equal to the drop energy.

The resulting spreadsheet for the side drop impact is given on Table 3.9.7-1.

From Table 3.9.7-1, it is seen that, when the target deformation is 2.46 inches, the total absorbed energy is approximately equal to the drop energy. The *g* load at this deformation is 44*g*.

3.9.7.8 Corner Drop Impact Analysis

The C. G. over corner drop is performed in a similar manner as the side drop. For the corner drop, both δ_e and impact area are a function of the penetration depth into the target.

$$\delta_e = \frac{W\beta}{2k} = \frac{226{,}900 \times \beta}{2 \times 60{,}000} = 1.8908\beta$$

And

$$\beta = \left(\frac{E_s}{4E_c I_c}\right)^{1/4} = \left(\frac{60{,}000}{4 \times 3.6 \times 10^6}\right)^{1/4} \times \left(\frac{1}{I_c}\right)^{1/4} = \frac{0.254}{I_c^{1/4}}$$

$$I_c = \frac{Lh^3}{12} = L \times \frac{36^3}{12} = 3{,}888L$$

The geometry relations used to evaluate of the impact area as a function of the deformation into the target are shown in Figures 3.9.7-3 to 3.9.7-6. The area, A, as a function of deformation is shown in Figure 3.9.7-5. Table 3.9.7-3 tabulates the results of the 'area vs. deformation' calculations, using a small ANSYS input file.

The next quantity that is needed is the deflection, δ_e. This deflection will occur as a result of only a small portion of the transfer cask being in contact with the target surface, with the area increasing as δ_e increases. The above L dimension calculation is developed in Figure 3.9.7-6.

$$L = 2\left[\left(\frac{2R\delta_e}{\cos 67.48°}\right) - \left(\frac{\delta_e^2}{\cos^2 67.48°}\right)\right]^{1/2} \quad \text{(See Fig. 3.9.7-3 for drop angle calculation)}$$

$$= 2\left[213.316\delta_e - 6.8166\delta_e^2\right]^{1/2}$$

To solve for *L*, iteratively, this is done in the spreadsheet given in Table 3.9.7-2. Which give

$$\delta_e = 0.03922, \quad L = 5.7815 \text{ in}$$

Using Reference 1, the target hardness number, S, is

$$S = \frac{M_u \sigma_u A}{W^2 \delta_e} = \frac{2.7559 \times 10^6 \times 4{,}000 \times A}{226{,}900^2 \times 0.03922} = 5.4594A$$

A spread sheet solution is carried out by incrementing Δ (penetration depth as shown in Figure 3.9.7-3) to obtain the Absorbed Energy that is equal to Drop Energy. The following steps are carried out in the spreadsheet:

1. Select Δ
2. Obtain Area, A, from Table 3.9.7-3
3. Compute $S = 5.4594\,A$
4. Obtain g from Figure 3.9.7-2
5. Compute Force, $F = W \times g$
6. Compute Energy Increment, $\Delta E = [1/2(F_i + F_{i\text{-}1})]\,(\Delta_i - \Delta_{i\text{-}1})$
7. Add ΔE to the previous to obtain current total absorbed energy
8. Compute total drop energy = $W\,(80 + x)$
9. Keep incrementing x till total absorbed energy is equal to the drop energy

The spreadsheet is given on Table 3.9.7-4. It is seen from this table that at a target deformation of 6.5 inches, the total absorbed energy is equal to the drop energy and the g load for this deformation is 15.9g.

3.9.7.9 Conclusions

The following table summarizes the results of the analysis described above.

Drop Orientation	Peak Deceleration (gs)	Target Penetration Depth (in.)
End Drop	49	3.10
Side Drop	44	2.5
Corner Drop	15.9	6.5

3.9.7.10 References

1. "Structural Design of Concrete Storage Pads for Spent Fuel Casks", EPRI NP-7551, August 1991 by Rashid, Nickell and James.

Table 3.9.7-1
Spreadsheet for 80 inch Side Drop Impact Load Calculations
(Using Non-Linear *S* vs. *g* relationship)

x	*A*	*S*	*g*	*F*	Δ*E*	Energy Absorbed	Drop Energy
0	0	0	0	0	0	0	18,152,000
0.5	2511.4	33,112	31.0	7,033,900	1,758,475	1,758,475	18,265,450
1	3540.7	46,683	36.0	8,168,400	3,800,575	5,559,050	18,378,900
1.5	4323.0	56,997	39.0	8,849,100	4,254,375	9,813,425	18,492,350
2	4976.2	65,609	42.0	9,529,800	4,594,725	14,408,150	18,605,800
2.1	5095.9	67,187	42.5	9,643,250	958,653	15,366,803	18,628,490
2.2	5212.5	68,725	42.9	9,734,010	968,863	16,335,666	18,651,180
2.3	5326.3	70,225	43.2	9,802,080	976,804	17,312,470	18,673,870
2.4	5437.4	71,690	43.5	9,870,150	983,612	18,296,082	18,696,560
2.42	5459.3	71,979	43.7	9,915,530	197,857	18,493,938	18,701,098
2.44	5481.2	72,267	43.8	9,938,220	198,538	18,692,476	18,705,636
2.46	**5502.9**	**72,554**	**43.9**	**9,960,910**	**198,991**	**18,891,467**	**18,710,174**
2.5	5546.0	73,123	44.0	9,983,600	398,890	19,290,357	18,719,250
2.51	5556.8	73,264	44.1	10,006,290	99,949	19,390,307	18,721,519
2.52	5567.5	73,405	44.15	10,017,635	100,120	19,490,426	18,723,788
2.53	5578.2	73,546	44.2	10,028,980	100,233	19,590,659	18,726,057
2.54	5588.8	73,687	44.24	10,038,056	100,335	19,690,995	18,728,326
2.55	5599.5	73,827	44.28	10,047,132	100,426	19,791,421	18,730,595

Table 3.9.7-2
C. G. Over Corner Drop – *L* Calculations

$L_{initial}$	I_c	β	δ_e	L_{final}
6	23328	0.020552	0.0388606	5.75475522
5.9	22939.2	0.020639	0.0390243	5.766842939
5.8	22550.4	0.020727	0.0391914	5.779163276
5.7	22161.6	0.020818	0.0393622	5.791724835
5.75	22356	0.020772	0.0392763	5.785413347
5.76	22394.88	0.020763	0.0392593	5.784158456
5.77	22433.76	0.020754	0.0392422	5.782906012
5.78	22472.64	0.020745	0.0392253	5.781656007
5.781	22476.53	0.020744	0.0392236	5.78153114
5.7815	**22478.47**	**0.020744**	**0.0392227**	**5.781468716**

Table 3.9.7-3
C. G. Over Corner Drop – Area Calculations

Δ	Δ_{CL}	α_{max}	α_{min}	Area, A
0.5	-15.146	37.942	36.529	19.361
1	-14.646	38.150	35.323	54.494
1.5	-14.146	38.357	34.117	99.620
2	-13.646	38.564	32.911	152.613
2.5	-13.146	38.772	31.705	212.213
3	-12.646	38.979	30.500	277.544
3.5	-12.146	39.186	29.294	347.950
4	-11.646	39.394	28.088	422.905
4.5	-11.146	39.601	26.882	501.977
5	-10.646	39.808	25.676	584.796
5.5	-10.146	40.015	24.470	671.043
6	-9.646	40.223	23.264	760.435
6.5	-9.146	40.430	22.058	852.716
7	-8.646	40.637	20.852	947.656
7.5	-8.146	40.845	19.646	1045.042
8	-7.646	41.052	18.440	1144.679
8.5	-7.146	41.259	17.234	1246.381
9	-6.646	41.467	16.028	1349.978
9.5	-6.146	41.674	14.822	1455.306
10	-5.646	41.881	13.617	1562.209
10.5	-5.146	42.089	12.411	1670.539
11	-4.646	42.296	11.205	1780.153
11.5	-4.146	42.503	9.999	1890.915
12	-3.646	42.710	8.793	2002.689
12.5	-3.146	42.918	7.587	2115.347
13	-2.646	43.125	6.381	2228.761
13.5	-2.146	43.332	5.175	2342.808
14	-1.646	43.540	3.969	2457.364
14.5	-1.146	43.747	2.763	2572.310
15	-0.646	43.954	1.557	2687.526
15.5	-0.146	44.162	0.351	2802.894
16	0.354	44.369	-0.855	2918.295
16.5	0.854	44.576	-2.060	3033.611
17	1.354	44.784	-3.266	3148.725
17.5	1.854	44.991	-4.472	3263.517
18	2.354	45.198	-5.678	3377.868
18.5	2.854	45.406	-6.884	3491.655
19	3.354	45.613	-8.090	3604.757
19.5	3.854	45.820	-9.296	3717.048
20	4.354	46.027	-10.502	3828.400

Table 3.9.7-4
C. G. Over Corner Drop – Energy Calculations

Δ	*AREA, A*	*S*	*g*	*Force, F*	*Energy Inc.*	*Total energy*	*Drop Energy*
0.00	0	0	-	0	0	0	18,152,000
0.50	19.361	105.70	14.04	3,186,193	796,548	796,548	18,265,450
1.00	54.494	297.50	14.12	3,203,602	1,597,449	2,393,997	18,378,900
1.50	99.620	543.87	14.22	3,225,961	1,607,391	4,001,388	18,492,350
2.00	152.613	833.18	14.33	3,252,219	1,619,545	5,620,933	18,605,800
2.50	212.213	1158.55	14.46	3,281,750	1,633,492	7,254,425	18,719,250
3.00	277.544	1515.23	14.61	3,314,122	1,648,968	8,903,393	18,832,700
3.50	347.950	1899.60	14.76	3,349,007	1,665,782	10,569,175	18,946,150
4.00	422.905	2308.81	14.92	3,386,147	1,683,789	12,252,964	19,059,600
4.50	501.977	2740.49	15.10	3,425,327	1,702,869	13,955,833	19,173,050
5.00	584.796	3192.64	15.28	3,466,364	1,722,923	15,678,755	19,286,500
5.50	671.043	3663.49	15.47	3,509,099	1,743,866	17,422,621	19,399,950
6.00	760.435	4151.52	15.66	3,553,392	1,765,623	19,188,244	19,513,400
6.50	**852.716**	**4655.32**	**15.86**	**3,599,117**	**1,788,127**	**20,976,371**	**19,626,850**
7.00	947.656	5173.63	16.07	3,646,159	1,811,319	22,787,690	19,740,300
7.50	1045.042	5705.30	16.28	3,694,413	1,835,143	24,622,833	19,853,750
8.00	1144.679	6249.26	16.50	3,743,783	1,859,549	26,482,382	19,967,200

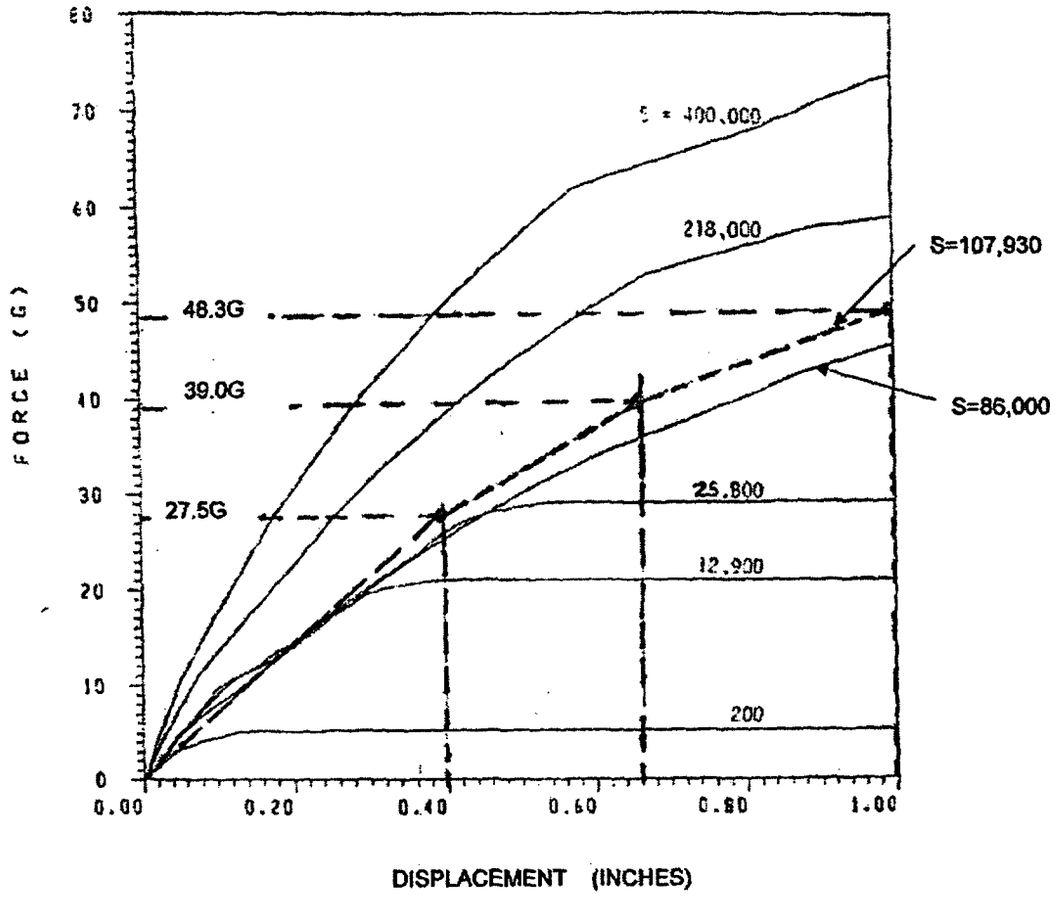

Figure 3.9.7-1
Force vs. Displacement – End Drop
(see Reference 1, Figure 14)

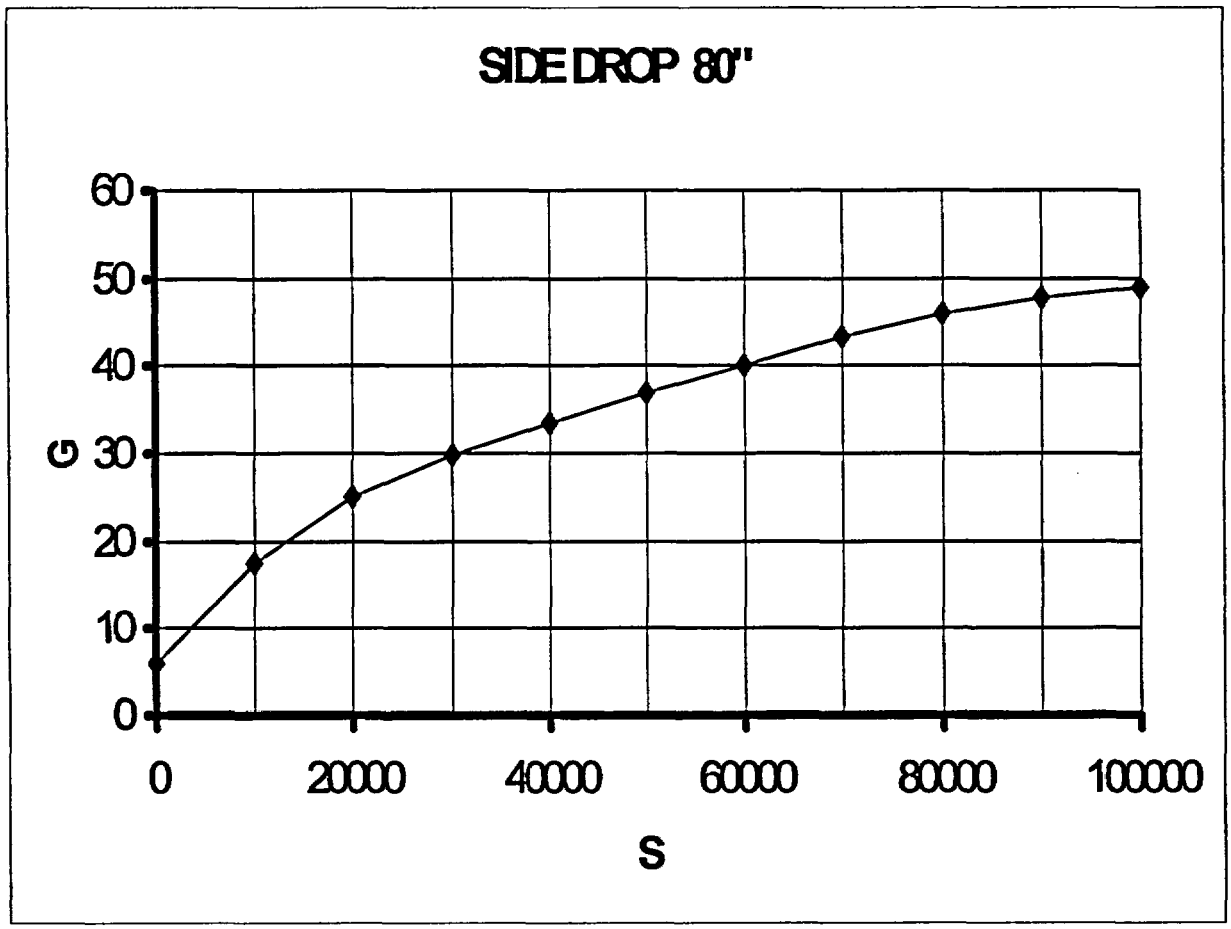

Figure 3.9.7-2
S vs. g Curve for 80 inch Height Side Drop

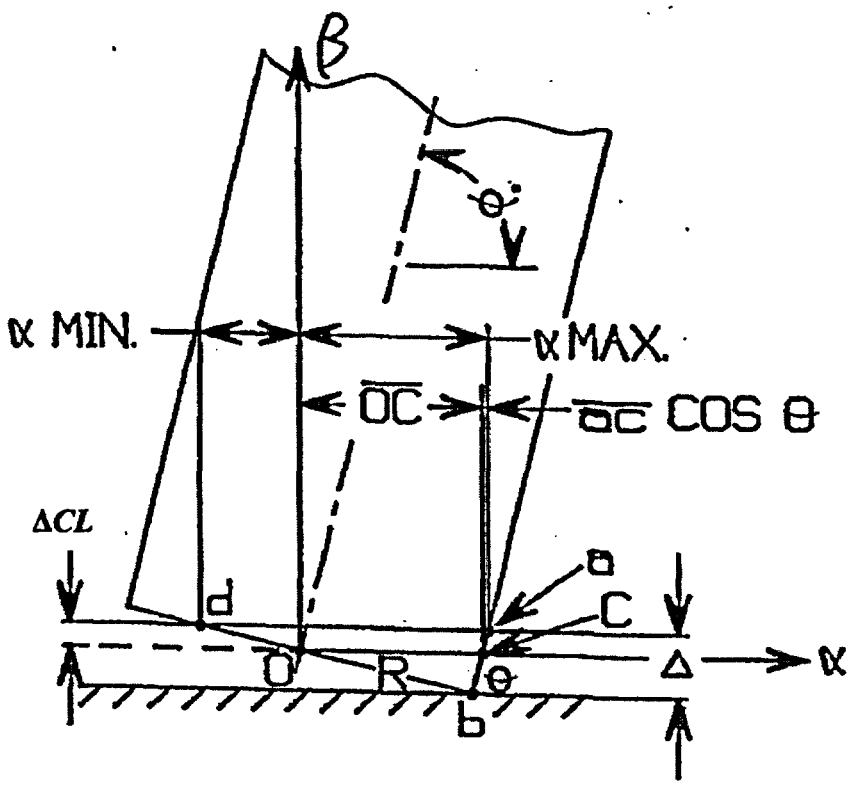

$$\sin\theta = \frac{R}{oc} \qquad \cos\theta = \frac{bc}{oc} \qquad \theta = \tan^{-1}\left(\frac{197.07}{81.7}\right) = 67.48°$$

$$bc = oc\cos\theta = R\left(\frac{\cos\theta}{\sin\theta}\right)$$

$$ac = ab - bc = \frac{\Delta}{\sin\theta} - R\left(\frac{\cos\theta}{\sin\theta}\right)$$

$$ad = \frac{ab}{\cos\theta} = \frac{\Delta}{\sin\theta\cos\theta}$$

$$\Delta CL = \Delta - bc\sin\theta = \Delta - R\cos\theta$$

$$\alpha_{max} = oc + ac\cos\theta = \frac{R}{\sin\theta} + ac\cos\theta$$

$$= \frac{R}{\sin\theta} + \Delta CL\left(\frac{\cos\theta}{\sin\theta}\right)$$

$$\alpha_{min} = ad - \alpha_{max} = \frac{\Delta}{\sin\theta\cos\theta} - \frac{R}{\sin\theta} - \Delta CL\left(\frac{\cos\theta}{\sin\theta}\right)$$

$$= \Delta CL\left(\frac{1}{\sin\theta\cos\theta} - \frac{\cos\theta}{\sin\theta}\right)$$

Figure 3.9.7-3
Geometry of C. G. Over Corner Drop

The area of the impact surface is obtained by first writing the equation for the intersection curves between the cylinder and plane surfaces. We set up the following coordinate systems with the origin at the bottom center of the cask.

By transforming coordinates:

$$\alpha = x\sin\theta + z\cos\theta \qquad x = \alpha\sin\theta - \beta\cos\theta$$
$$\beta = -x\cos\theta + z\sin\theta \qquad z = \alpha\cos\theta + \beta\sin\theta$$

The equation for a cylinder is,

$$x^2 + y^2 = R^2$$

Or by transforming coordinates,

$$\alpha^2\sin^2\theta - 2\alpha\beta\sin\theta\cos\theta + \beta^2\cos^2\theta + y^2 = R^2$$

By setting the intersection of this surface with target surface, $\beta = \Delta CL$, the equation of the intersection curve becomes the following.

$$\alpha^2\sin^2\theta - 2\Delta CL\sin\theta\cos\theta + \Delta CL^2\cos^2\theta + y^2 = R^2$$

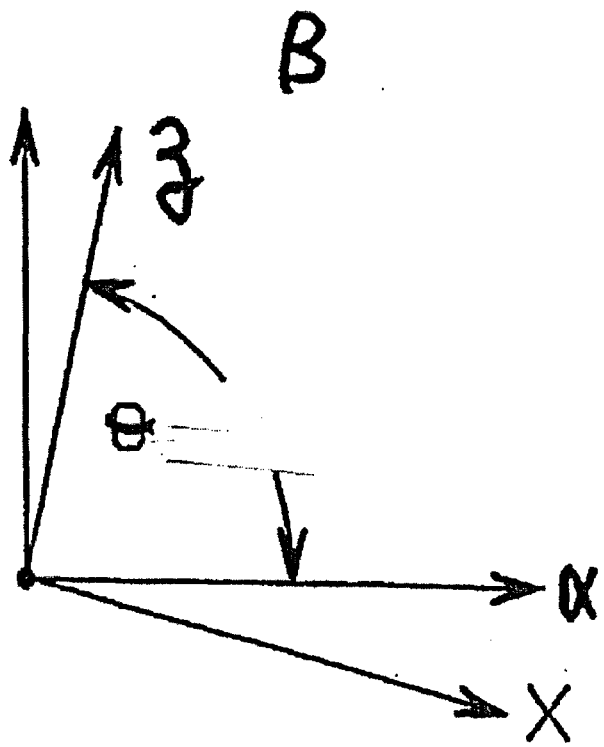

Figure 3.9.7-4
Geometry of C. G. Over Corner Drop (continued)

The area, A, as a function of the deformation is calculated by integrating the following.

$$\alpha^2 \sin^2\theta - 2\alpha\Delta CL \sin\theta \cos\theta + \Delta CL^2 \cos^2\theta + y^2 = R^2$$

$$A = 2\int_{\alpha\,\min}^{\alpha\,\max} y\,d\alpha$$

Where y is given in above equation.

This is numerically integrated using 100 divisions and the trapezoidal rule. The results are tabulated in Table 3.9.7-4.

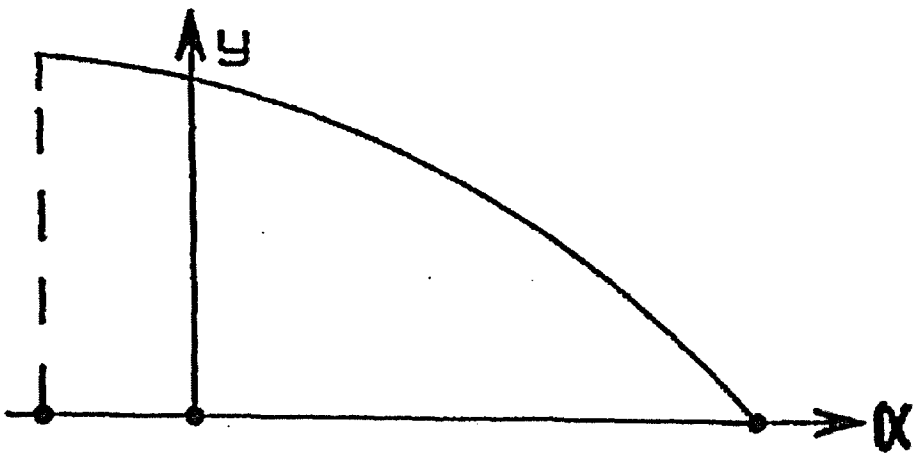

Figure 3.9.7-5
Geometry of the C. G. Over Corner Drop - Area Calculation (continued)

$$L = 2\left[\left(\frac{2R\delta_e}{\cos\theta}\right) - \left(\frac{\delta_e^2}{\cos^2\theta}\right)\right]^{1/2}$$

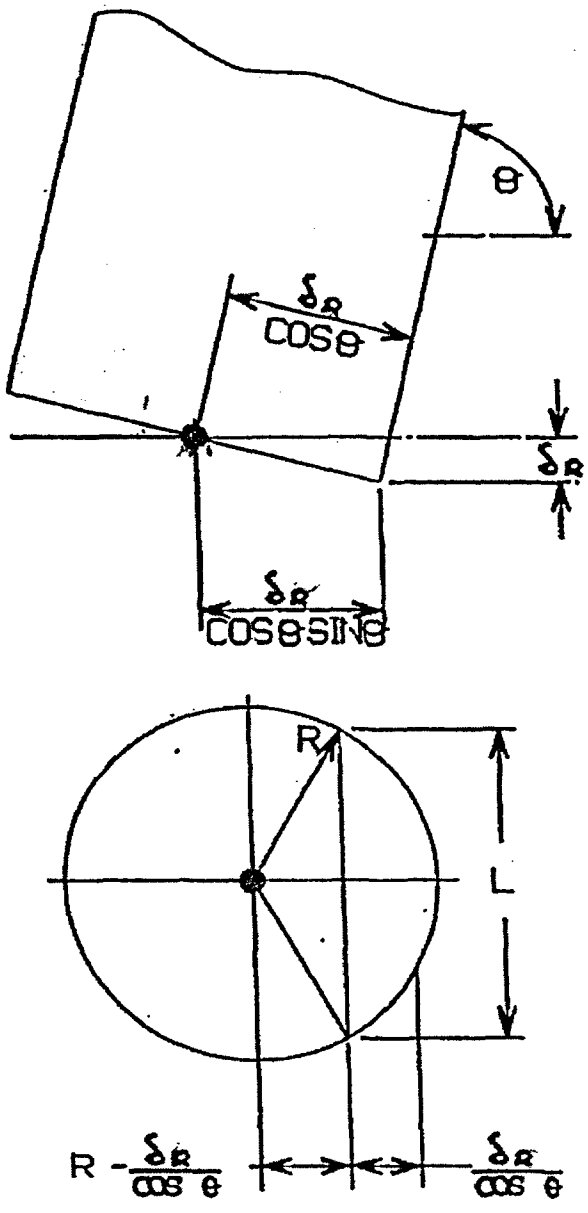

Figure 3.9.7-6
C. G. Over Corner Drop – *L* Dimension Calculation

APPENDIX 3.9.8
DAMAGED FUEL CLADDING STRUCTURAL EVALUATION

TABLE OF CONTENTS

3.9.8 DAMAGED FUEL CLADDING STRUCTURAL EVALUATION 3.9.8-1

3.9.8.1 Introduction 3.9.8-1

3.9.8.2 Design Input / Data 3.9.8-2

3.9.8.3 Loads 3.9.8-3

3.9.8.4 Evaluation Criteria 3.9.8-5

3.9.8.5 Evaluation Methodology 3.9.8-6

3.9.8.6 Trailer Acceleration from 0 mph to 5 mph during Transfer 3.9.8-8

3.9.8.7 Trailer Deceleration from 5 mph to 0 mph during Transfer 3.9.8-11

3.9.8.8 Normal Loading Condition during Insertion / Retrieval of DSC into / from HSM 3.9.8-13

3.9.8.9 Off-Normal Jammed Canister Loading during Insertion of DSC into HSM 3.9.8-14

3.9.8.10 One Foot End Drop Damaged Fuel Evaluation 3.9.8-15

3.9.8.11 One Foot Side Drop Damaged Fuel Evaluation 3.9.8-16

3.9.8.12 Conclusions 3.9.8-20

3.9.8.13 References 3.9.8-21

LIST OF TABLES

3.9.8-1 Westinghouse 15x15 - K_I Calculation using Fracture Geometry #2

3.9.8-2 Westinghouse 17x17 Std - K_I Calculation using Fracture Geometry #2

3.9.8-3 Framatome 17x17 MKBW - K_I Calculation using Fracture Geometry #2

3.9.8-4 Westinghouse 17x17 Vantage 5H - K_I Calculation using Fracture Geometry #2

3.9.8-5 Westinghouse 17x17 OFA - K_I Calculation using Fracture Geometry #2

3.9.8-6 Summary - Maximum Fuel Rod Stresses and Stress Ratios

3.9.8-7 Summary - Computed Fuel Tube Stress Intensity Factors and Ratios

3.9.8-8 Derivation of Tensile Force (T) and Applied Moment (M) Relationship for a Circular Tube

3.9.8-9 Tire Stiffness Calculation

LIST OF FIGURES

3.9.8-1 Fracture Geometry #1: Ruptured Section

3.9.8-2 Fracture Geometry #2: Through-Wall Circumferential Crack in Cylinder Under Bending

3.9.8-3 Stress Intensity Factor Solutions For Several Specimen Configurations

3.9.8 DAMAGED FUEL CLADDING STRUCTURAL EVALUATION

3.9.8.1 Introduction

The purpose of this appendix is to demonstrate structural integrity of the damaged fuel cladding in the NUHOMS® 32PTH DSC following normal and off-normal loading conditions of storage and onsite transfer (required for Part 72 License) and normal condition of offsite transport (required for Part 71 License).

In this appendix, the damaged fuel is defined as: "damaged PWR fuel assemblies are fuel assemblies containing missing or partial fuel rods or fuel rods with known or suspected cladding defects greater than hairline cracks or pinhole leaks. The extent of cladding damage in the fuel rods is to be limited such that a fuel pellet is not able to pass through the damaged cladding during handling and retrievability is assured following Normal/Off-Normal conditions".

This appendix evaluates stresses in the fuel cladding associated with normal and off-normal conditions of on-site transfer/storage and off-site transport. It also presents a fracture mechanics assessment of the cladding using conservative assumptions regarding defect size geometry and amount of oxidation in the cladding material. These evaluations demonstrate the structural integrity of the damaged fuel cladding under normal and off-normal conditions.

The NUHOMS® 32PTH DSC is designed to store 32 intact fuel assemblies, or no more than 16 damaged and the remainder intact, for a total of 32 standard PWR fuel assemblies per canister. All the fuel assemblies, intact or damaged, consist of PWR fuel assemblies with Zircaloy cladding. Damaged fuel assemblies may only be stored in the peripheral compartments of the NUHOMS® 32PTH DSC.

3.9.8.2 Design Input / Data

The design inputs, taken from References [2] and [12], are modified to include the reduction in cladding thickness due to oxidation. They are documented in the following table.

Fuel Assembly Type	WE15x15	WE 17x17std	17x17 MkBW	WE 17x17 Vantage5H	WE 17x17 OFA	Notes
Fuel Assembly Weight (lb)	1,555	1,575	1,575	1,575	1,575	(1,2)
No. of Rods	204	264	264	264	264	(1)
Active Fuel Length (in)	144.0	144.0	144.0	144.0	144.0	(1)
No. of Internal Spacers	6	6	6	6	6	(3)
Max. Fuel Rod Span (in)	27.0	25.0	25.0	25.0	25.0	(5)
Fuel Rod OD (in)	0.4193	0.3713	0.3713	0.3713	0.3573	(1,4)
Clad Thickness (in)	0.0216	0.0198	0.0213	0.0198	0.0198	(1,4)
Fuel Pellet OD (in)	0.3659	0.3225	0.3195	0.3225	0.3088	(1)
Fuel Tube Area (in^2)	0.0270	0.0219	0.0234	0.0219	0.0210	
Fuel Tube M.I. (in^4)	5.35E-04	3.39E-04	3.60E-04	3.39E-04	3.00E-04	
Fuel Pellet M.I. (in^4)	8.80E-04	5.31E-04	5.12E-04	5.31E-04	4.46E-04	
Fuel Tube + Pellet M.I. (in^4)	1.42E-03	8.70E-04	8.71E-04	8.70E-04	7.46E-04	
Fuel Rod Weight (lb)	7.62	5.97	5.97	5.97	5.97	(6)
Irradiated Yield Stress (psi)	80,500	80,500	80,500	80,500	80,500	(7)
Young's Modulus (psi)	10.4E6	10.4E6	10.4E6	10.4E6	10.4E6	(7)

Notes:

1. Data are obtained from Chapter 2, Table 2-1.
2. The fuel assembly weight includes BPRA weight.
3. The number of internal spacers is obtained from (Ref 12).
4. Include 0.00270 in thickness reduction to account for maximum oxide thickness.
5. Maximum fuel rod span is obtained from (Ref 12) and have been rounded up to whole number.
6. Fuel rod weight = Fuel Assembly Weight / No. of Rods.
7. Data are obtained from Reference 3 at 750 °F temperature.

3.9.8.3 Loads

3.9.8.3.1 Part 72 Normal and Off-normal Condition Loads

The damaged fuel inside the DSC is subjected to following normal and off normal condition Part 72 loads:

- Dead Weight
- Internal Pressure
- Thermal
- Transfer Load (Inertia Loads associated with moving the DSC from the fuel loading area to the ISFSI site), which consists of 1g in the longitudinal, 1g in the transverse and 1g in the vertical direction.
- HSM Loading/Unloading (Normal loads associated with inserting the DSC into and retrieving the DSC from the HSM)
- Jammed Canister Load (Off normal loads associated with jamming the DSC during DSC insertion into the HSM)

The stresses due to the dead weight are insignificant. No internal pressure is assumed for the damaged fuel. The cladding is assumed to be able to expand due to thermal loads and thus no thermal-induced stresses are considered. However, the temperature of the cladding is considered for selection of allowable stresses at temperature. Therefore, the structural integrity of the damaged fuel is evaluated in this appendix only for the Transfer/Handling loads (DSC Loading/transfer to ISFSI, HSM Loading/Unloading, and Jammed Canister Load conditions).

3.9.8.3.2 Part 71 Normal Condition Loads

The damaged fuel is evaluated for the following normal condition 10CFR Part 71 off-site transportation loads:

- 1 foot end and side drop loads
- Vibratory loads

Vibratory loads of 0.30g in longitudinal direction, 0.30g in the transverse direction and 0.60g in the vertical direction, taken from Reference [5] are considered representative for a truck loaded cask. This load case is considered enveloped by the 1g transfer load used for Part 72. Similarly, the vibration load of 0.19g in the longitudinal direction, 0.19g in the transverse direction and 0.37g in the vertical direction for a rail car loaded cask [Ref. 6] is also bounded by the Part 72 transfer load. The shock load of 4.7g in the longitudinal and 4.7g in the lateral and vertical directions for a rail car loaded cask (bounding values between rail and truck transport) [Ref. 6] during off-site transport are

bounded by 1 foot end drop (30g) and 1 foot side drop (30g) transport load. Therefore, structural integrity of the damaged fuel for the normal condition Part 71 load is evaluated only for the one-foot end and side drop conditions.

Note that for the normal and accident off-site transport drops the impact limiters are attached at both ends of the horizontal loaded cask.

3.9.8.4 Evaluation Criteria

The retrievability of the damaged fuel in the NUHOMS® 32PTH DSCs is assured if the damaged fuel cladding retains its structural integrity when subjected to normal and off normal loads. Per the damaged fuel definition in Section 3.9.8.1, the damaged fuel rods loaded in the 32PTH DSCs may have cladding defects greater than hairline cracks or pinhole leaks. However, under normal and off-normal loads, the original defects (such as cracks or pinholes) should not change significantly so that the damaged fuel can be retrieved.

The damaged fuel cladding needs to meet the following criteria to ensure their structural integrity and thus be retrievable:

- Fuel cladding stresses under normal and off-normal load conditions are less than the irradiated yield strength of the cladding material.
- Stability of the cladding tube is maintained (i.e., no buckling occurs).
- The stress intensity factor, K_I, of the fuel cladding tube geometry considering through-wall flaw is less than experimentally determined fracture toughness, K_{IC}, considering temperature and irradiation effects.

3.9.8.5 Evaluation Methodology

The onsite transfer of the fuel is accomplished using the OS 187H or Standard Transfer Cask loaded on a transfer trailer that is 10' 6" wide [8]. The transfer trailer has four axles with eight (8) 235/75 R17.5 SLR 184 tires per axle (total of 32 tires). The measured tire stiffness per tire is 1500 lbs/in [1].

During the on-site transfer operation, the trailer either accelerates from 0 initial velocity to a maximum velocity of 5 MPH [8] or decelerates from a maximum velocity of 5 MPH to 0 final velocity. Therefore, during the transfer operation the gap between the fuel assemblies and the DSC top or bottom plugs may close if friction is overcome. The kinetic energy during impact of the fuel assemblies' mass on the top or bottom plugs is absorbed as strain energy through the cask, skid, trailer, and ultimately in the tires, acting as springs.

The structural integrity of the fuel assembly is evaluated by using the principle of conservation of energy. Thus, for a spring/mass system the kinetic energy of the mass is equal to the strain energy absorbed by the spring at the time of impact.

Therefore: $(1/2)\ M*V^2 = (1/2)\ K*X^2$

Where:

M = Mass of the system (lb.sec^2/in) = W/g
W = Weight of the system (lbs)
g = Acceleration due to gravity = 386.4 in/sec^2
V = Velocity of the system (in/sec)
K = Stiffness of the spring (lbs/in)
F = Force acting on the mass and the spring (lbs)
X = Displacement of the spring (in) = F/K

Substituting F/K for X in the above equation and solving for F gives the force acting on the mass as:

$$F = (K*M)^{1/2} * V$$

Therefore, the equivalent g load acting on the mass = F/W

For the fuel rod once the force of impact (F) is known the stress may be computed knowing the area of cross section (A) of the cladding.

The following basic equations of kinematics relating distance, velocity, acceleration and time are used in this appendix:

$$s = u*t + (1/2)*a*t^2$$
$$v = u + a*t$$

where,

s = distance (in)

u = initial velocity (in/sec)
v = final velocity (in/sec)
a = acceleration or deceleration (in/sec ^{2})
t = time (sec)

The structural integrity of the damaged fuel rods is evaluated for the following five loading events:

- Damaged fuel rod assemblies subjected to 1g acceleration when the trailer accelerates from 0 initial velocity to constant velocity of 5 mph [8] during onsite transfer.
- Damaged fuel rod assemblies subjected to 1g deceleration when the trailer decelerates from 5 mph [8] constant velocity to 0 final velocity during onsite transfer.
- Normal condition of loading during insertion or extraction of the DSC into or from the HSM for storage.
- Off normal jammed canister loading during insertion or extraction of the DSC into the HSM for storage.
- Damaged fuel rod assemblies subjected to 1-foot drops during normal condition of off site transport.

For each of the above five loading events, the integrity of the damaged fuel assemblies is evaluated in the following sections.

3.9.8.6 Trailer Acceleration from 0 mph to 5 mph during Transfer

During onsite transfer of the cask from the fuel building to the ISFSI the loaded trailer picks up the velocity from 0 mph to 5 mph (88 in/s). The fuel assemblies inside the canister are subjected to a maximum postulated 1g (386.4 in/s^2) equivalent axial transfer load [1]. The maximum speed during this event is 5 mph and any sudden load on the fuel assemblies is transferred from the fuel assemblies to the cask, the support skid, the trailer, the rubber tires and to the road bed. The maximum transfer acceleration is +/- 1g.

Under the hot condition, the maximum gap between the fuel assemblies and the DSC plug = d (in)

Substituting in the kinematics equation $s = s_o + u_o t + a*t^2/2 = d$

Where:

Initial displacement, $s_o = 0$

Initial velocity, $u_o = 0$

Acceleration, $a = (1-0.3)\ g = 0.7g$

Where, 0.3 is the friction coefficient between the fuel assembly grid straps and the fuel compartment [9].

$g = 386.4$ in/s ^{2}

Solving for t

$$t = \{(2)*(d) / (0.7g)^{1/2}$$

At contact with top shield plug the velocity of the fuel assembly is

$$v = (0.7g)\ (t)$$

The contact force on the fuel assembly is equal to: $F = (K*M)^{1/2} * (v)$

Where:

M = total mass of the fuel assemblies = (W*n)/g
W = Weight of each fuel assembly
n = number of fuel assemblies/canister = 32
K= k*32 lb/in, where k = stiffness of each of 32 rubber tires
k = stiffness of each tire is computed as follows:

Tire pressure = 135 psi,

For 235 (tire width mm)/75 (height to width ratio in %) R 17.5 (rim diameter inch) SLR184 tires:

Tire width = (235 mm)/(25.4mm/in) = 9.25 in

Height of the tire = 75% of 9.25 in = 6.94 in

Diameter of the tire = (17.5 in) + 2*6.94 in = 31.4 in

Total loaded trailer weight = weight of (loaded cask +trailer + skid +ram)

Loaded Cask Weight (with impact limiters) = 250,000 lbs. (conservative, see Chapter 3, Section 3.2.3)

Weight (trailer + skid + ram) = 39,700(trailer)+ 26,500(skid)+ 6,400(ram) [1]
= 72,600 lb

Total Load = 250,000 + 72,600 = 322,600 lb

Load per tire = (322,600 lb)/(32 tires) = 10,081 lb

Area of contact of the tire = (10,081 lbs/135 psi) = 74.7 in^2

Length of compression of the tire = 74.7 in^2 / 9.25 in = 8.08 in

Therefore, deflection of the tire = $(31.4/2) - \{(31.4/2)^2 - (8.08/2)^2\}^{1/2}$ = 0.5287 in

Tire stiffness/tire = (10,081 lb)/(0.5287 in) = 19,068 lb/in

Total tire stiffness for 32 tires = (19,068)(32) = 6.1×10^5 lb/in

As per Table 3.9.8-9, the measured tire stiffness = 1500 x 32 = 4.8×10^4 lb/in

Conservatively, use tire stiffness of 6.1×10^5 lb/in

The force in the fuel assemblies is $F = (K*M)^{1/2} * (v)$

Therefore, load per assembly = F / 32 lb

Equivalent g load in the fuel rods = F / 32 / W

The axial stress in the rod is = F / Fuel Tube Area

Using the methodology described above, the fuel tube axial stresses for the prescribed condition are computed and presented in the following table.

Fuel Assembly Type	WE15x15	WE 17x17std	17x17 MkBW	WE 17x17 Vantage5H	WE 17x17 OFA
Total Fuel Weight (lb)	1,555	1,575	1,575	1,575	1,575
Fuel Tube Area (in^2)	0.0270	0.0219	0.0234	0.0219	0.0210
gap (in) (1)	6.0	6.0	6.0	6.0	6.0
t (s)	0.211	0.211	0.211	0.211	0.211
v (in/s)	56.97	56.97	56.97	56.97	56.97
M ($lb\text{-}s^2/in$)	128.8	130.4	130.4	130.4	130.4
W (lb)	48.6	49.2	49.2	49.2	49.2
No. of Fuel Assemblies	32	32	32	32	32
K, lb/in	610,000	610,000	610,000	610,000	610,000
F (lb)	504,946	508,183	508,183	508,183	508,183
Force / Assembly (lb)	15,780	15,881	15,881	15,881	15,881
No of Rod / Assembly	204	264	264	264	264
Force / Rod (lb)	77.4	60.2	60.2	60.2	60.2
Equivalent g load	10.1	10.1	10.1	10.1	10.1
Axial Stress (lb)	2,865	2,747	2,571	2,747	2,864

Note:

(1) The gap between the fuel assembly and the DSC end component is conservatively assumed to be 6" (the actual length is around 2 in.).

The axial stresses in the fuel rods are compressive stresses, and they are significantly less than the irradiated yield stress of the cladding material = 80,500 psi (See table of Section 3.9.8.2). Therefore, the fuel rods will maintain their structural integrity when subjected to the trailer acceleration during transfer.

3.9.8.7 Trailer Deceleration from 5 mph to 0 mph during Transfer

During onsite transfer of the cask from the fuel building to the ISFSI the loaded trailer travels at a maximum constant velocity of 5 mph (88 in/s). Any sudden loads, which may occur during an emergency stop, are transferred from the road bed through the rubber tires, the trailer, the support skid, and the cask to the fuel assemblies. The fuel assemblies inside the canister are subjected to maximum postulated 1g (386.4 in/s ^{2}) equivalent axial transfer load [7]. Therefore, the maximum transfer acceleration is +/- 1g.

The initial velocity is v_i = 88 in/s, the deceleration, g = 386.4 in/s ^{2}

The maximum velocity at impact of the fuel assemblies on the inner bottom cover plate is

v = 88 in/sec - v_f (due to friction) - v_d (due to deceleration)

Where, v_f is a function of work done by the force due to friction (F_f).

Therefore, $(M^* v_f^2)/2 = F_f {}^*d$

Where:

M = mass of the fuel assemblies

F_f = M*g*0.3 (where the coefficient of friction between grid straps and canister is 0.3 [9])

d = gap between fuel assembly and the DSC plug

$v_f = \{(2^*F_f{}^*d)/M)\}^{1/2}$

Conservatively assume that cask is tied to the trailer so that it does not move.

v_d is calculated as follows:

Substituting in the kinematics equation $s = s_o + ut + a^*t^2/2$ (Section 3.9.8.5)

$s_o = 0$, u = 88 in/sec, Acceleration, a = 386.4 in/s ^{2} and solving for 't'

$v_d = u + a^*t$

Conservatively, ignoring v_d (change in velocity due to deceleration), at contact with the inner bottom cover plate of the DSC the velocity of the fuel assembly is

$v = 88 - v_f$

The contact force on the fuel assembly = $F = (K^*M)^{1/2} * (v)$

Where:

M = total mass of the fuel assemblies = (W*n)/g

W = maximum weight of each fuel assembly

n = number of fuel assemblies/canister = 32

K= conservatively use tire stiffness of 6.1 x 10^5 lb/in (Section 3.9.8.6)

$F = (M * K)^{1/2} {}^*v$

Therefore, load per assembly = F / 32

Equivalent g load in the fuel rods = F / 32 / W.

The axial stress in the rod is = F / Fuel Tube Area.

Using the methodology described above, the fuel tube axial stresses for the prescribed condition are computed and presented in the following table.

Fuel Assembly Type	WE15x15	WE 17x17std	17x17 MkBW	WE 17x17 Vantage5H	WE 17x17 OFA
Total Fuel Weight (lb)	1,555	1,575	1,575	1,575	1,575
Fuel Tube Area (in^2)	0.0270	0.0219	0.0234	0.0219	0.0210
gap (in) (1)	6.0	6.0	6.0	6.0	6.0
M ($lb\text{-}s^2/in$)	128.8	130.4	130.4	130.4	130.4
W (lb)	48.6	49.2	49.2	49.2	49.2
F_f (lb)	14,928	15,120	15,120	15,120	15,120
v_f, (in/s)	37.3	37.3	37.3	37.3	37.3
v, (in/s)	50.7	50.7	50.7	50.7	50.7
K, lb/in	610,000	610,000	610,000	610,000	610,000
F (lb)	449,390	452,271	452,271	452,271	452,271
Force / Assembly (lb)	14,043	14,133	14,133	14,133	14,133
No of Rod / Assembly	204	264	264	264	264
Force / Rod (lb)	68.8	53.5	53.5	53.5	53.5
Equivalent g load	9.0	9.0	9.0	9.0	9.0
Axial Stress (lb)	2,550	2,445	2,288	2,445	2,549

Note:

(1) The gap between the fuel assembly and the DSC end component is conservatively assumed to be 6".

The axial stresses in the fuel rods are compressive stresses, and they are significantly less than the irradiated yield strength of the cladding material = 80,500 psi (See table of Section 3.9.8.2). Therefore, the fuel rods will maintain their structural integrity when subjected to the trailer deceleration during transfer.

3.9.8.8 Normal Loading Condition during Insertion / Retrieval of DSC into / from HSM

The insertion or retrieval of the DSC into the HSM is a highly controlled procedure, and the process is conducted slowly. For normal loading condition, the maximum ram push force for DSC insertion and grapple pull force for DSC retrieval are 80 kips and 60 kips, respectively. These applied forces are monitored and controlled. The acceleration/deceleration resulting from the procedure will be small and bounded by the transfer acceleration and deceleration as reported in Sections 3.9.8.6 and 3.9.8.7, respectively.

3.9.8.9 Off-Normal Jammed Canister Loading during Insertion of DSC into HSM

The insertion or retrieval of the DSC into the HSM is a highly controlled procedure, and the process is conducted slowly. For off-normal jammed canister loading condition, the maximum ram push for DSC insertion and grapple pull force for DSC retrieval are both 80 kips. This applied force is monitored and controlled. Similar to the normal loading condition, the acceleration/deceleration resulting from the procedure will be small and bounded by the transfer acceleration and deceleration as reported in Sections 3.9.8.6 and 3.9.8.7, respectively.

3.9.8.10 One Foot End Drop Damaged Fuel Evaluation

During off site transport (Part 71) the damaged fuel assemblies need to be evaluated for 1 foot end drop. The transport operation is carried out using the MP 187H Cask, with the DSC and the impact limiters in the horizontal position.

The maximum g load acting on the damaged fuel rod subjected to 1 foot end drop = 30g

The fuel tube axial stresses for the prescribed condition are computed and presented in the following table.

Fuel Assembly Type	WE15x15	WE 17x17 Std	17x17 MkBW	WE 17x17 Vantage5H	WE 17x17 OFA
Total Fuel Weight (lb)	1,555	1,575	1,575	1,575	1,575
Fuel Tube Area (in^2)	0.0270	0.0219	0.0234	0.0219	0.0210
1-Foot End Drop Equivalent g load	30	30	30	30	30
Force / Assembly (lb)	46,650	47,250	47,250	47,250	47,250
No of Rod / Assembly	204	264	264	264	264
Force / Rod (lb)	228.7	179.0	179.0	179.0	179.0
Axial Stress (lb)	8,469	8,172	7,649	8,172	8,523

The axial stresses in the fuel rods are compressive stresses, and they are significantly less than the irradiated yield stress of the cladding material = 80,500 psi (see table of Section 3.9.8.2). Therefore, the fuel rods will maintain their structural integrity when subjected to the 1 foot end drop load.

3.9.8.11 One Foot Side Drop Damaged Fuel Evaluation

During off site transport (Part 71) the damaged fuel assemblies need to be evaluated for 1 foot side drop. The transport operation is carried out using the MP 187H Cask, with the DSC and the impact limiters in the horizontal position.

The maximum g load acting on the damaged fuel rods under 1 foot side drop load = 30g. The damaged fuel rod structural integrity under 1 foot side drop load is assessed by computing the bending stress in the rod and comparing it with the yield stress of the cladding material. The fracture assessment of the damaged fuel rod structural integrity is made by using two fracture geometries (ruptured sections) as described below.

It is assumed that the damaged fuel tube is burst at the spacers (supports) location, which is the location of maximum bending moment. The loading assumed is on the opposite side of the rod at the burst location. The following two geometries, used for the fracture evaluation of the damaged fuel rods, are based on these assumptions.

Fracture Geometry #1: The first geometry is shown in Figure 3.9.8-1. In this damage mode the fuel tube is assumed to bulge from diameter D to diameter W ($W \geq D$) and rupture to a hole of diameter (2a) at the bulge location. It is assumed that $(2a/w) = 0.5$ for this geometry.

Fracture Geometry #2: The second geometry is shown in Figure 3.9.8-2. The stress intensities factors for this geometry are determined using the solution for a tube with a crack subjected to pure bending moment given in Reference 13. This evaluation is based on a crack length to diameter ratio of 0.5 (or $2a/D_m=0.5$).

The basis for the 0.5 crack length to equivalent plate width/diameter ratio for fracture geometries #1 and #2 is the experimental tests on "as received" Zircalloy fuel tubes with measured burst temperatures of up to 909°C, which showed flaw opening to diameter ratios of 0.4 to 0.5 [16]. The (2a/W) or $(2a/D_m)$ ratios used in this appendix are 0.5.

3.9.8.11.1 Structural Integrity Evaluation with Fracture Geometry #1

The fracture geometry #1 (Ruptured Section) is shown in Figure 3.9.8-1. With reference to Figure 3.9.8-1, the methodology for computing the stress intensity factor K_I is as follows:

Fuel Rod OD = D

Oxidized Clad Thickness = t

Average radius, R = (D-t)/2

I = net tube MI + net fuel MI, where it is conservatively assumed that the net tube MI is equal to one half of the total tube MI, and the net fuel MI is equal to one half of the total fuel MI.

Span Length = S

Assume (2a/W) = 0.5, where 2a = ruptured hole diameter,

W = bulged fuel tube diameter ≥ D.

Stress Intensity Factor, $K_I = (Y)(P*a^{1/2})/(t*W)$, [Reference 14, Fig. 8.7(c)]

Where:

Y = 2.11 {established using (2a/W) = 0.5 (for Forman et al. case) in Figure 3.9.8-3 }

P = average tensile force at the crack which is expressed as a function of moment on the cross section as:

$= (2MR^2t)/I$ (See Table 3.9.8-8)

$W = \pi R$

$M = 0.1058(W_s*S^2)$ (See Appendix 2 of Reference 3)

W_s = 30g Fuel Rod Weight / Length

Bending Stress = MD / 2I

Using the methodology described above, the stress intensity factors, K_I, for the prescribed condition are computed and presented in the following table.

Fuel Assembly Type	WE15x15	WE 17x17Std	7x17 MkBW	WE 17x17 Vantage5H	WE17x17 OFA
Fuel Rod OD, D (in)	0.4193	0.3713	0.3713	0.3713	0.3573
Clad Thickness, t (in)	0.0216	0.0198	0.0213	0.0198	0.0198
Average Radius, R (in)	0.1989	0.1758	0.1750	0.1758	0.1688
Fuel Tube M.I. (in^4)	5.35E-04	3.39E-04	3.60E-04	3.39E-04	3.00E-04
Fuel Pellet M.I. (in^4)	8.80E-04	5.31E-04	5.12E-04	5.31E-04	4.46E-04
I (in^4)	7.08E-04	4.35E-04	4.36E-04	4.35E-04	3.73E-04
Span Length, S (in)	27.0	25.0	25.0	25.0	25.0
(2a/W)	0.5	0.5	0.5	0.5	0.5
Y	2.11	2.11	2.11	2.11	2.11
W (in)	0.62	0.55	0.55	0.55	0.53
Fuel Assembly Weight (lb)	1,555	1,575	1,575	1,575	1,575
No. of Rods	204	264	264	264	264
Active Fuel Length (in)	144.0	144.0	144.0	144.0	144.0
1-Foot Side Drop Equivalent g load	30	30	30	30	30
W_s (lb/in)	1.59	1.24	1.24	1.24	1.24
Moment, M (kip. in)	0.12	0.08	0.08	0.08	0.08
Bending Stress (psi)	36,294	35,086	35,017	35,086	39,348
P (kip)	0.296	0.231	0.246	0.231	0.248
K_I (ksi $in^{1/2}$)	18.3	16.6	16.4	16.6	18.2

The computed stress intensity factor is compared with experimentally obtained plane strain fracture toughness, K_{IC} of irradiated Zircaloy cladding material as reported in

[15]. Reference15 reports a K_{IC} = 35 ksi $in^{1/2}$ at approximately 300°F which is greater than highest computed stress intensity factor, K_I of 18.3 ksi $in^{1/2}$ presented in the above table.

Therefore, the structural integrity of the damaged fuel rods, which are conservatively assumed to rupture as shown in Figure 3.9.8-1, will be maintained.

3.9.8.11.2 Structural Integrity Evaluation with Fracture Geometry #2

This geometry is shown in Figure 3.9.8-2. Stress intensity factors are computed for a crack in a fuel tube subjected to a uniform bending moment (M) using formulae given in Reference 13. As per Reference 13, page 472:

$$K_I = \sigma (\pi * R_m * \theta)^{1/2} F(\theta)$$

where,

$$F(\theta) = 1 + 6.8*(\theta/\pi)^{3/2} - 13.6*(\theta/\pi)^{5/2} + 20.0*(\theta/\pi)^{7/2}$$

σ = Bending Stress due to Uniform Moment 'M'

R_m = Average radius of the fuel tube

2θ = Angle which the crack makes at the center of the tube

K_I = Stress Intensity Factor at the crack

The K_I is computed for all the different fuel assemblies, and the results for all the fuel assemblies are presented in Table 3.9.8-1, 3.9.8-2, 3.9.8-3, 3.9.8- 4 and 3.9.8-5.

Based on the computed K_I using Fracture Geometries #1 & #2, a summary of the comparisons is presented as follows:

	Fracture Geometry #1 K_I	Fracture Geometry #2 K_I
WE 15x15	18.3	27.8
WE 17x17 Std.	16.6	25.3
17x17 MKBW	16.4	25.1
WE 17x17 Vantage 5H	16.6	25.3
WE 17x17 OFA	18.2	27.8

3.9.8.12 Conclusions

The maximum computed stresses in the fuel rods and their ratios to the irradiated yield stress of the cladding material are summarized in Table 3.9.8-6. From Table 3.9.8-6, it can be concluded that stresses for all load cases considered are significantly less than the yield stress of the Zircaloy cladding material (computed stresses are 4% to 49% of the yield stress).

It is important to note that, the stresses in the fuel rods for all analyzed normal and off normal load cases are compressive stresses (less than the critical buckling stress), except for the 1-foot transport condition side drop load.

For the 1-foot side drop it is demonstrated by using fracture mechanics procedures (by comparing computed stress intensity factors to critical crack initiation fracture toughness in Table 3.9.8-7), that the damaged fuel rods will maintain their structural integrity.

This calculation demonstrates that the damaged fuel assemblies in the NUHOMS® 32PTH DSC will retain their structural integrity when subjected to normal condition of storage and on site transfer loads. The damaged fuel assembly will also maintain their integrity when subjected to one-foot drop and vibration loads during normal condition of offsite transport. Therefore, the retrievability of the damaged fuel assemblies is assured when subjected to any of these normal and off normal loads.

3.9.8.13 References

1. Transnuclear Calculation No. NUH24PTH.0209 Rev. 0, "NUHOMS® 24PTH Damaged Fuel Cladding Structural Evaluation to Demonstrate the Retrievability of the Fuel Subject to Normal and Off-Normal Loads".

2. Transnuclear, Inc., "Design Criteria Document (DCD) for the NUHOMS®-32PTH System for Transportation and Storage," NUH32PTH.0101, Revision 0.

3. UCID - 21246, "Dynamic Impact Effects on Spent Fuel Assemblies," Lawrence Livermore National Laboratory, October 20, 1987.

4. Transnuclear Calculation No. 10494-6, Rev. 0, "NUHOMS-32PTH DSC, Transfer Cask, and 'Under Hook' Nominal Weight Calculation".

5. ANSI N14.23, "Draft American National Standard Design Basis for Resistance to Shock and Vibration of Radioactive Material Packages Greater than One Ton in Truck Transport", May 1980.

6. NRC -12 , SAND76-0427, NUREG766510, "Shock and Vibration Environments for Large Shipping Containers on Rail Cars and Trucks", June 1977.

7. Transnuclear Inc., "Final Safety Analysis Report for Standard NUHOMS® Horizontal Modular Storage System for Irradiated Nuclear Fuel," Document No. NUH-003, Revision 6

8. Transnuclear, Inc., "Technical Specification for the NUHOMS® 10' - 6" Wide Cask Transfer Trailer," Report No. NUH-07-106, Revision 3.

9. Baumeister, T., "Mark's Standard Handbook for Mechanical Engineers," McGraw-Hill Book Company, 8th Edition.

10. Transnuclear Calculation No. 10494-20, Rev. 0, "NUHOMS-32PTH Thermal Analysis of DSC in HSM for the Normal, Off-Normal, and Accident Storage Conditions".

11. Transnuclear Calculation No. 10494-46, Rev. 0, "NUHOMS-32PTH Thermal Expansions".

12. OCRWM Database, "Characteristics of spent fuel, high level waste, and other radioactive wastes which may require long term isolation" Appendix 2A, Volume 3 of 6, DOE/RW-0184, December 1987.

13. "The Stress Analysis of Cracks Handbook" Third Edition by Hiroshi Tada et al., ASME press.

14. R.W. Hertzberg," Deformation and Fracture Mechanics of Engineering Material" John Wiley & Sons, New York, 1976.

15. T.J. Walker, et al., "Variation of Zircaloy Fracture Toughness in Irradiation" Zirconium in Nuclear Applications, ASTM STP 551, American Society for Testing and Materials, 1974, pp. 328-354.

16. Light-Water Reactor Safety Research Program: Quarterly Progress Report July-September 1976, Section III, "Mechanical Properties of Zircaloy Containing Oxygen", Figs III-29 to III-32, ANL-75-72 (September 1975).

Table 3.9.8-1

Westinghouse 15x15 - K_I Calculation using Fracture Geometry #2

OD (in) =	0.4193
t (in) =	0.0216
R / t =	9.71
Rm (in) =	0.1989
M (kip-in) =	0.12
a / Rm =	0.5
Theta (radian) =	0.52
I (in^4) =	7.08E-04
Bending Stress (ksi) =	36.29
E (ksi) =	10,400

Theta (rad)	Theta/pi	Half Length (in)	F(Theta)	K_I (ksi $in^{1/2}$)
0.05	0.0159	0.0099	1.0132	6.5
0.10	0.0318	0.0199	1.0363	9.4
0.15	0.0477	0.0298	1.0646	11.8
0.20	0.0637	0.0398	1.0966	14.1
0.25	0.0796	0.0497	1.1312	16.2
0.30	0.0955	0.0597	1.1677	18.3
0.35	0.1114	0.0696	1.2058	20.5
0.40	0.1273	0.0795	1.2450	22.6
0.45	0.1432	0.0895	1.2853	24.7
0.50	0.1592	0.0994	1.3265	26.9
0.51	0.1623	0.1014	1.3348	27.3
0.52	0.1655	0.1034	1.3432	27.8
0.55	0.1751	0.1094	1.3686	29.1
0.60	0.1910	0.1193	1.4117	31.4
0.65	0.2069	0.1293	1.4557	33.7
0.70	0.2228	0.1392	1.5009	36.0

Table 3.9.8-2

Westinghouse 17x17 Std - K_I Calculation using Fracture Geometry #2

OD (in) =	0.3713
t (in) =	0.0198
R / t =	9.38
Rm (in) =	0.1758
M (kip-in) =	0.08
a / Rm =	0.5
Theta (radian) =	0.52
I (in^4) =	4.35E-04
Bending Stress (ksi) =	35.09
E (ksi) =	10,400

Theta (rad)	Theta/pi	Half Length (in)	F(Theta)	K_I (ksi $in^{1/2}$)
0.05	0.0159	0.0088	1.0132	5.9
0.10	0.0318	0.0176	1.0363	8.5
0.15	0.0477	0.0264	1.0646	10.8
0.20	0.0637	0.0352	1.0966	12.8
0.25	0.0796	0.0439	1.1312	14.7
0.30	0.0955	0.0527	1.1677	16.7
0.35	0.1114	0.0615	1.2058	18.6
0.40	0.1273	0.0703	1.2450	20.5
0.45	0.1432	0.0791	1.2853	22.5
0.50	0.1592	0.0879	1.3265	24.5
0.51	0.1623	0.0896	1.3348	24.9
0.52	0.1655	0.0914	1.3432	25.3
0.55	0.1751	0.0967	1.3686	26.5
0.60	0.1910	0.1055	1.4117	28.5
0.65	0.2069	0.1142	1.4557	30.6
0.70	0.2228	0.1230	1.5009	32.7

Table 3.9.8-3

Framatome 17x17 MKBW - K_I Calculation using Fracture Geometry #2

OD (in) =	0.3713
t (in) =	0.0213
R / t =	8.72
Rm (in) =	0.1750
M (kip-in) =	0.08
a / Rm =	0.5
Theta (radian) =	0.52
I (in^4) =	4.36E-04
Bending Stress (ksi) =	35.02
E (ksi) =	10,400

Theta (rad)	Theta/pi	Half Length (in)	F(Theta)	K_I (ksi $in^{1/2}$)
0.05	0.0159	0.0088	1.0132	5.9
0.10	0.0318	0.0175	1.0363	8.5
0.15	0.0477	0.0263	1.0646	10.7
0.20	0.0637	0.0350	1.0966	12.7
0.25	0.0796	0.0438	1.1312	14.7
0.30	0.0955	0.0525	1.1677	16.6
0.35	0.1114	0.0613	1.2058	18.5
0.40	0.1273	0.0700	1.2450	20.4
0.45	0.1432	0.0788	1.2853	22.4
0.50	0.1592	0.0875	1.3265	24.4
0.51	0.1623	0.0893	1.3348	24.8
0.52	0.1655	0.0910	1.3432	25.1
0.55	0.1751	0.0963	1.3686	26.4
0.60	0.1910	0.1050	1.4117	28.4
0.65	0.2069	0.1138	1.4557	30.5
0.70	0.2228	0.1225	1.5009	32.6

Table 3.9.8-4

Westinghouse 17x17 Vantage 5H - K_I Calculation using Fracture Geometry #2

OD (in) =	0.3713
t (in) =	0.0198
R / t =	9.38
Rm (in) =	0.1758
M (kip-in) =	0.08
a / Rm =	0.5
Theta (radian) =	0.52
I (in^4) =	4.35E-04
Bending Stress (ksi) =	35.09
E (ksi) =	10,400

Theta (rad)	Theta/pi	Half Length (in)	F(Theta)	K_I (ksi $in^{1/2}$)
0.05	0.0159	0.0088	1.0132	5.9
0.10	0.0318	0.0176	1.0363	8.5
0.15	0.0477	0.0264	1.0646	10.8
0.20	0.0637	0.0352	1.0966	12.8
0.25	0.0796	0.0439	1.1312	14.7
0.30	0.0955	0.0527	1.1677	16.7
0.35	0.1114	0.0615	1.2058	18.6
0.40	0.1273	0.0703	1.2450	20.5
0.45	0.1432	0.0791	1.2853	22.5
0.50	0.1592	0.0879	1.3265	24.5
0.51	0.1623	0.0896	1.3348	24.9
0.52	0.1655	0.0914	1.3432	25.3
0.55	0.1751	0.0967	1.3686	26.5
0.60	0.1910	0.1055	1.4117	28.5
0.65	0.2069	0.1142	1.4557	30.6
0.70	0.2228	0.1230	1.5009	32.7

Table 3.9.8-5

Westinghouse 17x17 OFA - K_I Calculation using Fracture Geometry #2

OD (in) =	0.3573
t (in) =	0.0198
R / t =	9.02
Rm (in) =	0.1688
M (kip-in) =	0.08
a / Rm =	0.5
Theta (radian) =	0.52
I (in^4) =	3.73E-04
Bending Stress (ksi) =	39.35
E (ksi) =	10,400

Theta (rad)	Theta/pi	Half Length (in)	F(Theta)	K_I (ksi $in^{1/2}$)
0.05	0.0159	0.0084	1.0132	6.5
0.10	0.0318	0.0169	1.0363	9.4
0.15	0.0477	0.0253	1.0646	11.8
0.20	0.0637	0.0338	1.0966	14.1
0.25	0.0796	0.0422	1.1312	16.2
0.30	0.0955	0.0506	1.1677	18.3
0.35	0.1114	0.0591	1.2058	20.4
0.40	0.1273	0.0675	1.2450	22.6
0.45	0.1432	0.0759	1.2853	24.7
0.50	0.1592	0.0844	1.3265	26.9
0.51	0.1623	0.0861	1.3348	27.3
0.52	0.1655	0.0878	1.3432	27.8
0.55	0.1751	0.0928	1.3686	29.1
0.60	0.1910	0.1013	1.4117	31.3
0.65	0.2069	0.1097	1.4557	33.6
0.70	0.2228	0.1181	1.5009	36.0

Table 3.9.8-6

Summary - Maximum Fuel Rod Stresses and Stress Ratios

Normal and Off Normal Load Case	Maximum [1] Stress (psi)	Stress [2] Ratio
On site Transport and Transfer Operations	2,865	0.04
One-foot End Drop (Part 71)	8,523	0.11
One-foot Side Drop (Part 71)	39,348	0.49

Notes:
(1) Maximum stress for all fuel assemblies.
(2) Stress ratio = maximum stress / 80,500 (yield stress for Zircaloy cladding).

Table 3.9.8-7

Summary - Computed Fuel Tube Stress Intensity Factors and Ratios

Fracture Geometry	Max K_I (1) (ksi $in^{1/2}$)	K_{IC} (2) (ksi $in^{1/2}$)	Ratio Max K_I / K_{IC}
Geometry #1	18.3	35.0	0.52
Geometry #2	27.8	35.0	0.79

Notes:

1. Maximum K_I for all fuel assemblies.
2. K_{IC} = Crack initiation fracture toughness (plane strain fracture toughness).

Table 3.9.8-8

Derivation of Tensile Force (T) and Applied Moment (M) Relationship for a Circular Tube

Consider a circular tube of average radius "R", thickness "t" subjected to a bending moment "M".

At angle "θ" from the neutral axis (N/A), for a segment of the tube with angle "dθ"

Area = A = $t*R*d\theta$,

Tensile stress = $\sigma = (M*R*\sin\theta)/I$

Where, I = moment of inertia of the section

Therefore,

Tensile Force $= \Delta P = (M*R*\sin\theta/I)*(t*R*d\theta)$

Total Tensile Force $= P = \int (M*R*\sin\theta/I)*(t*R*d\theta)$

Where, limits of integral are from angle "$\theta = 0$" to angle "$\theta = \pi$"

Therefore, $P = (M*R^2*t/I)\int \sin\theta \, d\theta$

$= (M*R^2*t/I)[-\cos\theta]_0^{\pi}$

$= 2*M*R^2*t/I$

Table 3.9.8-8 (continued)

Derivation of Tensile Force (T) and Applied Moment (M) Relationship for a Circular Tube

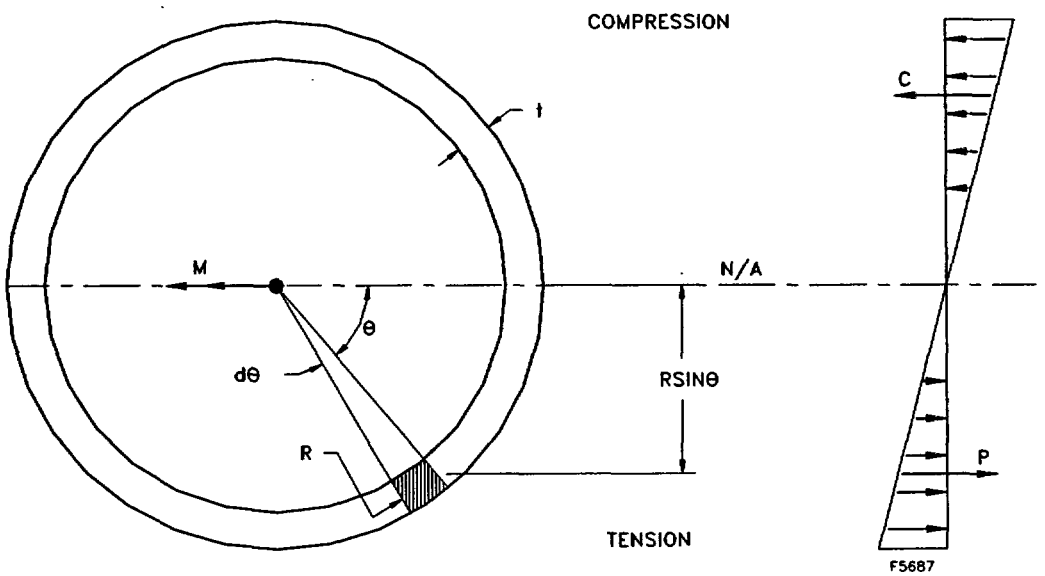

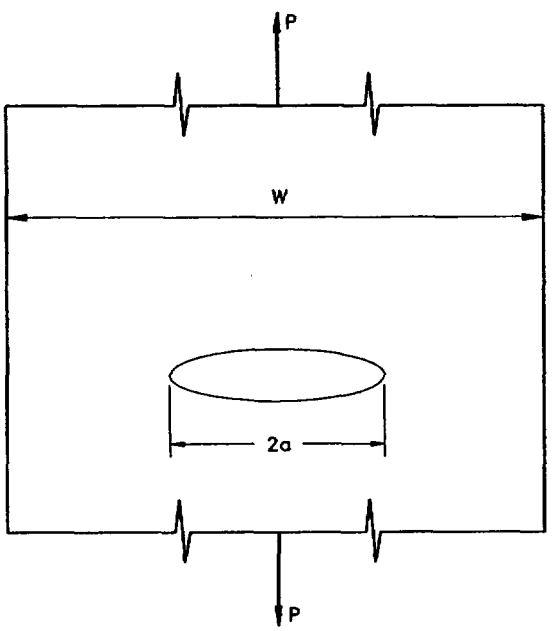

M = Applied moment
P = Resultant tensile force
R = Average radius of fuel tube
t = Thickness of fuel tube
I = Moment of inertia of fuel tube
2a = Crack width

$W = \pi R$

$P = \frac{2MR^2t}{I}$

Table 3.9.8-9

Tire Stiffness Calculation

The on-site transfer trailer has four axles with eight 235/75R 17.5 SLR 184 tires per axle (total of 32 tires). The tire stiffness is estimated based on tire measurements as follows:

For 235 (tire width in mm)/75 (height-to-width ratio in %) R 17.5 (rim diameter in inches) SLR184:
Tire width 235mm/25.4mm/in =9.25 inch

Height of tire = 75% of 9.25= 6.94 inch

Tire diameter = 17.5+2*6.94= 31.4 inch.

From trailer tire measurements:

	a (height) - in	b (width) - in	c (ground top) - in
A (front right tire)	6.5	7.4	30.0
B (front left tire)	7.3	7.4	30.8
C (rear right tire)	4.8	7.3	31.3
D (rear left tire)	4.0	7.2	31.4

Tire pressure: 140-145 psi

Trailer weight: 39,700 lbs.

Skid weight: 26,500 lbs

RAM weight: 6,400 lbs.

Average c dimension at front= (30+30.8)/2=30.4 inches

Average c dimension at rear = (31.3+31.4)/2=31.4 inches

Tire height: 33 inches, at approximately 145 psi pressure

Weight per tire (excluding RAM weight): 66,200/32=2070 lbs/tire

Weight per tire (assuming RAM weight is distributed on 8 tires): 6400/8= 1600 lb/tire

Front 8 tires: 2070+1600=3670 lbs/tire.

Table 3.9.8-9 (continued)

Tire Stiffness Calculation

All other tires: 2070 lbs/tire

Stiffness is determined as:

K_{front} = 3670/(33-30.4)=1411 lbs/in

$K_{all\ others}$ = 2070/(33-31.4)=1294 lbs/in

Use K/tire =1500 lbs/inch.

Total stiffness = 32x 1500= 4.8E 4 lbs/in

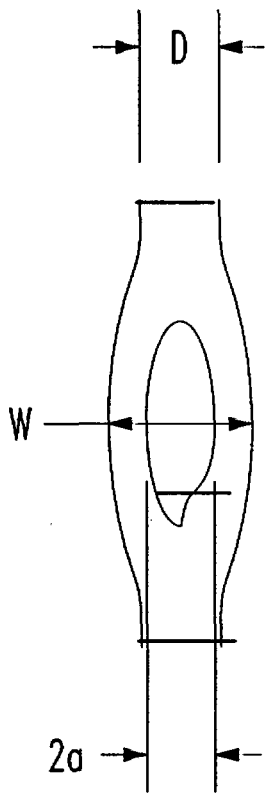

Figure 3.9.8-1

Fracture Geometry #1 - Ruptured Section

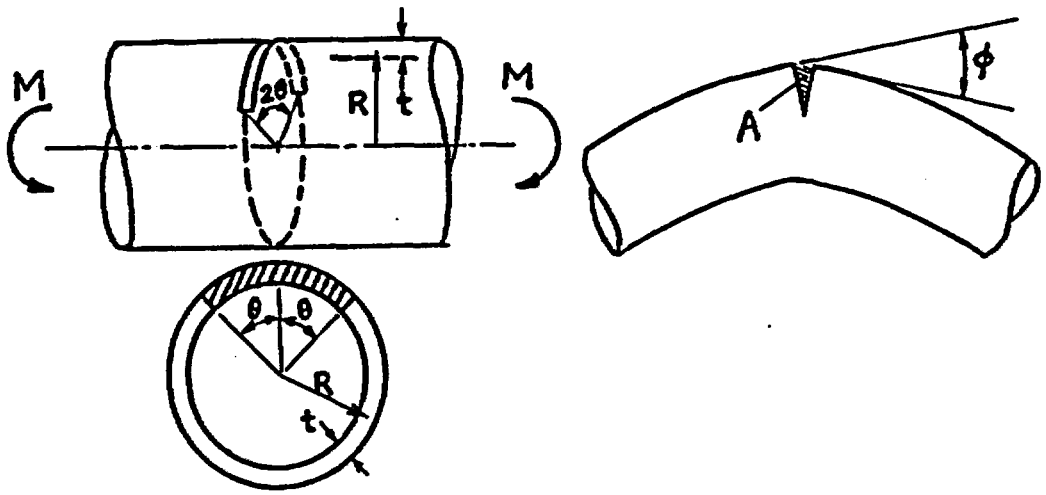

$$\underline{R/t \simeq 10} \qquad (\theta < 110^\circ)$$

$$\sigma = M/(\pi R^2 t)$$

$$K_I = \sigma\sqrt{\pi(R\theta)} \cdot F(\theta)$$

$$F(\theta) = 1 + 6.8\left(\frac{\theta}{\pi}\right)^{3/2} - 13.6\left(\frac{\theta}{\pi}\right)^{5/2} + 20.0\left(\frac{\theta}{\pi}\right)^{7/2}$$

Figure 3.9.8-2

Fracture Geometry #2: Through-Wall Circumferential Crack in Cylinder under Bending

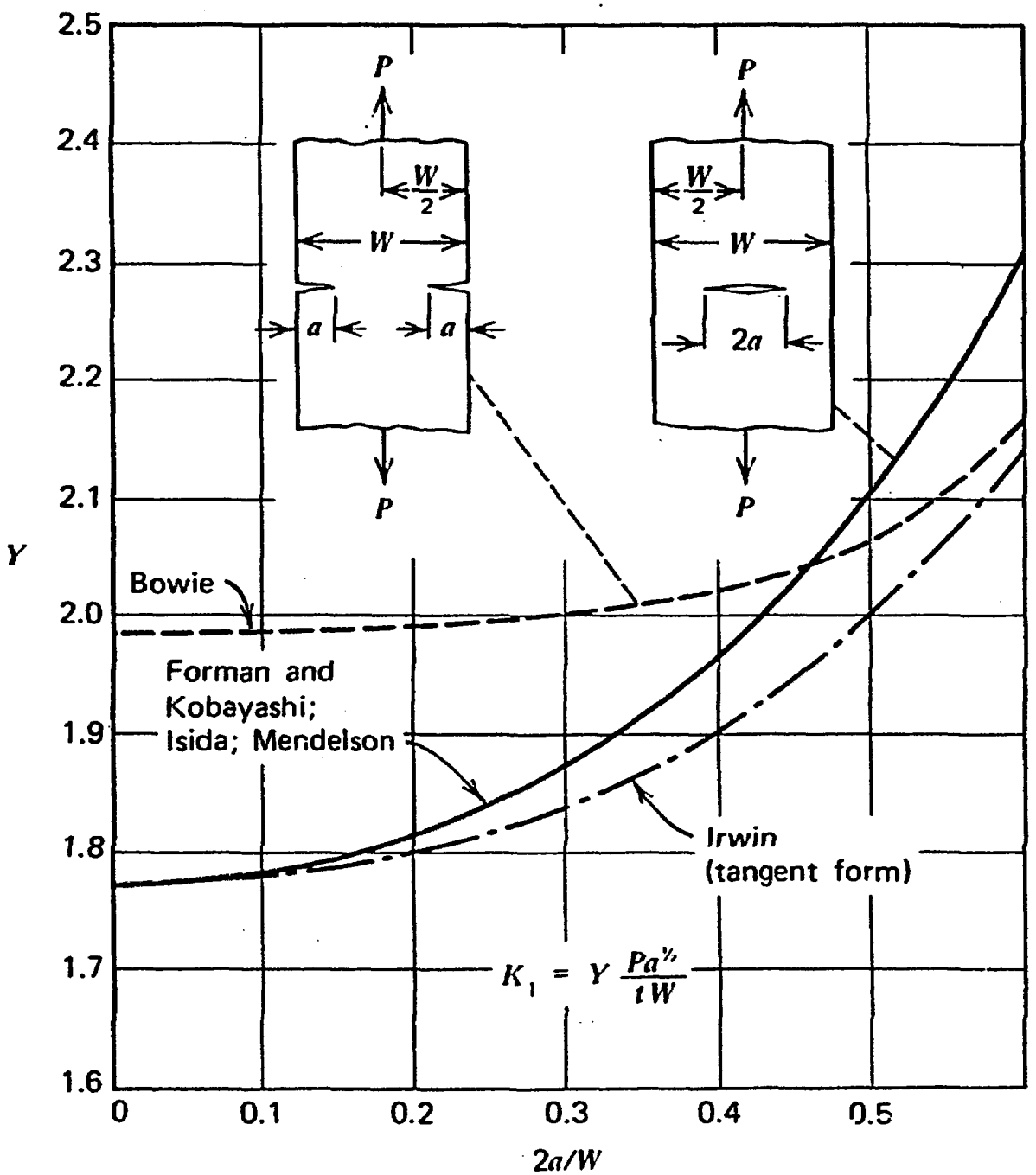

Figure 3.9.8-3

Stress Intensity Factor Solutions: For Several Specimen Configurations

APPENDIX 3.9.9
HSM-H STRUCTURAL ANALYSIS

TABLE OF CONTENTS

3.9.9 HSM-H STRUCTURAL ANALYSIS 3.9.9-1

3.9.9.1 Introduction 3.9.9-1

3.9.9.2 General Description of the HSM-H 3.9.9-1

3.9.9.3 Material Properties 3.9.9-3

3.9.9.4 Component Weights 3.9.9-4

3.9.9.5 Design Criteria 3.9.9-5

3.9.9.6 Load Cases 3.9.9-8

3.9.9.7 Finite Element Models 3.9.9-13

3.9.9.8 Normal Operation Structural Analysis 3.9.9-16

3.9.9.9 Off-Normal Operation Structural Analysis 3.9.9-18

3.9.9.10 Accident Condition Structural Analysis 3.9.9-20

3.9.9.11 Load Combinations 3.9.9-27

3.9.9.12 Conclusions 3.9.9-28

3.9.9.13 References 3.9.9-29

LIST OF TABLES

3.9.9-1 Summary of HSM-H Component Design Loadings

3.9.9-2 Summary of 32PTH DSC Support Structure Design Loadings

3.9.9-3 HSM-H Concrete Load Combinations

3.9.9-4 Ultimate Capacities of Concrete Components

3.9.9-5 Structural Design Criteria for DSC Support structure

3.9.9-6 HSM-H Support Steel Structure Load Combinations

3.9.9-7 Design Pressure for Tornado Wind Loading

3.9.9-8 Maximum HSM-H Concrete Component Forces and Moment for Normal & Off-Normal Loads

3.9.9-9 Summary of Thermal Forces and Moments in the HSM-H Concrete Components

3.9.9-10 Maximum HSM-H Concrete Component Forces and Moments for Accident Loads

3.9.9-11 Comparison of Highest Combined Shear Forces/Moments with the Capacities

3.9.9-12 Maximum/Minimum Forces/Moments in the Rail Components in the Local System

3.9.9-13 Maximum/Minimum Forces/Moments in the Rail Extension Plates in the Local System

3.9.9-14 Maximum/minimum Axial Forces in the Cross member Components

3.9.9-15 Rail component Results

3.9.9-16 Extension Plates and Cross Members Results

LIST OF FIGURES

3.9.9-1 Analytical Model of W12x96 Beam with Slotted, Nitronic and Stiffener Plates

3.9.9-2 Analytical Model of the HSM-H for Mechanical Load Analysis

3.9.9-3 Analytical Model of the 32PTH DSC Support Structure

3.9.9-4 Analytical Model of the HSM-H for Thermal Load Analysis

3.9.9-5 Symbolic Notations of Force and Moment Capacities

3.9.9-6 Components of Support Structure

3.9.9 HSM-H STRUCTURAL ANALYSIS

3.9.9.1 Introduction

The purpose of this appendix is to present the structural evaluation of the HSM-H due to all applied loads during storage loading operations.

The design of the HSM-H for 32PTH DSC is the same as the HSM-H which is under NRC review as Amendment 8 to CoC 1004 for 24PTH DSC. Analyses performed for HSM-H with 24PTH DSC used bounding values to envelop both 24PTH DSC and 32PTH DSC.

The HSM-H module design for 32PTH canister is identical to the HSM-H design for 24PTH canister except the following modifications:

1. The module for the 32PTH canister is designed such that the center line of the loaded 32PTH canister is approximately four inches higher compared to that of the 24PTH canister.

2. The diameter of the door openings in the front and rear of the front wall are approximately four inch and two inch larger for the 32PTH canister compared to those of the 24PTH canister.

3. The transfer cask docking surface in the module for the 32PTH canister transfer cask is approximately half inch wider compared to the cask docking surface for the 24PTH canister transfer cask.

4. The diameters of the front inner circular steel plate and rear circular concrete block of the shielded door for the 32PTH canister are approximately four inch and two inch larger compared to those of the 24PTH canisters.

5. For the 32PTH design the spacers at the canister stop plate of the module will be provided similar to the 24PTH short cavity design.

Analyses performed for HSM-H with 24PTH DSC used bounding values to envelop both 24PTH DSC and 32PTH DSC. The structural evaluation provided in this appendix is identical as the information provided in Amendment 8 to CoC 1004 for 24PTH DSC. Amendment 8 reference sections are indicated in this appendix for cross reference.

3.9.9.2 General Description of the HSM-H

The HSM-H is a free standing reinforced concrete structure designed to provide environmental protection and radiological shielding for the 32PTH DSC. Each HSM-H provides a self contained modular structure for the storage of a 32PTH DSC containing up to 32 PWR spent fuel

assemblies. The HSM-H provides heat rejection from the spent fuel decay heat by a combination of radiation, conduction and convection. Schematic sketch of the HSM-H showing the different components is provided in Chapter 1, Figure 1-1. The drawings in Chapter 1, Section 1.5 provide the principal dimensions and design parameters of the HSM-H.

The HSM-H is a reinforced concrete structure comprised of a base unit, where the 32 PTH DSC is stored and a roof unit that serves to provide environmental protection and radiation shielding. These two units are assembled together to form a single module.

The HSM-H modules may be prefabricated off-site, then transported to the ISFSI site and installed on a reinforced concrete basemat. The HSM-H is placed next to, and in contact with, adjacent module(s) to form a continuous single or double row arrays.

The 32PTC is supported inside the HSM-H by the DSC support structure. The DSC support structure (rail support assembly) is comprised of two rail sections, two slotted places and two rail support plates. The rail support assembly provides support for the DSC during storage and act as a sliding surface during DSC insertion and retrieval.

The air inlet vents are extending through the front on both sides of the front wall. The front wall and the rear wall of the base unit provide support for the rails and the rail extension flanges. The roof unit rests on the front, rear and side walls of the base unit. The air outlet vents are provided in the roof unit.

The HSM-H shield door consists of a rectangular circular steel plate at the front attached to a circular thick steel plate. The circular steel plate is attached to a thick circular reinforced concrete block at the rear. Both the circular steel and concrete blocks fit the circular opening in the front wall.

The concrete door provides missile protection and shielding. End shield walls are provided at the ends of a module array to provide the required missile and shielding protection. Similarly, an additional shield wall is used at the rear of the module for single module rows.

The side heat shields of the HSM-H consist of three panels. Each panel consists of optional anodized aluminum fins mounted on the stainless steel base plates. The base plates are provided with aluminum backing plates on the surface facing the concrete. The top louvered heat shield under the roof consists of seven panels. Each panel has two stainless steel mounting bars. Horizontal louvers are mounted on these bars. The heat shields provide thermal protection for the HSM-H concrete.

During DSC insertion/retrieval operations, the transfer cask is docked with the HSM-H docking surface and mechanically secured to the embedment provided in the front wall. The embedments are equally spaced on either side of the HSM-H access opening.

The drawings in Chapter 1, Section 1.5 provide the principal dimensions and design parameters of the HSM-H. The dimension differences between the HSM-H to be used for storing the 32PTH canister and 24PTH canister are listed in the following tables.

TN drawing No. 10494-72-104

HSM-H		
Dimension	System Type	
	For 32PTH Canister	For 24PTH Canister [13]
A	8' – 10"	8' – 6"
B	ø 5' – 11 5/8"	ø 5' – 9"
C	ø 7' – 5"	ø 7' – 1 1/2"

TN drawing No. 10494-72-107

HSM-H		
Dimension	System Type	
	For 32PTH Canister	For 24PTH Canister [13]
A	34.88"	33.60"

TN drawing No. 10494-72-108

HSM-H		
Dimension	System Type	
	For 32PTH Canister	For 24PTH Canister [13]
A	8' – 1 1/2"	7' – 10"
B	ø 7' – 3"	ø 6' – 11 1/2"
C	ø 5' – 8 5/8"	ø 5' – 6"
D	ø 7' – 7 1/4"	ø 7' – 3 3/4"
E	ø 1' – 10 1/2"	ø 1' – 10 1/2"

3.9.9.3 Material Properties

The temperature dependent material properties for concrete and reinforcing steel are provided in Chapter 3, Tables 3-6, 3-7 and 3-7A. The material properties of the Type 304 Stainless Steel rails are identical to the ASME Code properties listed in Chapter 3, Table 3-5.

3.9.9.4 Component Weights

The following table summarizes the weight of the loaded HSM-H.

Component Description	CALCULATED WEIGHT (kips)
32PTH DSC Empty Weight	58.04
32 PWR Spent Fuel Assemblies	50.72
Total Loaded DSC Weight (Dry)	**108.76**
HSM-H Single Module Weight (Empty)	306.1
HSM-H Single Module Weight (Loaded)	**414.86**

3.9.9.5 Design Criteria

Codes and Standards

The reinforced concrete HSM-H, including the 32PTH-DSC support structures, are important to safety NUHOMS® HD system components. Consequently, they are designed and analyzed to perform their intended functions under the extreme environmental and natural phenomena specified in 10CFR 72.122 [1] and ANSI 57.9 [2]. These include tornado, wind, seismic, and flood design criteria.

The following table summarizes Codes and Standards for design and fabrication of these components.

Component	Code of Construction
HSM-H and 32PTH DSC Support Structures	- ACI 349-97 (Concrete) - AISC Ninth Edition (Structural Steel) - AWS D1.1-98 (Structural Welds) - ASCE 7-95 (Loads) - ANSI 57.9-84 (Loads & Load Combinations)

Loadings

The loadings are listed in Tables 3.9.9-1 & 3.9.9-2 and discussed in details in Section 3.9.9.6.

Loading Criteria

The ultimate strength method of ACI 349 [3] is used for the design of the HSM-H reinforced concrete structural components. Required reinforcement is provided to meet the minimum flexural and shear reinforcement requirements of ACI 349 and to ensure that the provided design strength exceeds that required for the factored design loads specified in Table 3.9.9-3.

The following relationships from the ACI code are used to compute capacities of the concrete components:

Ultimate Moment Capacity (M_u)

$$M_u = \phi M_n = \phi A_s f_y (d-a/2)$$

where $a = (A_s f_y)/(0.85 f_c' b)$

Ultimate Tension Capacity (P_{tu})

$P_{tu} = \phi A_{st} f_y$

$\phi = 0.9$

$A_{st} = 2A_s$ (The reinforcement in two opposite faces are assumed to be same)

Ultimate Compression Capacity (P_{cu})

$P_{cu} = \phi P_n = 0.8\phi[0.85 f_c' (A_g - A_{st}) + f_y A_{st}]$

$A_{st} = 2A_s, \quad \phi = 0.7$

Ultimate In-Plane Shear Capacity (V_{ui})

$V_{ui} = \phi A_g (2\sqrt{f_c'} + \rho_n f_y)$

$\phi = 0.85, \rho_n = (2A_s/bT)$

Ultimate Out-Plane Shear Capacity (V_{uo})

$V_{uo} = \phi 2 \sqrt{f_c'} (bd)$

$\phi = 0.85$

where:

ϕ = Strength reduction factor

A_s = Area of reinforcing steel in tension

A_{st} = Total area of the reinforcing steel

A_g = Gross area of concrete section

fy = Yield strength of reinforcing steel

f_c' = Compressive strength of concrete

d = Distance of the top fiber of concrete from the center of the rebar

b = Width of the section = 12"

T = Depth of the section

The computed shear and moment capacities for all the concrete components of the HSM-H, calculated based on the preceding equations from ACI 349 [3] are provided in Table 3.9.9-4.

The capacities calculated in Table 3.9.9-4 for the accident condition consider a 10% reduction in compressive strength of the concrete and yield strength of the reinforcing rebar materials due to concrete temperatures exceeding 350°F.

The required steel strength, S, and required shear strength, S_v for critical sections of steel structure are calculated in accordance with the requirements of AISC Allowable Stress Design (ASD) method [4].

In addition to deadweight and normal and off normal handling loads, the steel support structure components are subjected to the normal operating thermal loads (TN), off-normal operating thermal loads (TO) and accident thermal loads (TA), which cause additional stresses. However, the steel support structure is protected from design wind load (WW), Tornado wind and missile impact loads (WT) and Flood loads (FL) by the concrete components of the HSM-H. Therefore, these loads do not cause stresses in the steel support structure.

The corresponding structural design criteria for the DSC support structure are summarized in Table 3.9.9-5 and 3.9.9-6.

3.9.9.6 Load Cases

3.9.9.6.1 HSM-H Normal Loads (*Section P.2.2.5.2.1 from CoC 1004 Amendment #8)*

(A) Dead Loads (DW)

Dead load includes the weight of the HSM-H concrete structure and the steel structure (the DSC weight is considered as a live load rather than a dead load).

The dead load is varied by +5% from the estimated value to simulate the most adverse loading condition in accordance with ANSI-57.9 [2].

(B) Live Loads (LL)

Live loads include the roof design basis snow and ice load of 110 psf conservatively derived from ASCE 7-95 [5]. A total live load of 200 psf (which includes snow and ice load) is used to envelope all postulated live loading, including such items as ladders, handrails, conduits, etc. added for personnel protection. In addition, the normal handling loads (RO), and off-normal handling loads (RA), and the DSC weight are treated as live loads for the concrete component evaluation.

In accordance with ANSI-57.9 [2], the live load is varied between 0% and 100% of the estimated load to simulate the most adverse conditions for the structure.

(C) Normal Operating Thermal Loads (TN)

The normal thermal loads on HSM-H include the effects of design basis internal heat load (40.8 kW maximum heat load) generated by the canister plus the effects of normal ambient conditions (0°F and 100°F).

(D) Normal Handling Loads (RO)

The most significant normal operational loading condition for the HSM-H components is the sliding of the DSC from the TC into the HSM-H. Friction forces are developed between the sliding surfaces of the DSC, the TC and the HSM-H support rails. Normal operation assumes the canister is sliding over the support structure due to a hydraulic ram force of up to 80,000 lbs (insertion) and 60,000 lbs (extraction) applied to the DSC base. It is assumed that the 80 or 60 kips load is resisted by an axial load (40 or 30 kips) in each support rail and front embedments. In addition the DSC weight is applied as a distributed load on both the rails. The normal handling loads are considered as live loads for the design of the concrete components.

(E) Design Basis Wind Load (WW)

Conservatively, this load case is assumed to be enveloped by tornado generated wind load (WT) described in Section 3.9.9.6.3.

3.9.9.6.2 HSM-H Off-Normal Loads (*Section P.2.2.5.2.2 from CoC 1004 Amendment #8)*

(A) Off-Normal Operating Thermal Loads (TO)

This load case is the same as the normal thermal load but with an ambient temperature range from -40°F to 117°F. The temperature distribution for the extreme ambient conditions is used in the analysis for the concrete and steel component evaluation.

(B) Off-Normal Handling Loads (RA)

This load case assumes that the TC is not accurately aligned with respect to the HSM-H resulting in binding of the DSC during a transfer operation causing the hydraulic pressure in the ram to increase. The ram force is limited to a maximum load of 80 kips during insertion and 80 kips during retrieval. Therefore, for the steel support structure, the off-normal jammed canister load (RA) is defined as an axial load on one rail of 80 kips during insertion and 80 kips during retrieval, plus a vertical load of one half the DSC weight (on both rails) at the most critical location. The off-normal operating handling loads are considered as live loads for the design of the concrete components.

3.9.9.6.3 HSM-H Accident Loads (*Section P.2.2.5.2.3 from CoC 1004 Amendment #8)*

(A) Accident Thermal Loads (TA)

The postulated accident thermal event occurs due to blockage of either the air inlet or outlet vents under off-normal ambient temperatures range from –40°F to 117°F.

(B) Tornado Wind and Tornado Missiles (WT, WM)

The design basis tornado (DBT) wind intensities used for the HSM-H design are obtained from NRC Regulatory Guide 1.76 [6]. Region I intensities are utilized since they result in the most severe loading parameters. For this region, the maximum wind speed is 360 mph, the rotational speed is 290 mph and the maximum translational speed is 70 mph. The radius of the maximum rotational speed is 150 ft, the pressure drop across the tornado is 3 psi and the rate of pressure drop is 2 psi per second [6].

Determination of Forces on Structure

Tornado loads are generated for three separate loading phenomena:

- Pressure or suction forces created by drag as air impinges and flows past the HSM-H. These pressure or suction forces are due to tornado generated wind with maximum wind speed of 360 mph.
- Pressure or suction forces created by tornado generated pressure drop or differential pressure load of 3 psi.
- Impact, penetration and spalling forces created by tornado-generated missiles impacting on the HSM-H.

The DBT velocity pressure is computed based on the following equation specified in ASCE 7-95 [5].

$$q_v = 0.00256\ K_z * K_{zt} * I * V^2 \text{ lb/sq ft}$$

Where:

K_z = velocity pressure exposure coefficient equal to 0.9 applied to the full HSM-H height of 18.5 ft for level C exposure (Table 6-3 of [5]).

K_{zt} = 1.0 for level C exposure and structures with height less than 30 ft. (Section 6.5.5 of [5]).

I = Importance Factor equal to 1.15 (Table 6-2 of [5]).
Since the generic design basis HSM-H dimensions are relatively small compared to 150 ft rotational radius of the DBT, the velocity value of combined rotational and translational wind velocity of 360 mph is conservatively used in the above equation to compute the DBT velocity pressure of 344 psf.

The design pressures for the tornado wind load are shown in Table 3.9.9-7.

Tornado Missiles

The determination of impact forces created by DBT generated missiles for the HSM-H is based on the criteria provided by NUREG-0800, Section 3.5.1.4, III.4 [7]. Accordingly, eight types of missiles are postulated:

1. The utility wooden pole, 13.5" diameter, 35' long missile weighing 1500 lbs at a horizontal velocity of 294 fps.
2. The armor piercing artillery shell 8" diameter, weighing 276 lbs at a horizontal velocity of 185 fps.
3. The steel pipe missile 12" diameter, Schedule 40, 30' long weighing 1500 lbs at a horizontal velocity of 205 fps.
4. The massive automobile missile weighing 4000 lbs at a horizontal velocity of 195 fps traveling through the air not more than 25 ft above the ground and having contact area of 20 square ft.
5. Wood plank missiles traveling end on, 200 lbs, traveling at 440 fps.
6. Steel Pipe 3" diameter, Sch 40, weighing 115 lbs, traveling at 268 fps.
7. Steel Pipe 6" diameter, Sch 40, 285 lbs, traveling at 230 fps.
8. Steel rod, 1" diameter, 3' long weighing 8 lbs traveling at 317 fps.

For the overall effects of a DBT missile impact, overturning and sliding of the HSM-H, the force due to the deformable massive missile impact is applied to the structure at the most adverse location. Conservation of momentum is assumed to demonstrate that sliding and/or tipping of the module will not result in an unacceptable condition for the module. The coefficient of restitution is assumed to be zero and the missile energy is transferred to the module to be dissipated as sliding friction, or an increase in potential energy due to raising the center of gravity. The force is evenly distributed over the impact area. The magnitude of the impact force for design of the local reinforcing is calculated in accordance with Bechtel Topical Report "Design of Structures for Missile Impact" [8].

For the local damage analysis of the HSM-H for DBT missiles, three governing missiles are used for the evaluation of concrete penetration, spalling, scabbing and perforation thickness. The modified National Defense Research Committee (NDRC) empirical formula is used for this evaluation as recommended in NUREG-0800, Section 3.5.3 [7]. The results of these evaluations are reported in Chapter 11.

(C) Flood Load (FL) *(Section P.2.2.2 from CoC 1004 Amendment #8)*

Flooding of the NUHOMS® ISFSI greater than 0.46 m (1'-6") above grade results in blockage of the HSM inlet vents. Flooding of the NUHOMS® ISFSI greater than 1.7 m (5'-8") above grade results in wetting of the DSC. Greater flood heights result in submersion of the DSC and blockage of the HSM outlet vents.

The DSC and HSM are conservatively designed for an enveloping design basis flood, postulated to result from natural phenomena such as a tsunami, and seiches, as specified by 10CFR72.122(b). For the purpose of this bounding generic evaluation, a 15 m (50 foot) flood height and water velocity of 4.6 m/sec (15 fps) is used. The HSM-H is evaluated for the effects of a water current of 4.6 m/sec (15 fps) impinging upon the side of a submerged HSM-H. The DSC is subjected to an external pressure equivalent to a 15 m (50 foot) head of water.

The calculated effects of the enveloping design basis flood are included in the load combinations and reported stresses presented in Section 3.9.9.10.3. The plant specific design basis flood (if the possibility for flooding exists at a particular ISFSI site) should be evaluated by the licensee and shown to be enveloped by the flooding conditions used for this generic evaluation of the NUHOMS® DSC and HSM-H.

(D) Seismic Load (EQ) *(Section P.2.2.3 from CoC 1004 Amendment #8)*

The design basis response spectra of NRC Regulatory Guide 1.60 [9] are selected as the design earthquake for qualifying different component of HSM-H. A damping value of seven percent of damping is used for the concrete structure [12]. The response spectra are anchored to a maximum ground acceleration of 0.3g for the horizontal component and 0.2g for the vertical component. The results of the frequency analysis of the HSM-H structure (which includes a simplified model of the DSC) yield a lowest frequency of 23.2 Hz in the transverse direction and 28.4 Hz in the longitudinal direction. The lowest vertical frequency exceeds 33 Hz. Thus, based on the R.G. 1.60 response spectra amplifications, the corresponding seismic accelerations used for the design of the HSM-H are 0.37g and 0.33g in the transverse and longitudinal directions respectively and 0.20g in the vertical direction. The corresponding accelerations applicable to the DSC are 0.41g and 0.36g in the transverse and longitudinal directions, respectively, and 0.20g in the vertical direction. The seismic analysis of the HSM-H is further discussed in Section 3.9.9.10.

3.9.9.6.4 Combined Load Criteria *(Section P.2.2.5 from CoC 1004 Amendment #8)*

A summary of the design loads for the HSM-H System is provided in Tables 3.9.9-1 and 3.9.9-2. These tables also present the applicable codes and standards for development of these loads. Table 3.9.9-3 and 3.9.9-6 summary the load combination requirements of the HSM-H module design. These tables comply with the requirements of 10CFR72.122, and ANSI 57.9.

3.9.9.7 Finite Element Model

3.9.9.7.1 ANSYS Finite Element Model of the Rail Assembly

Description of the Rail Assembly

The HSM-H support structure consists of two rail assemblies, each at 30 degrees from the vertical center line of the DSC. Four cross members connect the two rail assemblies (at the time they are shop fabricated) by four gusset plates welded to the rail web and the flanges. However, after the rail assemblies are installed at the ISFSI site, and before the DSC is loaded, the two outer most end cross members are removed. The steel support structure supports the DSC stored inside the module. Each rail assembly of the DSC support structure consists of the following components:

1. W 12x96 Rail Section 187" long made up off ASTM A992 material and with twelve (12) 6" diameter holes for airflow cooling of the DSC. The depth of the section is 12.71", thickness of the web is 0.55", width of the flange is 12.16" and thickness of the flange is 0.9" (Ref. 4).

2. A 1" thick slotted plate made up of A572 Grade 50 material with slots at angle of 30 degree to normal to the plate axis. The slot thickness range from 0.5" inside to 0.75" outside.

3. A 3/16" thick support plate made up of nitronic 60 (RC 29-35) material which provide a smooth support for the DSC to slide.

4. A rail extension flange which consists of 1" thick flange plate (A572, Grade 50 material), and 3/16" thick rail support extension plate (nitronic 60 material).

The rail extension flange is attached to a 1-1/4" thick embeded base plate (A36 material)by four bolts.

Finite Element Model of the Rail Assembly

A three dimensional finite element model of the rail section, slotted plate, rail support plate and rail extension flange was developed for the computer program ANSYS [10]. The rail flanges, slotted plate, rail support plate and extension flanges were modeled using SOLID 73 element. Each element has 8 nodes with six degrees of freedom (three translational and three rotational) per node. The web of the W section and the stiffeners were modeled using Shell 63 element. In order to establish compatability of the degrees of freedom between solid and plate elements, the ANSYS option for actvating realistic in-plane rotational stiffeness (Allman rotational stiffeness, KEYOPT(3)=2) is used for the plate elements. The model is inclined by 30 degrees from the vertical. A plot of the partial model (front end) is shown in Figure 3.9.9-1.

The model is completely restrained at the bottom end of the extension flange and supported vertically and transversely approximately 6" from the end to simulate the weld between the

extension flange and the base plate. The model also is supported in the vertical and transverse directions at approximately 12" on either side of the W section at the bottom flange (to simulate the simple support condition of the concrete pedestalls at the front and rear walls).

Finite element analysis of the above rail assembly model was performed to compute the maximum displacements of the model, subjected to unit load normal to rail axis in and out of plane of the curb and in the axial direction. The equivalent beam element properties such as area (A), moment of inertia about the major axis (I_{x-x}) and moment of inertia about the minor axis (I_{y-y}) are determined by equating the maximum deflection of the beam to displacement obtained from the finite element model.

3.9.9.7.2 ANSYS Finite Element Model of the HSM-H Combined Concrete and Steel Structure for Structural Analysis

The structural analysis of an individual module provides a conservative estimate of the response of the HSM-H structural elements under various static and dynamic loads for any HSM-H array configuration. Therefore, analytical models of a single free standing HSM-H is developed in this section for the computer program ANSYS [10]. The frame and shear wall action of the HSM-H concrete components are considered to be the primary structural system resisting the loads. The analytical models are evaluated for normal operating, off-normal and postulated accident loads acting on the HSM-H.

A three dimensional finite element model of the HSM-H which includes all the concrete components (rear wall, front wall, two side walls and the roof) was developed for the computer program ANSYS [10]. The eight node brick element type SOLID 73 element was used to model the concrete structure. Four layers of brick elements were used to model the concrete components. Each node of the eight node brick element has six degrees of freedom. The DSC was modeled using the beam elements (ANSYS element type BEAM4). The rails and the lateral bracing between the rails (Cross beams) were also modeled using beam elements with appropriate stiffness The mass of the DSC was lumped at the nodes representing the DSC using lumped mass elements (ANSYS element type MASS21). Plots of the model which includes the concrete structure and the support structure are shown in Figures 3.9.9-2. A plot of the support structure model (which includes the DSC, rails and the cross beams) is shown in Figure 3.9.9-3.

The material properties used in the DSC support structure model are provided in Chapter 3. The DSC support structure model is attached to the concrete at several locations (four locations at the rear shelf, four locations in the front shelf and two locations on the front wall opening. Each node of the support structure has three translational and three rotational degree of freedoms. The rails are supported such that they are completely restrained at the front extension plate locations and free to rotate in all three directions and free to translate only in axial direction at the other supports in the rear and the front shelf locations.

The DSC support structure analytical model is incorporated into the HSM-H analytical model. The various normal, off-normal and accident loads are applied to the analytical model and

internal forces and moments were computed in different members by performing a linear elastic finite element analysis.

The node coupling option of ANSYS was used to represent the appropriate connection between the different concrete components of the HSM-H model. The connections of the support structure to the concrete structure were modeled also using the node coupling option.

For the analysis performed in this calculation, due to applied loading, the model is assumed neither to uplift from the basemat (because of its dead weight) nor to slide on the basemat (because of friction). Therefore, the model is restrained vertically at all nodes on the bottom of the model, and also restrained laterally and axially at all nodes on the bottom of the model to prevent rigid body movement.

3.9.9.7.3 ANSYS Finite Element Model of the HSM-H for Thermal Stress Analysis

The thermal stress analysis of the HSM-H was performed using the three dimensional finite element model (developed for ANSYS) which includes the concrete and support steel components. The eight node brick elements of type SOLID73 were used to model the concrete structure. Four layers of brick elements were used to model the concrete components. Each node of the brick element has three translational and three rotational degrees of freedom. The connections between the HSM-H concrete structure and the door are designed such that free thermal growth is permitted in the door, when the HSM-H is subjected to thermal loads. Because of the free thermal growth, the door does not induce stresses in the concrete components of the HSM-H. Therefore, the analytical model of the HSM-H for thermal stress analysis of the concrete components does not include the door. The ANSYS model used to perform thermal stress analysis of the concrete and support steel components is shown in Figures 3.9.9-4. Conservatively, the roof and the base unit are coupled in this model. However, the DSC beam model is uncoupled from the support steel beam model.

The model base is restrained at one set of end nodes (in axial and lateral directions) and friction forces are applied in the axial and lateral directions at the opposite set of end nodes. For the thermal load analysis all the nodes at the base are restrained in the vertical direction.

3.9.9.8 Normal Operation Structural Evaluation

The evaluation of the HSM-H for 32PTH DSC is the same as the HSM-H which is under NRC review as Amendment 8 to CoC 1004 for 24PTH DSC [13]. Analyses performed for HSM-H with 24PTH DSC used bounding values to envelop both 24PTH DSC and 32PTH DSC. Following table shows how the bounding loads are used for structural evaluation of the HSM-H.

	Weight	Thermal
24PTH DSC (loaded weight)	93.7 kips	40.8 kw
32PTH DSC (loaded weight)	108.76 kips	34.8 kw
Weight used for HSM-H structural evaluation to envelop both 24PTH & 32PTH	110.0 kips (max.) (1) 72.0 kips (min.) (2)	
Thermal load used for HSM-H structural evaluation to envelop both 24PTH & 32PTH		40.8 kw

Notes:
1. Maximum weight is used for structural evaluation of the HSM-H.
2. Minimum weight is used for stability evaluation of the HSM-H.

The following table shows the normal operating loads for which the HSM-H components are designed. The table also lists the individual NUHOMS® HSM-H components which are affected by each loading.

Load Type	Affected Component	
	DSC Support Structure	HSM-H
Dead Weight	X	X
Normal Thermal	X	X
Normal Handling	X	X
Live Loads		X

The reinforced concrete and the support steel structure of the HSM-H are analyzed for the normal, off-normal, and postulated accident conditions using finite element models described in Section 3.9.9.7. These models are used to evaluate concrete and support structure forces and moments due to dead load, live load, normal thermal loads, and normal handling loads. The methodology used to evaluate the effects of these normal loads is addressed in the following paragraphs.

(A) HSM-H Dead Load (DW) Analysis (Section P.3.6.1.4(A) from CoC 1004 Amendment #8)

Dead loads are applied to the analytical model by application of 1.05g where g is the gravitational acceleration in the vertical direction (386.4 in/sec^2). The 5% variation in the dead

load is in accordance with ANSI/ANS 57.9. The results of the HSM-H concrete components dead load analysis are presented in Table 3.9.9-8.

(B) HSM-H Live load (LL) Analysis *(Section P.3.6.1.4(B) from CoC 1004 Amendment #8)*

Live load analysis is performed by applying 200 psf pressure on the roof and the DSC weight as a distributed load on the support structure. The normal handling load of 80 kips during DSC insertion and 60 kips during DSC retrieval is included as a live load for the concrete component evaluation. The results of the HSM-H concrete components live load analysis are presented in Table 3.9.9-8.

(C) HSM-H Normal Operating Thermal (TN) Stress Analysis *(Section P.3.6.1.4(C) from CoC 1004 Amendment #8)*

Normal operating thermal stress analysis of the concrete and steel support structure is performed for the enveloping thermal load case which is 40.8 kW heat load with ambient temperature of 100°F. An additional thermal load case with -40°F ambient and 40.8 kW heat load is also considered as a bounding case for the end module in an array of HSM-H. The results of the HSM-H concrete components thermal load analysis are presented in Table 3.9.9-9.

(D) HSM-H Operational Handling Load (RO) Analysis (Section P.3.6.1.4(D) from CoC 1004 Amendment #8)

The operation handling loads of 80 kips during DSC insertion and 60 kips during DSC retrieval are applied to the rail support structure in the axial direction. In addition, the DSC weight is applied as a distributed load on both rails of the HSM-H.

The normal operating handling loads are considered as live loads for the design of the concrete components. The results of the HSM-H concrete components operational handling load analysis are presented in Table 3.9.9-8.

(E) HSM-H Design Basis Wind Load (WW) Analysis (Section P.3.6.1.4(E) from CoC 1004 Amendment #8)

The DSC support structure and DSC inside the HSM-H are not affected by wind load. The concrete structure forces and moments due to design basis wind load are bounded by the result of tornado generated wind load discussed in Section 3.9.9.10. Therefore, no separate analysis is performed for this case.

The results of the HSM-H concrete components design basis wind load analysis are presented in Table 3.9.9-8.

3.9.9.9 OFF-Normal Operation Structural Analysis

This section describes the design basis off-normal events for the HSM-H modules and presents analyses which demonstrate the adequacy of the design safety features of the HSM-H modules.

The following table shows the off-normal operating loads for which the HSM-H components are designed.

Load Type	Affected Component	
	DSC Support Structure	HSM-H
Off-Normal Thermal	X	X
Off-Normal Handling	X	X

For an operating NUHOMS® HD system, off-normal events could occur during fuel loading, transfer cask handling, trailer towing, canister transfer and other operational events. Two off-normal events are defined which bound the range of off-normal conditions. The limiting off-normal events are defined as a jammed DSC during loading or unloading from the HSM-H and the extreme ambient temperatures of -40°F (winter) and +117°F (summer). These events envelope the range of expected off-normal structural loads and temperatures acting on the HSM-H. ANSYS finite element models described in Section 3.9.9.7 are used to evaluate concrete and support structure forces and moments due to these loads.

(A) HSM-H Off-Normal Thermal Loads (TO) Analysis (*Section P.3.6.2.3 (A) from CoC 1004 Amendment #8)*

This load case is the same as the normal thermal load but with an ambient temperature range from -40°F to 117°F. The temperature distributions for the extreme ambient conditions are used in the analysis for the concrete component evaluation. The results of the HSM-H concrete components thermal load analysis are presented in Table 3.9.9-9.

(B) HSM-H Off-Normal Handling Loads (RA) Analysis (*Section P.3.6.2.3 (B) from CoC 1004 Amendment #8)*

This load case assumes that the transfer cask is not accurately aligned with respect to the HSM-H resulting in binding of the DSC during a transfer operation causing the hydraulic pressure in the ram to increase. The ram force is limited to a maximum load of 80 kips during insertion and 80 kips during retrieval. Therefore, for the steel support structure, the off-normal jammed canister load (RA) is defined as an axial load on one rail of 80 kips during insertion and 80 kips during retrieval, plus a vertical load of one half the DSC weight (on both rails) at the most critical

location. The off-normal operating handling loads are considered as live loads for the design of the concrete components.

The results of the HSM-H concrete components for off-normal load analysis are presented in Table 3.9.9-8.

3.9.9.10 Accident Condition Structural Analysis

The design basis accident events specified by ANSI/ANS 57.9-1984, and other credible accidents postulated to affect the normal safe operation of the NUHOMS® HSM-H are addressed in this section.

In the following sections, each accident condition is analyzed to demonstrate that the requirements of 10CFR72.122 are met and that adequate safety margins exist for the HSM-H design. The resulting accident condition stresses in the HSM-H components are evaluated and compared with the applicable code limits set forth in Section 3.9.9.5. Load combination results for the HSM-H are presented in Section 3.9.9.11. The postulated accident conditions addressed in this section include:

- Tornado winds and tornado generated missiles (WT, WM)
- Design basis earthquake (EQ)
- Design basis flood (FL)
- Block Vent Thermal (TA)

ANSYS finite element models described in Section 3.9.9.7 are used to evaluate concrete and support structure forces and moments due to these loads.

3.9.9.10.1 Tornado Winds/Tornado Missile (WT, WM) (Section P.3.7.1 from CoC 1004 Amendment #8)

Stability and stress analyses are performed to determine the response of the HSM-H to tornado wind pressure loads. The stability analyses are performed using manual calculation methods to determine sliding and overturning response of the HSM-H array. A single HSM-H with both the end and the rear shield walls is conservatively selected for the analyses. The stress analyses are performed using the ANSYS finite element model of a single HSM-H to determine design forces and moments. These conservative generic analyses envelop the effects of wind pressures on the HSM-H array. Thus, the requirements of 10CFR 72.122 are met.
In addition, the HSM-H is evaluated for tornado missiles.

Effect of DBT Wind Pressure Loads on HSM-H

The HSM-H is qualified for maximum DBT generated design wind loads of 234 lb/ft^2 and 148 lb/ft^2 on the windward and leeward HSM-H walls (Table 3.9.9-7), respectively and a pressure drop of 3 psi.

A single stand-alone HSM-H is protected by shield walls on either side and at the rear. For an HSM-H array, the critical module is on the windward end of the array. This module has an end shield wall to protect the module from tornado missile impacts. The shield wall is also subjected to the 234 lb/ft^2 windward pressure load. The leeward side of the same end module in the array

has no appreciable suction load due to the presence of the adjacent module. The 148 lb/ft^2 suction load is applicable to the end shield wall on the opposite end module in the array. A suction of 207 lb/ft^2 is also applied to the roof of each HSM-H in the array.

For the stress analyses, the DBT wind pressures are applied to the HSM-H as uniformly distributed loads. The rigidity of the HSM-H in the transverse direction, due to frame and shear wall action of the HSM-H, is the primary load transfer mechanism assumed in the analysis. The bending moments and shear forces at critical locations in the HSM-H concrete components are calculated by performing an analysis using the ANSYS analytical model of the HSM-H. The resulting moments and shear forces are shown in Table 3.9.9-10 and are included in the HSM-H load combination results reported in Section 3.9.9.11.

For conservatism, the design basis operating wind pressure loads are assumed to be equal to those calculated for the DBT in the formulation of HSM-H load combination results.

A stability analysis is performed to evaluate the effects of overturning and sliding due to the postulated DBT. A single, freestanding HSM-H with end shield walls and rear shield wall is used for this analysis.

The pressure drop has no effect on the HSM-H, since the HSM-H is an open structure, due to the presence of the inlet and outlet vents.

HSM-H Overturning Analysis *(Section P.3.7.1.1.1 from CoC 1004 Amendment #8)*

For the DBT wind overturning analysis, the overturning moment and the resulting stabilizing moments are calculated.

A lower bound estimate of the stabilizing moment (M_{st}) for the windward module is:

M_{st} = Wd = 18,824 k-in.

Where:
- W = 362 K, [Lower bound weight of HSM-H (290 kips) + Lowest envelope of any DSC weight (72 kips)]
- d = 52 in., Horizontal distance between center of gravity of HSM-H to the outer edge of the module.

and the overturning moment (M_{ot}) for the windward module due to DBT wind pressure is:

$M_{ot} = [(W_1) A_w h/2 + W_3 A_r d]12$

Where:
- W_1 = 0.148 K/ft.^{2}, Wind load, leeward wall
- h = 18.5 ft, Wall height
- W_3 = 0.207 K/ft.^{2}, Wind uplift on roof
- A_r = 199.9 ft.^{2}, Roof area
- A_w = 382.4 ft.^{2}, Wall area
- d = 4.34 ft., Half of the transverse dimension of the roof

Therefore: M_{ot} = 8437.0 K-in.

Because the overturning moment is smaller than the stabilizing moment, the freestanding HSM-H will not overturn. The resulting factor of safety against overturning effects for the DBT wind loads is > 2.23.

HSM-H Sliding Analysis (*Section P.3.7.1.1.2 from CoC 1004 Amendment #8)*

To evaluate the potential for sliding of a single, freestanding HSM-H, the sliding force generated by the postulated DBT wind pressure is compared to the sliding resistance provided by friction between the base of the HSM-H and the ISFSI basemat.

The force (F_{sl}) required to slide the end module in an array is:

$$F_{sl} = [W - W_3 A_r]\mu$$

Where: μ = 0.6, coefficient of friction
W, W_3 and A_r are defined above.

Substituting gives:
F_{sl} = 192.4 K

The sliding force (F_{hw}) generated by DBT wind pressure for a single HSM-H is:

$$F_{hw} = (W_1 + W_2) A_w$$

Where: W_2 = 0.234 k/ft^2 wind load, windward wall
W_1, and A_w are as defined above.

Substituting gives:
F_{hw} = 146.1 K

Because the horizontal force generated by the postulated DBT is smaller than the force required to slide the end module in an HSM-H array, the HSM-H will not slide. The factor of safety against sliding of the HSM-H due to DBT wind loads is 1.32.

3.9.9.10.2 Earthquake (Seismic) *(Section P.3.7.2 from CoC 1004 Amendment #8)*

The peak horizontal ground acceleration of 0.30g and the peak vertical ground acceleration of 0.20g are utilized for the design basis seismic analysis of the HSM-H components.
Based on NRC Reg. Guide 1.61 [12], a damping value of three (3) percent is used for the DSC seismic analysis. Similarly, a damping value of seven (7) percent for DSC support steel and concrete is utilized for the HSM-H. An evaluation of the frequency content of the loaded HSM-H is performed to determine the amplified accelerations associated with the design basis seismic response spectra for the NUHOMS® HSM-H and DSC.

HSM-H Seismic Evaluation (*Section P.3.7.2.3 from CoC 1004 Amendment #8)*

Seismic Loads (EQ)

As described in Section 3.9.9.6.3, the design basis accelerations for the HSM-H are 0.3g in the horizontal directions and 0.2g in the vertical direction. These seismic accelerations are amplified based on the results of the frequency analysis of the HSM-H, as documented in Section 3.9.9.6.3. The resulting amplified accelerations are 0.37g and 0.33g in the transverse and longitudinal directions, respectively and 0.20g in the vertical direction. For conservatism, a value of 0.37g is used for both horizontal directions in the seismic analysis of the HSM-H.

Seismic Stress Analysis

An equivalent static analysis of the HSM-H is performed using the ANSYS model described in Section 3.9.9.7 and the seismic accelerations of 0.37g horizontally (longitudinal and transverse directions) and 0.2g vertically. These amplified accelerations are determined based on the frequency analysis of the HSM-H.

The responses for each orthogonal direction are combined using the SRSS method.
The seismic analysis results are shown in Table 3.9.9-10 and are incorporated in the loading combination C4C (Table 3.9.9-3) and C4S (Table 3.9.9-6) for the concrete and support structure components, respectively.

HSM-H Seismic Overturning Analysis

The following conservative analysis is performed to show that a single freestanding HSM-H with an end shield wall (in an array of two or more loaded modules) will not overturn due to seismic loads. Overturning about the long axis (i.e., in the short direction of the module) is considered.

Stabilizing moment = $M_{st} = (W_{hsm} + W_{dsc})\ b/2$
Overturning moment = $M_{ot} = (W_{hsm}\ 0.4a_{v1}+W_{dsc}0.4a_{v2})b/2+W_{hsm}\ d_1a_{h1}+W_{dsc}d_2a_{h2}$
(100% of horizontal acceleration is combined with 40% of vertical acceleration, Ref. [11])

Where:

W_{hsm}	=	310 K, Weight of the HSM-H (conservatively assumed)
W_{dsc}	=	110 K, Weight of DSC (conservatively assumed)
b/2	=	52 in, Horizontal distance from CG to corner(half width of the HSM-H)
d_1	=	123.45 in, Height of CG of HSM-H without the DSC
d_2	=	106 in, Height of the DSC center line
a_{v1}	=	0.20g, HSM-H peak vertical seismic acceleration
a_{v2}	=	0.20g, DSC peak vertical seismic acceleration
a_{h1}	=	0.37g, HSM-H peak horizontal seismic acceleration
a_{h2}	=	0.43g, DSC peak horizontal seismic acceleration (conservatively assumed)
M_{st}	=	21,840 K-in
M_{ot}	=	20,921 K-in

Because stabilizing moment is greater than the overturning moment the HSM-H will not overturn during the seismic event.

HSM-H Seismic Sliding Analysis

The friction force resisting sliding = $F_{st} = W_{hsm}(1-0.4*a_{v1})+W_{dsc}(1-0.4*a_{v2})]\mu$

The applied horizontal seismic force = $F_{hs} = [W_{hsm}a_{h1}+W_{dsc}a_{h2}]$

Where: μ = coefficient of friction between concrete HSM-H base on concrete basemat = 0.6.

W_{hsm}, W_{dsc}, a_{v1}, a_{v2}, a_{h1}, a_{h2} are defined above.

F_{st} = 231.8K
F_{hs} = 162.0K

The force required to slide the HSM-H is larger than the resulting lateral seismic force and therefore, the loaded HSM-H will not slide.

3.9.9.10.3 Flood Load (FL) *(Section P.3.7.3 from CoC 1004 Amendment #8)*

Since the source of flooding is site specific, the exact source, or quantity of flood water, should be established by the licensee. However, for this generic evaluation of the HSM-H, bounding flooding conditions are specified that envelop those that are postulated for most plant sites. As described in Section 3.9.9.6.3, the design basis flooding load is specified as a 50 foot static head of water and a maximum flow velocity of 15 feet per second. Each licensee should confirm that this represents a bounding design basis for their specific ISFSI site.

HSM-H Flooding Analysis

Because the HSM-H is open to the atmosphere, static differential pressure due to flooding is not a design load.

The maximum drag force, F, acting on the HSM-H due to a 15 fps flood water velocity is calculated as follows:

Where: $F = (v^2/2g)\, C_D\, A\, \rho_\omega$ [14]
v = 15 fps, Flood water velocity
C_D = 2.0, Drag coefficient for flat plate
A = 18.5 ft^2/ft, HSM-H area per foot length
ρ_w = 62.4 $lb./ft.^3$, Flood water density
F = Drag force (lb.)

$g = 32.2\ ft./s^2$ = Acceleration due to gravity

The resulting flood induced load is: F = 8.07 K/ft.

The following four flood load cases are considered:

Case 1: Flood water flow from front of HSM-H to rear of HSM-H
Case 2: Flood water flow from rear of HSM-H to front of HSM-H
Case 3: Flood water flow from left side of HSM-H to right side
Case 4: Flood water flow from right side of HSM-H to left side

Flood water flow from front of HSM-H to rear or rear of HSM-H to front (Cases 1 and 2)

Front/Rear wall, F_w = 8070*9' 8" = 78010 lbs
Conservatively, the total drag load on the front concrete components of the HSM-H is applied as a normal pressure load of magnitude (78010)/(18'6"*9'8"*144) = 3.1 psi.

Flood water flow in left side of HSM-H to right side or right side of HSM-H to left (Cases 3 and 4)

Side walls, F_w = 8070*20'8" = 166780 lbs

Conservatively, the total drag load on the left side concrete components of the HSM-H is applied as a normal pressure load of magnitude (166780)/(18'6"*20'8"*144) = 3.1 psi.

ANSYS finite element model described in Section 3.9.9.7 is used for the structural evaluation. The results for flood load case are obtained by enveloping results from above 4 load cases and shown on Table 3.9.9-10.

HSM-H Overturning Analysis

The factor of safety against overturning for the postulated flooding conditions is calculated using the stabilizing moment for a single HSM-H (with shield walls included) by summing moments about the bottom outside corner of a free-standing HSM-H. A net weight of 253.7 kips for a loaded HSM-H plus 100.4 kips for the upstream end shield wall, including buoyancy effects, is used to calculate the stabilizing moment that resists the overturning moment applied to the HSM-H by the flood water drag force. The stabilizing moment is:

$$M_{st} = 253.7 \times 52 + 100.4 \times 18$$

$$= 15{,}000 \text{ K-in.}$$

The maximum drag force due to the postulated water current velocity of 15 fps is 8.07 k/ft (see calculation above). The overturning moment due to the postulated flood current is based on drag

forces acting on a minimum of two modules in an array. The overturning moment is estimated as:

$$M_{ot} = 0.5 \times 8.07 \text{ K/ft.} \times 20.67 \text{ ft.} \times (18.5 \times 12/2)$$

$$= 9{,}258 \text{ K-in.}$$

The factor of safety (F.S.) against overturning for a freestanding HSM-H due to the postulated design basis flood water velocity is given by:

F.S. = 15,000 / 9,258 = 1.62

Therefore, a minimum of two (2) HSM-Hs adjacent to each other are required to prevent overturning.

HSM-H Sliding Analysis

The factor of safety against sliding of a freestanding HSM-H due to the maximum postulated flood water velocity of 15 fps is calculated using methods similar to those described above. The effective weight of the HSM-H including the DSC and end shield wall acting vertically downward, less the effects of buoyancy acting vertically upward is 354 K. The friction force resisting sliding of the HSM-H is equal to the product of the net weight of the HSM-H and the DSC and the coefficient of friction for concrete placed against another concrete surface such as that between the HSM-H and basemat, which is 0.6 [3]. Therefore, the force resisting sliding of the HSM-H is 0.6 x 354 or 212.5 kips. The drag force acting on a HSM-H (considering a minimum of two modules in an array) is 0.5 x 8.07 kips/ft x 20.67 = 83.4 kips total acting on the side wall of a single HSM-H, due to a flood velocity of 15 fps. The resulting factor of safety against sliding of a free standing HSM-H due to the design basis flood water velocity is 2.55. Therefore, a minimum of two (2) HSM-Hs adjacent to each other are required to prevent sliding.

3.9.9.10.4 Blocked Vent Thermal (TA) *(Section P.3.7.6 from CoC 1004 Amendment #8)*

This accident conservatively postulates the complete blockage of the HSM-H ventilation air inlet and outlet openings on the HSM-H side walls.

Since the NUHOMS® HSM-Hs are located outdoors; there is a remote probability that the ventilation air inlet and outlet vent openings could become blocked by debris. The NUHOMS® design features such as the perimeter security fence and the redundant protected location of the air inlet and outlet vent openings and the screens reduces the probability of occurrence of such an accident. Nevertheless, for this conservative generic analysis, such an accident is postulated to occur and is analyzed.

The postulated accident thermal event occurs due to blockage of either the air inlet or outlet vents under off-normal ambient temperatures range from –40°F to 117°F. The results of the HSM-H concrete components blockage thermal load analysis are presented in Table 3.9.9-9.

3.9.9.11 Load Combination

Concrete Components

To determine the required strength (internal axial forces, shear forces, and bending moments) for each HSM-H concrete component, linear elastic finite element analyses are performed for the normal, off-normal, and accident loads using the analytical models described in Section 3.9.9.7 for mechanical and thermal loads.

The individual load analysis results of the HSM-H concrete structure are presented in Table 3.9.9-8, 9 and 3.9.9-10. The load combination results for each component are presented in Table 3.9.9-11 for the load combinations defined in Table 3.9.9-3. The notations for the components of forces and moments and the concrete component planes in which capacities are computed are shown in Figure 3.9.9-5. All load combination results are below the computed section capacities.

Support Steel Structure

The support rails, rail stiffener plates, extension plates and cross members of the DSC support structure, shown in Figure 3.9.9-6 are evaluated using the allowable stress design method of the AISC Manual of Steel Construction [4]. The load combination results for each of these components are provided in Table 3.9.9-12 to 14.

The support rail stress comparison results are presented in Table 3.9.9-15. The extension plate and cross member stress comparison results are presented in Table 3.9.9-16.

HSM-H Shield Door

The shield door is free to grow in the radial direction when subjected to thermal loads. Therefore, there will be no stresses in the door due to thermal growth. The dead weight, tornado wind, differential pressure and flood loads cause insignificant stresses in the door compared to stresses due to missile impact load. Therefore, the door is evaluated only for the missile impact load. The maximum moment and shear force in the door are 28.8 kip-in/ft and 2.1 kips/ft. These computed moments and shear forces in the door are significant less than corresponding capacities.

HSM-H Heat Shield

The top heat shield (louvers) consists of seven panels. Each panel has two stainless steel mounting bars. The aluminum louvers are mounted on the mounting bars. Each mounting bar is suspended from the roof by two threaded rods. The natural lateral frequency of a typical rod is conservatively estimated to be 9.0 Hz. The combined axial and bending stress in the hanger rods is 34.63 ksi. The allowable axial and bending stress is 86.1 ksi.

The side heat shields consists of three panels. Each panel is suspended from the roof by two threaded rods, and supported laterally and longitudinally by four rods. The maximum axial plus

bending stress in the lateral and longitudinal support rods is 83.7 ksi. The allowable axial and bending stress is 86.1 ksi.

HSM-H Seismic Retainers

The seismic retainer consists of a capped tube steel embedment located within the bottom center of the round access opening of the HSM-H, and a tube steel retainer assembly that drops into the embedment cavity after DSC transfer is complete. The drop-in retainer extends approximately 4" above the rail to provide axial restraint of the DSC. The maximum seismically induced shear load in the retainer is 61 kips. The maximum shear stress in the retainer is 15.25 ksi. The allowable shear stress is 17.8 ksi.

3.9.9.12 Conclusions

The load categories associated with normal operating conditions, off-normal conditions and postulated accident conditions are described and analyzed in previous sections. The load combination results for HSM-H components important to safety are also presented. Comparison of the results with the corresponding design capacity shows that the design strength of the HSM-H is greater than the strength required for the most critical load combination.

3.9.9.13 References

1. Title 10, Code of Federal Regulations, Part 72 (10CFR72), "Licensing Requirements for the Storage of Spent Fuel in the Independent Spent Fuel Storage Installation," U.S. Nuclear Regulatory Commission, August 31, 1988.

2. ANSI/ANS 57.9-1984, "Design Criteria for an Independent Spent Fuel Storage Installation (Dry Storage Type)," American Nuclear Society.

3. "Code Requirements for Nuclear Safety Related Concrete Structures," ACI 349-97, American Concrete Institute, Detroit, MI.

4. "Manual of Steel Construction," American Institute of Steel Construction, Ninth Edition, 1990.

5. American Society of Civil Engineers, ASCE 7-95, "Minimum Design Loads for Buildings and Other Structures" (formerly ANSI A58.1).

6. "Design Basis Tornado for Nuclear Power Plants," Regulatory Guide 1.76, U.S. Atomic Energy Commission, April 1974.

7. "Missiles Generated by Natural Phenomenon," Standard Review Plan, NUREG-0800, U.S. Nuclear Regulatory Commission

8. Bechtel Topical Report, "Design of Structures for Missile Impact," BC-TOP-9-A, Revision 2, September 1974.

9. Regulatory Guide 1.60, "Design Response Spectra for Seismic Design of Nuclear Power Plants," U.S. Atomic Energy Commission, Revision 1, December 1973.

10. ANSYS Engineering Analysis System, Users Manual for ANSYS Rev. 5.6 and 7.0, Swanson Analysis Systems, Inc., Houston, PA.

11. "Structural Analysis and Design of Nuclear Plant Facilities," ASCE Publication No. 58.

12. Regulatory Guide 1.61, "Damping Values for Seismic Design of Nuclear Power Plants", U.S. Atomic Energy Commission, October 1973.

13. Amendment No. 8 to NUHOMS® CoC 1004, addition of 24PTH DSC to Standardized NUHOMS® System.

14. "Fluid Mechanics", Raymond C. Binder, 4th Edition, Prentice-Hall, Inc.

Table 3.9.9-1
Summary of HSM-H Component Design Loadings

Component	Design Load Type	Design Parameters	Applicable Codes
HSM-H Module	Dead Load (DW)	150 pcf concrete structure and weight of support steel structure	ANSI 57.9-1984 [2]
	Live Load (LL)	200 psf (including snow and ice load) on the roof DSC weight (110 kips)	ANSI-57.9-1984 [2] ASCE 7-95 [5]
	Normal Operating Temperature (TN) Off-Normal Operating Temperature (TO)	Normal: Ambient air temperature 0°F -100°F Off Normal: Ambient air temperature -40°F to 117°F	ANSI 57.9-1984 [2]
	Normal Handling Loads (RO)	Hydraulic ram load of 80,000 lb.(DSC HSM insertion) 60,000 lb (DSC HSM extraction) on the rails	ANSI 57.9-1984 [2]
	Design Basis Wind Load (WW)	Conservatively assumed to be same as tornado generated wind load.	ASCE 7-95 [5]
	Off-Normal Handling Loads (RA)	Hydraulic ram load of: 80,000 lb (DSC insertion) 80,000 lb (DSC extraction) on each rail, one rail at a time.	ANSI-57.9-1984 [2]
	Accident Temperature (TA)	Ambient air temperature of –40°F and 117°F with inlet and outlet vents blocked.	10CFR72.122(n) [1]
	Tornado Wind Load (WT)	Maximum wind speed of 360 mph and a pressure drop of 3 psi	ASCE 7-95 [5] NRC Regulatory Guide 1.76 [6]
	Tornado Missile Load (WM)	See Section T.2.2.1.3 for missiles considered.	NUREG-0800 Section 3.5.1.4 [7]
	Flood (FL)	Maximum water height: 50 ft. Maximum velocity of water 15'/sec.	10CFR72.122(b) [1]
	Seismic (EQ)	Horizontal ground acc: 0.30g Vertical ground acc.: 0.20g	NRC Reg. Guides 1.60 & 1.61 [9] and [12]

Table 3.9.9-2
Summary of 32PTH DSC Support Structure Design Loadings

Component	Design Load Type	Design Parameters	Applicable Codes
32PTH DSC Support Structure	Live Load (LL)	DSC weight (110 kips)	ANSI-57.9-1984 [2]
	Normal Operating Temperature (TN) Off-Normal Operating Temperature (TO)	Normal: Ambient air temperature 0°F -100°F Off Normal: Ambient air temperature -40°F to 117°F	ANSI 57.9-1984 [2]
	Normal Handling Loads (RO)	Hydraulic ram load of 80,000 lb.(DSC insertion) 60,000 lb (DSC extraction) on the rails	ANSI 57.9-1984 [2]
	Off-Normal Handling Loads (RA)	Hydraulic ram load of: 80,000 lb (DSC insertion) 80,000 lb (DSC extraction) on each rail. One rail at a time.	ANSI-57.9-1984 [2]
	Accident Temperature (TA)	Ambient air temperature of –40°F and 117°F with inlet and outlet vents blocked.	10CFR72.122(n) [1]
	Seismic (EQ)	Horizontal ground acc: 0.30g Vertical ground acc.: 0.20g	NRC Reg. Guides 1.60 & 1.61 [9] and [12]

Table 3.9.9-3
HSM-H Concrete Load Combinations

Load Combination No.	Combination Identifier	Load Combination
C1C	COMB1C	U > 1.4*DW+1.7*(LL+RO)
C2C	COMB2C	U > 1.05*DW+1.275*(LL+TN+WW)
C3C	COMB3C	U > 1.05*DW + 1.275*(LL+TN+RA)
C4C	COMB4C	U > DW+LL+TN+EQ
C5C	COMB5C	U > DW+LL+TN+WT
C6C	COMB6C	U > DW+LL+TN+FL
C7C	COMB7C	U > DW+LL+MAX(TO and TA)

Note: For definition of individual load cases see Table 3.9.9-1

Table 3.9.9-4
Ultimate Capacities of Concrete Components

Component	Thermal Condition	V_{ui}(1) Kips/ft	V_{uo1}(1) Kips/ft	V_{uo2}(1) kips/ft	M_{u1}(1) Kip-in/ft	M_{u2}(1) kip-in/ft
Rear Wall (upper)	Normal	76.8	14.5	14.5	305.9	305.9
	Accident	69.6	13.8	13.8	273.8	273.8
Rear Wall (lower)	Normal	98.4	36.2	36.2	778.1	778.1
	Accident	90.1	34.3	34.3	696.3	696.3
Side Walls (upper)	Normal	55.4	14.8	14.8	202.1	202.1
	Accident	50.5	14.0	14.0	180.8	180.8
Side Walls (lower)	Normal	64.0	23.4	23.4	322.9	322.9
	Accident	58.7	22.2	22.2	289.0	289.0
Roof	Normal	177.6	59.1	59.1	2438.1	2438.1
	Accident	162.4	56.1	56.1	2181.7	2181.7
Front Wall (upper)	Normal	174.7	56.3	56.3	2317.2	2317.2
	Accident	159.6	53.4	53.4	2073.5	2073.5
Front Wall (lower)	Normal	192.1	73.6	73.6	3042.5	3042.5
	Accident	176.0	69.8	69.8	2722.4	2722.4

NOTES:

(1) V_{ui} = Minimum of ultimate in plane shear capacities in planes 1 and 2.

Vuo1 = Minimum Ultimate out of plane shear capacity in plane 1

Vuo2 = Minimum Ultimate out of plane shear capacity in plane 2

Mu1 = Minimum Ultimate moment capacity in plane 1

Mu2 = Minimum Ultimate moment capacity in plane 2

Table 3.9.9-5
Structural Design Criteria for DSC Support Structure

Allowable Stress (S)	
Stress Type	Stress Value
Tensile	0.60 S_y
Compressive	(See Note 1)
Bending	0.60 S_y(2)
Shear	0.40 S_y
Interaction	(See Note 3)

Notes:

(1) Equations E2-1 or E2-2 of the AISC Specification (Ref. 4) are used as appropriate.

(2) For properly braced non-compact sections, for other cases see AISC Specification Chapter F.

(3) Interaction equations per the AISC Specification are used as appropriate.

(4) S_y = Yield strength of the material

Table 3.9.9-6
HSM-H Support Steel Structure Load Combinations

Load Combination No.	Combination Identifier	Load Combination
C1S	COMB1S	(1.5S or 1.4 S_v) > DW+LL+TN(1), (2)
C2S	COMB2S	S > DW+RO(3), (4)
C3S	COMB3S	1.3S > DW+TN+RA(3), (4)
C4S	COMB4S	(1.6S or 1.4S_v) > DW+LL+TN+EQ(2)
C5S	COMB5S	(1.7S or 1.4S_v) > DW+LL+MAX (TO and TA)(2)

Notes:

(1) This normal operating load combination applies to DSC storage condition.

(2) DSC weight is included as live load (LL) for this condition; the DSC spans between end supports

(3) These load combinations represent normal and off-normal handling conditions.

(4) DSC weight is included as a direct load on the rail.

Table 3.9.9-7
Design Pressures for Tornado Wind Loading

HSM-H Wall Orientation[1]	Velocity Pressure (psf)	Pressure Coefficient[2]	Max/Min Design Pressure (psf)
Front	344	+0.68	234
Left	344	-0.60	-207
Rear	344	-0.43	-148
Right	344	-0.60	-207
Roof	344	-0.60	-207

Notes:

1. Wind direction assumed to be from front. Wind load from other directions may be found by rotating table values to desired wind directions.
2. Pressure coefficient = guest factor (0.85) x max/min pressure coefficient from Figure 6-3 of reference 5.

Table 3.9.9-8
Maximum NUHOMS® HSM-H Concrete Component Forces and Moment for Normal and Off-Normal Loads

Load Case	Concrete Component	Forces/Moments			
		Shear, V_{01} (kips/ft)	Shear, V_{02} (kips/ft)	Moment, M_1 (kip-in/ft)	Moment, M_2 (kip-in/ft)
Dead Load (DW)	Rear Wall	1.20	0.60	5.40	20.10
	Side Wall	4.40	2.80	24.80	20.40
	Front Wall	5.30	5.10	75.30	190.80
	Roof	2.80	3.50	45.20	136.20
Live Load (LL)	Rear Wall	1.40	0.60	6.70	20.10
	Side Wall	1.20	0.80	8.50	9.60
	Front Wall	30.20	23.80	344.60	510.60
	Roof	0.90	1.30	16.00	47.20
Operational Handling Load (RO)	Rear Wall	Included in Live Load (LL)			
	Side Wall				
	Front Wall				
	Roof				
Off-Normal Handling Load (RA)	Rear Wall	Included in Live Load (LL)			
	Side Wall				
	Front Wall				
	Roof				
Design Wind Load (WW)	Rear Wall	4.88	2.20	81.50	124.88
	Side Wall	27.00	10.87	190.50	135.00
	Front Wall	12.75	12.12	179.00	289.12
	Roof	3.25	2.50	135.50	80.88

Table 3.9.9-9
Summary of Thermal Forces and Moments in the HSM-H Concrete Components

Thermal Case	Concrete Component	Forces/Moments			
		Shear, V_{o1}(1) (kips/ft)	Shear, V_{o2}(1) (kips/ft)	Moment, M_1(2) (kip-in/ft)	Moment, M_2(2) (kip-in/ft)
Normal Thermal (TN)	Rear Wall	4	6	47	60
	Side Wall	7	6	46	32
	Front Wall	16	23	1318	596
	Roof	3	5	111	234
Off-Normal Thermal (TO)	Rear Wall	4	5	51	39
	Side Wall	6	6	45	29
	Front Wall	16	23	1315	506
	Roof	3	5	93	233
Accident Thermal (TA)	Rear Wall	7	15	107	202
	Side Wall	92	32	184	340
	Front Wall	32	29	1353	2539
	Roof	11	20	349	830

Notes:

1. V_{o1} and V_{o2} are out of plane shear
2. M_1 and M_2 are out of plane moment

Table 3.9.9-10
Maximum HSM-H Concrete Component Forces and Moments for Accident Loads

Load Case	Concrete Component	Forces/Moments			
		Shear, V_{01}(1) (kips/ft)	Shear, V_{02}(1) (kips/ft)	Moment, M_1(2) (kip-in/ft)	Moment, M_2(2) (kip-in/ft)
Earthquake (EQ)	Rear Wall	4.71	1.31	23.92	89.41
	Side Wall	7.30	5.47	49.13	64.12
	Front Wall	17.71	13.37	133.16	498.61
	Roof	3.05	1.83	230.46	75.03
Flood (FL)	Rear Wall	6.34	3.42	146.03	106.63
	Side Wall	49.04	19.28	340.62	248.39
	Front Wall	20.5	17.57	309.27	351.48
	Roof	3.05	1.83	230.46	75.03
Tornado Wind (WT)	Rear Wall	4.88	3.81	151.94	124.88
	Side Wall	51.75	21.25	349.75	259.50
	Front Wall	16.62	13.94	295.69	289.12
	Roof	5.75	4.25	248.06	112.25

Notes:
(1) V_{01} and V_{02} are out of plane shears.
(2) M_1 and M_2 are out of plane moments.

Table 3.9.9-11
Comparison of Highest Combined Shear Forces/Moments with the Capacities

Component	Load Comb.(1)	Quantity	V_1 kips/ft	V_{01} kips/ft	V_{02} kips/ft	M_1 kip-in/ft	M_2 kip-in/ft
Rear Wall (Upper)	Comb 1c thru 6c	Computed	14.52	7.68	8.23	63.82	121 .65
		Capacity	76.8	14.5	14.5	305.9	305.9
		Ratio	**0.19**	**0.53**	**0.57**	**0.21**	**0.40**
	Comb 7c	Computed	9.73	8.52	2.93	92.68	227.1
		Capacity	69.6	13.8	13.8	273.8	273.8
		Ratio	**0.14**	**0.62**	**0.21**	**0.34**	**0.83**
Rear Wall (Lower)	Comb 1c thru 6c	Computed	17.34	9.48	13.25	159.40	167.70
		Capacity	98.4	36.2	36.2	778.10	778.10
		Ratio	**0.18**	**0.26**	**0.37**	**0.21**	**0.22**
	Comb 7c	Computed	6.92	4.78	14.82	110.79	180.69
		Capacity	90.10	34.30	34.30	696.30	696.3
		Ratio	**< 0.10**	**0.14**	**0.43**	**0.16**	**0.26**
Side Walls (Upper)	Comb 1c thru 6c	Computed	16.59	5.38	6.01	138.48	143.66
		Capacity	55.40	14.80	14.80	202.10	202.10
		Ratio	**0.30**	**0.36**	**0.41**	**0.69**	**0.71**
	Comb 7c	Computed	22.37	12.08	3.10	87.24	87.76
		Capacity	50.50	14.00	14.00	180.80	180.80
		Ratio	**0.44**	**0.86**	**0.22**	**0.48**	**0.49**
Side Walls (Lower)	Comb 1c thru 6c	Computed	36.17	17.43	21.12	308.10	216.77
		Capacity	64.00	23.4	23.4	322.9	322.9
		Ratio	**0.57**	**0.75**	**0.91**	**0.96**	**0.67**
	Comb 7c	Computed	19.28	21.12	15.34	97.25	180.24
		Capacity	58.70	22.2	22.2	289.0	289.0
		Ratio	**0.33**	**0.95**	**0.69**	**0.34**	**0.63**
Roof	Comb 1c thru 6c	Computed	13.18	5.87	12.38	265.53	401.25
		Capacity	177.60	59.10	59.10	2438.10	2438.10
		Ratio	**< 0.10**	**< 0.10**	**0.21**	**0.11**	**0.17**
	Comb 7c	Computed	7.42	11.48	24.06	330.77	897.67
		Capacity	162.40	56.10	56.10	2181.70	2181.70
		Ratio	**< 0.10**	**0.21**	**0.43**	**0.15**	**0.41**
Front Wall (Upper)	Comb 1c thru 6c	Computed	41.82	38.86	37.00	681.10	1042.27
		Capacity	174.70	56.30	56.30	2317.20	2317.20
		Ratio	**0.24**	0.69	0.66	0.30	0.45
	Comb 7c	Computed	13.72	36.20	19.42	1347.10	875.7
		Capacity	159.60	53.40	53.40	2073.50	2073.50
		Ratio	**<0.10**	**0.68**	**0.36**	**0.65**	**0.42**
Front Wall (Lower)	Comb 1c thru 6c	Computed	29.29	30.43	37.83	1783.50	836.92
		Capacity	192.10	73.60	73.60	3042.50	3042.5
		Ratio	**0.16**	**0.42**	**0.52**	**0.59**	**0.27**
	Comb 7c	Computed	32.06	33.32	29.66	1359.60	351.19
		Capacity	176.00	69.80	69.80	2722.40	2722.40
		Ratio	**0.18**	**0.48**	**0.42**	**0.50**	**0.13**

Note:

1. Com 1c thru 6c includes normal thermal. Com 7c includes accident thermal (see Table 3.9.9-3)

Table 3.9.9-12
Maximum/Minimum Forces/Moments in the Rail Components in the Local System

Load Combination		F_x Kips	F_y Kips	F_z Kips	M_x kip-in	M_y kip-in	M_z Kip-in
C1S	MAX	0.0	33.0	65.2	54.8	231.1	213.7
	MIN	0.0	-41.0	-61.3	-45.2	-1146.7	-236.2
C2S	MAX	38.5	39.8	77.0	0.22	428.2	247.8
	MIN	-28.9	-39.8	-60.9	-0.32	-1137.6	-247.8
C3S	MAX	86.5	30.7	89.6	54.9	592.7	199.4
	MIN	-86.5	-38.1	-63.0	-45.2	-1422.4	-230.4
C4S	MAX	22.3	38.2	102.1	54.9	562.5	-267.6
	MIN	-22.3	-46.3	-98.3	-45.2	-1869.0	-290.2
C5S	MAX	0.	43.8	72.6	162.4	234.1	236.3
	MIN	0.	-47.8	-71.5	-140.8	-126.8	-236.1

Table 3.9.9-13
Maximum/Minimum Forces/Moments in the Rail Extension Plates in the Local System

Load Combination		F_x Kips	F_y Kips	F_z Kips	M_x kip-in	M_y kip-in	M_z Kip-in
C1S	MAX	0.0	0.85	-0.25	2.7	6.8	13.8
	MIN	0.0	-4.0	-0.73	-2.7	-4.3	-45.9
C2S	MAX	40.0	2.6	-0.4	0.1	5.3	26.1
	MIN	-30.0	-2.6	-0.5	-0.1	-2.6	-26.1
C3S	MAX	80.0	0.8	-0.2	2.7	7.2	13.6
	MIN	-79.9	-3.9	-0.8	-2.8	-4.2	-44.9
C4S	MAX	38.5	1.5	-0.0	2.7	9.3	17.0
	MIN	-38.5	-4.7	-1.0	-2.8	-5.8	-53.2
C5S	MAX	0	0.9	0.3	8.3	10.9	16.1
	MIN	0.	-6.7	-1.3	-8.4	-8.6	-83.7

Table 3.9.9-14
Maximum/Minimum Axial Forces in the Cross Member Components

Load Combination		F_x Kips
C1S	MAX	6.2
	MIN	5.2
C2S	MAX	8.1
	MIN	5.8
C3S	MAX	5.2
	MIN	2.6
C4S	MAX	6.2
	MIN	5.2
C5S	MAX	6.2
	MIN	4.5

Table 3.9.9-15
Rail Component Results

Load Comb.	Interaction Ratio(1)	Shear Stress Ratio(2)	Stiffener Plate Stress Ratio(3)
C1S	0.35	0.64	0.16
C2S	0.58	0.83	0.00
C3S	0.57	0.89	0.18
C4S	0.50	0.92	0.15
C5S	0.34	0.89	0.14

Notes:

(1) Axial and bending stresses are computed using axial (F_x) and bending moment (M_y, M_z) results from Table 3.9.9-12. Interaction ratios are based on appropriate equations from Chapter H of AISC [4].

(2) Shear stresses are computed using shear forces (F_y, F_z) from Table 3.9.9-12. Shear stress ratio is the computed shear stress/shear stress allowable.

(3) Flexural stresses in the stiffener plates are computed using torsional moment (M_x) result from Table 3.9.9-12. Stiffener plate stress ratio is the bending stress in the plate/bending allowable stress.

Table 3.9.9-16
Extension Plates and Cross Members Results

Load Comb.	Extension Plates Interaction Ratio(1)	Cross Members Stress Ratio(2)
C1S	0.77	0.25
C2S	0.77	0.32
C3S	0.71	0.20
C4S	0.60	0.25
C5S	0.63	0.27

Notes:

(1) Axial and bending stresses are computed using axial (F_x) and bending moment (M_y, M_z) results from Table 3.9.9-13. Interaction ratios are based on appropriate equations from Chapter H of AISC [4].

(2) Axial stresses in the cross members are computed using axial (F_x) force results from Table 3.9.9-14. Cross member stress ratio is the axial stress in the member/axial allowable stress.

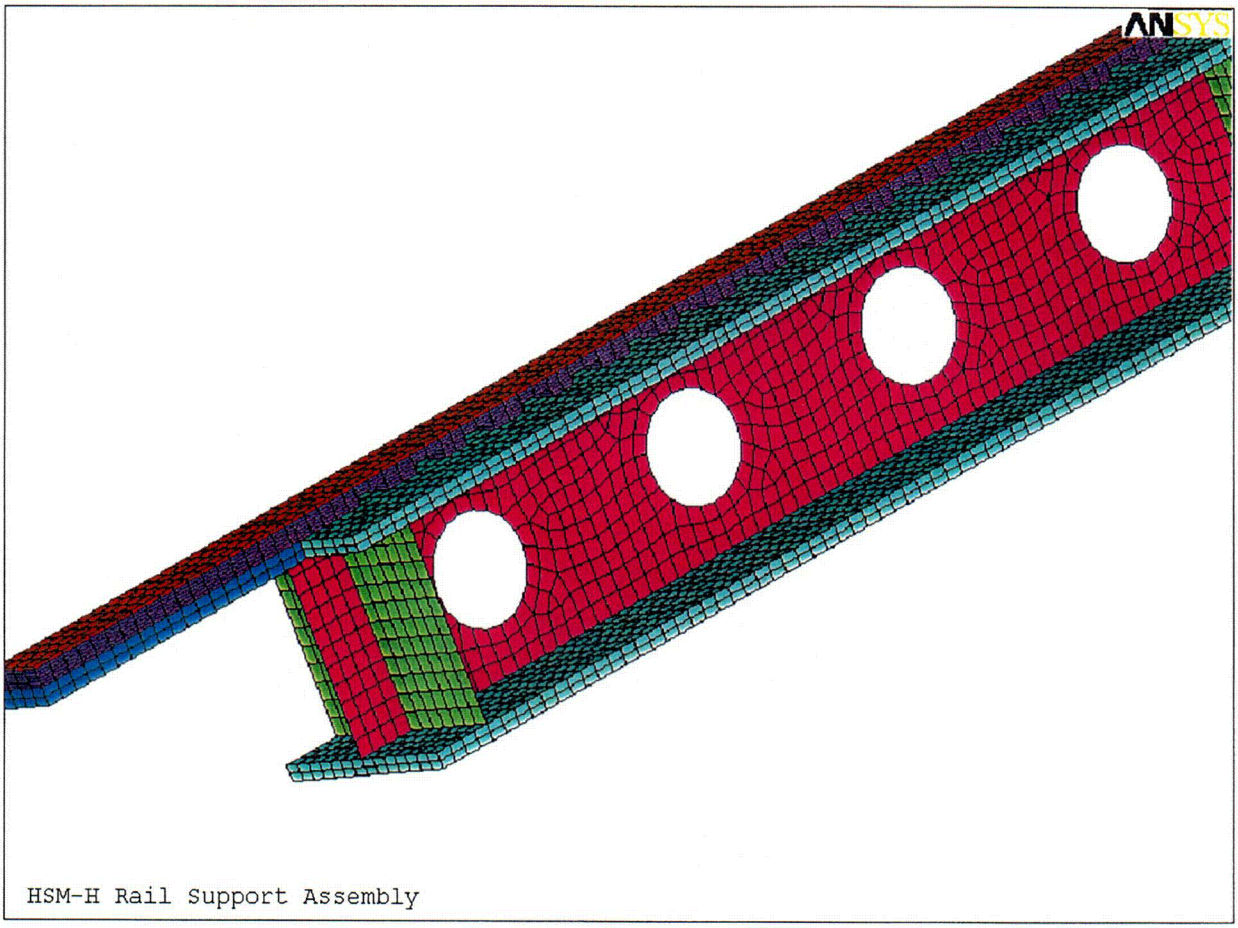

Figure 3.9.9-1
Analytical Model of the W12x96 Beam with Slotted, Nitronic and Stiffener Plates

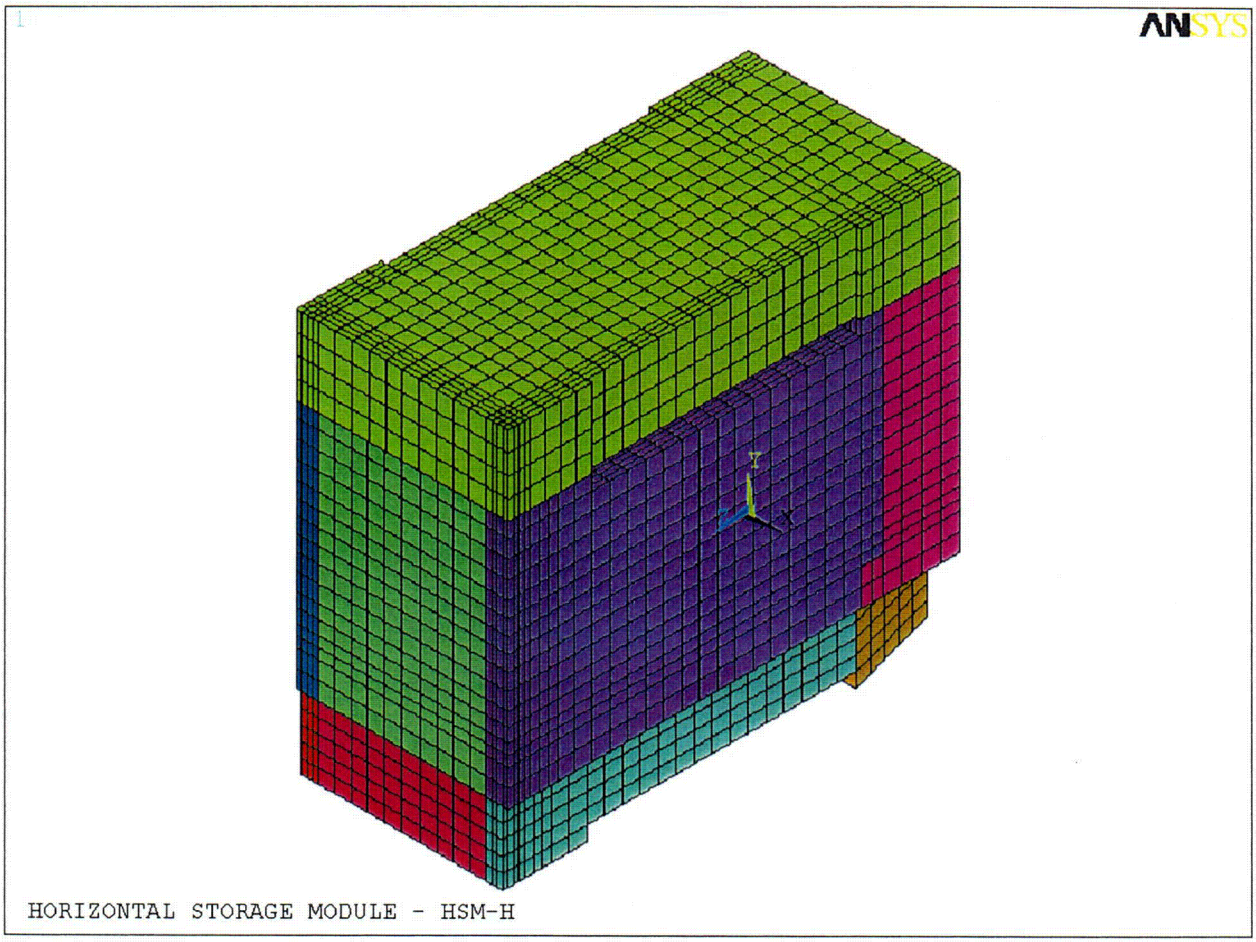

Figure 3.9.9-2
Analytical Model of the HSM-H for Mechanical Load Analysis

C32

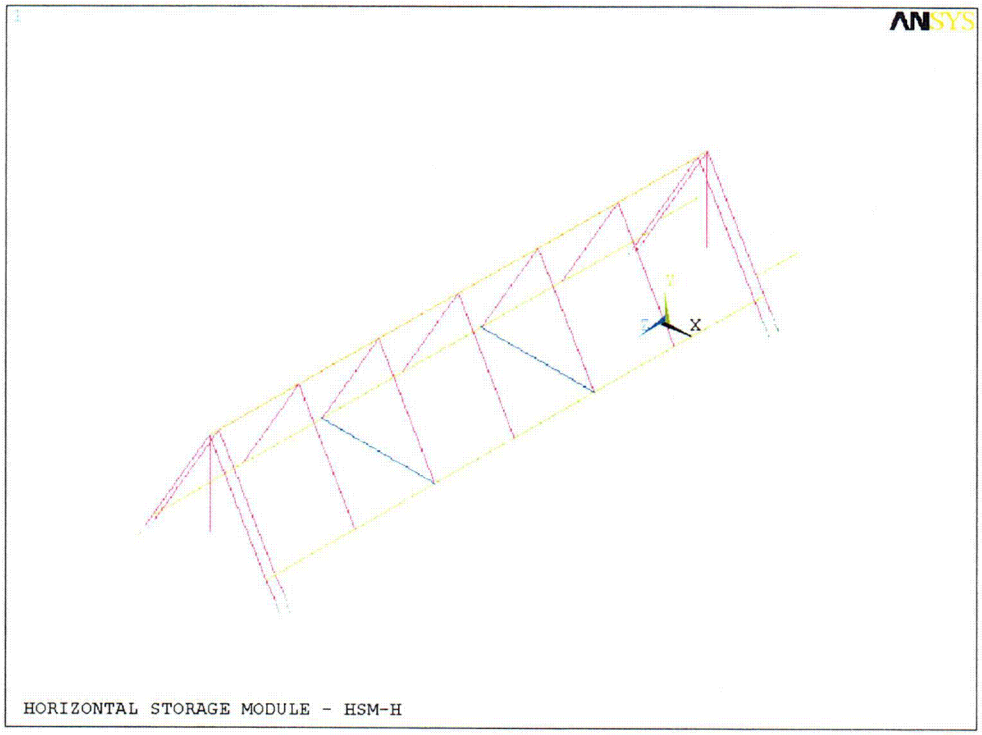

Figure 3.9.9-3
Analytical Model of the 32PTH DSC Support Structure

C33

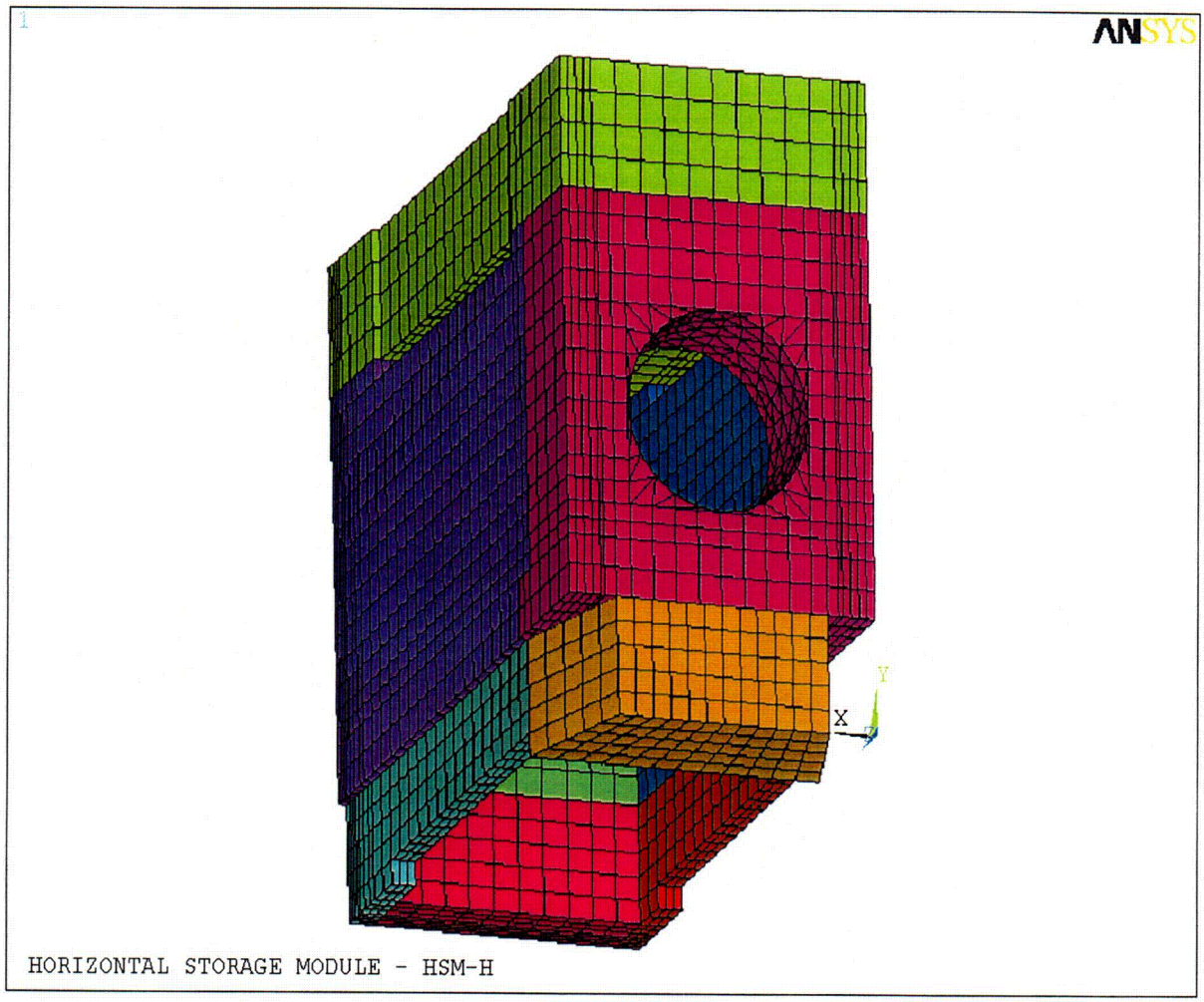

Figure 3.9.9-4
Analytical Model of the HSM-H for Thermal Load Analysis

C 34